



# A novel strategy for the treatment of Obesity using the small molecule ABX300, a modulator of the LMNA gene splicing

Celia Lopez Herrera

## ► To cite this version:

Celia Lopez Herrera. A novel strategy for the treatment of Obesity using the small molecule ABX300, a modulator of the LMNA gene splicing. Human health and pathology. Université Montpellier, 2015. English. NNT : 2015MONTT048 . tel-01549093

**HAL Id: tel-01549093**

**<https://theses.hal.science/tel-01549093>**

Submitted on 28 Jun 2017

**HAL** is a multi-disciplinary open access archive for the deposit and dissemination of scientific research documents, whether they are published or not. The documents may come from teaching and research institutions in France or abroad, or from public or private research centers.

L'archive ouverte pluridisciplinaire **HAL**, est destinée au dépôt et à la diffusion de documents scientifiques de niveau recherche, publiés ou non, émanant des établissements d'enseignement et de recherche français ou étrangers, des laboratoires publics ou privés.

# THÈSE

Pour obtenir le grade de  
**Docteur**

Délivré par l'Université de Montpellier

Préparée au sein de l'école doctorale CBS2 n°168  
Sciences Chimiques et Biologiques pour la Santé  
Et de l'unité de recherche CNRS-UMR5535

**Spécialité : Biologie moléculaire, Biologie cellulaire**

**Présentée par Celia LÓPEZ HERRERA**

**"Une Nouvelle stratégie pour le traitement de  
l'obésité en utilisant ABX<sub>300</sub>, une molécule  
modulatrice de l'épissage du gène *LMNA* "**

**Soutenue le 17 Décembre 2015 devant le jury composé de**

Anne-Dominique LAJOIX, PU, Université de Montpellier	Présidente
Philippe VALET, PU, Université de Toulouse	Rapporteur
Ez-Zoubir AMRI, DR2, Université de Nice	Rapporteur
François CASAS, DR2, Université de Montpellier	Examineur
Ramón GOMIS, PU, Universidad de Barcelona	Examineur
Jamal TAZI, PU, Université de Montpellier	Directeur de thèse

## RESUME EN FRANÇAIS



# Synthèse du mémoire

## Introduction

### I. Le tissu adipeux et l'obésité

La perception du tissu adipeux a considérablement changé au cours de ces dernières décennies avec la spectaculaire augmentation de l'incidence de l'obésité et sa morbidité associée. Au niveau mondial, mais plus particulièrement dans les pays industrialisés, l'obésité compte à présent parmi l'une des plus grandes préoccupations de santé publique. Même si cette maladie chronique a une étiologie multifactorielle, elle peut être simplement définie par une augmentation de l'accumulation de la graisse corporelle. Chez la majorité des patients, l'obésité est la conséquence d'un apport énergétique supérieur à la dépense. Peu de thérapies médicales sont actuellement reconnues et elles visent en général un ou plusieurs des mécanismes suivants: prévention de l'absorption des graisses, diminution de l'appétit et augmentation du métabolisme corporel.

Pour étudier les mécanismes liés à l'obésité, plusieurs modèles de rongeurs sont disponibles, permettant d'être en mesure d'émettre des hypothèses applicables à l'homme. Parmi ces modèles animaux ils existent par exemple des souris présentant des altérations concernant la leptine, une hormone qui régule les réserves de graisses dans l'organisme et l'appétit, parfois dite « hormone de la satiété ». Les souris *ob/ob*, sont mutées génétiquement au niveau du gène codant la leptine; et les souris *db/db* sont mutées au niveau du récepteur à la leptine. Très utilisés aussi ce sont les souris DIO (diet-induced obesity), chez lesquelles l'obésité est induite par un régime alimentaire riche en lipides.

Le tissu adipeux est susceptible aux changements diététiques, en effet il est sensible à l'insuline sécrétée suite aux repas, ainsi qu'à l'adrénaline produite lors d'un stress. De plus, un bon fonctionnement du système nerveux est requis pour détecter l'état des réserves énergétiques et faire correspondre les apports avec les dépenses. Des réponses métaboliques et comportementales sont ainsi



déclenchées, visant à maintenir l'équilibre énergétique. Dans l'ensemble, cet équilibre est sensible à divers facteurs, y compris des hormones, des neurotransmetteurs et des facteurs psychologiques et culturels.

Les adipocytes sont équipés de la machinerie biochimique nécessaire pour fonctionner efficacement en tant que site de stockage du carburant de l'organisme. Pour ce faire, ils sont aussi bien responsables de la conversion des acides gras libres en triglycérides permettant la lipogénèse (stockage des corps gras), que du processus inverse, la lipolyse (libération des corps gras). Outre ces deux fonctions fondamentales, le tissu adipeux est crucial pour l'activité du système endocrinien via sa fonction sécrétrice, qui est indispensable pour le maintien de l'homéostasie dans l'organisme. Des peptides et autres facteurs agissant de façon endocrine ou paracrine (adipokines/adipocytokines), sont libérés par ce tissu et/ou par sa fraction stroma vasculaire, et vont exercer des effets métaboliques très variés. Parmi ceux-ci on compte des adipocytokines pro-inflammatoires qu'on trouve augmentées en relation avec l'obésité tel que la leptine, la resistine, le TNF- $\alpha$ , l'IL-6 et le PAI-1; ainsi que d'autres adipokines comme l'adiponectine, l'apeline, l'adipsine et le FGF21.

Les deux principaux types de tissu adipeux sont le blanc et le brun. Typiquement, le tissu adipeux blanc représente environ 20% du poids corporel chez l'homme et 28% chez la femme (Thompson et al., 2012) mais chez les personnes obèses, il peut représenter jusqu'à 80% de ce poids. L'obésité est accompagnée d'une hausse généralisée des dépôts de tissu adipeux blanc en raison de l'hyperplasie (augmentation du nombre des adipocytes) et de l'hypertrophie (augmentation de la taille des adipocytes) (Dulloo et al., 2010). Les caractéristiques principales des adipocytes blancs sont le stockage d'excès d'énergie sous forme triglycérides dans de grosses gouttelettes uniloculaires, et la libération de cette énergie sous la forme d'acides gras libres dans des situations de besoin énergétique, comme le jeun, ou en réponse à un stimulus tel que la sécrétion d'adrénaline.

De leur côté, les adipocytes bruns stockent des triglycérides sous forme multiloculaire, de sorte qu'ils puissent être rapidement utilisés comme combustible pour la production de chaleur à travers un processus biochimique,

le "découplage" mitochondrial de la phosphorylation oxydative des acides gras libres (Sethi and Vidal-Puig, 2007). Chez les mammifères, le tissu adipeux brun peut dissiper l'énergie lipidique sous forme de chaleur dans un processus appelé thermogénèse sans frisson (Bartelt and Heeren, 2014). En effet les adipocytes bruns expriment au niveau de leur membrane mitochondriale interne une protéine de 32 kDa appelée UCP1 (protéine de découplage 1) permettant une dissipation du gradient électrochimique de protons généré par la respiration sous forme de chaleur (Cannon, 2004). Le tissu adipeux brun est donc unique en raison de sa fonction dans la thermogénèse comme forme de dépense énergétique, cette énorme capacité thermogénique apportant une contribution substantielle au métabolisme énergétique de l'organisme. Par ailleurs, il peut être distingué du tissu adipeux blanc morphologiquement par une vascularisation plus riche et une plus grande densité mitochondriale.

Récemment, une troisième catégorie d'adipocytes distincts des adipocytes blancs et bruns a été décrite. Ce sont des adipocytes bruns inductibles, qui ont été nommés des « adipocytes beiges/brite » (Giralt and Villarroya, 2013). Les adipocytes beiges sont notamment présents au sein du tissu adipeux blanc. Leur processus d'activation est décrit comme le " brunissement ". Ce phénomène est caractérisé par l'expression d'UCP1 et il entraîne des effets métaboliques bénéfiques. Le froid ainsi que l'activation de la voie  $\beta$ 3-adrénergique ont été reconnues entre autres comme activateurs du brunissage.

Finalement, dès leur développement, les trois types d'adipocytes sont bien distincts avec une expression différentielle de nombreux gènes (Baboota et al., 2015). L'utilisation de différentes lignées cellulaires (3T3-L1, 3T3F442A, C3H10T1/2, préadipocytes bruns, etc.) a permis récemment de mettre à jour le contrôle transcriptionnel au cours de la différenciation adipocytaire ainsi que les fonctions des adipocytes. L'une des caractéristiques qui permettent de mieux distinguer ces trois types d'adipocytes est la quantité de mitochondries.

## **II. Les Mitochondries et l'homéostasie énergétique**

Une fonction mitochondriale normale est nécessaire et requise pour la préservation d'un équilibre approprié entre le stockage et la dépense énergétique. Un excès de nutriments mène à des dysfonctionnements

mitochondriaux, qui sont accompagnés d'effets indirects sur le métabolisme des lipides et du glucose (Bournat et Brown, 2010).

Les mitochondries sont des organelles qui fournissent environ 90% de l'énergie requise pour le bon fonctionnement de la cellule eucaryote (Tao et al., 2014). L'énergie fournie par le glucose et les lipides contenus dans les aliments est transformée en ATP (adénosine-5'-triphosphate), de sorte qu'elle puisse être utilisée par la cellule. Ceci est possible grâce aux deux processus que sont la glycolyse et l'oxydation des acides gras. La glycolyse est un processus anaérobie transformant le glucose en pyruvate avec une faible production d'énergie comparativement à la respiration aérobie. Le processus d'oxydation des acides gras se caractérise quant à lui par une série de réactions diminuant la taille des acides gras. En fonction de la source de substrats, soit la glycolyse soit l'oxydation des acides gras prédomine pour produire de l'ATP.

Le cycle de Krebs, également connu comme cycle de l'acide citrique, est au centre du métabolisme énergétique des cellules et sert de base pour la production d'énergie via l'acétyl-CoA, un intermédiaire commun de la métabolisation du glucose et des acides gras. Deux cofacteurs, le NADH (nicotinamide adénine dinucléotide) et le FAD (flavine adénine dinucléotide), sont produits au sein du cycle de Krebs. Par leur intermédiaire, des électrons sont transportés successivement à travers les complexes de la chaîne de respiration mitochondriale, jusqu'à ce qu'ils soient reçus par l'O<sub>2</sub> pour générer du H<sub>2</sub>O et conduire à la production d'ATP.

La chaîne de respiration mitochondriale réunit cinq complexes enzymatiques présents dans la membrane mitochondriale interne (Lancaster, 2002) et désignés, avec le transporteur de phosphate inorganique et la translocase ATP/ADP, sous le nom de système OXPHOS. Ce système est constitué de protéines codées par les génomes nucléaires et mitochondriaux (van Waveren et Moraes, 2008) aux caractéristiques très différentes. La majorité des protéines impliquées dans la fonction mitochondriale sont codées au niveau nucléaire puis synthétisées dans le cytosol et pour ensuite rejoindre la mitochondrie (Elstner et al., 2009).

### **III. L'épissage de l'ARN pré-messager**

L'ARN pré-messager sera soit mûri suite au phénomène d'épissage en ARN messager pour être traduit en protéine, soit il exercera une fonction d'ARN non-codant. L'épissage est le processus par lequel des portions de l'ARN pré-messager, appelées introns, sont clivées, de sorte que l'ensemble des séquences restantes, nommées exons, soient associées pour former le produit final l'ARN messager qui suivra par la suite des modifications post-transcriptionnelles.

L'épissage joue un rôle essentiel dans le phénotype des cellules eucaryotes supérieures. Certaines fonctions tissulaires sont étroitement associées aux événements d'épissage tissu spécifiques (Wang et Burge, 2008; Taliaferro et al, 2011). Bien que la majorité des exons soient incluse dans l'ARN messager final, certains exons, ou des parties d'exons, peuvent être, dans certaines cellules ou dans des conditions spécifiques, éliminés à partir des ARN messager. Un même transcrit d'ARN peut être remanié de différentes façons et aboutir à des messagers, donc des protéines, très différentes. Ce processus est appelé épissage alternatif, et joue un rôle central dans la génération de protéomes complexes à partir de génomes définis. L'épissage alternatif s'applique à la grande majorité de nos gènes (>90%) et génère une considérable diversité protéique qui est modulée qualitativement en fonction du type de tissu ou au cours du développement d'un organisme (Modrek and Lee 2002).

Un épissage efficace nécessite, trois éléments dont les séquences sont plus ou moins conservées, permettent la définition des introns avant leur excision. Ces éléments sont le site donneur ou site d'épissage 5', le site accepteur ou site d'épissage 3', et le point de branchement, précédé par un tract polypyrimidine (Wahl et al., 2009). Outre ces trois éléments, d'autres séquences influencent l'épissage. En fonction de leur emplacement et leur activité, ces séquences sont soit des activateurs d'épissage exoniques (ESE) ou introniques (ISE), soit des inhibiteurs d'épissage exoniques (ESS) ou introniques (ISS). Certaines protéines reconnaissent les sites activateurs pour promouvoir l'épissage (protéines SR), et d'autres, au contraire, reconnaissent les sites inhibiteurs pour l'empêcher (hnRNP).

Le processus d'épissage comprend deux étapes impliquant des réactions de trans-estérification. La première est une attaque nucléophile du 2'-OH du ribose de l'adénosine du point de branchement sur le phosphate du site 5' d'épissage. La seconde est une attaque du phosphate au niveau du site 3' d'épissage par le 3'OH libéré précédemment en 5'. Ainsi les exons sont liés entre eux et l'intron est éliminé sous forme de lasso. Ces réactions sont réalisées grâce à un complexe multi-protéiniques appelé le spliceosome (Matera et Wang, 2014). Cette machinerie reconnaît des séquences consensus spécifiques qui aident à définir les sites d'épissage.

Le spliceosome est une structure très dynamique qui subit des réarrangements constants au cours du processus d'épissage. Son assemblage sur le transcrit cible requiert la liaison et la libération de différentes petites ribonucléoprotéines nucléaires, ainsi que d'autres facteurs d'épissage.

Des mutations dans les séquences normales d'épissage ont été décrites comme ayant un lien étroit avec des maladies. En effet, dans de nombreuses pathologies comme les maladies génétiques ou le cancer, le processus d'épissage est altéré (Orengo et Cooper, 2007; Tazi et al, 2009). C'est le cas du syndrome progérique (HGPS: Hutchinson-Gilford progeria syndrome) caractérisé par un vieillissement accéléré de l'organisme. À l'origine de ce syndrome une mutation synonyme (C>T) au niveau de l'exon 11 du gène *LMNA* codant pour les lamines A/C, induit l'utilisation exacerbée d'un site d'épissage cryptique et la production massive d'une protéine tronquée; appelée progérine. Cet épissage est régulé de façon opposée par deux protéines SR : SRSF1 (favorisant l'utilisation du site cryptique) et SRSF6 (promouvant l'utilisation du site authentique) (Lopez-Mejia et al., 2011). Cet exemple d'anomalie d'épissage a constitué le cœur du travail de criblage *in vitro* effectué chez ABIVAX afin de trouver de petites molécules ciblant la modulation pharmacologique de cet épissage alternatif. Ainsi, un composé, l'ABX300, a été sélectionné suite à ce crible et mon travail de thèse a porté sur l'étude de son mode d'action et l'identification de nouveaux analogues.

## Résultats

### I. Recherche du mode d'action d'ABX300

Il a été démontré au sein du laboratoire du Pr Tazi que les isoformes du gène *LMNA* issu d'un épissage alternatif jouent des rôles opposés sur le métabolisme lipidique et énergétique (Lopez-Mejia *et al.*, 2014). Ces travaux suggèrent que la modulation pharmacologique de cet épissage pourrait représenter une approche nouvelle et originale dans le traitement de l'obésité. Cette hypothèse a été testée dans les travaux ici présentés en utilisant 2 systèmes de criblage complémentaires, et ceci afin d'identifier un potentiel modulateur de l'épissage présentant un impact sur le métabolisme énergétique. Un premier crible basé sur la localisation de SRSF1, qui a été suivie par microscopie; et un second sur la base de l'événement d'épissage qui se produit entre les exons 11 et 12 du gène *LMNA* dans le cadre de HGPS (C>T → activation de progérine 5'SS). Un système rapporteur de l'épissage du gène *LMNA* basé sur l'activité de la luciférase nous a permis de rendre compte de l'utilisation des sites 5' authentique et cryptique d'épissage. Un composé appelé ABX300 a ainsi été sélectionné. Les données générées montrent aussi qu'ABX300 interagit directement avec SRSF1 avec pour conséquence un effet potentiel sur l'épissage de *LMNA*.

ABX300 a été testé par la suite sur deux modèles murins d'obésité, un modèle de souris génétiquement modifiées (*ob/ob* et *db/db*) et un modèle nutritionnel. L'administration journalière de la molécule a conduit à une perte de poids chez ces animaux.

Comme évoqué précédemment, mon travail de thèse a consisté à déterminer le mécanisme d'action de la molécule ABX300, ainsi que son impact sur le métabolisme. Les résultats ont montré qu'ABX300 n'a pas d'effet ni sur la différenciation adipocytaire, ni sur le contenu en triglycérides au sein de lignées cellulaires (cellules 3T3-L1 et préadipocytes de tissu adipeux brun). Cependant, des analyses *in vivo* de « pair-feeding », des analyses PET-scan, et des études en cages métaboliques, ont montré une différence entre les groupes traités et non-traités au niveau de leur prise alimentaire, la consommation d'oxygène et la

source énergétique utilisée. Parallèlement une série d'approches transcriptomiques ont permis de mettre en évidence une importante modulation par ABX300 de microRNA dont les cibles sont mitochondriales, et ceci en absence d'une restructuration globale du profil d'épissage.

Ces travaux montrent que l'identification de modulateurs de l'épissage alternatif du gène *LMNA* est une stratégie innovante et prometteuse pour la découverte de molécules bioactives dans le traitement de l'obésité.

## **II. Identification d'autres molécules ciblant l'épissage du gène *LMNA* basées sur l'analogie à la molécule ABX300**

En raison de plusieurs inconvénients empêchant le développement clinique de l'ABX300, l'identification de nouvelles molécules « back-up » (principalement des analogues d'ABX300, mais non exclusivement), ciblant l'épissage de *LMNA*, et ayant donc théoriquement un impact sur l'évolution du poids, a constitué le second objectif de mon travail de thèse. Idéalement, ces molécules seraient dépourvues d'effets secondaires indésirables mais conserveraient l'activité et l'efficacité d'ABX300 sur le poids. Pour cela, des modifications chimiques ont été apportées au squelette principal de la molécule ABX300.

De nombreuses molécules (887 plus exactement) de la chimiothèque d'ABIVAX ont ainsi été criblées puis en partie (21 molécules) testées *in vivo* dans des modèles de souris DIO mais malheureusement, aucune n'a montré un effet sur l'obésité.

## Discussion

Les récentes preuves indiquant que le gène *LMNA* joue activement un rôle dans le métabolisme (Tang et al., 2011; Liu et al., 2012) ont été complétées avec la découverte au sein de notre laboratoire des fonctions antagonistes que les différentes isoformes issues de ce gène exercent sur la dépense énergétique et la durée de vie (Lopez-Mejia et al., 2014). Nos études renforcent donc la proposition du gène *LMNA* comme cible pharmacologique potentielle dans le traitement de l'obésité.

Mon travail de thèse a abordé la compréhension du mécanisme d'action d'ABX300, une molécule modulatrice de l'épissage du gène *LMNA* avec un net effet sur l'obésité.

Concernant le système rapporteur de criblage *in vitro*, il serait pertinent de tester l'effet d'ABX300 sur le mini-gène WT/non muté correspondant. En faisant ceci, nous pourrions nous affranchir de tout effet potentiel de la drogue sur la transcription et pourrions vraiment utiliser cette construction avec une meilleure fiabilité.

Par ailleurs, comme il a été établi une interaction entre SRSF1 et ABX300, on ne peut pas exclure que d'autres membres de la famille n'interagissent aussi avec la molécule. Il serait certainement très intéressant de poursuivre le même type d'analyse avec d'autres protéines SR, notamment SRSF6 et SRSF5, deux protéines qui ont été rapportées comme ayant un rôle opposé à celui de SRSF1 sur cet épissage en particulier (Fong et al, 2009;. Lopez-Mejia et al., 2011).

De plus, dans des études futures, il serait également intéressant d'analyser comment ABX300 pourrait affecter les interactions des protéines SR avec les ARNm, par co-IP ou CLIP-Seq.

De plus, lorsque l'ensemble des épissages spécifiques du tissu adipeux a été évalué, nous n'avons pas pu déterminer un effet global d'ABX300 sur l'épissage. Néanmoins la réalisation d'analyses complémentaires du séquençage de l'ARN à haut débit (HTS) pourrait permettre d'avoir une vision globale du génome, et d'obtenir des informations concernant la biogénèse des microRNA.



Ce sont les microRNA ciblant spécifiquement des gènes qui participent à des processus mitochondriaux qui sont modulés par ABX300. Ce résultat suggère fortement que la molécule a un effet sur le fonctionnement de cette organelle. Bien que nous ayons échoué à identifier une hausse hypothétique de l'activité mitochondriale, nous pensons que le traitement avec ABX300 est inexorablement lié à un fonctionnement accru de cet organite. Néanmoins des analyses beaucoup plus complètes devraient être réalisées pour confirmer cette hypothèse. De plus, l'évaluation de l'activité locomotrice des animaux ainsi que la possibilité d'une mise en place d'un processus de browning, se présentent comme indispensables pour la bonne finalisation de l'étude du mode d'action de la molécule ABX300.

Enfin, la possibilité que ce soit le métabolite et non la molécule ABX300 elle-même qui soit responsable des effets observés phénotypiquement devrait être étudiée.

## INDEX

INDEX .....	
LIST OF ABBREVIATIONS.....	
PREFACE.....	1
ABSTRACT .....	3
INTRODUCTION .....	5
CHAPTER I: Adipose Tissue and Obesity .....	5
Adipose Tissue: a complex and heterogeneous organ.....	5
I.1 – Composition of Adipose Tissue .....	6
I.2 – Types of Adipose Tissue .....	7
<b>Browning/Whitening</b> .....	8
I.3 – Origin and Development of Adipose Tissue.....	10
<b>Cellular models</b> .....	14
I.4 – Functions of Adipose Tissue.....	15
<b>I.4a – Fat Deposition and Fat Mobilization</b> .....	16
<b>I.4a<sub>1</sub> – Triglycerides Synthesis in WAT: Lipogenesis</b> .....	17
I.4a <sub>1.1</sub> – Lipogenesis from diet.....	18
I.4a <sub>1.2</sub> – De novo lipogenesis .....	19
<b>I.4a<sub>2</sub> – Fatty Acids degradation: Lipolysis</b> .....	20
I.4a <sub>2.1</sub> – Insulin (anti-lipolytic effect).....	21
I.4a <sub>2.2</sub> – Adrenergic regulation (pro-lipolytic effect).....	22
<b>I.4a<sub>3</sub> –Regulation of appetite and satiety</b> .....	23
I.4a <sub>3.1</sub> – Secreted hormones.....	24
I.4a <sub>3.2</sub> – Neural circuits .....	24
I.4a <sub>3.3</sub> –Rewarding effects of food .....	25
<b>I.4b – Endocrine function</b> .....	25
<b>Oxidative stress &amp; Reactive Oxygen Species</b> .....	29
I.5 – WAT associated pathologies: obesity .....	30
<b>I.5a –Rodent models</b> .....	31
<b>I.5b –Treatment/Clinical Approaches</b> .....	34
<b>I.5c –Current Situation</b> .....	36

CHAPTER II: Mitochondria and Energy Homeostasis .....	37
Generalities .....	37
II.1 – Structure .....	38
II.2 – ATP Production.....	40
II.2a – Fatty Acids Oxidation ( $\beta$ -oxidation) .....	41
II.2b – The tricarboxylic acid (TCA) cycle (Krebs cycle) .....	43
II.2c – The electron transport chain (ETC) and ATP synthesis .....	45
<b>II.2c<sub>1</sub> –The complexes from the mitochondrial ETC .....</b>	<b>46</b>
<b>II.2c<sub>1.1</sub> – Complex I <math>\rightarrow</math> NADH-coenzyme Q oxidoreductase .....</b>	<b>46</b>
<b>II.2c<sub>1.2</sub> – Complex II <math>\rightarrow</math> Succinate-Q oxidoreductase .....</b>	<b>47</b>
<b>II.2c<sub>1.3</sub> – Complex III <math>\rightarrow</math> Cytochrome c oxidoreductase .....</b>	<b>47</b>
<b>II.2c<sub>1.4</sub> – Complex IV <math>\rightarrow</math> Cytochrome c oxidase.....</b>	<b>47</b>
<b>II.2c<sub>1.5</sub> – Complex V <math>\rightarrow</math> ATP synthase .....</b>	<b>47</b>
<b>II.2c<sub>2</sub> – The Decoupling proteins <math>\rightarrow</math>UCPs .....</b>	<b>48</b>
II.2d – The OXPHOS system regulation .....	49
II.3 – Mitochondrial DNA .....	50
II.3a – Origin and evolution.....	50
II.3b – Structure and organization.....	50
II.3c – Transcription regulation .....	52
<b>Nuclear control of mitochondrial functioning.....</b>	<b>53</b>
<b>II.3c<sub>1</sub> – Mitochondrial transcription factors coded by nDNA .....</b>	<b>53</b>
<b>II.3c<sub>2</sub> – Transcriptional regulators of nuclear genes coding mitochondrial proteins .....</b>	<b>54</b>
<b>NRF1 .....</b>	<b>54</b>
<b>NRF2 .....</b>	<b>54</b>
<b>PGC1<math>\alpha</math> .....</b>	<b>54</b>
<b>PGC1<math>\beta</math> .....</b>	<b>55</b>
II.4 – Mitochondrial dysfunction & disease.....	55
<b>Mitochondria in Obesity .....</b>	<b>56</b>
II.5 – Mitochondrial databases.....	57
<b>MitoCarta .....</b>	<b>58</b>

CHAPTER III: Pre-mRNA Splicing .....	59
Introduction to pre-mRNA Splicing .....	59
III.1 – Constitutive Splicing .....	59
III.2 – Alternative Splicing .....	60
<b>III.2a – Alternative splicing determinants</b> .....	62
<b>III.2b – Regulation of alternative splicing</b> .....	63
III.3 –The spliceosome .....	65
<b>Step wise spliceosome assembly</b> .....	65
III.4 – Alternative Splicing and Disease: The case of the LMNA gene and HGPS .....	67
<b>III.4a – Lamins</b> .....	67
<b>LMNA isoforms</b> .....	68
<b>III.4b – HGPS/Progeria</b> .....	69
<b>III.4c – Lamins and Metabolism</b> .....	71
III.5 – Other RNAs: microRNAs .....	72
<b>III.5a – MicroRNAs and Alternative Splicing</b> .....	74
<b>III.5b – MicroRNAs and Adipose Tissue</b> .....	75

RESULTS .....	77
Project 1: Investigation of the Mode of Action (MoA) of ABX300 .....	78
1. Aim of the project.....	78
2. Summary .....	79
3. Additional explored avenues.....	81
i) Effect of ABX300 on adipocytes differentiation .....	81
ii) Effect of ABX300 on adipocytes lipolysis/lipogenesis .....	87
iii) Effect of ABX300 on Browning.....	89
iv) Effect of ABX300 on mitochondria and oxygen consumption .....	92
v) Effect of ABX300 on LMNA .....	99
vi) Further phenotypic characterization of ABX300 treated mice.....	102
4. Clinical development of ABX300.....	106
i) Adverse effects of ABX300 on hERG .....	106
ii) Adverse effects of ABX300 on kidneys.....	108
iii) ABX300 skin biopsies in vitro (absorption experiments).....	109
Project 2: Identification of molecules targeting <i>LMNA</i> splicing to avoid use of the progerin 5' SS .....	110
1. Aim of the project.....	110
2. Modulation of the luciferase activity of the mini gene reporter by the ABIVAX Chemical Library .....	111
i) Regulation of body weight through splicing modulation .....	113
GENERAL DISCUSSION .....	116
APPENDIX .....	116
REFERENCES .....	126

# **“A Novel strategy for the treatment of Obesity using the small molecule ABX300, a modulator of the *LMNA* gene splicing”**

## **List of Tables**

Table 1: Differentially expressed genes in brown, beige and white adipocytes.....	9
Table 2: Summary of mentioned animal models of Obesity and metabolic features of human and mouse Lipodystrophy.....	32
Table 3: Summary of Adipose-related Splicing Regulators and Events.....	63
Table 4: Activity and cardiotoxicity of all the <i>in vivo</i> tested ABIVAX compounds. ....	107

## **List of Figures**

Figure 1: Components of the adipose organ.....	7
Figure 2: Brown, white and beige adipocytes; anatomical sites in mice and humans. ....	8
Figure 3: Developmental lineages of adipocytes. ....	11
Figure 4: Induction of adipogenesis by a cascade of transcription factors.....	12
Figure 5: Progression of differentiation on 3T3-L1 cells. ....	13
Figure 6: Energy balance. ....	17
Figure 7: Formation of Lipid Droplets. ....	19
Figure 8: Lipolysis and Lipid Signaling. ....	21
Figure 9: Effect of feeding and fasting on hunger.....	23
Figure 10: Factors released or secreted by adipose tissue. ....	26
Figure 11: Major adipokines, their roles and variations with weight modulation.....	29
Figure 12: Fat Distribution Influences Risks Associated with Obesity in Humans. ....	31
Figure 13: Lipid overflow in obesity and lipodystrophy.....	33
Figure 14: Approaches to increasing thermogenesis as an anti-obesity therapy.....	35
Figure 15: Interconnection of metabolic pathways. ....	37
Figure 16: Structure of mitochondria.....	39
Figure 17: Glycolysis and FAO. ....	40
Figure 18: Representation of the $\beta$ -oxidation of palmitic acid in the mitochondria. ....	42
Figure 19: Representation of mitochondrial FAO and OXPHOS in liver mitochondria. ....	43
Figure 20: Bioenergetics of the TCA/Krebs cycle. ....	44
Figure 21: The OXPHOS system.....	46
Figure 22: Mitochondrial genome and intercommunication between the nucleus and mitochondria.....	51

Figure 23: Mitochondrial transcriptional control over storage and thermogenesis gene programs. ....	56
Figure 24: Splicing reactive sites. ....	59
Figure 25: Chemistry in the splicing reaction. ....	60
Figure 26: Alternative Splicing Events (ASEs) in Metazoan Transcripts. ....	61
Figure 27: Overview of AS determinants. ....	62
Table 3: Summary of Adipose-related Splicing Regulators and Events. ....	63
Figure 28: Schematic representation of the 12 human SR proteins. ....	64
Figure 29: Dynamics of spliceosome assembly. ....	66
Figure 30: <i>LMNA</i> major lamin isoforms. ....	68
Figure 31: <i>LMNA</i> SS regulation by SRSF6 and SRSF1. ....	70
Figure 32: Schematic view of miRNA biogenesis and mechanism of action. ....	73
Figure 33: Regulatory Model of SS-Overlapping miRNA Biogenesis via AS. ....	74
Figure 34: Obesity / insulin resistance-related miRNA expression changes in humans and in murine models. ....	76
Figure 35: Absence of ABX300 effect on 3T3-L1 differentiation. ....	82
Figure 36: Absence of ABX300 effect on relative expression of key genes during 3T3-L1 differentiation. ....	84
Figure 37: Absence of ABX300 effect on protein expression of key genes involved in adipogenesis and phosphorylation of SR proteins during 3T3-L1 differentiation. ....	85
Figure 38: Absence of ABX300 effect on differentiated BAT preadipocytes. ....	86
Figure 39: Absence of ABX300 effect on lipolytic/lipogenic mechanisms in 3T3-L1 cells. ....	88
Figure 40: Absence of ABX300 effect inducing lipolysis on <i>ex-vivo</i> WAT explants. ....	89
Figure 41: Absence of a clear effect of ABX300 on browning. ....	91
Figure 42: ABX300 does not modulate the relative mRNA expression of key genes involved in mitochondrial biogenesis in WAT and BAT. ....	93
Figure 43: ABX300 influence on the mitochondrial amount and on the relative expression levels of genes implicated in mitochondrial ETC and Beta Oxidation. ....	95
Figure 44: Protein levels of mitochondrial total oxidative phosphorylation (OXPHOS) in WAT and BAT of ABX300 treated and untreated mice. ....	96
Figure 45: ABX300 does not change profiling of Seahorse XF Stress Test. ....	98
Figure 46: Tissue specific expression of lamins depending on diet condition and ABX300 treatment. ....	100
Figure 47: LCS mice response to ABX300 diverges according to their genetic background. ....	101
Figure 48: Different treatment schemes of ABX300 do not affect its effect on weight loss after one month treatment. ....	102

Figure 49: Noteworthy macroscopic effects induced by ABX300 on WAT. ....	103
Figure 50: Long term effect and efficacy of ABX300 to enhance weight loss in obese but not lean mice .....	104
Figure 51: ABX300 does not induce robust changes in glucose metabolism.....	105
Figure 52: Kidney sections of kidneys from ABX300 DIO treated mice.....	108
Figure 53: <i>In vitro</i> ABX300 dermal absorption experiment on skin biopsies.....	109
Figure 54: Histogram recapitulating all the drugs from the ABIVAX Chemical Library tested with the LMNA-luc mini gene reporter. ....	112
Figure 55: Modified moieties during the SAR studies.....	113
Figure 56: Absence of <i>in vivo</i> efficiency on weight loss of ABX .....	115



## LIST OF ABBREVIATIONS

### A

**AC:** Adenylate Cyclase

**ACC:** Acetyl-CoA Carboxylase

**AgRP:** Agouti-Related Peptide

**AKT/PKB:** Protein Kinase B

**AMPK:** 5' AMP-activated protein kinase

**AR:** Adrenergic Receptor

**AS:** Alternative Splicing

**AT:** Adipose Tissue

**ATGL:** Adipose Triglyceride Lipase

**ATP:** Adenosine Tri Phosphate

### B

**BAT:** Brown Adipose Tissue

**BMP:** Bone Morphogenetic Protein

**BMR:** Basal Metabolic Rate

**BP:** Branch Point

### C

**C/EBP:** CCAAT box enhancer binding protein

**cAMP:** Cyclic Adenosine Monophosphate

**CD:** Chow Diet

**Cidea:** Cell death activator CIDE-A

**CNS:** Central Nervous System

**COX:** Cyclooxygenase

**CPT:** Carnitine Palmitoyl Transferase

**CS:** Citrate Synthase

### D

**DEX:** Dexamethasone

**DIO:** Diet Induced Obesity

### E

**EE:** Energy Expenditure

**ER:** Endoplasmic Reticulum

**ESE:** Exonic Splicing Enhancer

**ESS:** Exonic Splicing Silencer

**ETC:** Electron Transport Chain

### F

**FA:** Fatty Acid

**FABP4:** Fatty Acid Binding Protein 4

**FADH<sub>2</sub>:** Flavin Adenine Dinucleotide

**FAO:** Fatty Acid Oxidation

**FAS:** Fatty Acid Synthase

**FBS:** Fetal Bovine Serum

**FFA:** Free Fatty Acids

**FGF:** Fibroblast Growth Factor

**FTIs:** Farnesyl Transferase Inhibitors

### G

**G3P:** Glycerol-3-phosphate

**GPCR:** G protein-Coupled Receptor

**GSK-3 $\beta$ :** Glycogen Synthase Kinase 3 beta

## H

**HFD:** High Fat Diet

**HGPS:** Hutchinson–Gilford Progeria Syndrome

**hMADS:** human Multipotent Adipose-Derived Stem cells

**HSL:** Hormone Sensitive Lipase

## I

**IL:** Interleukin

**IR:** Insulin Receptor

**ISE:** Intronic Splicing Enhancer

**ISS:** Intronic Splicing Silencer

## K

**KO:** Knock Out

## L

**LCFA:** Long Chain Fatty Acids

**LPL:** Lipoprotein Lipase

## M

**MCP-1:** Monocyte Chemoattractant Protein-1

**MEF:** Mouse Embryonic Fibroblast

**MEM:** Mitochondrial External Membrane

**MGL:** Monoglyceride Lipase

**MIM:** Mitochondrial Internal Membrane

**Mfn:** Mitofusis

**MIX:** Methylisobutylxanthine

**MSC:** Mesodermal/mesenchymal Stem Cells

**mtDNA:** Mitochondrial DNA

**mTERF:** Mitochondrial Transcription Termination Factor

**mTOR:** Mammalian Target Of Rapamycin

**Myf-5:** Myogenic factor-5

## N

**NA:** Noradrenaline

**NADH:** Nicotinamide adenine dinucleotide

**nDNA:** Nuclear DNA

**NEFA:** Non Esterified Fatty Acid

**NLS:** Nuclear Localization Signal

**NPY:** Neuropeptide Y

**NRF:** Nuclear Respiratory Factor

## O

**OCR:** Oxygen Consumption Rate

**ORO:** Oil Red Oil

**OXPHOS:** Oxidative Phosphorylation

## P

**PAI1:** Plasminogen activator inhibitor 1

**PDE:** Phosphodiesterase

**PET:** Positron Emission Tomography

**PGC1 $\alpha$ :** PPAR $\gamma$  coactivator 1 $\alpha$

**PI(3)K:** Phosphatidylinositol 3-kinase

**PIP:** Phosphoinositide-phosphate

**PKA/B/C:** Protein kinase A/B/C

**POLRMT:** Mitochondrial DNA-directed RNA polymerase

**PPAR:** Peroxisome proliferator-activator receptor

**PRDM16:** PR domain containing 16

**PTEN:** Phosphatase and tensin homolog

## R

**RC:** Respiratory Chain

**RER:** respiratory Exchange Ratio

**ROS:** Reactive Oxygen Species

**rRNA:** Ribosomal RNA

**RXR:** Retinoid X receptors

## S

**snRNP:** Small Nuclear Ribonucleic Protein

**SOD:** Superoxide Dismutase

**SP1:** Stimulatory Protein

**SR:** Serine-Arginine

## T

**T2D:** Type 2 Diabetes

**TAG:** Triacylglycerol

**Tbx1:** T-box transcription factor-1

**TCA:** Tricarboxylic Acid

**TF:** Transcription factor

**TFAM:** Mitochondrial transcription factor A

**TFB1M** et **TFB2M:** Mitochondrial Transcription Factor B1 et B2

**TGs:** Triglycerides

**TIM:** Translocase of the Inner Membrane

**TNF- $\alpha$ :** Tumor Necrosis Factor  $\alpha$

**TOM:** Translocase of the Outer Membrane

## **U**

**U:** Uracil

**UCP-1:** Uncoupling Protein-1

## **V**

**VDAC:** Voltage-Dependent Anion Channels

**VLDL:** Very Low Density Lipoprotein

## **W**

**WAT:** White Adipose Tissue

**WHO:** World Health Organization

**WNT:** Wingless-related integration site

## PREFACE

Metabolism, from the Greek Μεταβολισμός, *metabolē* change, from *metaballein* to change, from *meta-* + *ballein* to throw.

1. The sum total of the chemical processes that occur in living organisms, resulting in growth, production of energy, elimination of waste material, etc.
2. The sum total of the chemical processes affecting a particular substance in the body ⇒ carbohydrate metabolism, iodine metabolism.

From the Collins dictionary

The first documented references of metabolism date from the XIII<sup>th</sup> century:

“Both the body and its parts are in a continuous state of dissolution and nourishment, so they are inevitably undergoing permanent change.”

Ibn al-Nafis (1260)

However, it was not until four centuries later, that it took place the first experiment considered to be the one studying human metabolism. It was performed by Santorio Santorio and published in 1614 in his work entitled “*Ars de statica medicina*”. This book summarized his observations for a period of over 30 years in which he weighed himself recurrently; before and after sleeping, working, drinking, fasting, eating and excreting. He designed a movable platform attached to a steelyard scale that allowed for the quantification of changes in body weight of subjects who partook in their daily activities on the platform. After years of self-experimentation, he applied his device to the study of patients.

When analyzing his results, thus comparing the weights, he found out that most of the ingested food was lost through what he called *Perspiratio insensibilis* or *insensible perspiration of the body*. This concept designates how many grams the body loses during a certain period of time.

For his pioneering and detailed balance studies, he clearly deserves the title of founding father of metabolic studies. The importance and significance of weight measurement in medicine was revealed for the first time in this work, which makes Santorio still celebrated as the predecessor of experimental physiology.

- 1) Of the emotions anger and joy make the bodies lighter, fear and depression make them heavier; the effect of the other emotions is the effect of their constituents of the former.
- 2) In sorrow and fear the light substance is excreted through perspiration and the heavy substance remains; in joy and anger both substances are excreted.
- 7) In depression and fear the various parts of the body become filled with fluid and hard.
- 35) A body which is at rest whilst the mind is violently agitated has a stronger perspiration and less weight than a body that is strongly moved whilst the mind is at rest.
- 39) A too great emotion is more harmful than too great bodily movement.
- 47) Those who now are gay, now depressed, now angry, now afraid, have a more healthy perspiration than those who still enjoy a single emotion, even if it is a good one.

EMOTION AND PERSPIRATIO INSENSIBILIS (Weights and Confri)  
Referring to "*Ars de Statica Medicina*" from Santorio Santorio

## ABSTRACT

The discovery within our laboratory that the different LMNA isoforms play opposite roles on metabolism (Lopez-Mejia et al., 2014), led to the proposal that pharmacologically modulating this splicing could be a novel and original approach for the treatment of obesity. In this thesis I have challenged this proposal by performing experiments in order to identify potential modulators of splicing with impact on energy metabolism. Following an initial screen, a compound termed ABX300 was selected and tested on animal models of obesity. Specific modulation of the LMNA splicing by ABX300 was confirmed using splicing reporters. Moreover, our data show that ABX300 interacts directly with SRSF1 to mediate its effect on LMNA splicing.

The daily treatment with ABX300 lead to a weight loss in both, genetically modified mouse models and diet induced obesity mouse models. During my PhD I have established the mode of action of ABX300, along with its impacts on metabolism. Results demonstrated that ABX300 did not have an effect on adipocytes differentiation, nor in triglycerides content on *in vitro* cell lines (3T3-L1 and BAT preadipocytes). However, *in vivo* analysis, by means of pair-feeding experiments, Microcomputed tomography analysis, and metabolic chambers, among others, exhibited differences in between treated and untreated groups regarding food intake, oxygen consumption and fuel source. Concurrently, a series of transcriptomic approaches showed that ABX300 modulates the expression of miR whose targets encode proteins involved in mitochondrial functioning, but did not have an effect on global pre- mRNA splicing.

This work validates the screening for modulators of the LMNA alternative splicing as a promising strategy for the identification of bio-active small molecules and therefore promotes a complementary approach in the treatment of obesity.

# INTRODUCTION





## INTRODUCTION

### CHAPTER I: Adipose Tissue and Obesity

#### **Adipose Tissue: a complex and heterogeneous organ**

Considering fat as probably the most popular conversation topic nowadays, excepting weather and politics, it is surprising that the physiology of adipose tissue (AT), has been scarcely studied until forty years ago. Excess fat used to be associated with wealth, but this is no longer the case. Instead, obesity is now recognized as a risk factor for many diseases, such as insulin resistance, hypertension, hyperlipidemia, type 2 diabetes (T2D), and coronary heart disease. Indeed, the perception of AT has changed considerably with the dramatic increase in the incidence of obesity and obesity-related comorbidities over the past decades. These comorbidities are mostly related with the deposition of fat in the abdominal cavity. Even though fat distribution varies considerably inter- and intra-species, abdominal and subcutaneous represent the two main depots of white adipose tissue (WAT) generally described for mammals. Besides anatomical differences in between them, divergences have been also depicted at the cellular, molecular, physiological, and clinical level. Hundreds of genes have been shown to have a depot-dependent expression in both humans (Vidal, 2001; Vohl et al., 2004) and rodents (Gesta et al., 2006). Remarkably, metabolic complications are associated with this distribution. The relationships to health are different according to the emplacement of the WAT discrete depots susceptibility. In general, accumulation of WAT in the upper part of the body (abdominal obesity) is associated with detrimental effects on metabolic health and mortality (Ibrahim, 2010), whereas lower-body fat accumulation (gluteofemoral obesity) is associated with protective effects (Karpe and Pinnick, 2015).

Typically, AT makes up approximately 20% of body weight in men and 28% in women (Thompson et al., 2012), but in obese people it can expand manifold to more than 80% of body weight. Obesity is accompanied by a widespread increase in WAT deposits due to hyperplasia (increase in the adipocytes number) and hypertrophy (increase in the adipocytes size) of white adipocytes (Dulloo et al., 2010). Despite the slowly occurring turnover in humans, the total number of

adipocytes appears to be relatively constant throughout adult life under normal healthy conditions (Spalding et al., 2008). Adipocytes typically constitute 80 to 90% of AT volume, yet only 60 to 70% of cell number (Langin D, Frühbeck G, Frayn KN, 2009). The image of fat which was limited to a triglyceride (TG)-storage tissue is progressively disappearing since recent years studies describe AT as no longer simply a fat store, but a vital, complex endocrine organ. It is avidly being acknowledged as such, due to the discovery of its role as a producer of certain cytokines with endocrine, paracrine, and autocrine actions (Sikaris, 2004). AT major functions', encompassing its secretory role, will be described further in this manuscript (**I.3**).

### ***I.1 – Composition of Adipose Tissue***

Adipose tissue has thus been rebaptised as an adipose organ. It is composed in mammals of different kinds of adipocytes which are crucial for energy storage/mobilization and endocrine activity (**Figure 1**). Mature white adipocytes consist of a single large lipid droplet which “pushes” the cell nucleus against the plasmatic membrane. These droplets are the major components of WAT. The other cell types therein present constitute together the AT stromal vascular fraction (SVF). These are: precursor cells (including pre-adipocytes), fibroblasts, immune cells and vascular cells. These particular last-ones include both vascular smooth muscle cells and endothelial cells, which are associated with the major blood vessels. The blood vessels in AT are required for the proper flow of nutrients and O<sub>2</sub> to adipocytes, and they are the conduits that allow for the distribution of adipokines (described in **I.4b**). Vascular cells also secrete, and are responsive to AT-secreted proteins. On the other hand, immune cells (including macrophages and T-cells), have major roles in determining the status of the tissue. Particularly in obese people, there may be an increase in macrophages and other leukocytes. This occurs because immune cells are attracted into the AT by the altered secretory profile, coming from hypertrophic and hyperactive adipocytes that limit O<sub>2</sub> supply, rendering the tissue hypoxic and ultimately leading to AT dysfunction (Xu et al., 2003). To sum up, it can be concluded that the factors that are secreted by these different cellular components of AT, present themselves as being crucial for the maintenance of homeostasis throughout the whole organism.

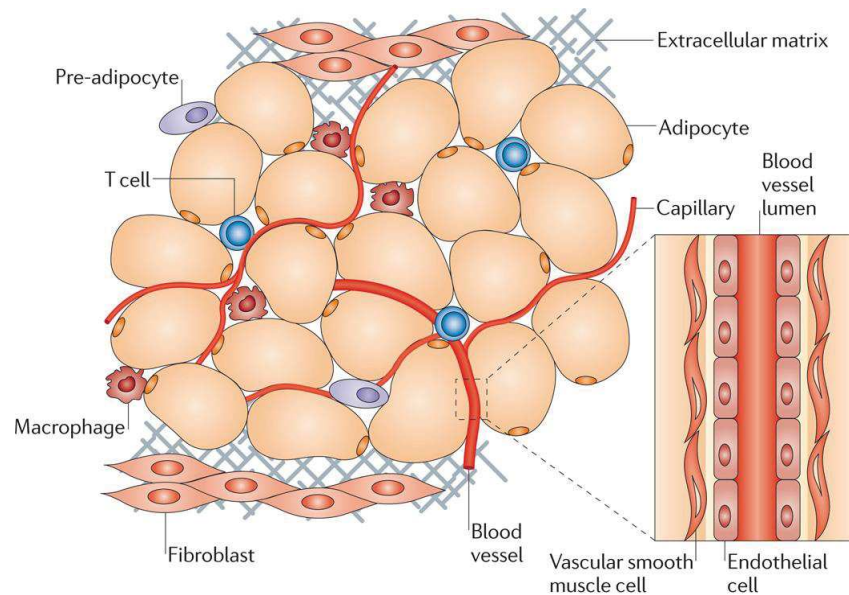


**Figure 1: Components of the adipose organ.**

Image from Ouchi et al., 2011.

## ***1.2 – Types of Adipose Tissue***

The two most popular features of white adipocytes are to store energy excess as TG, in the so-described large unilocular droplets, and to release this energy in the form of Free Fatty Acids (FFA). In contrast, brown adipocytes store TG in multilocular adipocytes as quick-access fuel for heat production through mitochondrial “uncoupling” of oxidative phosphorylation of FFA (Sethi and Vidal-Puig, 2007). BAT (Brown Adipose Tissue) in rodents is mainly concentrated in the interscapular region. However, physiologically relevant brown adipocytes can also be found in other areas, including typical WAT depots, the hind limbs and the intermuscular AT (Cinti, 2005; Almind et al., 2007; Xue et al., 2007) (**Figure 2A**). Morphologically, BAT can be distinguished from WAT by a richer vascularization, and a more abundant mitochondrial density. BAT is unique due to its function in thermogenic energy expenditure (EE). It possesses an enormous thermogenic capacity, making a substantial contribution to the whole-body energy metabolism.

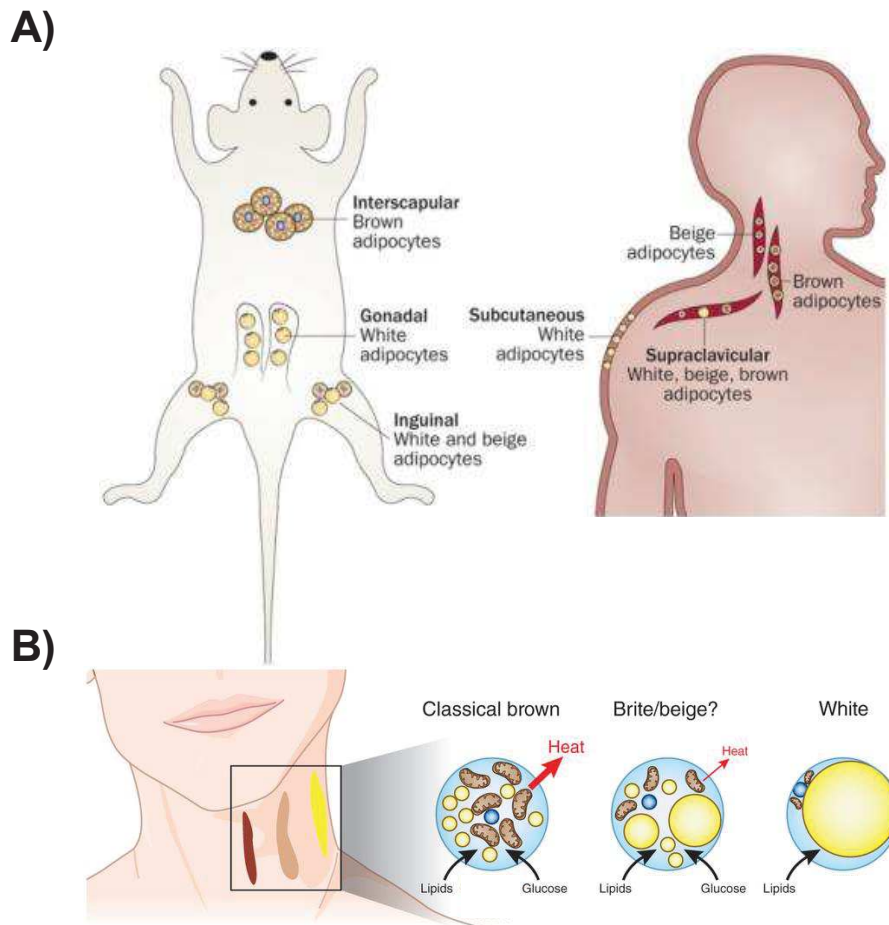


**Figure 2: Brown, white and beige adipocytes; anatomical sites in mice and humans.**

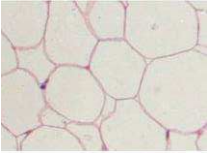
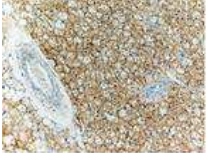
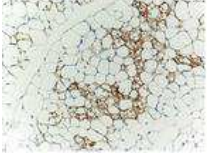
- A)** Interscapular, gonadal and inguinal adipocytes deposits are presented for mice. The neck and the supraclavicular stretch containing mixed populations are exhibited for humans. Adapted from Bartelt and Heeren, 2014.
- B)** Different types of AT are present within the relatively restricted region of the human neck. Adapted from Nedergaard and Cannon, 2013.

### Browning/Whitening

Recently, a third kind of adipocytes has been described, the so called beige, brown-in-white, or brite adipocytes (Giralt and Villarroya, 2013). These are inducible brown adipocytes, which are distinct from both white and brown adipocytes (**Figure 2B**). The appearance and activation of these cells within WAT, is referred to as “browning”. This phenomenon is hallmarked by the expression of UCP1 and the exertion of beneficial metabolic effects. It will be more extensively developed in the “Obesity Treatment approaches” section (**I.5**).

Brite adipocytes are thermogenic brown-like adipocytes which appear in mouse WAT upon particular stimuli such as  $\beta$ 3-adrenergic activation or cold exposure. Ez-Zoubir and colleagues, have latterly described a unique type of cells which are able to differentiate into cells which exhibit the key properties of human white adipocytes, and convert into functional brown adipocytes upon PPAR $\gamma$  activation. These cells have been named hMADS (human multipotent adipose-derived stem cells) (Elabd et al., 2009; Pisani et al., 2011). The potential of inducing even small amounts of brown fat in adult humans could provide a new approach to the treatment and prevention of obesity and its metabolic complications. Decisively, many genes are differentially expressed in mature white, brown and beige adipocytes (Baboota et al., 2015). These include Cidea, DIO2, PPAR $\alpha$ , PGC-1 $\alpha$ , and other factors involved in mitochondrial biogenesis and function (**Table 1**).

As opposed to this “browning” program, Hill and colleagues propose the presence of a “whitening” program, that occurs in adipocytes under conditions of chronic nutrient excess, and that would be critical for regulating AT remodeling under these conditions (Hill, 2015).

	Immunohistochemistry with anti-Ucp1	Location in humans	Location in mice	Developmental origin in mice	Enriched markers	Key Transcription factors	Activators
White		Beneath the skin (subcutaneous) Around internal organs (visceral) Bone marrow Intermuscular Breast tissue	Gonadal Retroperitoneal Mesenteric Omental Inguinal Subscapular Pericardial Popliteal	Myf5 <sup>-</sup> cells	Tcf21 Tle3 Lep Resistin HoxC8 Igfbp3 Inhbb	Bmp2, Bmp4 Krox20 Klf4 C/EBP $\alpha$ , $\beta$ , $\delta$ PPAR $\gamma$	High-fat diet Insulin/IGF1 RIP140 TIF2
Brown		Neck Interscapular (newborns) (Perirenal?)	Interscapular Cervical Axillary Perirenal (Endocardial?)	Myf5 <sup>+</sup> cells	Zic1 Lhx8 Eva1 Pdk4 Epsti1 miR-206 miR-133b	C/ebp $\beta$ Prdm16 Pgc-1 $\alpha$ Ppar- $\alpha$ Ebf2 TR	Cold Thiazolidinediones Natriuretic peptides Thyroid hormone Fgf21, Bmp7, Bmp8b Orexin
Beige		Supraclavicular (Paraspinal?)	Interspersed within WAT Subcutaneous fat > visceral fat	Myf5 <sup>+</sup> cells	Cd137 Tbx1 Tmem26 Cited1 Shox2	C/ebp $\beta$ Prdm16 Pgc-1 $\alpha$ (Ppar- $\alpha$ ?)	Cold Thiazolidinediones Natriuretic peptides (Thyroid hormone?) Fgf21 Irisin

**Table 1: Differentially expressed genes in brown, beige and white adipocytes.**

Adapted from Harms and Seale, 2013.

### ***1.3 – Origin and Development of Adipose Tissue***

The developmental patterns of WAT and BAT are also distinct. In rodents, WAT develops mainly shortly after birth, being present first in the perigonadal and subcutaneous depots, and only later in the omental depot. In humans, WAT development begins early in midgestation and by birth, it is well developed in both the visceral and subcutaneous depots. Anyhow, WAT depots gradually increase throughout life. BAT emerges earlier than WAT during fetal development. It is at its maximal size relative to body weight at birth, when the requirements for non-shivering thermogenesis are most needed, and then involutes in both humans and rodents with aging (Cannon, 2004).

At the cellular level, both appear to originate from mesodermal/mesenchymal stem cells (MSC), although several factors are involved in the development of one versus the other (**Figure 3**). Amidst others, bone morphogenetic proteins (BMPs), nodal, wingless (Wnt), and fibroblast growth factors (FGFs) control fat developmental signaling systems. The exact number of intermediate stages between the pluripotent state, the preadipocyte, and the mature adipocyte remains today uncertain. Nonetheless, it is believed that once committed, the MSC will give rise to undifferentiated precursors (osteoblast, adipoblast/preadipocyte, and myoblast), which, upon the expression of key transcription factors, will enter a differentiation program to acquire their specific functions (Gesta et al., 2007). At the level of preadipocytes (or myoblasts), the cells are already considered like committed to a specific differentiation. However, due to the lack of definite molecular markers, it should be noted that precursor cells and preadipocytes can be at least partly overlapping populations. Mature adipocytes will essentially develop from precursor cells known as preadipocytes by accumulating triacylglycerol (TAG).



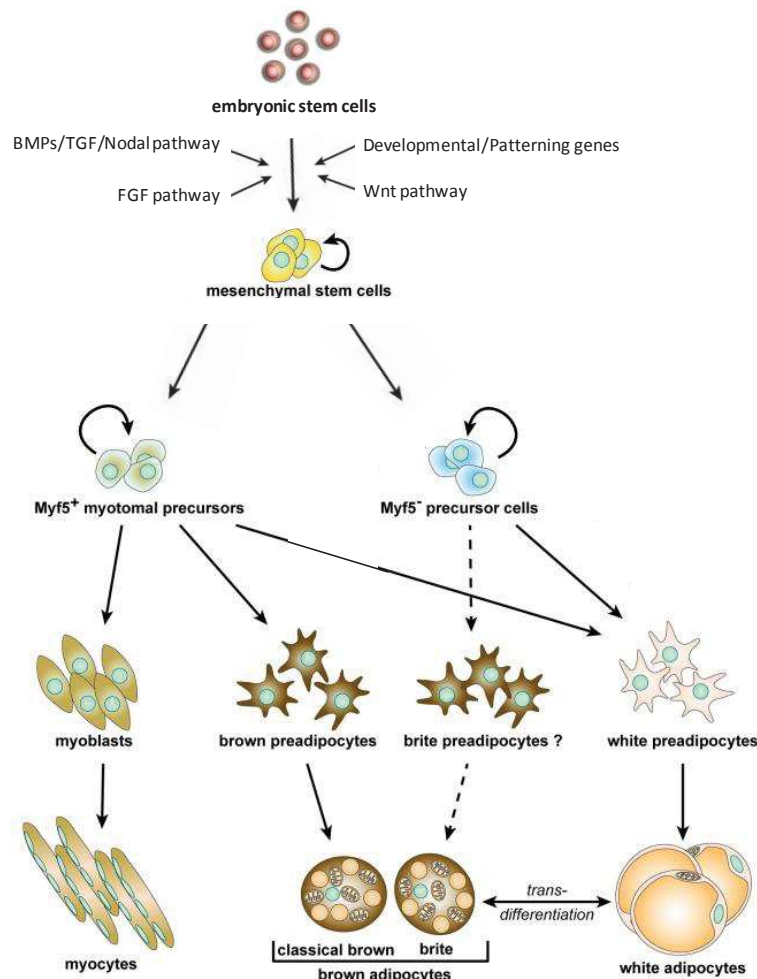


**Figure 3: Developmental lineages of adipocytes.**

Schematic representation of the possible developmental origins of murine adipocytes. Solid arrows represent conclusions from *in vivo* lineage tracing studies; dotted lines represent conclusions inferred from *ex vivo* or *in vitro* studies. Adapted from Rosenwald and Wolfrum, 2014.

Different cellular models (see next section), substantially 3T3-L1 cells have facilitated the study of the adipocyte differentiation process. Of note, cell proliferation and cell differentiation are two biological processes very closely related. Adipocyte differentiation is more accurately known as adipogenesis, and it might be described as a sequence of events characterized by the expression of specific markers which will allow for the acquisition of the phenotype of mature adipocytes. In fact, adipogenesis requires a prior proliferation stage. Once confluence accomplished, contact inhibition will prompt a growth-arrest and clonal expansion phase will follow. This is a stage caused by hormonal

stimulation consisting on a limited number of mitoses which represents a milestone for the differentiation process. The indispensability of clonal expansion has been elegantly shown by Fajas and colleagues. Their experiments showed no differentiation following the blockage of this phase (Fajas, 2003). Growth-arrest and clonal expansion constitute the first steps to take place on the transition from preadipocyte to adipocyte, which additionally counts among its ranks: early differentiation, and terminal differentiation. A transcriptional cascade involving members of the C/EBPs family and the nuclear receptor PPAR $\gamma$ , orchestrates this process (**Figure 4**). The different members composing the C/EBP family are sequentially expressed during adipocyte differentiation. Early expression of C/EBP $\beta$  and C/EBP $\delta$  promotes later expression of C/EBP $\alpha$  and PPAR $\gamma$  (**Figure 5**) (Farmer, 2006).

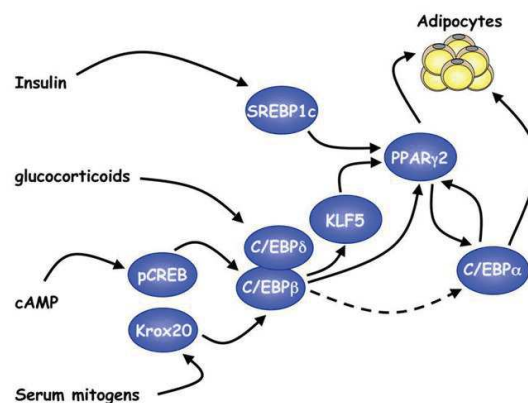


**Figure 4: Induction of adipogenesis by a cascade of transcription factors.**

Exposure of preadipocytes to a cocktail of adipogenic inducers and fetal bovine serum (FBS) activates expression of several transcription factors that converge on PPAR $\gamma$  and C/EBP $\alpha$  induction. Together, these factors oversee terminal adipogenesis. Image from Farmer, 2006.

PPAR $\gamma$  has been shown to be necessary and sufficient for adipocyte differentiation. It is required for maintenance of the terminal differentiated state of adipocytes. Proof being that the expression of a dominant-negative PPAR $\gamma$  or its inducible knock-out (KO) induced respectively dedifferentiation in 3T3-L1 cells, or death of mature adipocytes *in vivo*. Moreover, experiments performed by Zebisch and colleagues showed the dramatic effects of adding or not a PPAR $\gamma$  agonist to the cell culture media of adipocytes. The mere addition of this



compound, called rosiglitazone, permitted to achieve virtually complete differentiation of 3T3-L1 cells, whereas in contrast, only few of them succeeded differentiating into adipocytes in rosiglitazone's absence (Zebisch et al., 2012). This has earned PPAR $\gamma$  the position of "master regulator of adipogenesis". PPAR- $\gamma$  has an indispensable function in adipogenesis and an inseparable relationship with obesity, providing windows of opportunities for its treatment and for its associated metabolic syndromes (Shao et al., 2015).

There are at least three isoforms of PPAR gamma ( $\gamma$ 1,  $\gamma$ 2,  $\gamma$ 3), which differ at their 5' ends, each under the control of its own promoter (Martin et al., 1998). PPAR $\gamma$ 2 is mostly found in AT and the intestine (Fajas et al., 1997). Mature adipocytes are also noticeable by the presence of makers of terminal differentiation, such as FABP4 (Fatty Acid Binding Protein 4), GLUT4 (Glucose transporter type 4) and FAS (Fatty-Acid Synthase) (Rosen and MacDougald, 2006).

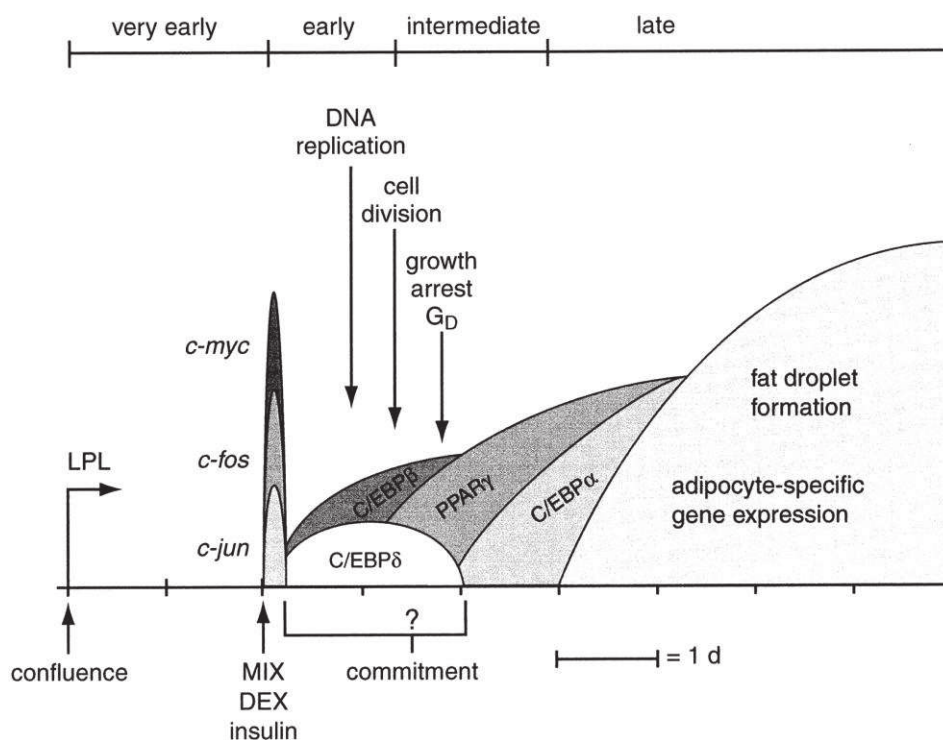


**Figure 5: Progression of differentiation on 3T3-L1 cells.**

The major identified events of preadipocyte differentiation are presented chronologically. Areas labeled by gene names represent periods of gene expression during the differentiation program. The distinct stages of differentiation (very early, early, intermediate and late) are also depicted. Image from Ntambi and Kim, 2000.

## Cellular models

Recently, considerable light has been shed on the cell biology and the transcriptional control underlying adipocytes differentiation thanks to the accessibility of various cell lines. Besides primary preadipocytes, diverse cellular models are currently available to help us understand and identify the molecular mechanisms involved within the differentiation process. Since the development of the murine adipose 3T3-L1 cell culture system by Green and colleagues, this one has become the most popular cellular model for the study of adipocytes differentiation (Green and Kehinde, 1975). But additional cell lines, like 3T3F442A and C3H10T1/2, are also used. Nevertheless, it is important to realize that even if they are handy, these remain solely cellular models. Despite being considered good tools for the study of WAT, they do not express all WAT markers. For example, 3T3-L1 cells produce little, if any, leptin compared to normal white adipocytes (Gesta et al., 2007). In addition, *in vitro* differentiation of 3T3-L1 adipocytes is known to be easily disrupted by a variety of pharmacologic interventions, suggesting a rather delicate balance between terminal differentiation and continued proliferation that may not accurately reflect *in vivo* adipogenesis.

It is obvious that the signals received by the adipocyte precursors *in vivo* are very complex and cannot be one hundred percent reproduced on *in vitro* cellular models. A transcriptomic study sustained this idea by showing that the cell program associated with *in vivo* adipocyte differentiation was substantially more complex than the data obtained with cellular models (Soukas et al., 2001). When comparing *in vitro* and *in vivo* differentiation, a great part of the characteristics of the fat cells were similar, expressing many of the same genes. All the same, what varied was the expression pattern. Therefore, to avail oneself of animal models comes as essential in the end.

Brown preadipocyte cell lines have also been immortalized but they prevail much less extensively characterized (Rosen and Spiegelman, 2000). Created from single newborn mice of different KO models (Klein et al., 2002; Whittle et al., 2012), they are known to retain the main characteristics of primary cells including UCP1 expression. They display sensitive and diverse metabolic

responses to insulin and adrenergic stimulation and have proven to be useful in the characterization of UCP regulation and the role of key insulin signaling elements for insulin action.

#### ***1.4 – Functions of Adipose Tissue***

The best-known function of WATs is to store nutrients in the form of TG for energy demands, such as starvation, and to mobilize them under particular stimuli such as adrenaline signaling. These two roles are undeniable, but besides AT possesses a secretory function. An important number of peptides and other factors that can act in an endocrine or paracrine fashion are released by AT, which makes it increasingly identified as a fundamental, complex endocrine organ, and not simply as a fat stock.

In mammals, BAT can both store nutrients as lipids and dissipate their energy as heat in a process called nonshivering thermogenesis (Bartelt and Heeren, 2014). Brown adipocytes express in their mitochondrial inner membrane (MIM) a 32 kDa protein called UCP1 (uncoupling protein 1), that allows for dissipation of the proton electrochemical gradient generated by respiration in the form of heat (Cannon, 2004). After BAT, skeletal muscle is the other important organ for thermogenesis (Himms-Hagen, 2004). Depots of UCP1-positive brown adipocytes have been identified, interspersed between skeletal muscle bundles in the legs of obesity-resistant strains of rodents, suggesting that “ectopic brown adipocytes” may play an important role in the regulation of whole-body energy homeostasis (Almind et al., 2007). In mice, BAT induction by cold exposure of  $\beta 3$  agonists, resulted in promoted EE, reduced adiposity, and protection from Diet Induced Obesity (DIO) (Ghorbani et al., 1997; Guerra et al., 1998). Conversely, BAT ablation led to reduced EE, diabetes, hyperlipidemia and obesity (Rothwell et al., 1983; Bouchard, 1990; Lowell et al., 1993). Interestingly, mice lacking UCP1 were cold-sensitive but not obese (Maes et al., 1997). Taken together, these genetic models suggest that BAT might influence whole-body energy metabolism in ways not fully explained by the expression of UCP-1. However, it is clear that overexpression of this protein in WAT results in reduced adiposity (Mifflin et al., 1990).

In humans, gradual reduction in the levels of BAT is known to take place with ageing, and this phenomenon seems to be accelerated in individuals with obesity. The amount of metabolically active brown adipocytes seems to be particularly low in patients with this one pathology or with T2D (Bartelt and Heeren, 2014). Furthermore it has been proposed that decreased BAT function in rodents would participate in the origin of these diseases.

#### **I.4a – Fat Deposition and Fat Mobilization**

Energy balance in animals is governed by the first law of thermodynamics, and is often expressed as a simple equation:

$$\text{Energy Intake} = \text{energy expended} + \text{energy stored}$$

As this law must be obeyed, any treatment for obesity must have an effect on one of the equation components. Despite this simple reality, treatment of this condition remains an unresolved challenge, and fat continues accumulating in human beings reflecting the imbalance existing in between the processes of deposition and mobilization. Because the body's capacity to store is finite and relatively small, long-term imbalances are reflected in changes in the amount of TAG stored in adipocytes (Shi and Burn, 2004). In other words: in leanness, weight maintenance, or obesity. Multiple mechanisms regulate these processes and in general, regulation is reciprocal so that fatty acids flow "in" and "out" of the adipocyte according to the nutritional and physiological state of the organism (**Figure 6A**).

Adipocytes are equipped with the biochemical machinery to function effectively as the body's fuel store. To do this, they must mediate the conversion of FFA to TG for storage, also called lipogenesis (see section **I.4a<sub>1</sub>**), and the breakdown of TG to FFA and glycerol, or lipolysis (see section **I.4a<sub>2</sub>**) (**Figure 6B**). This is a tissue exquisitely designed to respond to acute changes in nutritional cues. For example, it is insulin-sensitive (insulin stimulates glucose uptake and lipogenesis and inhibits lipolysis) and subject to adrenergic regulation (epinephrine stimulates lipolysis and adaptive thermogenesis).

Finally, energy balance requires an ability of the brain to detect the status of energy stores and match energy intake with expenditure, triggering metabolic and behavioral responses designed to maintain energy balance (section I.4a<sub>3</sub>).

A)

Energy intake	Energy expenditure
Feeding	Basal metabolism Physical activity Adaptive thermogenesis Diet-induced Cold-induced

B)

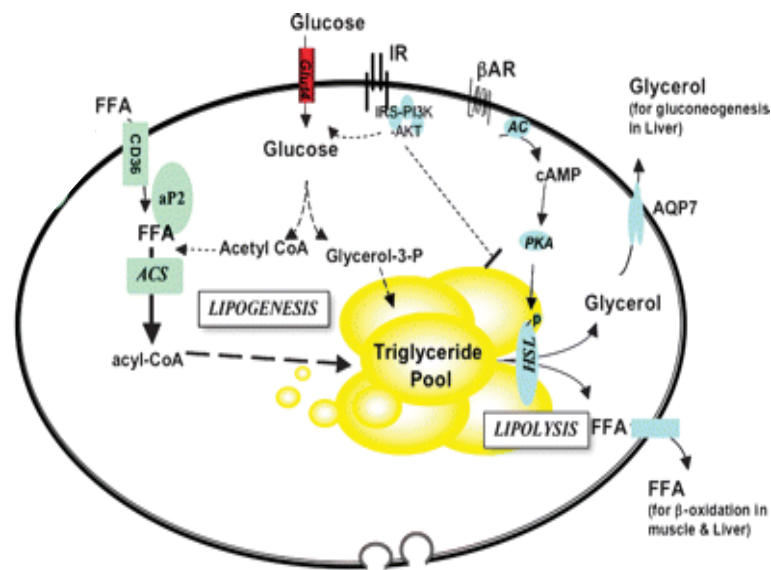


**Figure 6: Energy balance.**

- A) Energy intake depends upon the balance between caloric intake and EE.  
Adapted from Rosen and Spiegelman, 2006.
- B) Schematization of lipids metabolism. Adapted from Sethi and Vidal-Puig, 2007.

#### ***I.4a<sub>1</sub> – Triglycerides Synthesis in WAT: Lipogenesis***

Through lipogenesis and subsequent TG synthesis, our organism can efficiently store energy in the form of fats. Lipogenesis is the process by which acetyl-CoA, a central metabolic intermediate, is converted to FAs. Latter TG synthesis can be apprehended as the creation of FAs from acetyl-CoA and

malonyl-CoA precursors, through the action of enzymes called fatty acid synthases (FAS). This is indeed a very important part of the lipogenesis process, which – together with glycolysis – functions to create fats from blood sugar.

Glycolysis is the metabolic pathway that converts glucose into pyruvate. Along the process, glycerol 3-phosphate (G3P) is produced. During lipogenesis, G3P is esterified with three molecules of FA to synthesize fat. Depending on the nutritional and hormonal status of the body, the availability of FA and glucose will vary, and thus TG synthesis will vary too. In the fed state, liver and WAT will capture FA and glucose from diet, which are later stored as TG into lipid droplets. Within the adipocyte we can distinguish two different TG synthesis mechanisms. Either they will be formed by harvesting circulating FAs from food (I.3a<sub>1.1</sub>), either by *de novo* lipogenesis from carbohydrate precursors (I.3a<sub>1.2</sub>).

#### ***I.4a<sub>1.1</sub> – Lipogenesis from diet***

Indeed, it is a fact that fat mobilization fluctuates along the day. After meals, the dietary lipids undergo digestion by bile salts within the intestines. And only afterwards, they are hydrolyzed by pancreatic enzymes, to become FAs. Under this form, lipids will penetrate the intestinal absorptive cells, or enterocytes. They are ensuing secreted into the lymphatic system under the form of chylomicrons to finally enter the bloodstream. Once there, these lipids are hydrolyzed into glycerol and AG by the LPL (lipoprotein lipase). This is a fascinating multifunctional enzyme, whose activity is increased following elevated plasma insulin levels, and who contributes to the many aspects of obesity and other metabolic disorders that relate to insulin action, energy balance, and body weight regulation (Wang and Eckel, 2009; Thompson et al., 2012). The released FAs are transported to other tissues by albumin. To enter the adipocytes, they either diffuse, either utilize specific transporters, like FABP2.

**Figure 7** depicts the uptake of FAs through NEFA and lipoproteins, together with the formation of lipid droplets in the adipocytes. Green arrows follow the path of lipid storage in the postprandial state. Blue arrows illustrate the degradation and subsequent release of lipid droplets in the post-absorptive state, to provide



energy for other tissues. And black arrows indicate glucose uptake by adipocytes for *de novo* synthesis of FAs which will be developed in the following section.

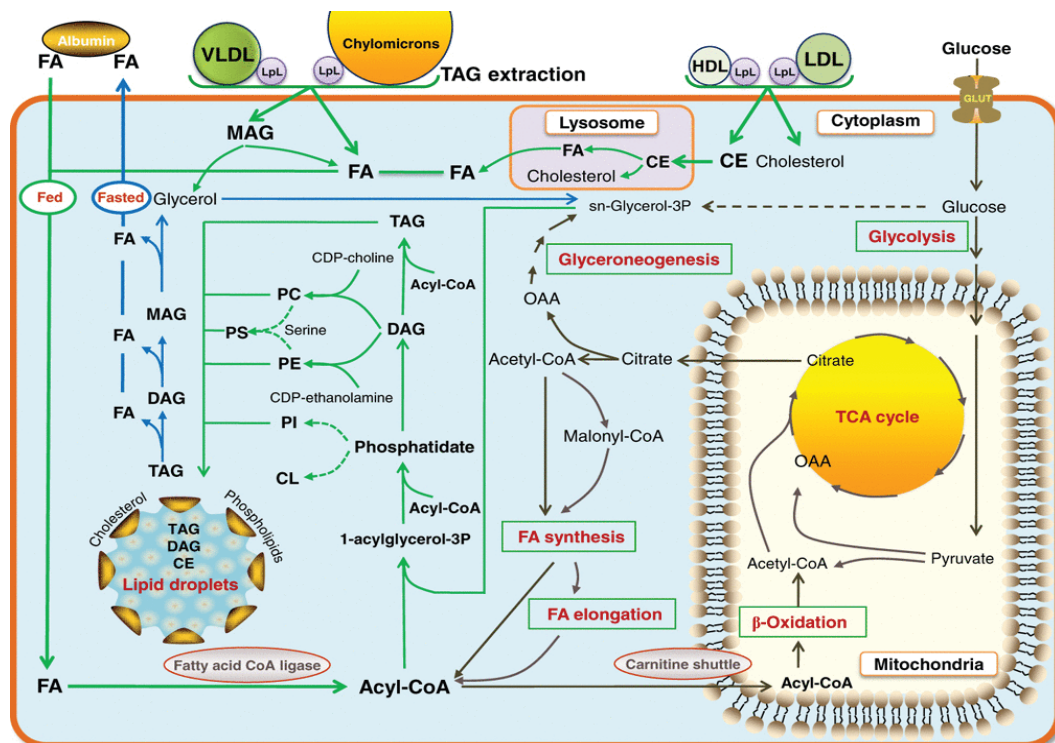


**Figure 7: Formation of Lipid Droplets.**

Uptake of fatty acids through NEFA and lipoproteins and formation of lipid droplets in adipocytes. Image from Mardinoglu et al., 2013.

#### 1.4a<sub>1,2</sub>– *De novo* lipogenesis

*De novo* lipogenesis is the metabolic pathway that synthesizes FAs from excess carbohydrates. These FAs are released into the bloodstream in the form of VLDL, and can then be incorporated into TGs for energy storage. Though it also takes place in adipocytes, *de novo* lipogenesis is mainstream in liver. In obesity, it has been revealed to be down regulated in AT from mice and humans (Ortega et al., 2010), suggesting an adaptive process in order to limit an ongoing increase of fat mass.

The increase of insulin after a meal causes the activation (dephosphorylation in this case) of the enzyme responsible for the transformation of Acetyl-CoA into malonyl-CoA, whose name is acetyl-CoA carboxylase (ACC). This conversion entails the renewal of carbohydrates into FAs. On the contrary, during starvation and exercise, epinephrine and glucagon are released into the bloodstream, leading to the inactivation (phosphorylation) of ACC, and inhibition of lipogenesis in favor of FA oxidation via beta-oxidation (see **chapter II**). Phosphorylation of ACC is mostly carried out by AMPK (AMP-activated protein kinase), which is activated following ATP is depletion, thus 5'AMP rise. AMPK acts as a master metabolic sensor, regulating several intracellular systems including the cellular uptake of glucose, the  $\beta$ -oxidation of FA and the biogenesis GLUT4 and mitochondria. The energy-sensing capability of AMPK can be attributed to its ability to detect and react to fluctuations in AMP and ATP (Sethi and Vidal-Puig, 2007). Indeed, concentrations of AMP and ATP in the cell act as a measure of the energy needs. This is a useful way to ensure that glucose is not diverted down a storage pathway in times when ATP levels are low. Glucose and insulin act synergistically to stimulate the expression of lipogenic enzymes, such as ACC, FAS DGAT (Diglyceride acyltransferase) or GPAT (G3P acyltransferase) (Lenhard, 2011).

#### ***1.4a<sub>2</sub> – Fatty Acids degradation: Lipolysis***

The key process in fat catabolism and the provision of energy substrate during times of nutrient deprivation (fasting) or enhanced energy demand (exercise) is the hydrolytic cleavage of stored TG, also known as lipolysis (**Figure 8**). Since WAT is the primary fuel reserve in mammals, this is the site where this mechanism takes place. Lipolysis is translated in terms of generation of FAs and glycerol, which will be released from adipocytes to the bloodstream. A complex, hormonally controlled regulatory network regulates its initiation, ultimately activating key intracellular enzymes called lipases that will hydrolyze the TG (Zechner et al., 2009).



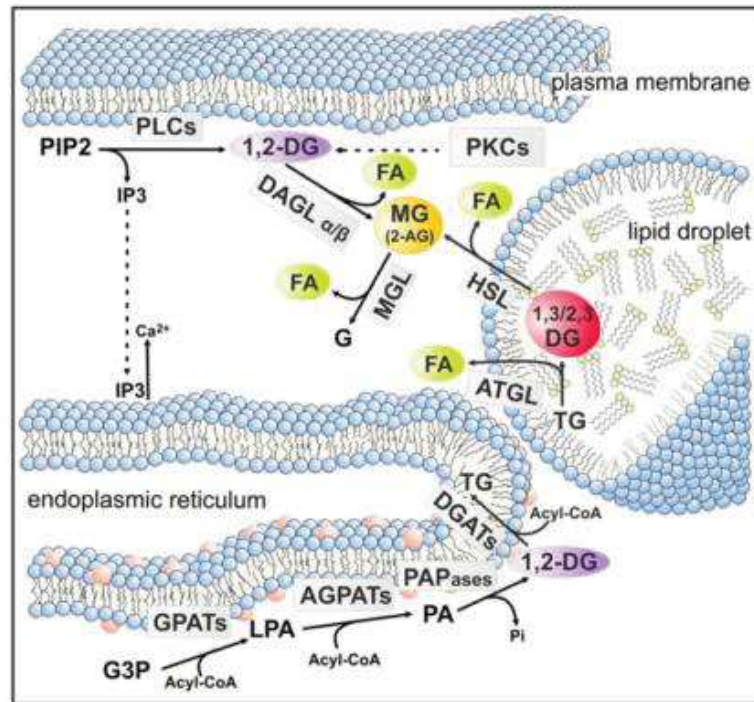


**Figure 8: Lipolysis and Lipid Signaling.**

Lipid intermediates involved in cellular signaling are generated by anabolic and catabolic reactions in distinct cellular compartments. Image from Zechner et al., 2012.

Lipolysis occurs in three stages, with different cytosolic lipases performing in each of them: Firstly, ATGL (Adipose triglyceride lipase) will catalyze the conversion from TAG to DAG (diacylglycerols). Subsequently, HSL (Hormone-sensitive lipase) will mediate the next hydrolysis in order to obtain MG (monoacylglycerols). Finally, MGL (Monoacylglycerol lipase) will allow for the acquisition of glycerol. It is important to mention that a FA is released at each stage. This process is affected in multiple steps. To date, numerous effectors, including adipokines, hormones and cytokines, have been described as being anti-lipolytic (insulin), or pro-lipolytic (epinephrine, norepinephrine, growth hormone, glucagon, and glucocorticoids).

#### *1.4a<sub>2.1</sub> – Insulin (anti-lipolytic effect)*

Changing insulin concentrations largely determines fat mobilization. Insulin and insulin-like growth factor represent the most potent inhibitory hormones in lipolysis. Their effects are primarily communicated through the

insulin receptor (IR) (Langin, 2006). In peripheral tissues, insulin auto-phosphorylates the IR, leading to activation of the PI3K enzyme system which then activates PKB/AKT. Recently, a team working on development of pharmacologically active small compounds, has found a synthetic PI3K inhibitor which increases EE and hyper-activates BAT in mice (Ortega-Molina et al., 2012).

#### ***1. 4a2.2 – Adrenergic regulation (pro-lipolytic effect)***

The lipases' activation befalls principally through the initiation of adrenergic pathways, largely dependent on  $\beta$ -adrenoceptor ( $\beta$ -AR) stimulation. While in human WAT only two subtypes of  $\beta$ -AR induce lipolysis, mouse adipocytes express three subtypes of  $\beta$ -ARs: b1-AR, b2-AR, and b3-AR. The relative distribution of  $\beta$ -AR determines the lipolytic activity in a cell type- and tissue -specific manner (Zechner et al., 2009). Adipocytes of patients with obesity have a higher density of  $\beta$ -3 AR and lower insulin receptor density, a situation that has several metabolic consequences. In mice where the  $\alpha$ 2/ $\beta$ -AR balance was genetically manipulated, Valet and colleagues showed an influence on fat mass due to an interaction between  $\beta$ 3-AR and  $\alpha$ 2 genes, along with the diet.

Adrenergic pathways depend on the sympathetic nervous system (SNS) innervations in WAT, which are presented as indispensable. Two catecholamines appear as essential: adrenaline/epinephrine and noradrenaline/norepinephrine (Ardilouze et al., 2004). When they bind to  $\beta$ -AR, G proteins are stimulated, that in turn activate AC (Adenylate Cyclase), generating a rise in cAMP levels which translates in an elevated activity of PKA. Target proteins of PKA include HSL and perilipin, a lipid-droplet associated protein, whose phosphorylation induces an increased release of FAs and glycerol from AT up to 100-fold.

Lipolysis is crucial for all the rest of the organs, including BAT, where the generated FAs will be used for UCP1 activation for thermogenesis and mitochondrial  $\beta$  –oxidation, among others. Regulated increases in thermogenesis occur in brown adipocytes with the stimulation of  $\beta$ -AR, initiating a signal transduction cascade that converts the catabolic end products of macronutrients (carbohydrates, fats and proteins) into mitochondrial fuel (Tseng et al., 2010).

### ***1.4a<sub>3</sub> –Regulation of appetite and satiety***

As we have previously seen, excessive food intake together with a sedentary lifestyle are to a large degree at the origin of obesity in humans. Interest in the control of feeding has increased in parallel to the evolution of the obesity epidemics and the rise in the incidence of metabolic diseases. Metabolic signals emanate from peripheral organs, the gastrointestinal tract, and AT. These signals target the brain to regulate feeding, EE and hormones. In response, the brain triggers metabolic and behavioral feedback designed to maintain the equilibrium (Ahima and Antwi, 2008). Overall, energy balance is responsive to various factors, including hormones (I.3a<sub>3.1</sub>), neural inputs (I.3a<sub>3.2</sub>), and psychological and cultural factors (I.3a<sub>3.3</sub>) (**Figure 9**) (Abizaid et al., 2006). A thematic review on the current knowledge on the homeostatic regulation of energy balance was published last year by Marc Schneeberger and colleagues (Schneeberger et al., 2014).

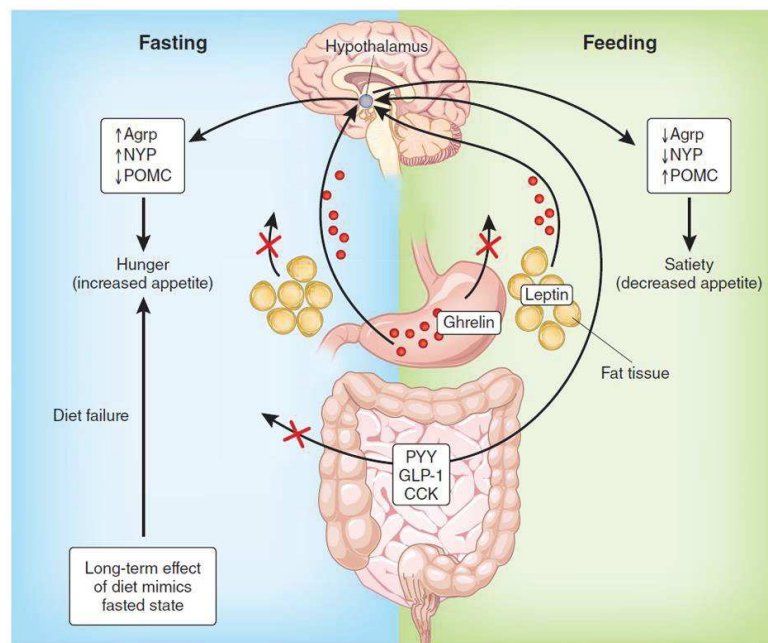


**Figure 9: Effect of feeding and fasting on hunger.**

During and after regular feeding, there is a reduction in the production of ghrelin by the stomach. In contrast, production of PYY, GLP-1 and CCK from the gut is increased, and serum leptin levels also rise. These changes are detected by the brain, resulting in modulation of gene expression which result in decreased appetite and a feeling of satiety such that caloric intake is stopped. During fasting, the opposite situation is established, leading to hunger. Image from Larder and O’Rahilly, 2012.

***1.4a<sub>3.1</sub> – Secreted hormones***

Appetite and satiety are mainly controlled by the gut–brain axis via hormonal and neuronal signals. From the moment nutrients enter the small intestine in the body, a set of peptides are released in order to reduce meal size and ultimately terminate feeding. Hormones and cytokines secreted by peripheral organs also partake of this mission. In response to meals, the hormones secreted by the gut comprise among others:

- CCK (Cholecystokinin), a peptide that acts as a satiety factor decreasing meal size (Liebling et al., 1975).
- GLP-1 (Glucagon-like peptide-1), an incretin which increases satiety and promotes insulin sensitivity. Agonists are widely regarded for therapeutic utility and applications in metabolic disorders (Finan et al., 2013).
- Ghrelin, a critical signal stimulating food intake and promoting weight gain, whose antagonists have the potential for obesity and diabetes therapy (Ahima and Antwi, 2008). Farhana and colleagues recently showed that ghrelin resistance was caused by DIO by promoting inflammation (Naznin et al., 2015).

Opposing the actions of ghrelin by inhibiting hunger, a hormone to be mentioned is:

- Leptin, a hormone secreted mostly by AT which has pleiotropic effects on glucose homeostasis and feeding behavior. It holds an imposing ability to acutely reduce food intake. In obesity, a decreased leptin sensitivity occurs, resulting in an inability to detect satiety despite high energy stores (Ahima and Antwi, 2008) (see **1.4b**).

***1.4a<sub>3.2</sub> – Neural circuits***

During and after feeding, there are changes in the production the so-described hormones. These alterations are detected by the brain, resulting in modulation of gene expression which normally results in decreased appetite and a feeling of satiety such that caloric intake is stopped. Protein levels of orexigenic neuropeptides [Agouti-related protein (AGRP) and neuropeptide Y (NPY)], are found decreased whereas anorexigenic peptides' levels, originating from pro-

opiomelanocortin (POMC), are found increased. During fasting, up-regulation of orexigenic and down-regulation of anorexigenic gene expression occurs within the hypothalamus, leading to hunger (**Figure 9**). Dieting results in a gut hormone profile that mimics the fasted state (Larder and O’Rahilly, 2012).

#### ***1.4a<sub>3.3</sub>—Rewarding effects of food***

Even with the existence of a beautiful panel of intricate and very well designed control circuits, food has pleasurable and rewarding qualities which drive appetite beyond metabolic needs. The motivational and premium aspects of feeding are mediated by the limbic system. First, although food intake is relatively easy to measure, it is not the precise parameter that determines the amount of energy brought into the system. The efficiency of calorie absorption in the gut, which is much more difficult to assess, and is usually ignored in practice, must also be accounted for. A second consideration is that the body’s response to alterations in energy input or expenditure is not static. In general, energy homeostasis is regulated to defend the highest weight achieved (Schwartz et al., 2003). Thus voluntary reductions in food intake are countered by involuntary reductions in EE, making weight loss more difficult than a simple interpretation the previous equation (**1.3a**) would indicate.

#### **1.4b – Endocrine function**

An important aspect of AT endocrinology is the recognition that numerous other cell types, in addition to adipocytes, are also present within this tissue. Together, these additional cell types, which are called SVF (section **1.1**), play important roles in regulating AT function. Interestingly, even if adipocytes represent more than half of the total cell number, the non-adipocyte cells can have effects on multiple biological systems, including energy homeostasis (lipid and carbohydrate metabolism, thermogenesis, appetite), the immune system, the reproductive function, hemostasis, blood pressure, and angiogenesis. The SVF may also be, besides fat, the source of some secreted factors, more decorously known as adipokines or adipocytokines (**Figure 10**).

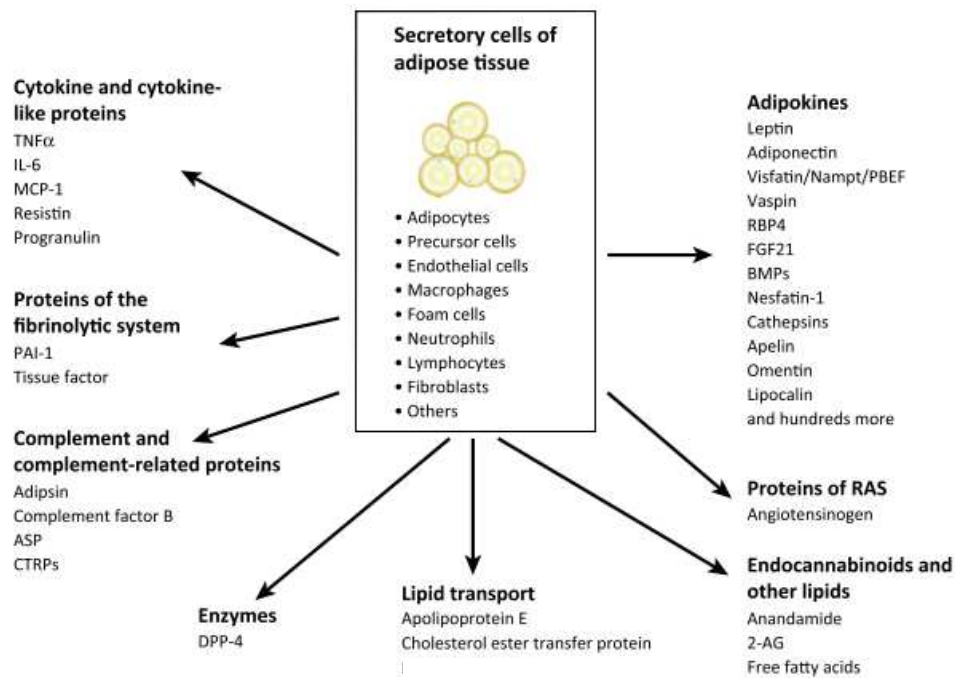


**Figure 10: Factors released or secreted by adipose tissue.**

Adipocytes, immune cells, fibroblasts, endothelial cells, and others contribute to the release of metabolites, lipids, and adipokines. Examples of adipose tissue-derived molecules are provided here. Image from Fasshauer and Bluher, 2015.

I will briefly describe the most influential adipokines hereafter:

Leptin is secreted almost exclusively by fat, whose mass abundance is mirrored by leptin circulating levels. It does not only regulate feeding behavior, by repressing food intake and promoting EE, but it also serves as a bridge between peripheral metabolically active tissues and the central nervous system (CNS). Leptin acts on the limbic system by stimulating dopamine uptake, creating a feeling of fullness. During the onset and progression of obesity, the dampening of leptin sensitivity often occurs, preventing the efficacy of leptin replacement therapy from overcoming obesity and its comorbidities (Santoro et al., 2015). Six distinct leptin receptors, LRA–LRf, derived from alternative splicing (AS) of *lepr* mRNA have been identified in mice (Myers et al., 2008). A functional leptin system is required for the effectiveness of some agents in the treatment of obesity, such as tungstate (Canals et al., 2009).



Adiponectin is almost exclusively produced by adipocytes, where its mRNA transcript is the most highly expressed. Its levels have been shown to inversely correlate with obesity, visceral fat distribution, T2DM, and other obesity-related diseases (Ye and Scherer, 2013; Fasshauer et al., 2014). It protects against a cluster of obesity-related metabolic complications through multiple mechanisms (Hui et al., 2015). This is maybe due to its insulin sensitizing, anti-inflammatory, and antiapoptotic properties. Adiponectin also acts in the brain to increase EE and thereby it may promote weight loss (Turer and Scherer, 2012; Fasshauer and Bluher, 2015).

Apelin is a widely expressed adipokine identified over the past years as a new player in energy metabolism, in addition to leptin and adiponectin. Apelin exerts pleiotropic actions throughout the whole body (Knauf et al., 2013). By interacting with its receptor APJ, apelin determines many physiological metabolic functions such as, glucose uptake, lipids utilization, and modulation of insulin secretion. These actions globally lead to improvement of insulin resistance. Following apelin secretion by AT, glycaemia decreases due to glucose uptake within that same tissue, muscle, intestine and others. Even if further studies are required, this adipokine presents promising anti-diabetic properties given its beneficial roles on both EE and insulin sensitivity (Bertrand et al., 2015).

Resistin is primarily expressed in and secreted from mature adipocytes. It appears as an important link between obesity and inflammatory processes. Levels of resistin are elevated in many murine models of obesity (Rosen and Spiegelman, 2006). Maybe that's the reason why resistin was initially considered as a determinant of the emergence of insulin resistance in obesity. The amount of evidence supporting this link remains ample. Notwithstanding, since the number of studies presenting evidence against this statement continues to expand, not the entire scientific community agrees on it.

TNF- $\alpha$  seems to be derived from macrophages and other cells belonging to the immune system, aside from adipocytes. Its levels are elevated in insulin-resistant states such as obesity and sepsis, and in mouse models of obesity (Warne, 2003), undoubtedly contributing to inflammation and the maintenance of the obese state.

IL-6 is furthermore another pro-inflammatory cytokine, principally secreted by the macrophages present in AT (Fain, 2010). Anti-inflammatory properties are also noticeable through its inhibitory effects on TNF- $\alpha$  and other interleukins.

Adipsin is secreted by adipocytes. It has insulin-like effects. It is positively related to adiposity, insulin resistance, dyslipidaemia, and cardiovascular disease.

PAI-1 can be secreted by AT although it is mainly produced by the endothelium. Elevated levels of PAI-1 are associated with obesity. These are a common finding in plasma from both mice and humans, and have thus been considered as one of the biomarkers used to predict obesity-associated diseases (González et al., 2012). In addition, PAI-1 is an important regulator of extracellular matrix turnover, tissue remodeling, and fibrosis (Lund et al., 1988).

FGF21 is produced by the AT, liver, and skeletal muscle, and released into the circulation. Its action requires the interaction with a co-receptor,  $\beta$ -Klotho. In their presence, thermogenic effects as well as glucose and lipid lowering, have been observed in rodent animal models (Fisher et al., 2012; Gaich et al., 2013; Itoh, 2014). FGF21 also stimulates glucose uptake in 3T3-L1 and primary human adipocytes, and this in an insulin additive fashion (Kharitonov et al., 2005). These effects could be due, at least in part, to its role in adaptive thermogenesis and in promoting browning of WAT. The metabolic effects of FGF21 on glucose homeostasis and insulin sensitivity in mice have been shown to be mediated by adiponectin (Lin et al., 2013).

Some of these actions underscore the links between obesity and its related pathologies. For instance, in obesity there is an imbalance in adipokines production, which results in a process of adipose tissue dysfunction (**Figure 11**). Adipokines appear like promising candidates both for novel pharmacological treatment strategies and as diagnostic tools for obesity (Fasshauer and Bluher, 2015). Some pro-inflammatory and atherothrombotic adipokines such as leptin, resistin, IL-6, TNF-  $\alpha$  and PAI-1 are increased in obesity, whereas the anti-inflammatory adipokine adiponectin tends to be decreased.



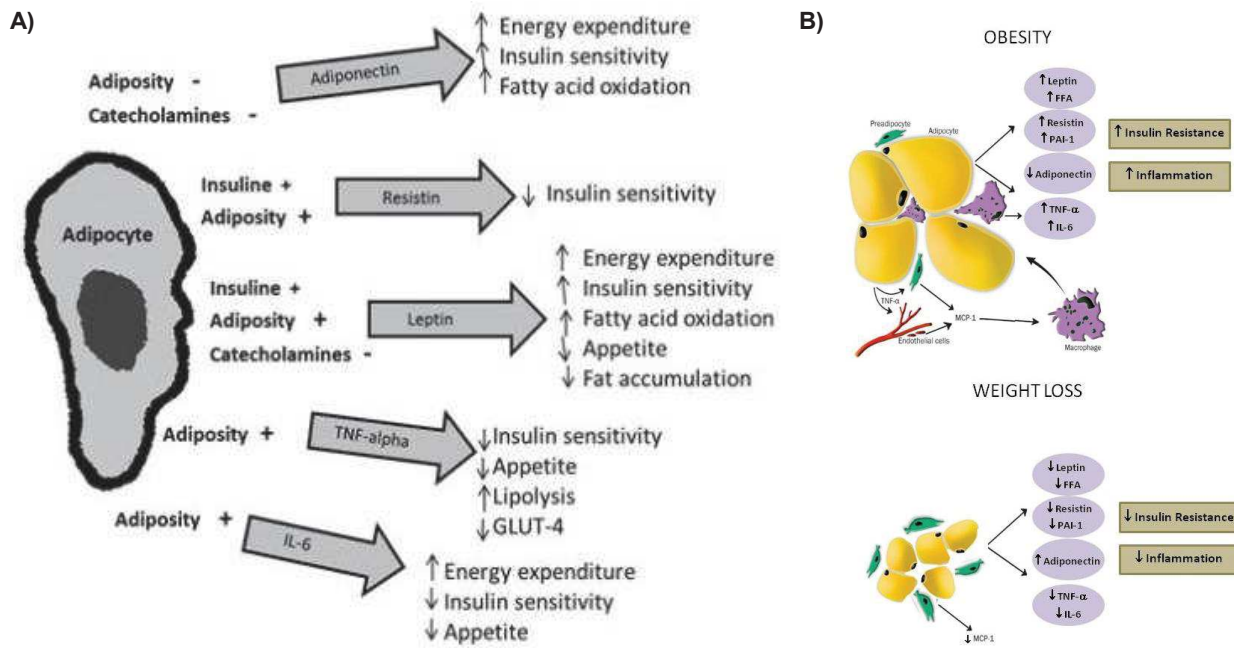


**Figure 11: Major adipokines, their roles and variations with weight modulation.**

- A)** Insulin, catecholamines, and adiposity regulate AT adipokines production. These will exert next distinct metabolic effects. Image from Fernández-Sánchez et al., 2011.
- B)** Weight loss reverts the alterations caused by obesity typical hypertrophic and hyperactive adipocytes, which leads to improved insulin resistance and inflammation. Image from Azevedo et al., 2012.

### ***Oxidative stress & Reactive Oxygen Species***

Adipokines are known to induce the production of reactive oxygen species (ROS), generating a process known as oxidative stress. There are several mechanisms by which obesity produces ROS, like for instance: mitochondrial and peroxisomal oxidation of FA, over-consumption of O<sub>2</sub> and alteration of oxygen metabolism by lipid rich diets (Chentouf et al., 2011). Upon the increase of AT, the activity of antioxidant enzymes such as superoxide dismutase (SOD), catalase (CAT), and glutathione peroxidase (GPx), was found to be significantly diminished. Although obesity and oxidative stress are clearly correlated, it still remains unclear whether this relationship is causal and if so, which factor is responsible for driving the other (Ristow and Wolfrum, 2013).

### ***1.5 – WAT associated pathologies: obesity***

In a worldwide fashion, but especially in industrialized first world countries, one of the largest public health concerns is obesity. This is a disease that results the common denominator of many WAT associated pathologies. Obesity is associated among others with: insulin resistance, diabetes, cardiovascular disease, nonalcoholic fatty liver disease, gallstones, Alzheimer's disease, and several cancers. These are co-morbidities that can lead to further morbidity and mortality. In modern times, the social stigma of obesity has created negative psychosocial impacts and has caused disadvantages for overweight and obese people. Furthermore, childhood obesity is associated with a greater chance of premature death and disability in adulthood.

Obesity is a chronic disease of multifactorial origin and can be defined as an increase in the accumulation of body fat. It develops when energy intake exceeds energy expenditure. Although fat accumulation is a familiar phenomenon to most healthy individuals, it only appears to become clinically relevant when abnormal changes in adipose mass are associated with health problems. The most common index defining obesity is the body-mass index (BMI). This reference number is calculated by dividing an individual's weight (Kg) by the square of its height (m). A healthy status is outlined for digits comprised in between 20 and 25 kg/m<sup>2</sup>. When the resulting number is between 25 and 30 kg/m<sup>2</sup> the person is considered to be overweight. Obesity can be attributed to those above 30 kg/m<sup>2</sup>. And although the number of brown adipocyte-like cells is inversely correlated with BMI in humans (Qian et al., 2013), weight is not everything. People over 30 kg/m<sup>2</sup> can be absolutely in good conditions and on the contrary, normal-weight individuals may be "metabolically-obese". As already mentioned in section 1.1, fat distribution plays an important role in metabolic risk. Higher negative connotations are associated to visceral compared to subcutaneous fat (**Figure 12**).

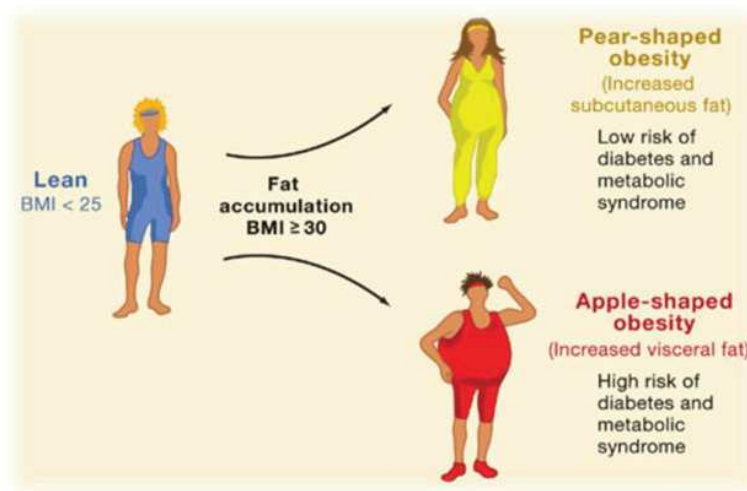


**Figure 12: Fat Distribution Influences Risks Associated with Obesity in Humans.**

Adapted from Gesta et al., 2007.

Lately, new definitions of obesity which take this into consideration are in the spotlight. Research starts distinguishing the obese people into metabolically healthy (MHO), or unhealthy (MUO) individuals, independently of their BMI. In this two groups insulin sensitivity, together with the ability to adapt to a caloric challenge has been shown to be different (Badoud et al., 2015).

Lean subjects can also have a disproportionate amount of fat. These are referred to as TOFI (Thin-Outside-Fat-Inside), and have been described as being at higher risk of developing insulin resistance and T2D. The metabolic opposites are the 'fit fat' or FOTI (Fat-Outside-Thin-Inside), which are MHO, presenting little internal fat relative to their size.

### **1.5a –Rodent models**

*Bona fide* results proving that body weight and composition are regulated by specific genes have been provided by transgenic mice and rats models. They provide a powerful resource for the study of obesity, as well as the discovery of the underlying mechanisms and the development of drugs to fight this syndrome. Thanks to these models, we are now able to generate hypothesis regarding humans.

Two primary rodent models are used to study obesity, the monogenic (a single gene) and polygenic (more than one gene). Two of the most famed spontaneous mutations leading to a monogenic massive obesity are the *Lep ob/ob* and the *Lepr db/db* mice strains. They respectively lack leptin or have a loss of function of the leptin receptor, resulting in deficiency of leptin signaling. This causes hyperphagia and impaired thermogenesis. However, obesity in humans is considered a polygenic multi-factorial disease. A high energy intake enormously contributes to this pathology. Consequently one of the most accurate employed animal models is the DIO (Diet Induced Obesity). These animals long-term receive a HFD (high fat diet) before a research protocol can begin. Unfortunately, there is no easy way to select the appropriate mouse model to study obesity. Every one of them has got strengths and weaknesses to discuss.

### Obesity

Model name	Mutation	Hyperphagia	Decreased Energy Expenditure	Hyperglycemia	Insulin Resistance
<b>MONOGENIC MUTATIONS IN THE LEPTIN PATHWAY</b>					
<b>Leptin and its receptor</b>					
<i>ob/ob</i> mouse	<i>Lep<sup>ob</sup>/Lep<sup>ob</sup></i> (leptin deficiency)	X	X	X	X
<i>db/db</i> mouse	<i>Lep<sup>db</sup>/Lep<sup>db</sup></i> (leptin receptor)	X	X	X	X
<b>DIET-INDUCED MODELS; POLYGENIC MODELS</b>					
Diet induced obese (DIO) rat	Polygenic	X	X	[X]	X
Cafeteria diet-induced obesity	Polygenic	X	X	[X]	X
High-fat diet-induced obesity	Polygenic	X	X		X

### Lipodystrophy

Metabolic feature	Human generalised lipodystrophy	Mouse generalised lipodystrophy	Human partial lipodystrophy	Mouse partial lipodystrophy
Insulin resistance	+++	+++	++	?
Diabetes	+++	++	++	?
Leptin/adiponectin	Reduced	Reduced	Reduced	?
Fatty liver	+++	+++	++	+
Dyslipidaemia	+++	++	++	+
Hyperphagia	++	++	+	?
Elevated metabolic rate	+	+	+	?
Organomegaly	++	+	+	?
PCOS*	++	?	++	?

\*Many women with generalised or partial lipodystrophy manifest features of polycystic ovary syndrome (PCOS).

**Table 2: Summary of mentioned animal models of Obesity and metabolic features of human and mouse Lipodystrophy.**

“[ ]” indicates mild or late phenotype. Adapted from Lutz and Woods, 2013 and Savage, 2009

Of note is that protection from obesity in different genetically engineered models can typically be attributed to increased nutrient oxidation, increased thermogenesis, increased activity, and reduced lipogenesis. Besides these popular models, many other KO mice are currently available into which the genetic engineering of one specific gene, leading to its invalidation, entails metabolic consequences, either obesity or lipodystrophy (**Table 2**), which allows researchers to further deepen into the intrinsic pathways of these two conditions.

Having too little of AT, like having too much, leads untoward undesired metabolic consequences, from which the most alarming one is ectopic fat deposition. The severe metabolic disturbances seen in human and mouse syndromes of partial and complete lipodystrophy provide a cautious reminder that the safest place to store excess TG is certainly AT (Moitra et al., 1998; Reitman et al., 2000). In both cases, obesity and lipodystrophy, the lipids spill over into the circulation and subsequently accumulate ectopically in other tissues where their effects are harmful (**Figure 13**) (Guénantín et al., 2014). Different pathologies, such as laminopathies imply lipodystrophy among their symptoms. This aspect will be further developed in section III.5a2.

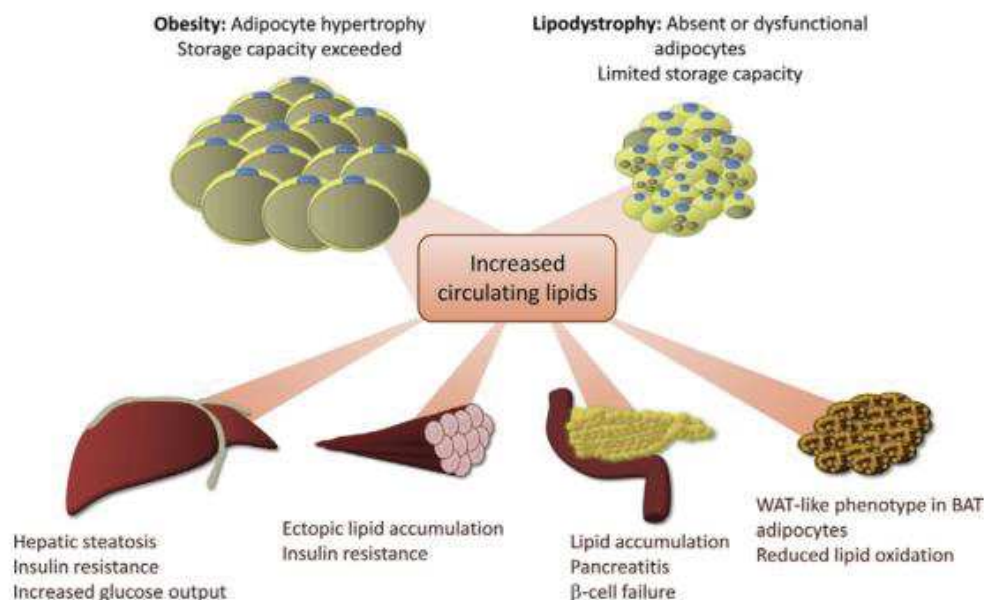


**Figure 13: Lipid overflow in obesity and lipodystrophy.**

Adapted from Rochford, 2014.

### ***1.5b –Treatment/Clinical Approaches***

Parallel to the increase of obesity, the study of this condition has undergone considerable development. This has been accomplished thanks to research in various fields of knowledge that have broken down old paradigms providing a solid foundation for understanding the disease and for developing strategies for prevention and treatment. Even if in theory energy balance obeys to a “simple” rule, and focusing on diet and exercise should work, many additional factors kick in the presented equation (1.3a) and unluckily reality is not as simple. For extremely obese individuals (BMI >35) bariatric surgery is usually the answer, whereas for the treatment of less severe obese patients current approved medical therapies ordinarily aim at one or more of the following mechanisms:

- Preventing fat absorption: Interfering with the body's ability to assimilate specific nutrients from food for the purpose of inhibiting digestion and lowering caloric absorption. For example fiber supplements or Orlistat.
- Suppressing appetite: Drugs blocking the cannabinoid receptors or catecholamines and their derivatives are the main molecules used for this goal. The endocannabinoid system has significant effects on appetite and metabolism. Over nutrition activates this system, resulting in hyperphagia, reduction in EE and obesity.
- Increasing the body's metabolism: Targeting EE, that is, cellular bioenergetics is an attractive strategy that could be used alone or in conjunction with other approaches. Two organs appear attractive for this purpose, BAT and muscle.

#### **BAT**

With the recognition that adult humans have BAT, targeting cellular bioenergetics has become an increasingly attractive way to dissipate energy excess and provides a potential therapeutic approach for the treatment and prevention of obesity as well as its associated diseases (Tseng et al., 2010). The existence of beige adipocytes, a pool of inducible brown adipocytes, mixed in with white adipose depots (Mori et al., 2014) encourages researchers to combine efforts towards this direction. In addition, thanks to modern technologies of fluorescence imaging, it is nowadays relatively easy to visualize BAT in living



mice and check whether this activation is taking place (Rice et al., 2015). In the past few years different approaches envisaging browning have been investigated (Bartelt and Heeren, 2014; Dempersmier and Sul, 2015). The **Figure 14** recapitulates different approaches based on increasing thermogenesis.

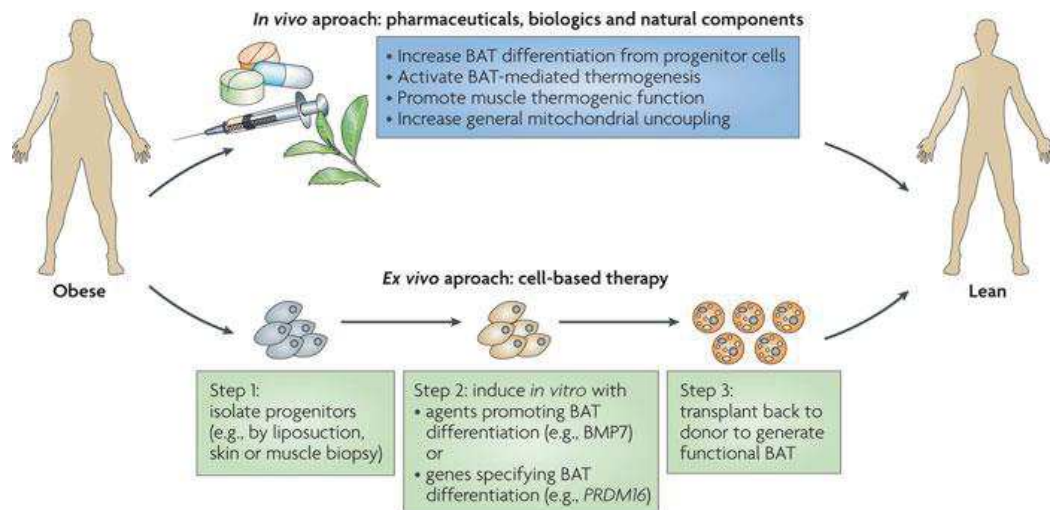


**Figure 14: Approaches to increasing thermogenesis as an anti-obesity therapy.**

Based on the current knowledge of bioenergetics, four potential therapeutic approaches could be envisioned: increasing brown fat differentiation from progenitor cells; activating brown fat thermogenesis; promoting skeletal muscle thermogenesis; or increasing general mitochondrial uncoupling. Image from Tseng et al., 2010.

This approach of EE increase has already proven to be effective in achieving weight loss. In rodents, treatment with CL-316243, a  $\beta$ 3-AR-specific agonist, substantially functioned (Harper et al., 2008). Moreover, treatment with resveratrol increased BAT thermogenesis markers and EE, decreasing fat accumulation in AT (Andrade et al., 2014) and protecting mice against DIO and insulin resistance while increasing lifespan (Lagouge et al., 2006; Baur et al., 2006). Another example that has complementarily been used by humans would be DNP, a non-selective uncoupler of mitochondrial oxidation that lessens the efficiency of ATP energy production in a dose-dependent manner. As the dose increases, energy production is made more inefficient, hence metabolic rate increases, and more fat is burned in order to compensate for the inefficiency and to meet energy demands.

## Muscle

To burn excess energy exercising is the first thing that comes to anybody's mind when pondering about weight loss. There is no doubt that to mobilize our muscles is an effective tactic that in addition has profound beneficial effects on virtually all biological systems. When we do sports we are increasing our body's metabolism and the scientifically appropriate definition for what is happening in our organism is "exercise-induced thermogenesis". Together with non-exercise activity thermogenesis and cold-induced shivering thermogenesis, these are the three types of thermogenesis occurring in skeletal muscle, which will increase EE. Furthermore, endurance exercise training (Himms-Hagen, 2004; Goodyear, 2008), or chronic cold exposure (Puigserver et al., 1998; Lin, 2002) may trigger a remodeling of muscular fibers, helping protect against obesity and related metabolic disorders. In this organ different types of myofibers differ in speed of contraction, mitochondrial content and pattern of energy use. Type I (red) myofibers have a slow-twitch speed of contraction, a higher mitochondrial content, and thus a higher rate of oxidative metabolism. Type II (white) myofibers have a more rapid speed of contraction and both oxidative and glycolytic properties (Tseng et al., 2010). A shift in skeletal muscle fiber types has been reported for different genetically modified mouse models, among which we count p43 overexpressing mice; p43 mitochondrial T3 receptor induces a shift toward the contractile slow type phenotype (Casas et al., 2008).

### ***1.5c –Current Situation***

Because of the unacceptable side effects or inadequate long-term clinical efficacy, these medications have so far met with limited success, and thus the American Food and Drugs Administration (FDA) has only approved very few drugs specifically for weight loss. Unfortunately, effectiveness remains limited. To continue improving the chances of identifying most successful therapeutic approaches, a better understanding of the mechanisms linking adipose tissue development, function, and expansion is required.



## CHAPTER II: Mitochondria and Energy Homeostasis

### Generalities

In complex organisms, such as mammals, it is crucial that the metabolic demands of the various tissues are coordinated to ensure that the energy needs of the whole body are effectively met. The ability of an organism to convert organic molecules from the environment into energy is essential for the development of cellular structures, cell life, growth, differentiation and death. All these are attainable thanks to mitochondria. Mitochondria are organelles that provide about 90% of the energy required by a normal eukaryotic cell to function (Tao et al., 2014). The processes of glycolysis and oxidative phosphorylation (OXPHOS), allow for the transformation of the 'power' contained in the nutrients into a form of energy suitable for the cell: ATP; the currency of life.

Although mitochondria are best known for this main role, they fulfill a plethora of other functions such as homeostasis maintenance; cell death pathways coordination; heat production; steroid hormones, phospholipids and amino acids synthesis; and participation in stress associated events (Winklhofer and Haass, 2010; Snyder and Stefano, 2015). Moreover, mitochondria house and regulate a myriad of interconnected biochemical pathways (Pagliarini et al., 2008) (**Figure 15**).

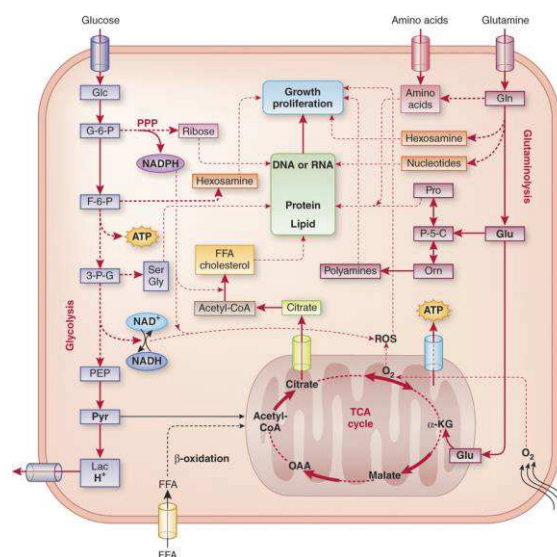


**Figure 15: Interconnection of metabolic pathways.**

Image from Wang and Green, 2012.

Secondly, mitochondria are highly dynamic structures. They respond with precise architectural modifications to  $\text{Ca}^{+2}$  signaling and other regulatory mechanisms (Liesa and Shirihai, 2013). However, they are not isolated or fixed in the cell; but instead form a dynamic network which is tightly regulated by two main phenomena: fusion and fission (Jakobs, 2006). This network is associated with cytoskeletal microtubules and with other organelles. Tight control of mitochondrial dynamics and functions is essential for maintaining an adequate energy balance.

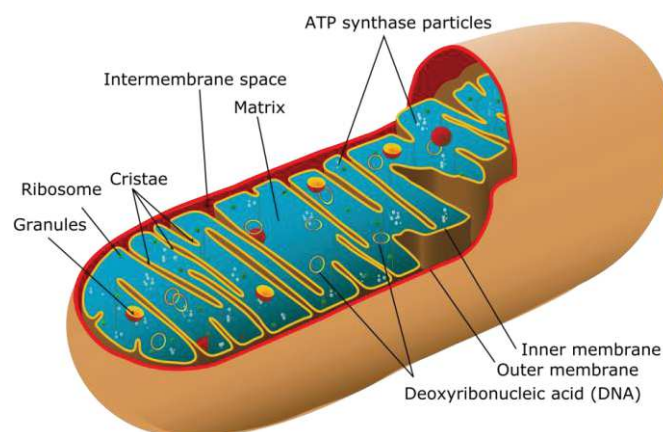
Mitochondria are present in all eukaryotic cells except for red blood cells. They are inherited maternally via the oocyte. Their shape, size and number are closely related to cellular activity, cell type and energy needs. Specific tissues — and perhaps even different sub-cellular locations — contain mitochondria of markedly different protein composition (Johnson et al., 2007). Nevertheless, they usually have an ovoid shape, and generally range from 1-2 to 10  $\mu\text{m}$  in length, and from 0.5 to 1  $\mu\text{m}$  in width. Regarding number, a somatic mammalian cell carries thousands of copies of the mitochondrial DNA (mtDNA) (Ameur et al., 2011).

## II.1 – Structure

Mitochondria are surrounded by two membranes, an external (MEM) and an inner (MIM) membrane, which delimit two separate compartments: the matrix and the intermembrane space (**Figure 16**).

- **MEM:** lipid bilayer composed of about 50% proteins and 50% lipids. This membrane is highly porous. On the one hand, molecules smaller than 10 kDa, such as ions, metabolites and the different nucleotides enter through channels called porins, or VDAC (voltage-dependent anion channel). On the other hand, proteins containing a mitochondrial targeting signal cross via translocases (TOM: translocase of the outer membrane). Thanks to the acquisition of ATP/ADP translocase, mitochondria have the ability to exchange ATP with the cells cytoplasm (Gabaldón and Huynen, 2004). The MEM also accommodates CPT-1 (Carnitine PalmitoylTransferase-1), which allows for the transport of the activated LCFA (Long Chain Fatty Acids) from the cytosol into the intermembrane space (see section **II.2a**).

- The **intermembrane space** is about 100 Å. It has a composition close to the cytosol and it is positively charged due to its richness in protons ( $H^+$ ).
- **MIM**: composed of 80% proteins and 20% phospholipids. Contrary to the MEM, this membrane is impermeable to ions, due to the presence of a particular phospholipid named cardiolipin (Clostre, 2001). Only  $O_2$ ,  $H_2O$ ,  $CO_2$ ,  $N_2O$  and  $NH_4$  may 'freely' move across. Shuttling systems, co-transporters, symporters and carriers such as ANT (Adenine Nucleotide Translocator), CPT II (Carnitine Palmitoyl Transferase II), or TIM (Translocase of the Inner Membrane) are necessary for other molecules. One of the peculiarities of the MIM is the so called mitochondrial crests. Tomographic studies have helped to highlight these foldings which imbibe the complexes of the respiratory chain (RC) (Hunte et al., 2000; Dimroth et al., 2000).
- The **matrix** is the inner compartment of mitochondria. Many metabolic pathways occur here:  $\beta$ -oxidation of FA, Krebs cycle, etc. It contains mtDNA, mitochondrial ribosomes and transfer RNA (tRNA).



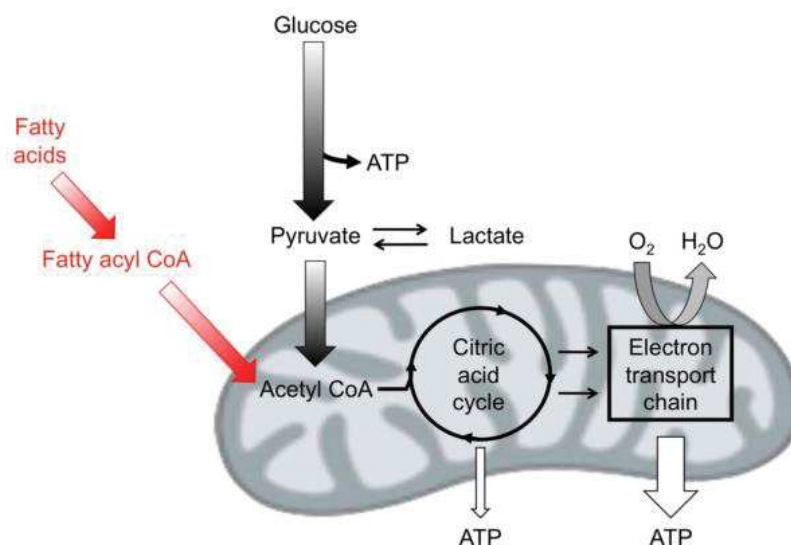
**Figure 16: Structure of mitochondria.**

Diagram showing the internal structure of mitochondria with the convoluted MIM housing the RC. Image from an internet source.

## II.2 – ATP Production

The main role of mitochondria involves ATP production and energy metabolism. We need so much energy in the form of ATP that in average, at the end of one's life we will have used over 40 kg of it (Bland and Birnbaum, 2011). Our cells are capable of metabolizing a variety of carbon substrates, including glucose, FAs, ketone bodies, and amino acids. Cellular fuel choice does not only fulfill specific biosynthetic needs, but also enables programmatic adaptations to stress conditions beyond compensating for changes in nutrient availability.

A cycle exists which serves as a basis for the analysis of energy production through ATP synthesis, and which is at the center of cells energy metabolism. This is the Krebs cycle, also known as Tricarboxylic Acid (TCA) cycle. To fuel it, glucose and FAs must be metabolized, in order to produce the same common intermediate, acetyl-CoA, which is fed into the TCA cycle. This is made thanks to a dyad of processes named Glycolysis and Fatty Acid Oxidation (FAO) (**Figure 17**).



**Figure 17: Glycolysis and FAO.**

Glycolysis and lipolysis provide Acetyl-CoA, which serves as a substrate for TCA, where NADH and FAD are produced. Through these two cofactors,  $e^-$  are donated to the ETC resulting in significantly larger production of ATP.

Glycolysis was defined in section **I.3a**, as the metabolic pathway that converts glucose into pyruvate. Within the mitochondria, pyruvate is converted to Acetyl-CoA and CO<sub>2</sub> in a process called pyruvate decarboxylation. Subsequently, Acetyl-CoA enters the so mentioned TCA cycle, where it is fully oxidized (Stanley et al., 2014). Glycolysis is an anaerobic process, and entails a low-energy production compared to aerobic respiration. One molecule of glucose can enter glycolysis and be fully processed to 2 pyruvate molecules, producing two NADH (reduced nicotinamide adenine dinucleotide) and two ATP molecules; or can enter the TCA cycle and generate bigger quantities of NADH, further 30 or so ATP molecules and another intermediary molecule: FADH<sub>2</sub> (Flavin Adenine Dinucleotide). NADH and FADH<sub>2</sub> are high energy reduced co-enzymes, which act as reducing equivalents, donating e<sup>-</sup> to the ETC (Electronic Transport Chain). As the e<sup>-</sup> pass down the chain, energy is captured in the form of a proton gradient which is then utilized to generate ATP. In the presence of alternative sources of anaerobically oxidizable substrates, such as FAs, FAO predominates over glycolysis regarding ATP production. Emerging evidence indicates that specific switches from utilization of one substrate to another, glucose to FAs and vice-versa, can have protective or permissive roles in disease pathogenesis (Stanley et al., 2014). FAO will be next described.

### ***II.2a – Fatty Acids Oxidation (β-oxidation)***

FAO is characterized by a series of reactions that decrease the size of FAs, reducing the Acyl-CoA chains by two carbons at every cycle (**Figure 18**). In this pathway, Acyl-CoAs are cyclically dehydrogenated, hydrated and decarboxylated, which results in the progressive shortening of the chains and the production of two RedOx cofactors which are: NADH and FADH<sub>2</sub>. These will then fuel the ETC, for ATP production. Higher quantities of them can be obtained by FA degradation than by glucose or pyruvate.

Approximately 80% of the energy needed by the heart and skeletal muscle is provided by FAO (Carracedo et al., 2013). In addition, this process is also used for BAT thermogenesis. In fact, FAO implies heat production instead of ATP synthesis in the presence of UCP1.

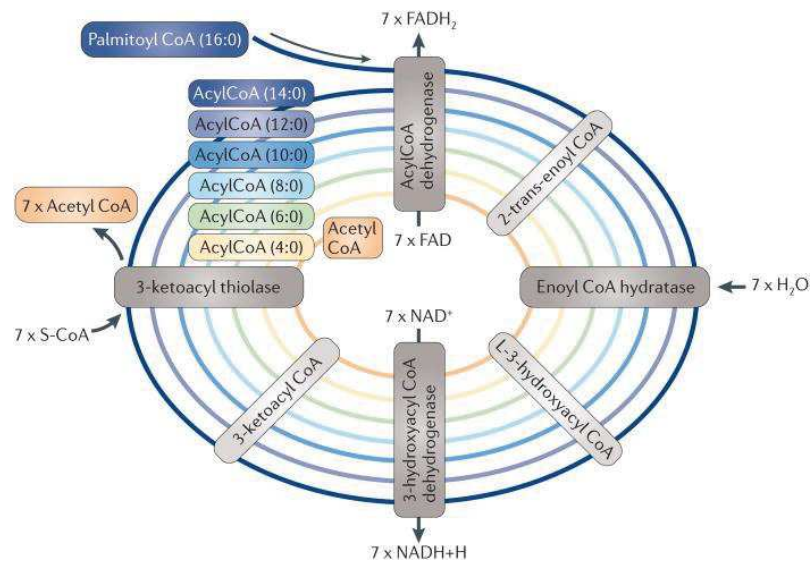


**Figure 18: Representation of the  $\beta$ -oxidation of palmitic acid in the mitochondria.**

Free Acyl-CoAs can be metabolized by FAO. FAO is characterized by a series of reactions that decrease the size of FAs, reducing the Acyl-CoA chains by two carbons at every cycle. Image from Carracedo et al., 2013.

Interestingly, FAO progression depends on the number of carbons of the FAs' aliphatic chain. Medium (6 to 12 C) and short (less than 6 C) chains can passively diffuse across the MEM and MIM to the matrix, where they are thought to be activated by different Acyl-CoA Synthetases (ACS). However, long chain fatty acids (LCFA), whose aliphatic chains' length is comprised in between 13 and 21 C, such as Palmitoyl-CoA (16:0), cannot freely diffuse through the MIM. Beforehand they require an activation step. To do so, LCFA are modified to fatty Acyl-CoAs thioesters, hence activated, by ACS located in the MEM. Then, prior to their entry into the intermembrane space via the carnitine shuttle, the long-chain Acyl-CoAs are converted into acyl-carnitine derivatives by CPT1, also located in the MEM. These acyl-carnitine derivatives are finally translocated across the MIM into the mitochondrial matrix by carnitine-acylcarnitine translocase. Another enzyme located on the matrix side of the MIM, CPT2, renews the acyl-CoA units. Once carried through the MIM and inside the matrix, FAs are oxidized to acetyl-CoA units so that, as previously mentioned, the FA chain length is reduced by two carbons in every cycle of  $\beta$ -oxidation. **Figure 19** depicts this process.



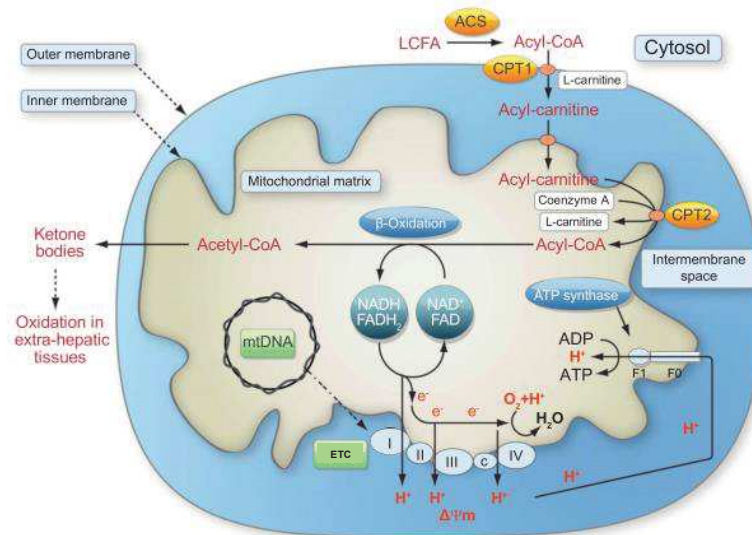


**Figure 19: Representation of mitochondrial FAO and OXPHOS in liver mitochondria.**

Adapted from Begriche et al., 2011.

It is important to mention that in response to a decrease of carbohydrate intake (e.g. fasting or starvation), CPT-1 will be up-regulated resulting in FAs entering FAO. On the contrary, upon feeding, FAs synthesis will be enhanced. This phenomenon is accompanied by high expression levels of malonyl-CoA, an allosteric inhibitor of CPT-1.

### **II.2b – The tricarboxylic acid (TCA) cycle (Krebs cycle)**

It takes its name from the German Hans A. Krebs (1900-1986). Despite the lack of support of his supervisor Otto Warburg, who even wrote that Krebs would never make it to a good biochemist (Kornberg, 2000), he disemboweled a series of sequential, reversible and irreversible reactions of carbohydrate oxidation that earned him a Nobel Prize in Physiology or Medicine in 1953 (Krebs and Johnson, 1937).

The TCA cycle or Krebs cycle is connected with many other metabolic pathways participating in cellular energy exchange (**Figure 15**). Glucose, lipids, amino acids and nucleic acids are broken down and re-synthesized in order to keep cell vital functions. Intracellular signaling controls the entrance of metabolites to the Krebs cycle and its regulation towards biosynthesis of macromolecules. **Figure 20** shows the enzymatic process related to this cycle.

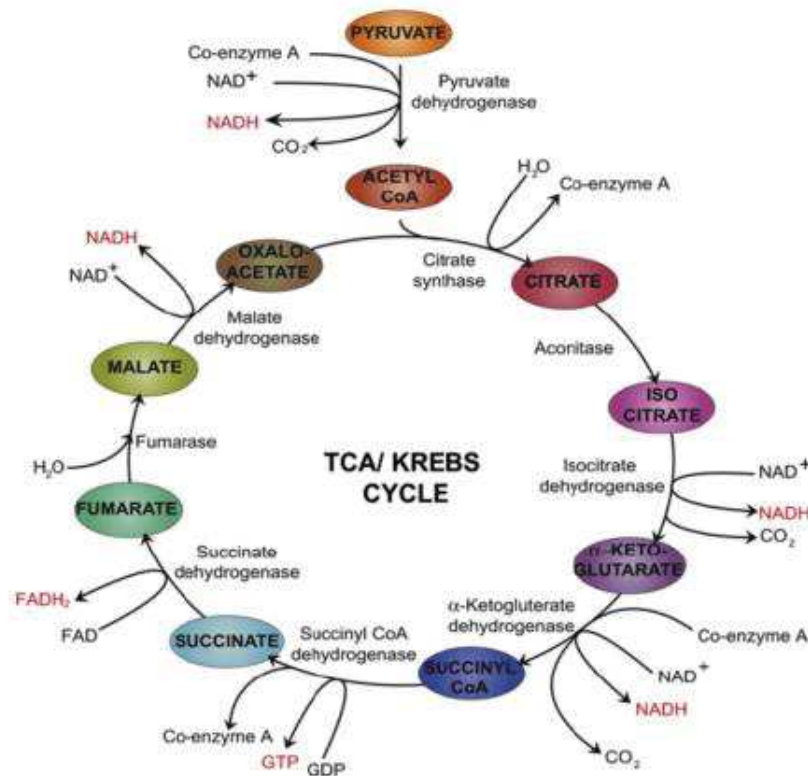


**Figure 20: Bioenergetics of the TCA/Krebs cycle.**

Pyruvate is converted to high-energy molecules like NADH, GTP and FADH<sub>2</sub> through catalyzation by TCA/Krebs cycle enzymes. Adapted from Osellame et al., 2012.

In the first step of the TCA, Acetyl-CoA plus oxaloacetate and water form citrate by a reaction catalyzed by the enzymatic activity of the citrate synthase. The next three steps, isocitrate, α-ketoglutarate and succinyl-CoA formation, are important for the release of NADH and CO<sub>2</sub>. The aconitase, isocitrate and α-ketoglutarate dehydrogenases catalyze these three oxidation steps. Subsequently, succinyl-CoA and succinate dehydrogenases will give rise to succinate and fumarate, releasing GTP and FADH<sub>2</sub> in the process. The succinate dehydrogenase directly connects the Krebs cycle to the ETC in a reaction that can be reversed. The liberated FADH<sub>2</sub> serves as an energy carrier that feeds e<sup>-</sup> to the complexes of the ETC. In the next reaction, the fumarate hydratase catalyzes the hydration of fumarate to generate malate. Finally, closing the cycle, the malate dehydrogenase converts the malate to oxaloacetate again, producing a final NADH molecule (Quinlan et al., 2012; Stobbe et al., 2012) (**Figure 20**).



## ***II.2c – The electron transport chain (ETC) and ATP synthesis***

To generate ATP, phosphorylation of ADP needs to take place. This reaction is catalyzed by the ATP synthase ( $F_0F_1$ -ATPase). This enzymatic complex is capable of pumping  $H^+$  back into the mitochondrial matrix thanks to the existence of an electrochemical gradient ( $\Delta\mu H^+$ ) ( $\Delta p$ ), also known as “the proton motive force” (Divakaruni and Brand, 2011). This was the basis of the Chemiosmotic Theory formulated by Peter Mitchell in 1961 for which he received the Nobel Prize (MITCHELL, 1961). Two components might be distinguished within this gradient:

- A pH gradient ( $\Delta pH$ ): the matrix becomes more basic
- A charge gradient ( $\Delta\psi m$ ): the matrix side of the MIM is negatively charged.

The charge difference normally rests at -150 to -180mV. It serves as a store of the oxidation energy for the various processes that take place across the MIM, and thus couples phosphorylation and  $O_2$  consumption (respiration). Meanwhile, the  $e^-$  are transported in successive steps through the ETC complexes, until they are received by  $O_2$  to generate  $H_2O$ .

The ETC is composed by five respiratory chain enzymatic complexes, held within the MIM (Lancaster, 2002), and together with the  $P_i$  carrier and the ATP/ADP translocase, they are referred to as the OXPHOS system (**Figure 21**). The first four enzyme complexes are involved in substrate oxidation and formation of the energy gradient, while the fifth (ATP synthase) employs this gradient to generate ATP. The order of intervention of these complexes is established by their RedOx potential, ranging from the most reducing to the most oxidant one. NADH and  $FADH_2$  donate  $e^-$  to complexes I and II, respectively. These  $e^-$  are then passed to complexes III and IV where  $O_2$  acts as the terminal oxygen acceptor. Oxidized  $NAD^+$  and FAD then re-enter the cycle.

To maintain a constant  $H^+$  gradient, respiration rate increases when proton pumps undergo “slip-redox”. This fleeing phenomenon results in reduced pumping of  $H^+$  for the same number of  $e^-$  transferred along the respiratory chain. This is theoretically possible in complexes I, III and IV, the three  $H^+$  pumping sites.

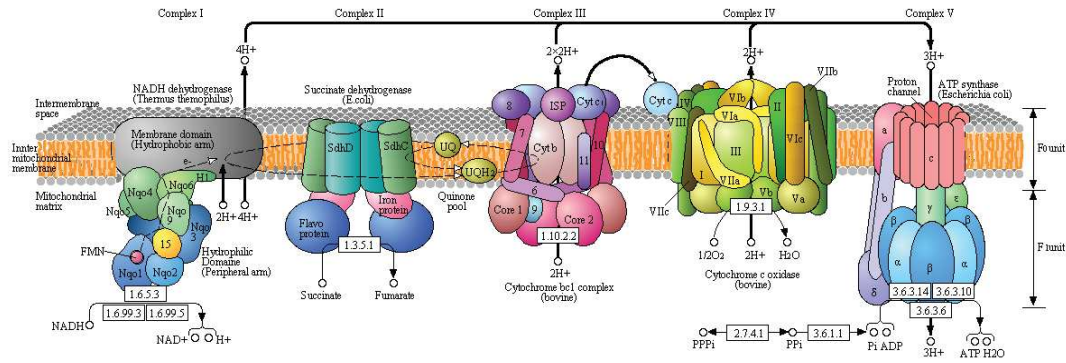


**Figure 21: The OXPHOS system.**

Image from Granata et al., 2009.

## II.2c<sub>1</sub> –The complexes from the mitochondrial ETC

The OXPHOS complexes (**Figure 21**) consist of proteins encoded by both the nuclear ( $n$  = approximately 100 in humans) and the mitochondrial genome ( $n$  = 13) (**Figure 22A**) (van Waveren and Moraes, 2008), except for complex II which contains proteins exclusively coded by the nDNA (nuclear DNA). The cells modulate the activity of these complexes depending on their energetic requirements.

### II.2c<sub>1.1</sub> – Complex I $\rightarrow$ NADH-coenzyme Q oxidoreductase

Complex I consists of 45 subunits; 38 nDNA coded, and 7 mtDNA coded (Carroll et al., 2006). This complex catalyzes the first OXPHOS reaction which consists on the oxidation of NADH and the transfer of two  $e^-$  to ubiquinone. The reaction is coupled to the translocation of two  $H^+$  from the mitochondrial matrix to the intermembrane space, contributing to the necessary force for driving ATP synthesis (Yagi and Matsuno-Yagi, 2003). Flavin mononucleotide (FMN) is the first  $e^-$  acceptor. It contains a catalytic site consisting on a Fe-S center (Sazanov, 2007) and it is located at the hydrophilic domain of the complex that contains the NADH binding site.

***II.2c<sub>1.2</sub> – Complex II → Succinate-Q oxidoreductase***

Complex II is composed by four subunits - A to D -, encoded by four different nuclear genes (Rustin and Rötig, 2002). It catalyzes the oxidation of succinate to fumarate via the intermediate oxidation of FADH<sub>2</sub> and the reduction of ubiquinone, allowing the transfer of two e<sup>-</sup> to complex III.

***II.2c<sub>1.3</sub> – Complex III → Cytochrome c oxidoreductase***

Complex III encloses 10 nDNA and 1 mtDNA coded subunits. It catalyzes the reduction of cytochrome C. During this reaction the coenzyme Q is oxidized and two H<sup>+</sup> move from the matrix to the intermembrane space (Link, 1995).

***II.2c<sub>1.4</sub> – Complex IV → Cytochrome c oxidase***

Complex IV accommodates 13 subunits; 10 nDNA coded, and 3 mtDNA coded. These proteins are synthesized in the cytoplasm and transported to the mitochondria (Borisov, 2002). Complex IV catalyzes the RedOx reaction from molecular O<sub>2</sub> to H<sub>2</sub>O. The produced e<sup>-</sup> are transferred to complex V. During this reaction, two H<sup>+</sup> are consumed and two other are transferred from the matrix to the intermembrane space.

***II.2c<sub>1.5</sub> – Complex V → ATP synthase***

Complex V is composed of two main linked subunits, F<sub>0</sub> and F<sub>1</sub>, located in the MIM and the matrix respectively. Acting as a rotor, this complex uses the passage of H<sup>+</sup> to operate. The F<sub>0</sub> portion, starts conducting the H<sup>+</sup> from the intermembrane space to the matrix (Schon et al., 2001). Later, they will go through the F<sub>1</sub> portion, which uses the ΔpH created thanks to the expulsion of H<sup>+</sup> by complexes I, III and IV to convert ADP into ATP. This conversion depends upon the magnitude of Δψ<sub>m</sub> and the ability of the respiratory chain to maintain it. The ATP formed during this reaction is anew exported to the cytosol in exchange for ADP.

## II.2c<sub>2</sub> – The Decoupling proteins →UCPs

UCPs may also be considered a part of the Oxidative Phosphorylation Pathway. As I have just explained, in classical mitochondrial dynamics fuel oxidation is linked to  $e^-$  transport, resulting in the development of an electrochemical gradient and in ATP synthesis. However, there is a tissue into which  $H^+$  flow back across the MIM without concomitant ATP synthesis. This tissue is BAT, a specialized organ which expresses the UCP1 isoform (see section I.1). UCP1, was actually herein discovered (Nicholls et al., 1978). This protein plays an indispensable role in thermogenesis, dissipating the  $e^-$  gradient at the ETC, in order to generate heat against certain physiological situations, or for other purposes (Lin and Klingenberg, 1980; Cannon, 2004). In the presence of UCP1, FAO (section II.2.1) implies heat production instead of ATP synthesis.

The UCP family features today five members which also locate within the MIM. Even if their general role in regulating cellular energy transduction has been described in the literature, the detailed impact of the rest of UCPs on body metabolism remains not fully understood. However, an association with conditions such as insulin resistance in diabetes and atherosclerosis, as well as an increase with starvation and sepsis have been shown (Cadenas et al., 1999; Blanc et al., 2003; Chan and Harper, 2006). Given these linkages, UCPs have been suggested as attractive therapeutic target for diseases rooted in metabolic imbalance and oxidative stress (Divakaruni and Brand, 2011).

The rest of the isoforms, other than UCP1, were later identified in different tissues, based on their sequence similarity. A 57% homology is shared by both, UCPs -2 and -3 (Pecqueur et al., 2001). UCP2 (Fleury et al., 1997) is widely expressed in most mammalian tissues (Azzu et al., 2008), whereas we find UCP3 (Boss et al., 1997) predominantly expressed in fat, skeletal and cardiac muscle (Krauss et al., 2003; Aguirre and Cadenas, 2010). Studies using KO animal models for these UCPs prevail conflicting (Nedergaard and Cannon, 2003). UCP3 (-/-) mice showed no changes in  $O_2$  consumption compared to WT in muscle mitochondria (Cadenas et al., 2002). However, one year before, an increase in skeletal muscle ATP synthesis *in vivo* in UCP3 (-/-) mice was shown by Gary W. and colleagues (Cline et al., 2001), which was accompanied by a

concomitant reduction in  $H^+$  leak (Vidal-Puig et al., 2000). Moreover, over-expression of UCP3 in mice caused fat-specific weight loss (Clapham et al., 2000; Cadenas et al., 2002).

The fourth (Mao et al., 1999) and fifth (Yu et al., 2000) members of this family, UCP-4 and -5, exhibit a tissue-specific distribution, being largely expressed in mouse brain. Furthermore, they have been suggested to be involved in tissue-specific thermoregulation and metabolic changes associated with nutritional status (Yu et al., 2000).

### ***II.2d – The OXPHOS system regulation***

The OXPHOS system is mainly regulated by the cellular calcium ( $Ca^{2+}$ ) signaling,  $H^+$  and phosphorylation. The permeability of the MEM to  $Ca^{2+}$  is voltage dependent, meaning that the VDACS become impermeable or permeable according to  $\Delta\Psi$ . When the cell demands more energy, more  $Ca^{2+}$  is transferred to the mitochondria matrix. Here, the  $Ca^{2+}$  accumulation is counteracted by the mitochondrial  $Na^+/Ca^{2+}$ ,  $H^+/Ca^{2+}$  exchangers.

Natural leak of  $H^+$  across the MIM is the main cause of incomplete coupling of mitochondria. This is at the origin of the lost as heat of some of the RedOx energy in substrates during oxidative phosphorylation (Brand, 2000; Divakaruni and Brand, 2011). “Futile”  $H^+$  cycling comes at a tremendous energetic cost: up to 20–25% of an animal’s BMR (Basal Metabolic Rate) may be attributable to  $H^+$  leak (Rolfe et al., 1999). The Basal proton leak is nonetheless physiologically essential. It is cell-type specific, correlates with metabolic rate (Jastroch et al., 2011), is inversely proportional to body mass (Bourne, 1993; Brand et al., 2003) and is exclusively related to the physicochemical properties of the MIM.

In relation to phosphorylation, several studies have shown that all OXPHOS components can be phosphorylated, even the small  $e^-$  carrier cytochrome C is Tyr phosphorylated *in vivo* (Hüttemann et al., 2007).

### **II.3 – Mitochondrial DNA**

#### ***II.3a – Origin and evolution***

The idea that mitochondria could have originated from preexistent prokaryotic organisms has become a paradigm in biology. Many questions concerning the coexistence of these two separated organisms have been raised. Mitochondria are thought to have joined the pre-eukaryotic cell at its very origin, 3 billion years ago, descendants of the bacterial phylum  $\alpha$ -proteobacteria, instituting an advantageous metabolic cooperation that has allowed the maintenance of this association over centuries (Baluka, 2009; Martin, 2010; Lukeš et al., 2011; Gray, 2012; Blackstone, 2013). It is difficult to clearly define which were the exact events that gave rise to the symbiotic alliance currently existing between the mitochondria and the cells. Some theories postulate that pre-eukaryotic cells interiorized mitochondria by phagocytosis (de Duve, 2007). Another hypothesis states that the mitochondrion may have been an invasive, parasitic bacterium and that the symbiosis emerged by a nutritional synchrony, based on nutrients transfer (Searcy, 2003). These queries are difficult to answer because there are no physical records of the extinct transition forms of mitochondria and eukaryotic cells, only current observations. Thus, explaining the first interactions between mitochondria and the eukaryotic cells is still a matter of debate.

#### ***II.3b – Structure and organization***

Nuclear and mtDNA possess very different characteristics. Rigorously speaking, the replication of this last one is nuclear independent, but the enzymatic components required for this process, along with transcription and translation, have a nuclear origin (Scarpulla, 1997; Enríquez et al. 1999; Taanman, 1999).

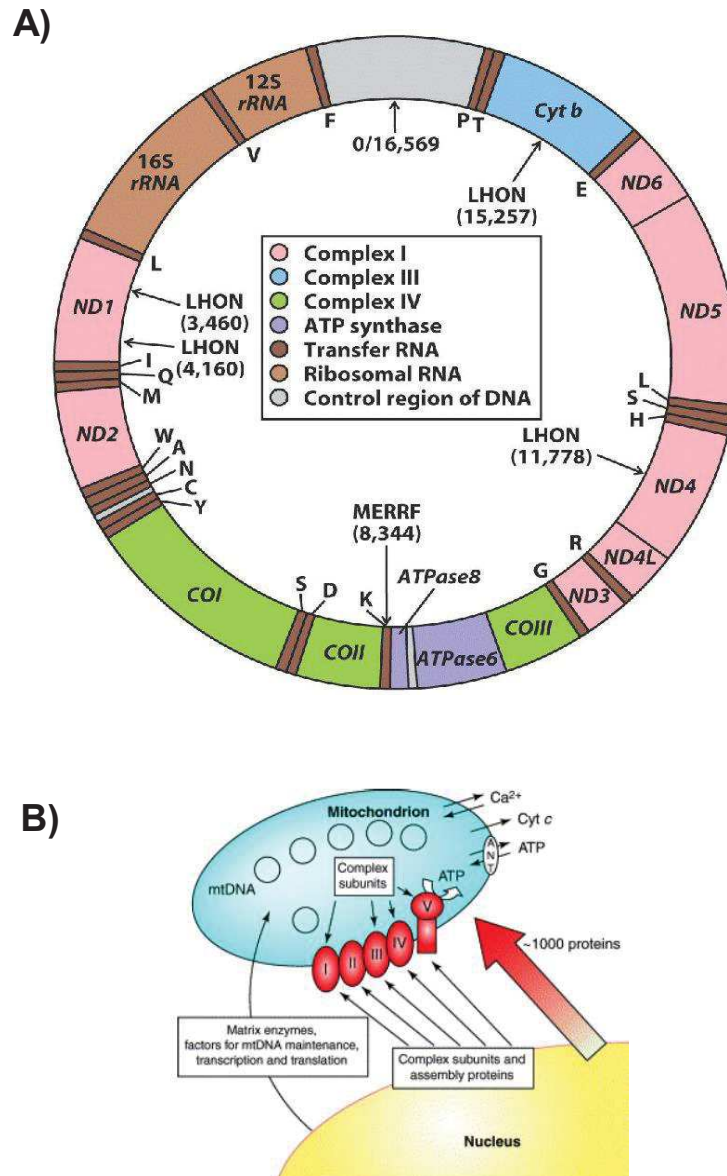


**Figure 22: Mitochondrial genome and intercommunication between the nucleus and mitochondria.**

**A)** Mitochondrial genome. Image from source internet.

**B)** Thirteen essential polypeptide respiratory chain complex subunits are synthesized in the mitochondrial matrix from mtDNA. More than 1000 different mitochondrial proteins are synthesized in the cytosol from nuclear DNA. Image from Chinnery, 2003.

In mammals, the mitochondrial genome is a double stranded circular DNA of about 16.600 bps. Concretely, in mouse, a 16.295 bps closed circular DNA has proved to be a model system for studies of mtDNA replication (Gillum and Clayton, 1978; Bogenhagen et al., 1981). The human one is 16.569 bps long



(Cotter et al., 2004), self-replicating and contains a double-stranded, circular DNA. The strands differ in terms of their G+C content, thus distinguishing a light chain (L) and a heavy chain (H), where most of the information is encoded.

The hallmark of mammalian mtDNA organization is the extreme economy of DNA sequence management. The genome displays exceptional economy of space, with a high degree of organization. Genes lack introns and both tRNAs and rRNAs are unusually small, with tRNA genes interspersed between rRNA, and protein coding genes with zero or few non-coding nucleotides between the coding sequences. Some of these genes overlap and it occurs sometimes that the generation of the stop codons befalls post-transcriptionally (Taanman, 1999).

The majority of proteins involved in mitochondrial function are nonetheless nuclear encoded. They are synthesized in the cytosol and then targeted to mitochondria (Elstner et al., 2009). It is estimated that more than 1000 mitochondrial proteins are derived from nuclear genes. In mouse and human, mitochondrial coded genes include overall: 12S and 16S rRNAs, tRNAs required for protein synthesis and essential genes for OXPHOS. Mouse mtDNA is highly homologous in global sequence and in gene organization to the human mtDNA (Bibb et al., 1981). However, mouse mtDNA is unique concerning the translational start codon. Any of the four nucleotides may occupy the third position on the AUN triplet codon, whereas the only translational stop codon is the orthodox UAA. **Figure 22A** displays the mitochondrial genome and **Figure 22B** partially illustrates the so described intercommunication between the nucleus and mitochondria. One example worth mentioning is the mitochondrial nucleoid protein M19 for whom a modulatory functional link has been established with the activity of the ETC, leading to the regulation of major cellular processes such as myogenesis and insulin secretion (Cambier et al., 2012).

### ***II.3c – Transcription regulation***

As described before, mitochondria have their own genome, but it only encodes a part of the ETC proteins. Farther mitochondrial proteins are encoded by the nuclear genome. This double origin requires a detailed and coordinated regulation (Scarpulla, 2006). Therefore, there exist key regulatory factors



encoded by nDNA which will allow firstly the transcription of the mtDNA and secondly the expression of nuclear genes encoding mitochondrial proteins.

### **Nuclear control of mitochondrial functioning**

The main feature of the genes coding for the members of the OXPHOS system is that they are located within two different genomes. The vast majority of them are nuclear genes, with only a few being encoded by the mitochondrial genome. Apart from the implications derived from the different position of both genomes, it is important to note that these are two very different genetic systems. Each of them has a particular arrangement of genes and distinct requirements for the transcription and translation processes (Enriquez et al., 1999b). OXPHOS genes which are nuclear encoded exhibit the typical characteristics of the RNA polymerase II transcription, thus presenting a particular number and distribution of introns and exons. Each strand contains a promoter for the initiation of transcription, the HSP (heavy strand promoter) and LSP (light strand promoter). Transcription results in the formation of polycistronic RNA precursors which encompass the entire genetic information of each strand. These RNA are processed to produce mRNAs, tRNAs and rRNAs.

#### ***II.3c<sub>1</sub> – Mitochondrial transcription factors coded by nDNA***

Mitochondria have their own transcription machinery, whose elements are encoded by the nuclear genome.

- POLRMT (mitochondrial DNA-directed RNA polymerase): this is an enzyme responsible for mitochondrial gene expression as well as for providing RNA primers for initiation of replication of the mtDNA. To interact with the promoter, it requires TFAM and TFB1M or TFB2M.
- TFAM (mitochondrial transcription factor A): this is a key activator of mitochondrial transcription as well as a participant in mitochondrial genome replication.
- p43 (truncated c-ErbA protein): this is a mitochondrial T3 receptor that acts as a mitochondrial transcription factor and consequently stimulates mitochondrial activity and mitochondrial biogenesis (Casas et al., 1999).

- TFB1M and TFB2M (mitochondrial transcription factor B1 and B2): these enzymes act as methyltransferases regulating the assembly and stability of the mitochondrial ribosome.
- mTERF (mitochondrial transcription termination factor): it plays different roles which are not restricted to transcription termination, but concern also transcription initiation and the control of mtDNA replication.

### ***II.3c<sub>2</sub> – Transcriptional regulators of nuclear genes coding mitochondrial proteins***

The expression of nuclear genes encoding mitochondrial proteins, and regulating mechanisms of mtDNA replication and transcription is finely coordinated. This coordination is possible thanks to 'actors' such as:

#### **NRF1**

NRF1 (Nuclear Respiratory Factor-1) is a transcription factor which has been shown to interact with promoters of several genes encoding for different subunits of the ETC complexes, and for proteins involved in mtDNA replication and transcription, like POLRMT, TFAM, TFB1M and TFB2M (Scarpulla, 2006).

#### **NRF2**

This transcription factor has been identified as a transcriptional activator of the gene encoding the subunit IV of cytochrome c oxidase, TFAM, TFB1M, TFB2M and three of the four subunits of succinate dehydrogenase (Scarpulla, 2002 ; Kelly and Scarpulla, 2004).

#### **PGC1 $\alpha$**

This protein belongs to a family of transcriptional coactivators playing an essential role in the integration and orchestration of the mitochondrial biogenesis program. PGC1 $\alpha$ 's expression and activation are regulated by signaling pathways initiated by environmental stimuli. It represents an energy sensor capable of inducing the appropriate mitochondrial modifications. PGC1 $\alpha$  notably interacts with NRFs, inducing the expression of genes encoding for proteins of the ETC as well as for factors required for mitochondrial replication and transcription (Scarpulla, 2006; Scarpulla, 2008). Furthermore, PGC1 $\alpha$  regulates the expression of genes encoding proteins involved in the mitochondrial FAO

(Vega et al., 2000), by interacting with PPAR $\alpha$  and ERR $\alpha$  (Estrogen Related Receptor alpha).

### ***PGC1 $\beta$***

This transcriptional coactivator exhibits strong structural homology with PGC1 $\alpha$  (Austin and St-Pierre, 2012). They partially co-activate several transcription factors; importantly those inducing the expression of genes involved in the regulation of mitochondrial energy metabolism (Meirhaeghe et al., 2003).

## ***II.4 – Mitochondrial dysfunction & disease***

Mitochondrial dysfunction is a generic term, which includes alteration of different metabolic pathways and damage to mitochondrial components (Begrache et al., 2011). Mitochondrial dysfunction causes over 50 diseases ranging from neonatal fatalities to adult-onset neurodegeneration (Dimauro and Schon, 2003; Lowell and Shulman, 2005; Wallace, 2005). Recent epidemiological studies have provided evidence that disorders of the mitochondrial respiratory chain affect at least 1 in 5000 of the population (Schaefer et al., 2004). These figures make these disorders some of the most common genetic diseases (Chinnery, 2003; Peng et al., 2015). Mitochondrial disease results in different degrees of failure of this organelle. Proceeding from different casualties, the consequences are collective; defeat to produce the energy needed for the sustainment of life and growth of an organism. Post-mitotic tissues, such as muscle and brain, are the most sensitive to mtDNA changes, due to their high energy requirements and non-proliferative status. Most of the damage related to mitochondria is caused in such organs, with high energy consumption. Less often, heart, liver and kidney are also affected. However, if the mitochondrial weakness happens throughout the organism, the whole system begins to fail.

A growing body of research demonstrates that altered mitochondrial energy production, particularly in skeletal muscles, is a major anomaly capable of setting off a chain of metabolic events leading to obesity (Rogge, 2009).

## Mitochondria in Obesity

A normal mitochondrial function is required for maintaining the appropriate balance between energy storage and expenditure. Nutrient excess leads to mitochondrial dysfunction with the consequential effects on lipid and glucose metabolism (Bournat and Brown, 2010). This is partially due to the harmful effects of ROS. Affecting mitochondrial metabolism generally favors ROS generation and the subsequent development of oxidative stress. A mechanism involving a deleterious effect of high TG on the functioning of the mitochondrial ETC by promoting superoxide generation has been proposed (Martínez, 2006; Monteiro and Azevedo, 2010).

Recent studies also suggest that the actions of mitochondria would extend beyond their conventional role as generators of heat. There is mounting evidence that impaired mitochondrial respiratory capacity is accompanied by attenuated expression of UCP1 and other BAT-selective genes, implying that mitochondria would exert transcriptional control over gene programs involved in oxidative metabolism and thermogenesis (Nam and Cooper, 2015) (**Figure 23**).

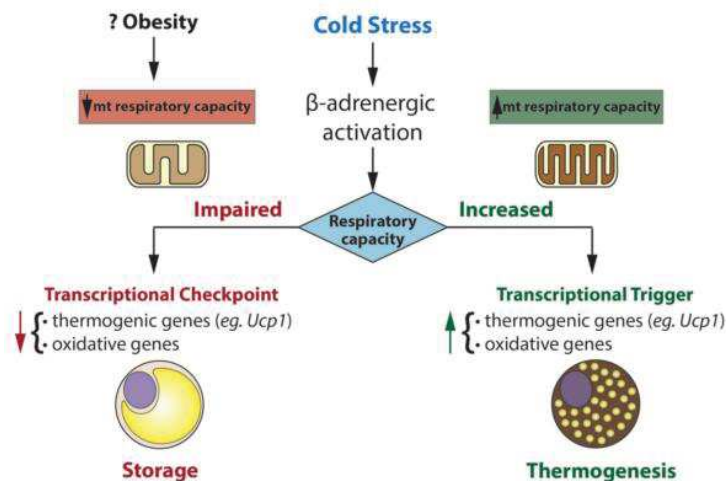


**Figure 23: Mitochondrial transcriptional control over storage and thermogenesis gene programs.**

Transcriptional control is dependent on mitochondrial respiratory capacity. In this model, impaired respiratory capacity acts as a transcriptional checkpoint, whereas augmented respiratory capacity acts as a transcriptional trigger. Adapted from Nam and Cooper, 2015.

Additionally, Gospodarska and colleagues have described differences in between BAT and WAT concerning mitochondrial turnover during temperature transitions (Gospodarska et al., 2015). Their results indicated that dynamics of brown adipocytes turnover during reversible transition from warm to cold may determine the thermogenic capacity of an individual in a changing temperature environment. Mitochondrial dynamics, fusion and fission, together with the two main regulators, mitofusins (Mfn1 and Mfn2) have also been implicated in studies where the participation of mitochondrial dysfunction for metabolic disorders is highlighted. Moreover, an important role of mitochondrial dynamics has been revealed regarding the neuronal populations orchestrating the regulation of hunger and satiety (Nasrallah and Horvath, 2014). Furthermore, it has been shown that when mitochondrial abnormalities cannot be dealt with, there is an increased chance that major illnesses like T2D, Alzheimer's disease, and cancer may occur (Snyder and Stefano, 2015).

## **II.5 – Mitochondrial databases**

If we search on Pubmed for “mitochondrial databases” without any other filter, we will encounter a digit slightly higher than 1500 results. If we further specify for “homo sapiens” or “mus musculus” results are reduced to 765 and 106 respectively (summer 2015).

To study and illustrate the biology of this organelle, an expanded mitochondrial inventory and several tools are nowadays available. Among them we find: ChloroMitoSSRDB, GOBASE, HMPDb, InterMitoBase, MamMiBase, MitoCarta, MitoDat, MitoData, MitoDrome, MitoGenesisDB, MitoInteractome, MitoMiner, MitoProteome, MitoRes, MitoZoa, MitPred, MPIMP db, mtDB, OGRe, etc.

Since MitoCarta, is a very complete and reliable database for rodents, this is the one we have used for analyzing our results. Therefore, this is the only one I will describe in brief in this manuscript.

***MitoCarta***

MitoCarta is a compendium of genes encoding proteins with strong support of mitochondrial localization which is freely available in the net. The first version dates from seven years ago (Meisinger et al., 2008; Pagliarini et al., 2008). A second one, MitoCarta2.0 released 2015, is in review for publication (Calvo, S.E., Klauser, C.R., Mootha, V.K. MitoCarta2.0: an updated inventory of mammalian mitochondrial proteins). MitoCarta2.0 is an inventory of 1013 human and 1098 mouse genes. To generate this inventory, the authors performed mass spectrometry of mitochondria isolated from fourteen different tissues. They assessed protein localization through large-scale GFP tagging and microscopy. Then, these results were integrated with six other genome-scale datasets of mitochondrial localization (Pagliarini et al., 2008).

## CHAPTER III: Pre-mRNA Splicing

### Introduction to pre-mRNA Splicing

Splicing is the process by which portions of eukaryotic pre-messenger RNA (pre-mRNA), called introns, are removed and the remaining sets of sequences, exons, are ligated together to form the final mRNA product. Only the processed mRNA is translated into a protein or exerts a function as non-coding RNA, and so splicing plays an essential role in the phenotype of higher eukaryotic cells. While the majority of exons are constitutively included in the final mRNA, some exons, or just portions of exons, may be excluded from the mRNA in certain cells or under specific conditions. This process is referred to as Alternative Splicing (AS) and plays central role in generating complex proteomes from defined genomes.

#### III.1 – Constitutive Splicing

Introns must be defined prior to their excision. Three conserved sequence elements are required for efficient pre-mRNA splicing (Lim and Burge, 2001). They allow intron recognition and subsequent removal, and constitute the binding platform for the spliceosome. These essential sequences are: the 5' splice site (5'SS) or splice donor, the 3' splice site (3'SS) or splice acceptor, and the branch point sequence (BPS), that is preceded by a polypyrimidine tract (Wahl et al., 2009) (**Figure 24**).

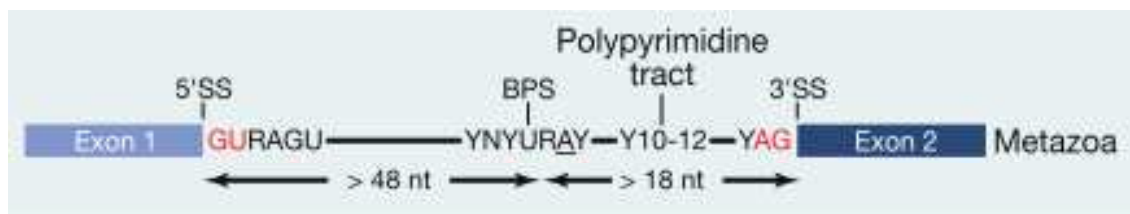


**Figure 24: Splicing reactive sites.**

Conserved sequence elements within pre-mRNAs intron in metazoan. Adapted from Wahl and Lührmann, 2015.

Nuclear pre-mRNA splicing encompasses a two-step process that involves two transesterification reactions. These are simple chemical processes involving the splicing reactive sites that I have just described above. In the first place, the

phosphodiester bond at the 5' SS is attacked by the 2'-hydroxyl of the adenosine of the BPS in the intron, which generates a free 5' exon and an intron lariat-3' exon. Subsequently, during the second step, the 3'-hydroxyl from the free 5' exon attacks the phosphodiester bond at the 3'SS, leading to exon ligation and excision of the lariat intron (Wahl et al., 2009) (**Figure 25**).

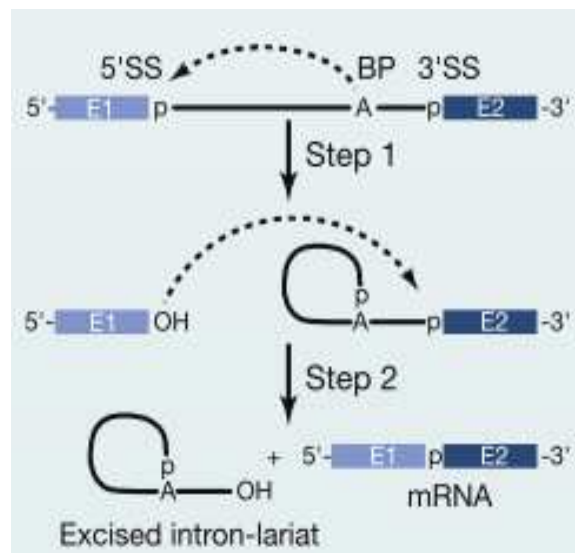


**Figure 25: Chemistry in the splicing reaction.**

The splicing reaction requires two subsequent transesterification reactions, which allow for the excision of intron-lariat and the ligation of the 5' and 3' exons. Adapted from Wahl and Lührmann, 2015.

### III.2 – Alternative Splicing

Alternative splicing is one of the mechanisms by which two different cells with the exact same genetic code can have entirely different structures and functions. So far, the mammal species with the highest proportion of AS is human, with 95% of multi-exon genes showing evidence of AS (Pan et al., 2008). There are important aspects for specificity in AS like species specific, development stage specific, sex specific and tissue specific AS. Tissue specific AS events are closely associated with specific tissue functions (Wang and Burge, 2008; Taliaferro et al., 2011). If we compared the cells in our skin to the cells in our eyeball, we would see that they have virtually identical genetic information, despite their obvious differences. The combinatorial nature of expressing different parts of different genes, at different stages or conditions, literally



results in an infinite number of possible ways to determine how our cells look and behave.

In eukaryotes, different categories of AS events can provide a multitude of isoforms of RNA from the same pre-mRNA (Blencowe, 2006; Wahl and Lührmann, 2015b). So far seven AS events compose the list of alternative mRNA processing. These are illustrated in **Figure 26**.

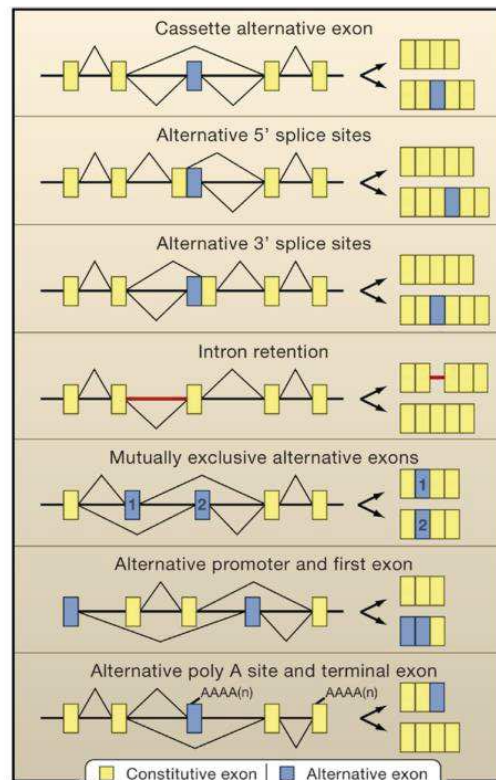


**Figure 26: Alternative Splicing Events (ASEs) in Metazoan Transcripts.**

Types of AS that are responsible for the generation of functionally distinct transcripts are depicted. Blue boxes indicate alternative exons. Adapted from Blencowe, 2006.

AS regulation of eukaryotic exons is increasingly recognized as playing a central role in the phenotypic variation of genotypically identical cells, and the misregulation of AS has been implicated in many of the complex and unsolved diseases burdening today's society (Matlin et al., 2005). The ability to control AS in a targeted and predictable fashion *in vivo* would give us some degree of power to control the phenotype of individual cells, as well as entire tissues, organs, and possibly even whole organisms. Potential applications of this ability include the treatment, prevention, and

curing of diseases driven by AS misregulation (Garcia-Blanco et al., 2004; Tang et al., 2013) and the reprogramming of stem cells in order to regenerate vital tissues and/or organs (Salomonis et al., 2010).

### III.2a – Alternative splicing determinants

Splicing can occur either co- or post-transcriptionally (Pandya-Jones and Black, 2009). A wide variety of factors are thought to contribute to AS outcome. An integrated model for the regulation of AS is summarized in **Figure 27** (Luco et al., 2011). The splicing reaction is conducted by a specific set of proteins that collectively make up a molecular machine called the spliceosome (Matera and Wang, 2014), that will be further detailed in section III.3. Specific consensus sequences are recognized by spliceosomal components and help define the SS. Those sequence elements are highly conserved in yeast, but extremely degenerated in higher eukaryotes. In fact, not all exons contain the consensus sequences at their SS, distinguishing them as strong and weak. SS resembling the consensus sequence are referred to as strong, while the remaining are denominated weak. As their names imply, strong SS are bound efficiently by the spliceosome, while weak SS are not. Competition between adjacent SS is thought to be one of the main drivers of AS outcomes (Kornblihtt et al., 2013).

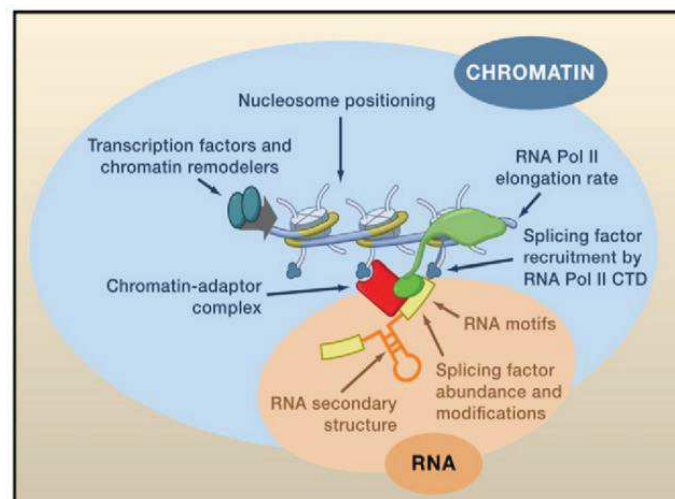


**Figure 27: Overview of AS determinants.**

Alternative splicing patterns are determined by a combination of parameters including cis-acting RNA regulatory elements and RNA secondary structures (highlighted in orange) together with transcriptional and chromatin properties (highlighted in blue) that modulate the recruitment of splicing factors to the pre-mRNA. Image from Luco et al., 2011.

### III.2b – Regulation of alternative splicing

Besides, the above described well characterized sequence elements (5'SS, 3'SS and BPS), a number of other sequences have been reported to influence pre-mRNA splicing. Splice site choice is also regulated through cis-acting splicing regulatory elements (SREs) and trans-acting splicing factors. Such sequences can be found within introns or exons and can stimulate or inhibit the splicing of a given exon. On the basis of their relative locations and activities, SREs are classified as exonic splicing enhancers (ESE), intronic splicing enhancers (ISE), exonic splicing silencers (ESS) or intronic splicing silencers (ISS). The recruitment of spliceosomal components can be enhanced or inhibited by the binding of these regions on the nascent transcript and by the binding of splicing factors (SF's), typically the Serine-Arginine Rich family of proteins (SR proteins) (Fu, 2014). Distinct SF's modulate a set of adipogenesis-related ASEs with biological relevance. The so far known adipose-related splicing regulators and events are summarized in **Table 3**.

#### Distinct SF's modulate a set of adipogenesis-related ASEs

Splicing Factor or Regulator	AS Event	Adipocyte	Biological Signatures
Sam68	<i>mTOR</i>	WAT	Promote adipogenesis
SRSF10	<i>Lipin1</i>	WAT	Differentiation/Lipid storage
SRp40	<i>PPAR<math>\gamma</math></i>	Pre-adipocyte	Promote adipogenesis
SRSF2 & FTO	<i>RUNX1T1</i>	WAT	Promote adipogenesis
RBM4a	<i>PPAR<math>\gamma</math></i> , <i>Pref-1</i>	BAT	Enhance differentiation and metabolism of BAs
	<i>INSR</i> , <i>MEF2C</i>		

#### Exon usage and biological relevance of adipocyte-related ASEs

Gene	AS Region	Adipocyte Isoform	Biological Signatures
<i>mTOR</i>	Intron 5	Excluded	Promote white adipogenesis
<i>Lipin 1</i>	Exon 7	Included/Excluded	Differentiation/Lipid storage
<i>INSR</i>	Exon 11	Included	Promote brown adipogenesis
<i>MEF2C</i>	Alternative 3' splice site of Exon 10	Distal	Promote brown adipogenesis
<i>NcoR</i>	Exon 37b	Included/Excluded	Proliferation/Differentiation
<i>PKC<math>\delta</math></i>	Alternative 5' splice site of Exon 9	Proximal	Promote adipogenesis
<i>CETP</i>	Exon 9	Included	Promote lipid metabolism
<i>RUNX1T1</i>	Exon 6	Included	Promote white adipogenesis
<i>ODC</i>	Exon 1, 2 and 3	Selection of exon 2 and 3	Promote lipid accumulation

**Table 3: Summary of Adipose-related Splicing Regulators and Events**

Adapted from Lin, 2015.

Common SF's include the so-mentioned SR proteins, which recognize ESEs to promote splicing, as well as various heterogeneous nuclear ribonucleoproteins (hnRNPs), which typically recognize ESSs to inhibit splicing. These antagonistic activities are essential determinants of SS selection in a concentration dependent manner.

SR proteins constitute a family of proteins currently integrated by 12 members (**Figure 28**). Their principal role consists on the regulation of both constitutive and alternative splicing, but they can also participate in other functions such as regulation of mRNA stability (Zhang and Krainer, 2004) and microRNA processing (Wu et al., 2010). This family of proteins is characterized by one or more RNA recognition motifs in their N-terminal (RRM domain), and by a serine-arginine rich region in C-terminal (RS domain). Their activity is mainly regulated by posttranslational modifications of their RS domain, essentially serine phosphorylations.

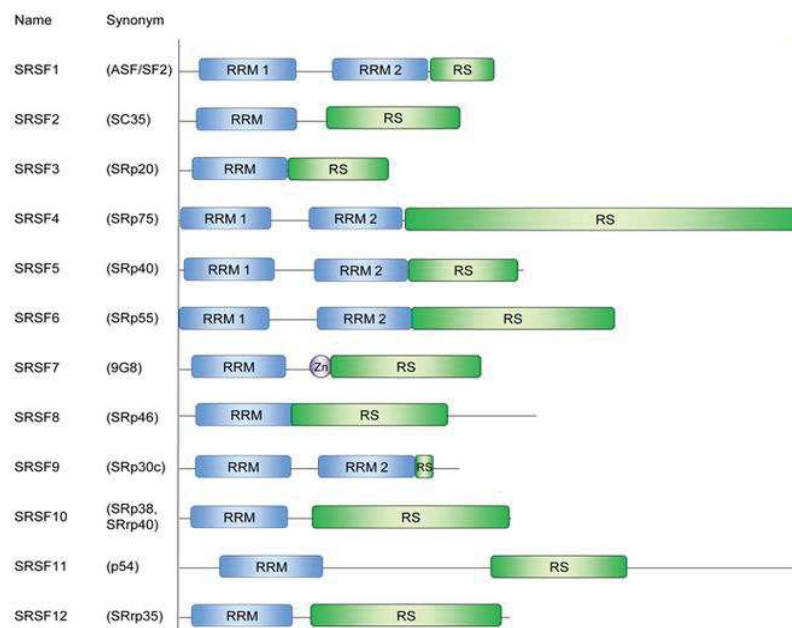


**Figure 28: Schematic representation of the 12 human SR proteins.**

Adapted from Twyffels et al., 2011.

The hnRNP family plays the opposite role in AS regulation, counteracting the activity of SR proteins. Besides this established association with the splicing apparatus, hnRNP proteins are involved in preventing folding of pre-mRNA into

secondary structures and transporting mRNA out of the nucleus. This family incorporates more than 20 proteins, which generally include one or more RRM. Nonetheless some hnRNPs rather bind RNA via another domain.

### **III.3 –The spliceosome**

RNA splicing, whether constitutive or alternative, is catalyzed by the macromolecular machinery known as the spliceosome. The spliceosome consists on a set of small nuclear ribonucleoprotein particles (snRNPs) such as U1, U2, U4/U6, and U5, which assemble together with associated proteins into different complexes. Many other non-snRNP proteins are also a part of this machinery (Zhou et al., 2002). Each snRNP consists of a snRNA (or two in the case of U4/U6) and a variable number of complex-specific proteins.

The spliceosome is a highly dynamic structure that constantly re-arranges during a pre-mRNA splicing cycle and whose assembly on the target transcript is a stepwise process that requires binding and releasing of its different snRNPs as well as the other splicing factors.

#### **Step wise spliceosome assembly**

Although spliceosome assembly is best-understood in budding yeast, the key assembly steps are well conserved in evolution (Matera and Wang, 2014). First, assembly begins with the recognition by U1 snRNP of the 5'SS via base pairing of U1 snRNA to the mRNA, forming the early complex (complex E). This process is facilitated by the Pol II CTD. The interaction between the 5'SS and U1 snRNP in complex E is ATP- independent and fairly weak. It is stabilized by other factors, such as members of the SR protein family (Cho et al., 2011) and the cap-binding complex (CBC) (Pabis et al., 2013). Indeed, most of the functionally important RNA-RNA interactions formed within the spliceosome are weak and generally require the assistance of proteins to enhance their stability (Wahl et al., 2009). The 3'SS of the pre-mRNA is recognized by the U2 snRNP and associated factors, such as splicing factor 1 (SF1) and U2 auxiliary factors (U2AFs), which are also components of the complex E. After that, U2 snRNA recognizes sequences around the BPS adenosine and interacts with U1 snRNP in an ATP-dependent manner, to form the pre-spliceosome (complex A). In a subsequent transition step, U1 and U2 snRNPs undergo rearrangements, which bring the 5'SS, BPS and 3'SS into close proximity (De Conti et al., 2013). After the assembly of



complex A, the U4–U6 and U5 snRNPs are recruited as a preassembled tri-snRNP to form complex B. At this step, major spliceosomal snRNP are recruited to the transcript. However, the splicing reaction does not occur yet. The resulting complex B goes through a series of compositional and conformational rearrangements including the release of U1 and U4, which result into the formation of a catalytically active complex B (complex B\*). The activated spliceosome, complex B\*, completes then the first catalytic step of splicing, generating complex C. Complex C undergoes then additional ATP-dependent rearrangements before carrying out the second catalytic step of splicing (Konarska et al., 2006). This results in a post-spliceosomal complex that contains the lariat intron and the spliced exons. Finally, the U2, U5 and U6 snRNPs are released from the mRNP particle and recycled for additional rounds of splicing. Disassembly of the post-catalytic spliceosome is also driven in an ATP-dependent manner (Wahl et al., 2009; Hoskins and Moore, 2012) (**Figure 29**).

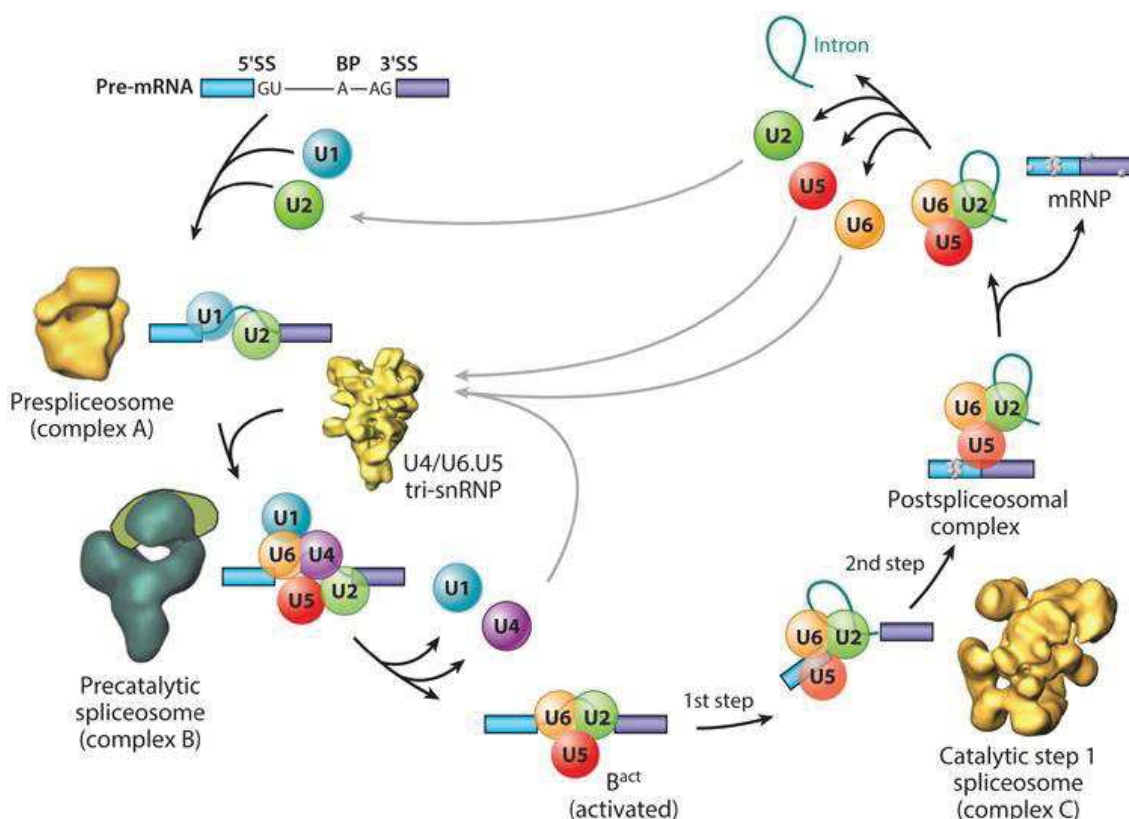


**Figure 29: Dynamics of spliceosome assembly.**

The spliceosome assembly and disassembly cycle, with known structures of individual complexes, as well as the cross-intron assembly and disassembly of the major spliceosome. Image from Lee and Rio, 2015.

### III.4 – Alternative Splicing and Disease: The case of the *LMNA* gene and HGPS

Alterations in normal AS patterns are known to have a close link with disease (Orengo and Cooper, 2007; Tazi et al., 2009). Changes in regulatory sequences can drastically change or invalidate essential gene products due to the complexity of the process (Zhang et al., 2015). Estimates attribute up to half of human disease mutations to changes of splice regulatory regions (Wang and Cooper, 2007). There are also documented cases of disease product of overexpression of trans-acting regulation genes of AS in other mammals (Anczuków et al., 2012). AS has been frequently associated with cancer (Tazi et al., 2009; Kelemen et al., 2013), diabetes (Prokunina-Olsson et al., 2009) and obesity (Kaminska and Pihlajamäki, 2013). In this last condition, splicing has moreover been correlated with changes in weight loss, FA and glucose metabolism (Kaminska and Pihlajamäki, 2013).

#### III.4a – Lamins

Lamins are intermediate filament proteins forming a fibrous meshwork, called nuclear lamina, between the inner nuclear membrane and peripheral heterochromatin of metazoan cells. Lamin functions have been proven to present cell-type specific differences (Zwerger et al., 2015) of which the main ones are structural function and transcriptional regulation in the cell nucleus. Proper integration of lamin A/C into the lamina is required for correct nuclear mechanical properties and nuclear envelope integrity.

There are two types of lamins: A type lamins and B type lamins.

In humans, B type lamins (B1 and B2) are coded by two different genes (*LMNB1* and *LMNB2*), whereas A-type lamins are encoded by a single gene, *LMNA*. Alternative RNA processing of *LMNA* pre-mRNA produces three main nuclear protein isoforms; that is, lamin C, progerin, and lamin A (**Figure 30**).



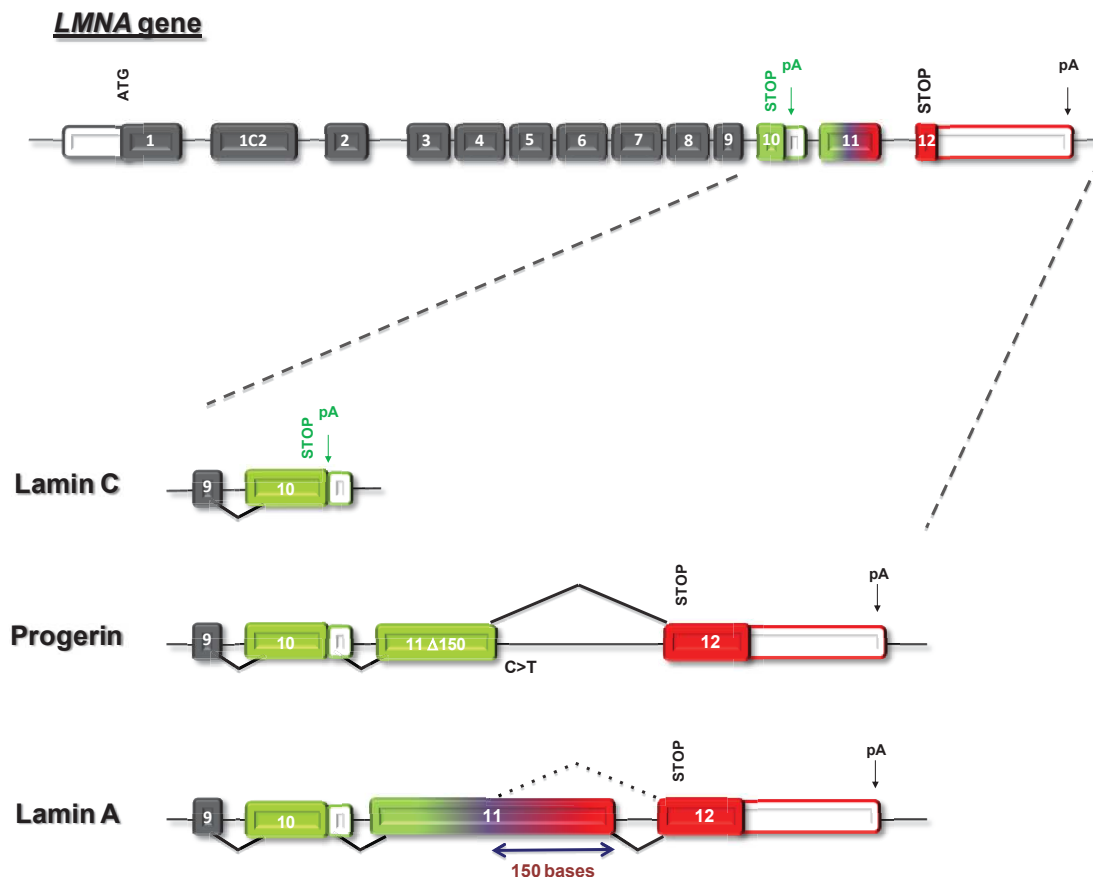


**Figure 30: LMNA major lamin isoforms.**

Schematic representation showing the production of lamins C and A by the use of different polyadenylation sites, and the obtainment of progerin by differential AS. The main mutation giving rise to HGPS (C>T) is also depicted.

### LMNA isoforms

As I just explained, the *LMNA* gene produces three main protein isoforms by RNA processing of the primary transcript. Lamins C and A originate from the use of different polyadenylation sites. When this process takes place at the level of exon 10, lamin C will be produced whereas when polyadenylation occurs at the level of exon 12, the resulting isoform will be lamin A.

A process of maturation is required for the procurement of Lamin A. It implicates a step of farnesylation that will give rise to prelamin-A, which in turn will mature into lamin A. The third isoform, a shorter form of lamin A, can be obtained by AS. The regulation of the splicing takes place at the level of exon 11. Highly used SS will give rise to lamin

A, whereas less used SS will originate a truncated form of the protein, called progerin (**Figure 30**). This isoform lacks the 150 nucleotides that contain the necessary sequence for the farnesyl group enzymatic cleavage. Therefore it remains farnesylated and accumulates around the nuclear envelope, leading to dominant deleterious effects in nuclear organization.

### **III.4b – HGPS/Progeria**

Progerin accumulation is largely responsible of HGPS (Hutchinson-Gilford Progeria Syndrome). This disease is more frequently plainly called progeria. It is an extremely rare genetic disease characterized by signs of premature ageing. This severe form of early-onset accelerated senescence is narrowly associated with lipodystrophy (Eriksson et al., 2003).

Babies are born normally and healthy, but they have an accelerated senescence and at the age of 14 they resemble old people. The main characteristics are: stunted growth, alopecia, accelerated aging of the skin (subcutaneous AT loss), lipodystrophy, atherosclerosis, and cardiovascular problems. This last feature is usually the cause of death. Surprisingly, mental development is not affected, due to the presence of a specific microRNA in the brain: miR-9 (Jung et al., 2012; Nissan et al., 2012).

Most cases are sporadic and caused by *de novo* single point silent mutations in the *LMNA* gene (c.1824C>T; p.Gly608Gly) which results in aberrant AS. This alteration on the process consisting on the removal of introns gives rise to an exacerbated production of progerin, the truncated isoform of the protein (Navarro et al., 2006). Consequently, as previously mentioned, abnormal progerin agglomerates at the nuclear periphery and causes the appearance of shape abnormalities in the nucleus.

In the laboratory, a role of two serine-arginine (SR)-rich proteins, SRSF1 and SRSF6, has been elucidated for the regulation of progerin production (**Figure 31A**) (Lopez-Mejia et al., 2011). The authors portrayed a model into which the progerin 5' SS was sequestered in a conserved secondary RNA structure that prevented it to be used (**Figure 31B**). The progeria mutation would disrupt this structure allowing then SRSF1 to indirectly favor progerin 5'SS, while SRSF6 would directly repress progerin production. According to their data, the mechanism by which the SS is selected depends then on two features. Firstly, a RNA secondary structure which prevents the

use of the progerin 5' SS. The progeria mutation would open up the secondary structure and allow accessibility to SR proteins. Aright secondly, two SR proteins, SRSF1 and SRSF 6 that are described as having two opposite effects: SRSF1 activates progerin 5'SS, while SRSF6 represses it.

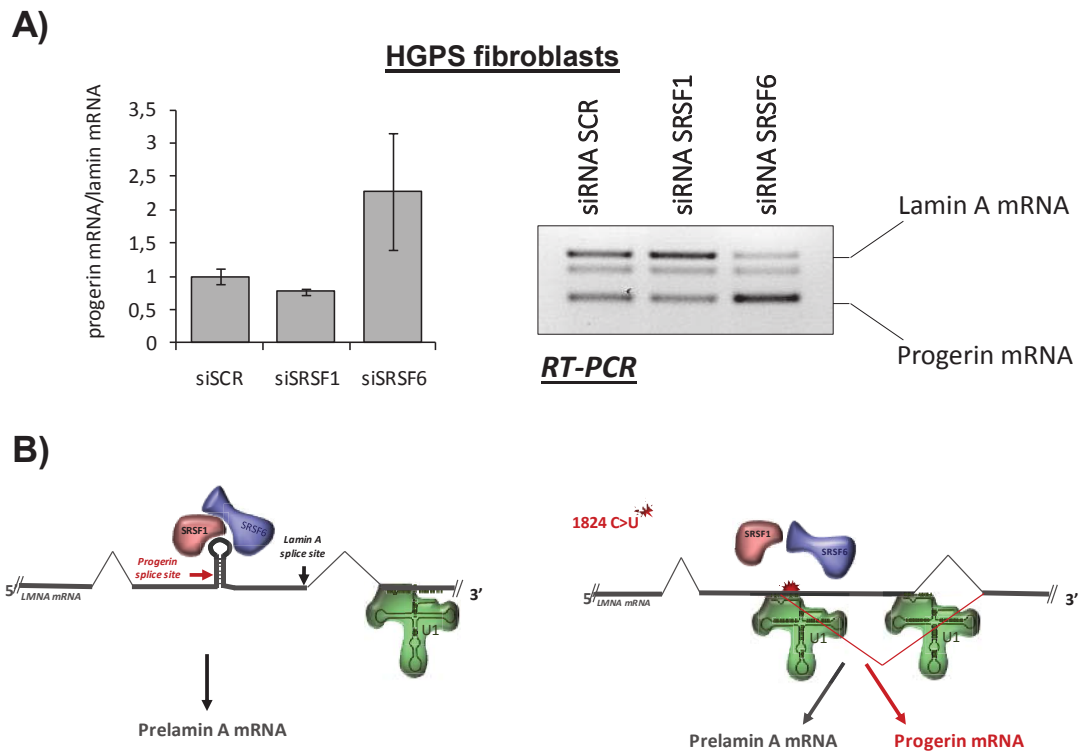


**Figure 31: LMNA SS regulation by SRSF6 and SRSF1**

**A)** SRSF6 prevents usage of progerin 5'SS in fibroblasts from progeria patients. Left panel is the quantification of the mRNA ratio between truncated (progerin) and full-length (lamin A) isoforms from the RT-PCR experiment on the right panel (SRSF1 and SRSF6 siRNA knockdown). SCR: scrambled. Adapted from Lopez-Mejia et al., 2011.

**B)** Model of the progerin 5' SS activation.

In HGPS, loss of AT correlates with adipokine dysregulation, insulin resistance, and atherosclerosis, suggesting a critical role of AT function in controlling whole body energy metabolism, age-related pathologies, and longevity (Arai et al., 2011). It is difficult to extrapolate the metabolic abnormalities with lamin deregulation, however, it is known that modifications in lamin A/C may be induced by common metabolic pathways involved in both diabetes and obesity before hyperglycemia is established (Miranda et al., 2008).

### III.4c – Lamins and Metabolism

Existing literature has oftentimes designated the importance of the interface between metabolism and lamins, nuclear proteins encoded by the *LMNA* gene (Liu et al., 2012; Tang et al., 2011; Lloyd et al., 2002; Rochford, 2014). Recently, our laboratory has shown that the production of different LMNA isoforms is causative of distinct physiological metabolic outcomes (Lopez-Mejia et al., 2014). The entire publication can be found in **Annex 1**. This discovery suggests that lamins would act as regulators of energy homeostasis. LMNA isoforms were shown to affect mitochondrial gene expression and contribute to metabolic adaptations of AT in mice, resulting in opposed energy expenditure (EE) and lifespan. Strikingly, lamin isoforms correlates with opposing effects on lifespan and distinct effects on mitochondrial activity (Lopez-Mejia et al., 2014). The experiments leading to these conclusions evidently involved mouse models expressing different isoforms of the *Lmna* gene. Progeria mice (G609G/G609G), expressed the three main *Lmna* isoforms I explained above and were lypodistrophic. They also had a very short life span (dying usually before the age of 5 months), and a high EE which was related with mitochondrial activity. Wild type (WT) mice lived around one year and a half and their EE was intermediate. And last but not least, the mice expressing exclusively Lamin C lived even longer. It is important to remark that under normal nourishment conditions these animals became obese over time. The underlying explanation seems to be in connection with a low EE, which correlates with a low mitochondrial activity, and a capacity to compensate for the deleterious effects triggered by obesity; suggesting that lamin C would protect against increased oxidative stress associated with fat accumulation.

To sum up, results supported the notion that RNA processing of the *Lmna* gene is an active conserved mechanism that contributes to metabolic adaptations of AT in mammals, ascribing *Lmna* an additional important role. This outcome is in line with previous evidence suggesting a role for lamins into metabolism, which would be complementary with their structural function (López-Otín et al., 2013).

### III.5 – Other RNAs: microRNAs

RNAs may carry information from the DNA to the ribosome resulting in protein production. This is the case for mRNAs which contain a coding sequence that will determine the amino acid sequence. However, many RNAs do not code for proteins. In eukaryotes, about 97% of the transcriptional output is non-protein-coding (Mattick, 2003).

Examples of these so-called non-coding RNAs are: tRNAs, rRNAs, snoRNAs, siRNAs, snRNAs, exRNAs, piRNAs, and microRNAs. They can be encoded by their own genes or derive from mRNA introns and are oftentimes conserved across species. This fact highlights the importance of their functions, which include among others splicing regulation (Kishore and Stamm, 2006; Lee and Rio, 2015) and gene expression (Phillips, 2008).

MicroRNAs (miRNAs/miRs) are small non-coding RNAs of approximately 22 nucleotides that play important roles in post-transcriptional regulation of gene expression and, therefore, biological processes in different tissues. A given target may be regulated by multiple miRNA and a given miRNA might have hundreds of different mRNA targets (Friedman et al., 2009). MicroRNAs are able to regulate a multitude of effector genes in a multi-level regulatory mechanism that profoundly affects the gene expression program in the cells (Makeyev and Maniatis, 2008).

The genesis of microRNAs from the primary miRNA transcript is mediated by the microprocessor complex. The pri-miRNA is cleaved thanks to Drosha's RNase III activity, who acts in a complex with its co-factor DGCR8 (DiGeorge syndrome critical region 8 homolog) to create the pre-miRNA. Later on, exportin 5 deals with the transport of the pre-miRNA from the nucleus to the cytoplasm, where they are processed by the RNA-mediated interference machinery (Gregory et al., 2004).

Cytoplasmic pre-miRNAs will be anew cleaved by another RNase III-type enzyme, Dicer, who also features two TRBP co-factors. Following Dicer cleavage, the short RNA duplex is bound by an AGO (Argonaute) protein, a component of a complex termed RISC (RNA-induced silencing complex).

Since their discovery, miRNAs have been described as repressors, but recently new RNA stabilization roles and thus consequent translational activation are being ascribed

to these RNAs (Rusk, 2008; Orang et al., 2014). Nevertheless, silencing remains the most studied aspect among the distinct miR functions. Different mechanisms are known to lead to this outcome. These presently stand: destabilization of the mRNA through shortening of its poly-A tail, cleavage of the mRNA strand into two pieces, and less efficient translation of the mRNA into proteins. Moreover, silencing is possible thanks to RISC but chiefly thanks to the existence of complementary sequences that will base-pair in between microRNAs and the 3'UTR of the corresponding mRNA molecules. To recognize their targets, pairing does not need to be perfect, except for in a region called the “seed sequence”. This area corresponds to the nucleotides in positions 2 to 7 of the miRNA 5'-end, and it must be perfectly complementary (Lewis et al., 2005).

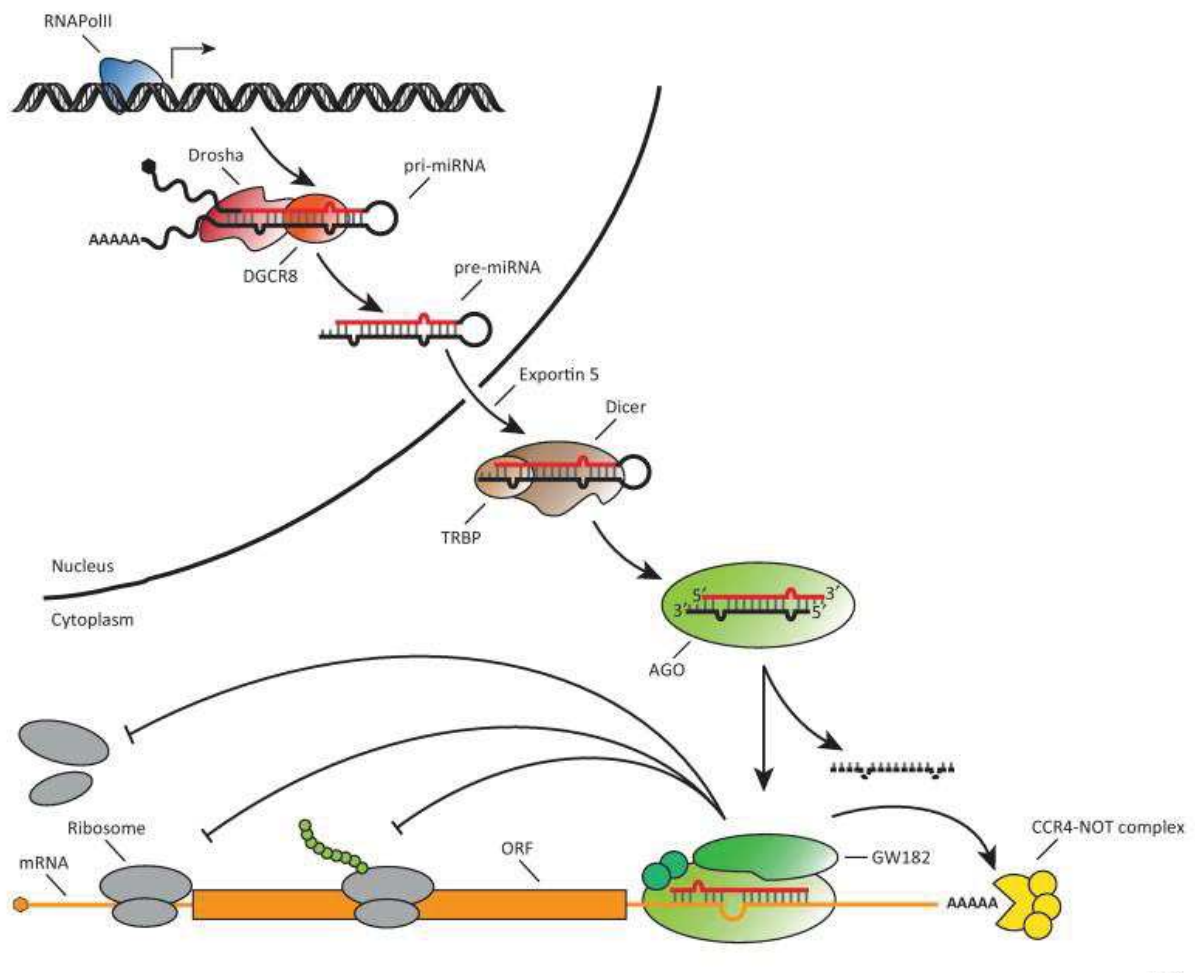


**Figure 32: Schematic view of miRNA biogenesis and mechanism of action.**

Image from Rüegger and Großhans, 2012.

### III.5a – MicroRNAs and Alternative Splicing

Many studies point to the importance of the dialogue established between the microprocessor and the spliceosome to regulate miRNA biogenesis. The production of microRNAs might be affected by AS (**Figure 32**) (Melamed et al., 2013). Given that mammalian miRNAs are expressed from intronic, exonic or polycistronic regions, if inclusion and/or exclusion are stimulated, a variation within the microRNAs population will likely follow.

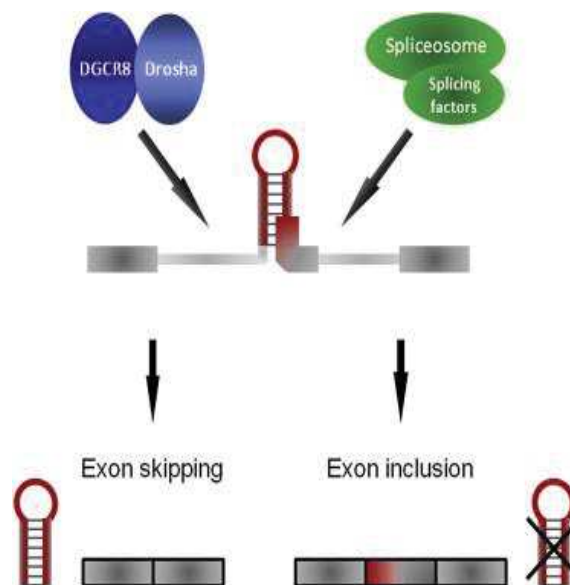


**Figure 33: Regulatory Model of SS-Overlapping miRNA Biogenesis via AS.**

The spliceosome and the Microprocessor complex compete for processing of the same RNA region, leading to two possible scenarios. Image from Melamed et al., 2013.

Furthermore, the involvement of an SR protein in the production of a specific miR has been recently demonstrated (Wu et al., 2010). A self-regulating loop has been described for this regulation into which SRSF1 promotes miR-7 production by binding the pri-miRNA structure and in turn miR-7 targets the mRNA of the gene encoding SRSF1 in the cytoplasm.



### ***III.5b – MicroRNAs and Adipose Tissue***

A major function of miRNAs in AT is to stimulate or inhibit the differentiation of adipocytes, and to regulate specific metabolic and endocrine functions. Moreover, miRNAs are likely to be involved in communication between fat cells, as well as between adipose and other tissues. They also play a major role in maintaining cell identity by fine-tuning cell-specific transcriptional networks and have been shown to play important roles in both brown and white fat differentiation (Mori et al., 2014).

The miR-193b-365 cluster of miRNAs and miR-155 participate in brown adipogenesis, while miR-143 and miR-103 have been implicated in white adipocyte differentiation and insulin resistance. Likewise, miR-196a, which is expressed primarily in WAT progenitor cells in response to cold or adrenergic stimulation, can suppress a white fat gene to favor brown adipogenesis over white adipogenesis. Moreover, several other microRNAs are differentially expressed in various adipose depots and altered expression has been reported in individuals with obesity and T2D. Mori and colleagues described last year a collection of miRNAs in AT that changed in response to obesity, insulin resistance, or cold exposure (Mori et al., 2014). **Figure 33** displays a summary of changes in miR expression related with obesity and insulin resistance, both in humans and rodents. Besides, miRNAs can also be secreted from fat cells into the circulation and serve as markers of disturbed AT function. This is the case for miR-197, miR-23a, miR-509-5p, miR-130a-b, miR-195, miR-27a and miR-320a, whose expression appears dysregulated in association with metabolic syndrome (Arner and Kulyté, 2015).

Finally, given their role in regulating transcriptional networks, miRNAs in AT might offer tangible targets for treating additional metabolic disorders. They appear very attractive as therapeutics that can be specifically targeted to AT.

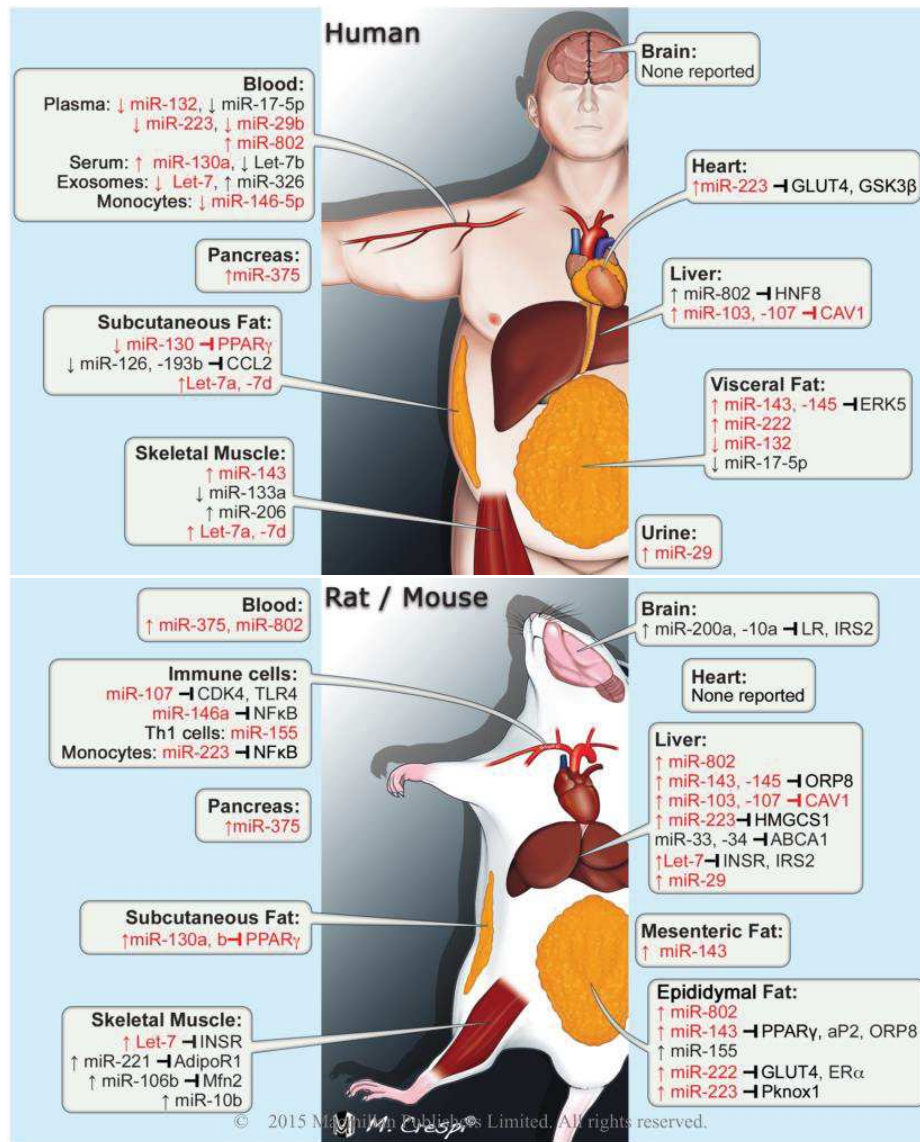


**Figure 34: Obesity / insulin resistance-related miRNA expression changes in humans and in murine models.**

miRNAs in red font were differentially expressed in human and murine obesity with arrow indicating up- or down regulation. Image from Deiluiis, 2015.

## RESULTS

---

## RESULTS

### Project 1: Investigation of the Mode of Action (MoA) of ABX300

#### 1. Aim of the project

Compelling data have recently shown the association between LMNA isoforms and energy metabolism (Tang et al., 2011; Liu et al., 2012; López-Otín et al., 2013; Rochford, 2014). In addition, the idea that lamin A/C may influence obesity-related traits was already suggested a few years ago (Hegele et al., 2000; Hegele et al., 2001; Wegner et al., 2007). Furthermore, our laboratory published last year pretty conclusive data indicating that the different LMNA isoforms played opposite roles on metabolism (Lopez-Mejia et al., 2014). This finding led to the proposal that pharmacologically modulating this splicing could be a novel and original approach for the treatment of obesity. By means of two screening systems, a compound labeled ABX300 was selected and tested on mice models of obesity, having an enormous impact on weight evolution. We confirmed the influence of the identified molecule on *LMNA* splicing by studying the behavior of splicing reporters in cultured cell lines.

The acronym labeling this molecule is comprised of the digit three hundred, which simply happens to refer to the position of this small compound in the ABIVAX chemical library; and the characters ABX, which stand for the name of this enterprise. ABIVAX is an emerging science-driven drug discovery company, which develops novel small molecule therapeutics. To do so, it focuses on the initial small molecule discovery through cell-based screening protocols and on the posterior development of these drugs. The first aim of my PhD project in ABIVAX was to investigate the mode of action (MoA) of the previously identified molecule, ABX300. In order to determine it, we carried out an extensive number of experiments. In collaboration with Ez-Zoubir Amri, we performed Microcomputed tomography aiming to identify the specific kinds of adipose tissue, if any, mostly affected by our treatment. We further completed the mechanistic analysis of the drug by performing indirect calorimetric analysis in concert with François Casas, and the help of the Metamus platform held in Montpellier. Furthermore, since differences in food intake were attributable to the treatment, we verified to which extent they were responsible for the observed phenotype. We also conducted a series of transcriptomic approaches to identify splicing events and/or microRNAs into which the treatment could have an impact.

In association with the Sherbrook University, we checked for favoring or limitation of alternative exons inclusion and exclusion. Ultimately, in parallel, we used commercial arrays to check for microRNAs modulations (in partnership with Pierre de la Grange), allowing us to decipher an apparent mitochondrial “preference” of our drug.

## 2. Summary

Screening experiments revealed that ABX300 associated with SRSF1, and thus modulated *LMNA* alternative splicing profile. Since the *LMNA* gene is known to play an important role into white adipose tissue (WAT) homeostasis, the compound was thereafter tested in diet induced obesity (DIO) mouse models to further study its mode of action (MoA). ABX300 treatment provoked a global reshuffling of WAT, by restoring a lean like profile in treated animals. This was evident in sight as well as, both at the splicing and the transcriptomic level. Moreover, we found that ABX300 specifically modulated 10 microRNAs, and surprisingly that these importantly targeted mitochondria related processes. Hence, oxygen consumption, which mitochondria are largely responsible for, was increased after drug administration. These results present a new approach to obesity treatment, based on the modulation of *LMNA* splicing, by interacting with serine/arginine-rich splicing factor 1.

## Pharmacological modulation of the splicing factor SRSF1 mitigates Diet Induced Obesity in mice

---

## Pharmacological modulation of the splicing factor SRSF1 mitigates Diet Induced Obesity in mice

Celia Lopez-Herrera<sup>1, 7</sup>, Julien Santo<sup>1, 7</sup>, Cécile Apolit<sup>1, 7</sup>, Yacine Bareche<sup>2</sup>, Laure Lapasset<sup>2</sup>, Carine Chavey<sup>2</sup>, Florence Mahuteau<sup>3</sup>, Romain Naijman<sup>3</sup>, Pauline Fornarelli<sup>3</sup>, Isabel C. Lopez-Mejía<sup>2</sup>, Guillaume Béranger<sup>6</sup>, François Casas<sup>5</sup>, Ez-Zoubir Amri<sup>6</sup>, Bernard Pau<sup>4</sup>, Didier Scherrer<sup>1</sup>, and Jamal Tazi<sup>2\*</sup>

1) ABIVAX, 1919 Route de Mende, 34293 Montpellier Cedex 5, France

2) Institut de Génétique Moléculaire de Montpellier, CNRS UMR 5535, 1919 Route de Mende, 34293 Montpellier Cedex 5, University of Montpellier

3) Institut Curie, UMR176, Bâtiment 110, Centre universitaire 91405 ORSAY CEDEX, France

4) Université de Montpellier, UFR Pharmacie, 15 Avenue Charles Flahault, 34000 Montpellier

5) UMR Dynamique Musculaire et Métabolisme, INRA - CAMPUS SUPAGRO 2 place Viala 34060 CEDEX 2 Montpellier

6) Institut de Biologie de Valrose, UMR CNRS 7277 – UMR INSERM 1091, Université de Nice Sophia Antipolis, Faculté de Médecine, 28 avenue de Valombrese, 06107 Nice Cedex 2, France

7) These authors contributed equally to this work

**Running title:** ABX300 new drug for obesity treatment

**\* Corresponding author:** Prof. Jamal Tazi, PhD

Senior Member “Institut Universitaire de France”

Institut de Génétique Moléculaire de Montpellier

1919 route de Mende

34293 Montpellier Cedex 5

France

E-mail: jamal.tazi@igmm.cnrs.fr

Tel: (33) 4 34 35 96 85 / Fax: (33) 4 34 35 96 34



## Abstract

Alternative Splicing (AS) and/or polyadenylation enable the *LMNA* gene to originate distinct protein isoforms that yield opposing effects on energy metabolism and lifespan.

Two splicing factors, SRSF1 and SRSF6, contribute to the production of these different isoforms. By pharmacological screening of compounds that potentially modulate SRSF1 activity and *LMNA* AS, we identified a small molecule that specifically interacted with the RS domain of SRSF1. This molecule, ABX300, affected adiposity of Diet Induced Obese (DIO) mice, leading to a global beneficial restoration of white adipose tissue (WAT) depots *in vivo*. Global analysis of alternative splicing in the WAT from treated and untreated animals showed that ABX300 treatment reversed most of the AS altered by obesity. Similarly, transcriptomic analysis revealed that WAT from DIO mice treated with ABX300 had the same profile as that from untreated mice fed with chow diet. Interestingly, ABX300 treatment largely affected the expression of microRNA whose target mRNAs were involved in mitochondrial metabolism. Consistently, *in vivo* studies showed that mice treated with ABX300 had an increase in O<sub>2</sub> consumption, along with a switch in fuel preference toward lipids, thereby suggesting a protection against diet induced fat accumulation.

Targeting SRSF1 by ABX300 represents therefore a novel and complementary approach for the treatment of obesity.

## 1 Introduction

2 Obesity, the imbalance of income and expenditure of energy, is a rapidly  
3 growing worldwide epidemic (Ng et al., 2014). The establishment of a sedentary  
4 lifestyle combined with excessive caloric intake has made the number of overweight  
5 individuals grow markedly in the last century. Obesity is characterized by increased fat  
6 mass due to energy storage in White Adipose Tissue (WAT) (Cummings and Schwartz,  
7 2003; Frayn et al., 2003). An increase in fat mass can be achieved by an increase in  
8 the size of adipocytes (hypertrophy), or by an expansion of their number (hyperplasia)  
9 (Rosen and MacDougald, 2006). In addition, obesity is associated with a collection of  
10 clinical problems known as the metabolic syndrome: insulin resistance, diabetes,  
11 cardio-vascular disease, dyslipidemia, and fatty liver (Kahn, Buse, Ferrannini, & Stern,  
12 2005; Van Gaal, Mertens, & De Block, 2006). Increased physical activity and better  
13 feeding habits are clearly a requisite to limit or reverse weight excess and its  
14 deleterious metabolic consequences. However, dietary management and exercise are  
15 not usually successful as an intervention, underscoring the need for efficient  
16 medication to treat metabolic disorders (Feige et al., 2008). Integrated metabolic  
17 networks, which are governed at the transcriptional level by transcription factors and  
18 co-regulators, enable the organism to adapt the metabolic state of different organs to  
19 nutrient availability (Spiegelman and Heinrich, 2004; Desvergne et al., 2006; Feige and  
20 Auwerx, 2007). The limited success to date in the pharmacotherapy of obesity likely  
21 reflects the existence of multiple redundant and compensatory pathways in energy  
22 homeostasis (Guan et al., 2010). Intense drug discovery efforts in the metabolic field  
23 highlight the need for novel mechanisms for the treatment of obesity. Compelling data  
24 suggest that targeting cellular bioenergetics may provide an exciting new therapeutic

approach for the treatment or prevention of this disorder (Harper et al., 2008; Tseng et al., 2010; Locke et al., 2015).

We recently reported opposed Energy Expenditure (EE) and lifespan on mice, depending on LMNA isoforms (Lopez-Mejia et al., 2014). Existing literature had oftentimes designated the importance of the merge between metabolism and lamins, nuclear proteins encoded by the *LMNA* gene (Liu et al., 2012; Tang et al., 2011; Lloyd et al., 2002; Rochford, 2014). Alternative RNA processing of *LMNA* pre-mRNA produces three nuclear protein isoforms; that is, lamin A, progerin, and lamin C. Mutations in lamin A/C can cause several syndromes collectively described as laminopathies which include several lipodystrophies, but also progeroid syndromes (Worman and Bonne, 2007). The lipodystrophy mutations strongly support the idea that lamins can have cell-type-specific functions (Wilson et al., 2001). A *de novo* silent mutation in *LMNA* (c.1824C>T; p.Gly608Gly) results in aberrant Alternative Splicing (AS) of the Lamin-A isoform. This alteration, will give rise to a truncated isoform of the protein, termed progerin (Navarro et al., 2006). The importance of two serine-arginine (SR)-rich proteins, SRSF1 and SRSF6, for the regulation of progerin production was previously described by our laboratory (Lopez-Mejia et al., 2011). Exacerbated accumulation of progerin is the predominant cause of Hutchinson-Gilford Progeria Syndrome (HGPS), a severe form of early-onset premature aging associated with lipodystrophy (Eriksson et al., 2003; De Sandre-Giovannoli et al., 2003). In HGPS, loss of adipose tissue correlates with adipokine dysregulation, insulin resistance, and atherosclerosis, suggesting a critical role of adipose tissue function in controlling whole body energy metabolism, age-related pathologies, and longevity (Arai et al., 2011). The lamin isoforms, by changing the nuclear envelope architecture, may also

1 contribute to changes in the expression of genes involved in mitonuclear imbalance  
2 controlling longevity (Houtkooper et al., 2013).

3 Our previous work showed how the RNA processing and thus the production of  
4 the distinct LMNA isoforms had physiopathological outcomes; affecting mitochondrial  
5 gene expression and contributing to metabolic adaptations of the adipose tissue in  
6 mammals. Given the described antagonistic functions of the LMNA isoforms on EE,  
7 we designed two screening systems based on SFSRF1 localization and the LMNA AS,  
8 for the identification of potential candidates to treat metabolic disorders, such as  
9 obesity.

10 In this study, we report the endorsement of an *in vitro* luciferase reporter assay,  
11 based on the structure of the LMNA gene. Our lead compound, ABX300, was shown  
12 to prevent weight gain in animals under a high fat diet (HFD) and to induce weight loss  
13 on Diet Induced Obese (DIO) mice. We found that the decrease of body weight in the  
14 ABX300 treated animals was accompanied by a reduction in the food intake. However,  
15 a pair-feeding (PF) experiment determined that this phenomenon was not sufficient to  
16 explain the observed phenotype. Furthermore, the size of lipid droplets, as well as the  
17 oxygen consumption, the respiration exchange ratio (RER), and diverse mitochondrial  
18 features in conjunction with microRNA targeting mitochondria, were altered in ABX300  
19 treated mice.

20 Our data reveal for the first time that drug screening for pharmacological  
21 modulators of LMNA AS could be a valid strategy to approach obesity therapy. We  
22 strongly believe that this unexplored/novel/original approach, based on the modulation  
23 of splicing, is of great potential, not only to treat obesity but a wide range of diseases  
24 (Soret et al., 2005).

## Results

### Identification of ABX300 a SRSF1 partner that modulates *Lmna* splicing

More than 6,000 molecules were screened for their ability to inhibit the kinase activity of topo I and thereby the specific phosphorylation of SR proteins. This approach had led to the identification one indole derivative (IDC16) targeting specifically the SR protein SRSF1, and inhibiting HIV multiplication *in vitro* (Bakkour et al., 2007). Based on IDC16 structure, a new library was developed by ABIVAX to encounter the toxic effect of this molecule. In the first place, we designed a screening based on the localization of the SRSF1 protein. We used HeLa cells expressing the GFP protein in fusion with endogenous SRSF1 protein and selected the molecules that did not disturb GFP distribution (**Figure 1A**). The selected molecules were farther used for a next step of screening based on the AS of the *LMNA* gene known to depend on SRSF1 protein (Lopez-Mejia et al., 2011). More precisely, we generated a HEK-293FRT reporter cell line (HEK-293FRT-LMNA-luc) that stably expressed luciferase fused with a portion of LMNA cDNA, under the control of the CMV promoter (**Figure 1B**). This cell line contained the main mutation responsible for HGPS, (c.1824C>T; p.Gly608Gly), and thus was used as reporter for the distinct use of the *LMNA* exon 11 5' splice sites (5'SS), which are, as previously mentioned, under the control of SRSF1. Interestingly among 900 compounds (**Figure S1A and S1B**), the ones belonging to family number 8 seemed to be very active in our test (**Figure 1C**). In this family, one lead compound was identified, ABX300. It increased luminescence in a dose-dependent manner, reaching values of 4.95 RLU/mg protein at 4.28  $\mu$ M (**data not shown**). Notably, cell viability was not troubled under ABX300 treatment (**data not shown**). Moreover, following a classical fluorimetric titration protocol, we demonstrated a direct interaction

1 between SRSF1 and ABX300 with a stoichiometry of 1:1 (**Figure 1D**). To further  
2 characterize this result we generated a SRSF1 protein without the RS domain  
3 (SRSF1 $\Delta$ RS), and carried out the same kind of experiments. As expected, we had a  
4 different profile of fluorescence spectra, which revealed a lack of interaction in these  
5 conditions. Besides, we used hnRNPK as a negative control (**Figure S1C**). This led us  
6 to conclude that ABX300 interacts with SRSF1 through its RS domain.

### 7 **ABX300 modulates weight evolution under High Fat Diet**

8 LMNA isoforms have been shown to play important opposite roles in the  
9 regulation of metabolic adaptations of adipose tissue in mammals. The luciferase  
10 reporting system described in Fig.1B, led us to the selection of ABX300 by revealing  
11 the distinct use of the *LMNA* 5'SS. To further study the effects of this compound in  
12 energy metabolism, we used a diet-induced obesity (DIO) mouse model, which we  
13 treated subsequently or simultaneously to High Fat Diet (HFD) administration. Average  
14 treatment length was one month, and the chosen dose, 50 mg/Kg. This was the highest  
15 non-toxic dosage according to the "Maximal Tolerated Dose Test" that we carried out  
16 (**Figure S2A**). The adequacy of the DIO animal model for mimicking human obesity  
17 had been largely recognized by the scientific community (Nilsson et al., 2012). Our  
18 treatment remarkably influenced weight evolution. In a curative context, ABX300  
19 enhanced weight loss (**Figure 2A**, left panel), reaching a plateau (**Figure S2B** left  
20 panel). In addition, ABX300 prevented weight gain in the same mouse strain, and this  
21 in a constant manner (**Figure 2B**, left panel). Indeed, a noticeable decrease in food  
22 intake was revealed in parallel to ABX300 administration under HFD conditions, shortly  
23 after the first administrations (**Figures 2A** and **2B** right panels). Cumulative food intake  
24 for the whole period is shown in the bottom part of these panels, where significant  
25 differences are displayed accompanying weight transformation. Nevertheless, both



effects on body mass were steady and time persistent (**Figure S2B**). To assess whether the drug required the presence of fat to take action, and check for its efficiency under standard diet conditions, we prosecuted our treatment within chow diet. Monitoring of mice weight and food intake showed no differences between groups (**Figure 2C**), for any of the mentioned parameters. Hence, the weight loss for HFD ABX300 treated mice could result from the ingest differences. To determine to which extent this phenomenon contributed to weight loss in these mice, we pair-fed animals to restrict their daily food intake to that of the ABX300 DIO treated mice. Each day, we restricted pair-fed animals to the amount of calories consumed by ABX300 DIO treated mice on the previous day. Concurrently, we did not pair-fed untreated and ABX300 DIO treated mice and instead gave these mice *ad libitum* access to food. Consequently, untreated mice gained weight, ABX300 DIO treated mice significantly lost weight, and the body weights of the pair-fed mice were significantly different from both of them, throughout the 30 days pair-feeding period (**Figure 2D**). In conclusion, these data indicate that ABX300 is an anorexigenic drug, affecting weight in a fat and food-dependent manner, but that hypophagia alone is not sufficient to explain the observed phenotype.

### **ABX300 decreases adiposity in DIO mice**

We have shown in our previous results that HFD ABX300 treated mice had a significant reduction in weight. To determine which tissues were affected, animals were sacrificed and their organs were weighted. Results showed significantly reduced WAT size in ABX300 DIO treated mice when compared to untreated mice after one month of drug administration. Adipose mass was five times lower in these individuals while weight of all other organs did not vary (**Figure 3A**). Moreover, to have a more



comprehensive view of the fat distribution in mice, we performed a computed tomography. This technique allows to differentiate the different body parts, producing detailed three-dimensional images of soft tissue and bone structure. Our analysis revealed that ABX300 treated DIO mice were leaner and had a reduced adiposity, both in visceral and subcutaneous WAT, without marked changes on the lean mass (**Figure 3B**), confirming the results shown in **Figure 3A**. Areas of low density (WAT) are represented in purple, medium density areas (organs) are shown in orange, and areas of high density (bones) are shown in white. The total fat volumes were calculated for each group, presenting a 5.5 fold decrease for ABX300 treated DIO mice, resembling animals under chow diet (**Figure 3C**).

Using Haematoxylin-Eosin staining of representative sections of WAT, Brown Adipose Tissue (BAT), Liver and Muscle, we observed that ABX300 had a global effect on fat. Indeed, the treatment visibly reduced the strong lipid accumulation induced by HFD in WAT (**figure 3D**), liver and BAT (**Figure S3A**). These results were confirmed by the surface size quantification of adipocytes. In WAT 80% of adipocytes in treated mice were cells of small size ( $<2000\mu\text{m}^2$ ) whereas in untreated mice the WAT was composed by heterogeneous cell sizes. Interestingly, we didn't find very large fat cells ( $> 10000\mu\text{m}^2$ ) in treated mice while we found a proportion of 10% in untreated (**Figure 3E**). All these results suggested that ABX300 induced delipidation by a breakdown of cellular lipid stores to provide endogenous free fatty acids. To verify if enhanced lipolysis was involved in the observed effect of ABX300, we assessed glycerol, non-esterified fatty acids (NEFA) and triglycerides (TGs), in plasma and serum from ABX300 treated and untreated animals. None of them differed between groups (**Figure S3B**) dismissing the idea of ABX300 inducing lipolysis.

## **ABX300 does not modulate global splicing**

To analyze the possible effect of ABX300 on AS we designed a large-scale screening strategy and compared a pool of RNA from treated and DIO untreated mice. Among a library of 1.330 alternatively spliced events (ASEs) we selected 537 high-quality PCRs from across the alternative exons. We used these high-quality PCRs to study the ASEs expressed in WAT from ABX300-treated mice compared to untreated obese mice (535 events). We farther selected the ones with the most important variations between the two conditions (**Figure S4**). The portrayed Percent Splicing Index (PSI), provides useful information about the inclusion level of each exon. This measure was computed according to the formula shown in **Figure 4**, where it is also depicted a heat map containing the 12 ASEs into which intragroup variations fall in a homogeneous manner. To confirm these results, we performed manual end-point PCRs. In the case of Myo9e01, Myo9b02 and Pdlim5 we observed strong PSI changes, corroborating our first analysis. The 9 remaining ASEs seemed to be less affected or not at all (**data not shown**). Moreover, we analyzed ASEs of non-obese mice and we found that their splicing status importantly correlated with the modulations induced by ABX300 treatment (**data not shown**). Altogether, our data suggests that ABX300 effect on splicing is rather specific and that the treatment provokes a reversal of most of the events altered by HFD and obesity.

## **ABX300 induces WAT restoration in DIO mice**

To understand how adipose tissue could be affected by the treatment, we designed an experiment into which the expression of 84 key genes involved in the differentiation and maintenance of mature adipocytes was checked. In the first comparison, we showed that 22/84 genes (26, 2 %) were significantly modulated in

1 treated obese mice (**Figure 5A**). Further, we compared the adipogenesis profile in lean  
 2 mice versus obese mice and found that 8/84 genes (9, 5 %) were robustly modulated  
 3 (**Figure 5B**). A last comparison between lean mice and treated obese mice revealed  
 4 that only Shh (Sonic Hedgehog) and Gata3 (Trans-acting T-cell-specific transcription  
 5 factor GATA-3) were modulated. Shh is thought to be a repressor of stem cell  
 6 commitment through adipocyte lineage (Suh et al., 2006; Huang et al., 2009; James et  
 7 al., 2010) (**Figure 5C**). A large number of genes that were modulated in the treated  
 8 mice, were due to a return to a normal state of adipose tissue. This reinforced the idea  
 9 that ABX300 would induce a way back to a normal healthy condition of adipose tissue.

#### 10 **ABX300 regulates microRNA notably targeting mitochondria**

11 A biological role of alternative splicing in the regulation of miRNA biogenesis has  
 12 been recently demonstrated, together with a competitive interaction between the  
 13 microprocessor complex and the splicing machinery (Melamed et al., 2013).  
 14 MicroRNAs (miRNAs) constitute a growing class of non-coding regulatory RNAs that  
 15 primarily regulate gene expression by reducing mRNA stability and/or repressing  
 16 translation. Several miRNAs exhibit tissue-specific expression, and those present in  
 17 WAT are known to have crucial implications for understanding adipose tissue,  
 18 connecting regulatory networks underlying adipogenesis and adipose dysfunction in  
 19 obesity. In order to outright the results shown in Figure 4, and to evaluate the potential  
 20 modulation of non-coding RNAs by our treatment, we determined the population of  
 21 miRNAs in visceral WAT from HFD/CD Untreated and ABX300 Treated DIO mice using  
 22 Affymetrix microarrays. We examined 1.111 murine miRNAs in WAT and found a set  
 23 of these small RNAs fluctuating in between untreated and treated animals (Fold-  
 24 change  $\geq 1.5$ ; P-value  $\leq 0.05$ ). More precisely, 52 miRNAs were differentially expressed  
 25 for these two conditions. The heat map in **Figure 6A** shows the 26 elevated and the

26 down regulated miRNAs when comparing HFD Untreated to HFD Treated animals (see also Figure S5A). Similarly, Figures 6B and S5B show the shifts of the 113 microRNAs (54 up-59 down regulated) varying between HFD and CD Untreated mice. Among the above mentioned variations, 42 miRNAs overlapped for the two comparisons (Figure 6C), suggesting that the treatment could restore the normal expression levels of these microRNAs, supporting observations from Figures 4 and 5. Importantly, only one microRNA was found to be significantly altered in the absence of weight loss, when the drug was administered under standard diet conditions (data not shown). Interestingly, we noticed that several miRNAs known to be up-regulated during obesity (Ortega et al., 2010; Arner et al., 2012; Chen et al., 2014) tended to be down regulated in the treated animals, and vice versa. For instance, miR-221, miR-222, miR-342-3p, and miR-146b, were induced during hyper-caloric diet, and down regulated with the treatment. Conversely, miR-30c, miR-92a, miR-193b and miR-378 were decreased during obesity but were upregulated in WAT from ABX300 treated mice. To test our observations more rigorously, and focus exclusively of the microRNAs that were modulated by ABX300, we centered ourselves on a set of 10 miRNAs whose expression varied exclusively in response to the drug. We then compared the list of miRNAs enriched in the ABX300 DIO Treated animals, with predicted targets of miR retrieved from the miRDB database (<http://mirdb.org/> miRDB; see material and methods section). Notably, a substantial number of the ABX300 modulated miR had predicted miR targets addressing mitochondria (score target  $\geq 80$ ). To assay the statistical significance of these regulations, we performed a similar calculation for 1.912 additional murine miRNAs. Only 315 of them (16.47%) were predicted to target these organelles (Mouse MitoCarta), indicating that the identified ABX300-modulated miRNAs were likely mitochondrial-enriched following treatment.

Amid these eight, miR-29a has been predicted to target Slc16a1 (**Figure S5D**), which has been uncovered to play a critical role in the regulation of energy balance when animals are exposed to an obesogenic diet (Lengacher et al., 2013). Given that each miRNA regulates, on average, about 200 target genes, these ABX300 specific modulations of a mitochondria related miR population, could most likely have a widespread impact on protein output and partially but importantly account for the observed phenotype. We conclude that ABX300 treatment significantly influenced the modulation of relevant endogenous miRNA mitochondrial targets.

### **ABX300 increases oxygen consumption**

Results on miRNA analysis showed that ABX300 modulated a series of miRNA that are regulators of several genes involved in the functioning of mitochondria. To continue the exploration we decided to study energy homeostasis more in detail by assessing the respiration at the level of the whole animal. ABX300 treated and untreated mice were placed in metabolic cages. Oxygen consumption ( $VO_2$ ) and  $CO_2$  production ( $VCO_2$ ) were monitored during a 12h dark/ 12h light cycle using the Oxymax Lab Animal Monitoring System (**Figure 7A**).

HFD ABX300 treated mice showed no differences in  $VO_2$  and  $VCO_2$  over a period of 24h (**Figure 7B** and **Figure 7C** right panels). However, if we focused on the light period, that is on the eight hours following ABX300 administration, treated DIO mice showed a marked tendency to display a higher  $O_2$  consumption and  $CO_2$  production compared to untreated DIO mice (**Figure 7B** and **Figure 7C** left panels). These eight hours corresponded to the Light period, when mice are normally in a resting state, characterized by a decrease in metabolism, at rest and their metabolism decreases. These outcomes seem to indicate an increase of the basal metabolic rate

of ABX300 treated DIO mice succeeding drug administration. The Respiratory Exchange Ratio (RER) was calculated by the ratio  $VCO_2/VO_2$ . Likewise, ABX300 treated DIO mice demonstrated a RER close to 0.7 which indicates that fatty acids are mainly metabolized source to provide energy. In contrast, untreated animals presented a RER ratio close to 0.8, showing a mixed consumption of fat and carbohydrates (**Figure 7D** right panel). All these results indicate that ABX300 drives higher metabolic rates leading to a rapid metabolization of lipids, which is likely carried out by the mitochondrial  $\beta$ -oxidation.

## Material & Methods

### Cell culture

#### - HeLa cells

SRSF1-GFP HeLa cells (gift from Edouard Bertrand's group) were maintained in Dulbecco's Modified Eagle Medium (DMEM, Invitrogen) containing 10% heat-inactivated Fetal Bovine Serum (FBS, PAA), 2 mM L-Glutamine, and 1% penicillin and streptomycin (all from ThermoFisher).

#### - HEK-293 FRT-LMNA-Luc cells (luminescence assay)

HEK-293 FRT-LMNA-Luc cells were seeded 48h prior to luminescence lecture at 10,000 cells per well. Then culture medium was removed, and cells were washed with sterile DPBS once. Cells were lysed using Passive Lysis Buffer 1X (E1941, Promega, Madison, WI, United States) directly added to cells. Half of the cell lysate was then mixed with Luciferase Assay Reagent (E1501, Promega, Madison, WI, United States) and luciferase activity was measured within 1 second per well. The other half was used for protein normalization in the well (Pierce™ 660nm Protein Assay Reagent).



## **Immunofluorescence analysis**

Cells were fixed in 4% (w/v) paraformaldehyde for 20 min. The nuclei were stained with Hoechst 33342 (SIGMA). Cells were washed in PBS and water, mounted with DAKO mounting medium, and observed under the fluorescence microscope. Cell imaging was performed with a confocal Leica SP5-SMD. Images were processed using Fiji software.

## **Fluorimetric titrations**

The fluorimetric titrations were performed at a constant dye concentration (ABX300) (1.2  $\mu$ M) with increasing concentrations of SRSF1 in 0.6 mM guanidine buffer (up to 120  $\mu$ M). Fluorescence spectra were recorded on a FluoroMax-3 (Jobin Yvon), at room temperature. Measurements were performed with solutions of OD<0.1 to avoid reabsorption of the emitted light, and data were corrected with a blank and from the variations of the detector with the emitted wavelength. The binding curves were obtained by plotting the fluorescence enhancement  $F/F_0$  ( $F$ = integrated fluorescence area of the complex and  $F_0$  = integrated fluorescence area of the free dye) versus the concentration in SRSF1.

## **Animals & Ethics Statement**

All animal procedures were executed according to European directive 2010/63/UE. Mice were maintained under pathogen-free conditions in our animal facility (E34-172-16) and experiments were conducted by authorized personnel. The study plan was approved by the Institutional Review Board at the Animal Facility of the Institut de Génétique Moléculaire de Montpellier and the Regional Ethics Committee for Animal Experimentation of Languedoc-Roussillon (agreement n° CEEA-LR-1061).



## **Synchronized Pair-feeding Test**

DIO mice were divided into three groups and housed by experimental class. HFD untreated and ABX300 treated animals had *ad libitum* access to food, whereas in an Untreated Pair-Fed (PF) group, food was calorie restricted. These animals received the same amount of aliment consumed by the ABX300 treated group over the preceding 24 h. Body weight was registered twice a week.

## **Organs Collection**

After one month of treatment, mice were anesthetized by intraperitoneal injection (Xylazine/Ketamine/Rompun combination) and euthanized by cervical dislocation. Organs were collected, rapidly weighed and immediately snap-frozen in liquid nitrogen or fixed in 4% Paraformaldehyde.

## **Histological Analysis**

Organs fixed in 4% Paraformaldehyde were dehydrated, embedded in paraffin and stained with Haematoxylin/Eosin for histological analysis. Slides were scanned with the NanoZoomer equipment (HAMAMATSU). Virtual slides were analyzed with the NDP.view software and Image J complemented with MRI Adipocytes Tools to measure the size of white adipose tissue cells.

## **Micro-computed Tomography**

The adipose tissue quantification was performed as previously described with the similar parameters (Lopez-Mejia et al., 2014).

## **Total RNA extraction**

For total RNA, extraction 30mg of WAT were grinded in liquid nitrogen and powder was dissolved in TRIreagent (SIGMA) according to the manufacturer's protocol, followed by a DNase digestion and a Phenol-Chloroform-Isoamyl alcohol purification. RNA quantity and

integrity were controlled by Nanodrop ND-1000 (Thermoscientific) and Agilent Bioanalyzer (Agilent Technologies) respectively.

### **miRNAarray experiments**

Small non-coding RNA transcripts were assessed throughout the Affymetrix technology, where RNAs were hybridized to the Affymetrix miRNA v3.0 arrays (GenoSplice- Evry- France).

### **Reverse-transcription and PCR**

1µg of RNA samples were reverse-transcribed using First-strand cDNA synthesis kit (GE Healthcare) according to the manufacturer's instructions. Gene expression was assessed by PCR using Platinum Taq DNA Polymerase (PCR buffer 1x, MgCl<sub>2</sub> 1,5 mM, primers forward and reverse 0,6 µM of each, dNTP 0,25 mM of each, Platinum Taq DNA Polymerase 2U/rxn, 1µl of cDNA and add nuclease-free water to 50 µl final volume (# 10966-034 Life Technologies). PCR was performed with Roche ThermoCycler (2 min 94°C, 35 cycles of 30 sec 94°C/30 sec 55°C/1min 72°C, 2 min 72°C). Products of PCR were analyzed with Elmer Perkin Caliper.

### **Metabolic Chamber Experiments**

DIO mice were switched to *ad libitum* CD one week before the metabolic chamber experiments. Single-housed animals were accustomed for 24 hours prior to recording. Immediately before the run, they were weighed and treated. Oxygen consumption (VO<sub>2</sub>) and Carbon dioxide production (VCO<sub>2</sub>) were monitored every "two" minutes over a 24 hours period using a Comprehensive Lab Animal Monitoring System (Columbus Instruments, Columbus, OH) thermostated at 22°C. The respiratory exchange ratio (RER) corresponds to the VCO<sub>2</sub>/VO<sub>2</sub> ratio.

## **Statistical analysis**

All results were expressed as the mean  $\pm$  standard error mean (S.E.M). Significance of differences was determined with the Student t test or Mann & Whitney test with significance at \*  $P < 0.05$ ; \*\* $P < 0.01$ ; \*\*\* $P < 0.001$ ; \*\*\*\* $P < 0.0001$ .

## **Supplemental methods**

### **Animal Feeding & Treatment**

Six-week old male mice C57BL/6J were purchased from Charles River Laboratory (69592 L'Arbresle) and housed under a normal light cycle (12h light-dark) and a constant temperature of 22°C, with free access to food and water. Experiments began after one week of acclimatization to our installations under CD conditions. At this point, either mice continued to receive CD (from Safe, 3% energy from fat), either they switched to a High-Fat Diet (HFD from Research Diet 58Y1, 60% energy from fat). Two treatment protocols were designed for the HFD condition. For the curative schema, mice were fed for up to ten weeks to generate diet-induced obesity (DIO) mice and were treated after. For the preventive schema the treatment started along with the diet. For both nourishment conditions, mice were divided into 2 groups of treatment, half of them received the vehicle (Labrafil M1944CS – 5% DMSO) and the other half received the active compound ABX300 at 50 mg/kg. The chose route was intragastric, to accurately manage the delivered dose. Mice were weighed weekly and food intake was measured four times per week.

### **Target Prediction Analysis**

Putative miRNA targets were identified using the mirDB online database (<http://mirdb.org/miRDB/>), which is a database for miRNA target prediction and functional annotations. Target prediction is performed by an algorithm (MirTarget) which analyses all the NCBI RefSeq 3'-UTR in order to predict both, conserved and

non-conserved target's motifs. A target prediction score is also computed in order to inform the user about the confidence he may have on the prediction. The range is comprised between 50 and 100, but below 80 cautiousness is recommended. As the microarray analysis was based on a previous version of mirBase (<http://www.mirbase.org/>) (v.17), the selected miRNA names were updated on the actual mirBase version (v.21). The miRNA were then applied against the mirDB database in order to retrieve all the predicted targets whose prediction score was  $\geq 80$ . Using the MitoCarta database (<https://www.broadinstitute.org/pubs/MitoCarta/>), the selected target's genes were then filtered in order to retrieve exclusively specific mitochondrial's target genes. The two heat maps presented in the Figures 6 A and B were generated by using a custom R script (<https://cran.r-project.org/>) containing gplots (<https://cran.r-project.org/web/packages/gplots/gplots.pdf>). The data were clustered using the Pearson correlation co-efficient method and the Heatmap2 function (<http://www.inside-r.org/packages/cran/gplots/docs/heatmap.2>).

### **Serum and Plasma Biochemistry**

For blood lipid content analysis (Figure S3B), mice were fasted 5h after treatment and few microliters of blood were removed at the tail vein, every week, with anticoagulant for serum or without anticoagulant for plasma. Blood was centrifuged at 4°C, 8000 rpm for 10 minutes to analyze plasma glycerol (Free Glycerol Reagent- F6428 SIGMA, Glycerol Standard solution – G7793 SIGMA), serum triglycerides (Triglycerides FS – 157609910021 DiaSys Diagnostic Systems GmbH) and serum non-esterified fatty acids (NEFA-HR(2) R1 Set – 434-91795 Wako Chemicals GmbH, NEFA-HR(2) R2 Set - 434-91995 Wako Chemicals GmbH, NEFA Standard – 270-77000 Wako Chemicals GmbH) .

## Discussion

In this study we developed a screening assay based on the AS regulation of the *LMNA* gene, and we used this assay to identify a particularly interesting compound, ABX300. This molecule was capable of enhancing weight loss in DIO animals. Our results endorse cell-based screening for modulators of *LMNA* AS, as a promising approach to the discovery of new metabolic drugs; henceforth an important goal of metabolic research.

Most drug discovery efforts in the metabolic field have focused elsewhere. Examples are peptide targets or monoamine and cannabinoid targets (see Kennett and Clifton, 2010; Powell et al., 2011; Jackson et al., 2015 for more details). Nevertheless previous studies have already supported the relevance of AS isoforms for the regulation of metabolism (Goodson et al., 2011; Huot et al., 2012; Ruas et al., 2012; Li et al., 2014). It is important to note that AS increases the amount of functionally different protein isoforms which lead in some cases to metabolic diseases (Kaminska and Pihlajamäki, 2013). Therefore, understanding the underlying molecular mechanisms of AS may provide opportunities for new diagnostic approaches. Remarkably, compelling data have recently shown the association between *LMNA* isoforms and energy metabolism (Tang et al., 2011; Liu et al., 2012; López-Otín et al., 2013; Rochford, 2014; Lopez-Mejia et al., 2014). In addition, the idea that lamin A/C may influence obesity-related traits was already suggested a few years ago (Hegele et al., 2000; Hegele et al., 2001; Wegner et al., 2007). These studies made *LMNA* a positional and biological candidate gene in the pathogenesis of type 2 diabetes, obesity, and quantitative traits of growth and metabolism. *LMNA* was highlighted as a collaborator in these metabolic phenotypes, following observations of altered lamin A-

to-C mRNA expression ratio, which correlated with a pleiotropic impact on lipid metabolism (Aebi et al., 1986), and affected signaling cascades in adipose cells (Lin and Worman, 1993). Theoretically, changes in mRNA stability or AS favoring one lamin mRNA may cause relative differences in lamin A/C expression. In the present study, we emphasize the idea that influencing LMNA isoforms might be beneficial in obesity. Specifically, we show here that ABX300 interacts with SRSF1, and it is tempting to hypothesize that this interplay affects *LMNA* splicing favoring Lamin-A production. Moreover, not shown data reveal a slight increase in the expression of Lamin-A after ABX300 treatment and this specifically in several metabolic organs. This result supports the notion of a role for lamin proteins in metabolism, complementary to their structural functions (Kumaran et al., 2002; Spann et al., 2002; López-Otín et al., 2013). For concretizing our data, it would be of great interest to test ABX300 in murine models deficient for A-type lamins (Fong et al., 2006; Davies et al., 2010; Coffinier et al., 2010). We would expect a decrease of its efficiency, or even an absence of efficacy.

Since we are promoting *LMNA* AS modulation as an attractive mechanism of anti-obesity therapies, it was necessary to demonstrate that the effect of ABX300 did not have a global effect on the AS of endogenous genes. While analyzing AS events in visceral WAT of treated animals, only a few of them were found to be altered by the molecule. Even more to our advantage, these changes pointed to a return to normality, because AS in ABX300 treated mice revisited the profile of lean animals (**Figure 4D**). Perhaps, the most intriguing concept opened by the results conferred here is that small molecules targeting the core splicing machinery, display tiny effects on different genes and alternative SS (**Figure 4E**). Understanding the molecular basis for these differential effects may pave the way towards the rational design of compounds that can modulate the versatile effects of SS selection on gene expression (Bonnal et al.,



2012). Further studies using RNA-sequencing and global analysis of transcript variants and splicing regulators would be of great utility for exploring the association of AS with metabolic alterations in obesity.

AS has also been described to affect microRNA biogenesis and regulation (Passetti et al., 2009). Withal it is conceivable that splicing regulation *in vivo* represents a system-wide response to the composition of miRNAs (Fu and Ares, 2014). Nevertheless, how the impact on gene regulation by miRNAs will affect drug metabolism remains unknown (Kwan et al., 2008). In recent years, there has been a rapidly growing interest in the role of miRNAs in fat cell development and obesity. Understanding their role in the proliferation and differentiation of adipocytes during fat cell development may provide new therapeutic targets for anti-obesity drugs and early biomarkers for clinical diagnosis ((Heneghan et al., 2010 A. McGregor and S. Choi, 2011). Moreover, miRNAs have been shown to play important roles in both brown and white fat differentiation (Jordan et al., 2011; Trajkovski et al., 2011; Sun et al., 2011; Trajkovski et al., 2012; Yin et al., 2013; Mori et al., 2014) and in maintaining cell identity by fine-tuning cell-specific transcriptional networks (Christodoulou et al., 2010; Ebert and Sharp, 2012). In response to obesity, insulin resistance, or cold exposure, miRNAs have been delineated to change in adipose tissue (Xie et al., 2009; Mori et al., 2012). This is consistent with our results indicating a modulation of ABX300 of mitochondrial microRNAs (**Figure 5**), and seems to correlate with the observed phenotype of treated animals.

Numerous are the proposals to create new therapies for obesity targeting mitochondrial dynamics and energy homeostasis. Screening of chemical libraries, as well as collections of known drugs and drug-like compounds, to determine if synthetic chemicals can activate BAT, and thus increase EE, concern among others PRDM16



(Seale, 2010) PGC1 $\alpha$  (Vaughan et al., 2014), UCP1 (Tomás et al., 2004), and AMPK (Cool et al., 2006) . Furthermore, we have explored the browning mechanism as another possible avenue for ABX300 to reduce fat mass, but this does not seem to be the launched mechanism (data not shown). Brown and white adipocyte identity is defined during development but can be modified by a myriad of complex events including genetic factors, epigenetic factors, hormonal factors, and other environmental challenges that might occur during adipocyte differentiation (Gesta et al., 2007; Seale et al., 2008; Schulz et al., 2013). Experiments carried out with 3T3-L1 and BAT cellular models did not allow us to confirm any robust effect of the molecule on the differentiation process (data not shown).

Here, we provide evidence that EE and metabolic homeostasis is markedly influenced by ABX300. The drug increases basal metabolic rate during the light period (**Figure 6**). Besides its influence on EE, ABX300 seemed to act to control feeding, and while based on the literature we do believe that our data *in vivo* and biochemically are related to mitochondrial activity, we could not completely exclude the possibility that at least part of the responses observed might be related to other functions, such as its anorexigenic action. However a pair-feeding experiment demonstrated that reduced food intake alone was not sufficient to explain the observed phenotype (**Figure 2D**). The involvement of ABX300 in the regulation of food intake could indicate that it was exclusively acting like an appetite suppressant. ABX300, is capable of crossing the blood brain barrier (data not shown). Consequently, it could potentially act on the centers controlling hunger (Ahima and Antwi, 2008), a fact which usually relates to toxicity. Nevertheless, ABX300 selectivity (weight loss exclusively under HDF conditions) (**Figure 2**), pointed to a positive safety profile, and made us enthusiastic about the possibility of developing ABX300 for therapeutic purposes. We hypothesize

that action of ABX300 is only relevant in the presence of an hyperlipidic regime, this particularity has been already been observed for other compounds (Tang et al., 2011; Ortega-Molina et al., 2012). Unfortunately, despite these facts and ABX300 efficacy, the development and clinical use of this drug is limited by some other adverse effects. In this regard, small molecules are known to be disadvantaged by the need to interact with the often more conserved active site of a target. This exquisite specificity is the basis for the existence of non-mechanistic (or 'off-target') toxicity, a major disadvantage of small-molecule drugs (Hughes et al., 2011).

In summary, we showed that ABX300 induces weight maintenance or loss in HFD fed animals through SRSF1 interaction, which increases oxygen consumption, upregulates mitochondrial related miRNAs, and switches adipocyte size, leading altogether to metabolic tuning. Our data add more evidence to the fact that modulation of AS, specifically *LMNA*'s, is a valid strategy to approach obesity therapy. These results provide insights into the physiological regulation of energy balance and its perturbation in *LMNA* mutation states.

#### **Authors' contributions**

CA, CLH and JS performed the in vivo experiments (drug treatments) and the analytical methods (PCR, histology and metabolites measurements). They also analyzed and collected the data. LL performed and analyzed the microscopy data together with western blotting. FM, RN and PF designed and produced the ABX drugs, along with the performance of the affinity experiments. ICLM produced the HEK293-Imna luc cell line. YB performed the micro RNA analysis. EZA and FC contributed to CT scan and metabolic cages experiments. CA, CLH, JS, CC, BP, DS and JT designed the experiments and analyzed, discussed, and interpreted the data. CA, CLH, JS, LL and

CC reviewed and edited the manuscript; CA, CLH, JS, LL and YB made the figures. JT developed the hypothesis, coordinated and directed the project, and wrote the manuscript. All authors had final approval of the submitted manuscript.

#### **Acknowledgements**

This work was supported by the collaborative laboratory ABIVAX, OSEO-ISI CaReNA grant. JT is senior member of the Institut Universitaire de France. CLH is an ESR fellow of the EU FP7 Marie Curie ITN RNPnet program (289007). ICLM was supported by a graduate fellowship from the Ministère Délégué à la Recherche et aux Technologies and CNRS. We are grateful to the Montpellier-RIO imaging platform (Montpellier, France), to the Histology Experimental Network of Montpellier, to the “Centre de Ressources en Imagerie Cellulaire de Montpellier” (France), and to the IGMM animal facilities. The authors are grateful to R. Klinck (Université de Sherbrooke) for their splicing experiments, to P. de la Grange (Genosplice) for their microRNA experiments and to Edouard Bertrand for the SRSF1-GFP HeLa cells.

#### **Conflict of interests/ Competing interests**

The authors declare that they have no conflict of interest. All the authors of this paper declare that they are aware that the work has been funded by ABIVAX a private company that holds patents on ABX300. These patents are shared with the CNRS and Institut Curie. CA, CLH, JS, LL, RN, PF and DS are ABIVAX employees. JT, and BP have received funding from ABIVAX to perform the work. CC, FM, ICLM, YB and JT are members of a collaborative laboratory that has received financial support from ABIVAX.

## References

- A. McGregor, R., and S. Choi, M. (2011). microRNAs in the Regulation of Adipogenesis and Obesity. *Curr. Mol. Med.* *11*, 304–316.
- Aebi, U., Cohn, J., Buhle, L., and Gerace, L. (1986). The nuclear lamina is a meshwork of intermediate-type filaments. *Nature* *323*, 560–564.
- Ahima, R.S., and Antwi, D. a. (2008). Brain Regulation of Appetite and Satiety. *Endocrinol. Metab. Clin. North Am.* *37*, 811–823.
- Arai, Y., Takayama, M., Abe, Y., and Hirose, N. (2011). Adipokines and aging. *J. Atheroscler. Thromb.* *18*, 545–550.
- Bonnal, S., Vigevani, L., and Valcárcel, J. (2012). The spliceosome as a target of novel antitumour drugs. *Nat. Rev. Drug Discov.* *11*, 847–859.
- Chen, L., Dai, Y.M., Ji, C.B., Yang, L., Shi, C.M., Xu, G.F., Pang, L.X., Huang, F.Y., Zhang, C.M., and Guo, X.R. (2014). MiR-146b is a regulator of human visceral preadipocyte proliferation and differentiation and its expression is altered in human obesity. *Mol. Cell. Endocrinol.* *393*, 65–74.
- Christodoulou, F., Raible, F., Tomer, R., Simakov, O., Trachana, K., Klaus, S., Snyman, H., Hannon, G.J., Bork, P., and Arendt, D. (2010). Ancient animal microRNAs and the evolution of tissue identity. *Nature* *463*, 1084–1088.
- Coffinier, C., Jung, H.J., Li, Z., Nobumori, C., Yun, U.J., Farber, E. a., Davies, B.S., Weinstein, M.M., Yang, S.H., Lammerding, J., et al. (2010). Direct synthesis of lamin A, bypassing prelamin a processing, causes misshapen nuclei in fibroblasts but no detectable pathology in mice. *J. Biol. Chem.* *285*, 20818–20826.
- Cool, B., Zinker, B., Chiou, W., Kifle, L., Cao, N., Perham, M., Dickinson, R., Adler, A., Gagne, G., Iyengar, R., et al. (2006). Identification and characterization of a small molecule AMPK activator that treats key components of type 2 diabetes and the metabolic syndrome. *Cell Metab.* *3*, 403–416.
- Cummings, D.E., and Schwartz, M.W. (2003). Genetics and pathophysiology of human obesity. *Annu. Rev. Med.* *54*, 453–471.
- Davies, B.S.J., Barnes, R.H., Tu, Y., Ren, S., Andres, D. a., Peter Spielmann, H., Lammerding, J., Wang, Y., Young, S.G., and Fong, L.G. (2010). An accumulation of non-farnesylated prelamin A causes cardiomyopathy but not progeria. *Hum. Mol. Genet.* *19*, 2682–2694.
- Desvergne, B., Michalik, L., and Wahli, W. (2006). Transcriptional regulation of metabolism. *Physiol. Rev.* *86*, 465–514.
- Ebert, M.S., and Sharp, P. a. (2012). Roles for MicroRNAs in conferring robustness to

- 1 biological processes. *Cell* **149**, 505–524.
- 2 Eriksson, M., Brown, W.T., Gordon, L.B., Glynn, M.W., Singer, J., Scott, L., Erdos,  
3 M.R., Robbins, C.M., Moses, T.Y., Berglund, P., et al. (2003). Recurrent de novo point  
4 mutations in lamin A cause Hutchinson-Gilford progeria syndrome. *Nature* **423**, 293–  
5 298.
- 6 Feige, J.N., and Auwerx, J. (2007). Transcriptional coregulators in the control of energy  
7 homeostasis. *Trends Cell Biol.* **17**, 292–301.
- 8 Feige, J.N., Lagouge, M., Canto, C., Strehle, A., Houten, S.M., Milne, J.C., Lambert,  
9 P.D., Matak, C., Elliott, P.J., and Auwerx, J. (2008). Specific SIRT1 Activation Mimics  
10 Low Energy Levels and Protects against Diet-Induced Metabolic Disorders by  
11 Enhancing Fat Oxidation. *Cell Metab.* **8**, 347–358.
- 12 Fong, L.G., Ng, J.K., Lammerding, J., Vickers, T.A., Meta, M., Côté, N., Gavino, B.,  
13 Qiao, X., Chang, S.Y., Young, S.R., et al. (2006). Prelamin A and lamin A appear to  
14 be dispensable in the nuclear lamina. *116*, 743–752.
- 15 Frayn, K.N., Karpe, F., Fielding, B. a, Macdonald, I. a, and Coppack, S.W. (2003).  
16 Integrative physiology of human adipose tissue. *Int. J. Obes. Relat. Metab. Disord.* **27**,  
17 875–888.
- 18 Fu, X.-D., and Ares, M. (2014). Context-dependent control of alternative splicing by  
19 RNA-binding proteins. *Nat. Rev. Genet.* **15**, 689–701.
- 20 Van Gaal, L.F., Mertens, I.L., and De Block, C.E. (2006). Mechanisms linking obesity  
21 with cardiovascular disease. *Nature* **444**, 875–880.
- 22 Gesta, S., Tseng, Y.H., and Kahn, C.R. (2007). Developmental Origin of Fat: Tracking  
23 Obesity to Its Source. *Cell* **131**, 242–256.
- 24 Goodson, M.L., Mengeling, B.J., Jonas, B. a., and Privalsky, M.L. (2011). Alternative  
25 mRNA splicing of corepressors generates variants that play opposing roles in  
26 adipocyte differentiation. *J. Biol. Chem.* **286**, 44988–44999.
- 27 Guan, X.M., Chen, H., Dobbelaar, P.H., Dong, Y., Fong, T.M., Gagen, K., Gorski, J.,  
28 He, S., Howard, A.D., Jian, T., et al. (2010). Regulation of Energy Homeostasis by  
29 Bombesin Receptor Subtype-3: Selective Receptor Agonists for the Treatment of  
30 Obesity. *Cell Metab.* **11**, 101–112.
- 31 Harper, M.-E., Green, K., and Brand, M.D. (2008). The efficiency of cellular energy  
32 transduction and its implications for obesity. *Annu. Rev. Nutr.* **28**, 13–33.
- 33 Hegele, R. a., Huff, M.W., and Young, T.K. (2001). Common genomic variation in  
34 LMNA modulates indexes of obesity in Inuit. *J. Clin. Endocrinol. Metab.* **86**, 2747–  
35 2751.
- 36 Hegele, R.A., Cao, H., Harris, S.B., Zinman, B., Hanley, A.J., and Anderson, C.M.



- 1 (2000). Genetic variation in LMNA modulates plasma leptin and indices of obesity in  
2 aboriginal Canadians. *Physiol. Genomics* 3, 39–44.
- 3 Heneghan, H.M., Miller, N., and Kerin, M.J. (2010). Role of microRNAs in obesity and  
4 the metabolic syndrome. *Obes. Rev.* 11, 354–361.
- 5 Houtkooper, R.H., Mouchiroud, L., Ryu, D., Moullan, N., Katsyuba, E., Knott, G.,  
6 Williams, R.W., and Auwerx, J. (2013). Mitonuclear protein imbalance as a conserved  
7 longevity mechanism. *Nature* 497, 451–457.
- 8 Huang, H., Song, T.-J., Li, X., Hu, L., He, Q., Liu, M., Lane, M.D., and Tang, Q.-Q.  
9 (2009). BMP signaling pathway is required for commitment of C3H10T1/2 pluripotent  
10 stem cells to the adipocyte lineage. *Proc. Natl. Acad. Sci. U. S. A.* 106, 12670–12675.
- 11 Hughes, J.P., Rees, S.S., Kalindjian, S.B., and Philpott, K.L. (2011). Principles of early  
12 drug discovery. *Br. J. Pharmacol.* 162, 1239–1249.
- 13 Jackson, V.M., Breen, D.M., Fortin, J.-P., Liou, A., Kuzmiski, J.B., Loomis, A.K., Rives,  
14 M.-L., Shah, B., and Carpino, P.A. (2015). Latest approaches for the treatment of  
15 obesity. *Expert Opin. Drug Discov.* 1–15.
- 16 James, A.W., Leucht, P., Levi, B., Carre, A.L., Xu, Y., Helms, J. a, and Longaker, M.T.  
17 (2010). Sonic Hedgehog influences the balance of osteogenesis and adipogenesis in  
18 mouse adipose-derived stromal cells. *Tissue Eng. Part A* 16, 2605–2616.
- 19 Jordan, S.D., Krüger, M., Willmes, D.M., Redemann, N., Wunderlich, F.T., Brönneke,  
20 H.S., Merkwirth, C., Kashkar, H., Olkkonen, V.M., Böttger, T., et al. (2011). Obesity-  
21 induced overexpression of miRNA-143 inhibits insulin-stimulated AKT activation and  
22 impairs glucose metabolism. *Nat. Cell Biol.* 13, 434–446.
- 23 Kahn, R., Buse, J., Ferrannini, E., and Stern, M. (2005). The Metabolic Syndrome :  
24 Time for a critical appraisal. *Blood Press.* 28, 2289–2304.
- 25 Kaminska, D., and Pihlajamäki, J. (2013). Regulation of alternative splicing in obesity  
26 and weight loss. 143–147.
- 27 Kennett, G. a., and Clifton, P.G. (2010). New approaches to the pharmacological  
28 treatment of obesity: Can they break through the efficacy barrier? *Pharmacol.*  
29 *Biochem. Behav.* 97, 63–83.
- 30 Kumaran, R.I., Muralikrishna, B., and Parnaik, V.K. (2002). Lamin A/C speckles  
31 mediate spatial organization of splicing factor compartments and RNA polymerase II  
32 transcription. *J. Cell Biol.* 159, 783–793.
- 33 Kwan, T., Benovoy, D., Dias, C., Gurd, S., Provencher, C., Beaulieu, P., Hudson, T.J.,  
34 Sladek, R., and Majewski, J. (2008). Genome-wide analysis of transcript isoform  
35 variation in humans. *Nat. Genet.* 40, 225–231.
- 36 Lengacher, S., Nehiri-Sitayeb, T., Steiner, N., Carneiro, L., Favrod, C., Preitner, F.,

- 1 Thorens, B., Stehle, J.C., Dix, L., Pralong, F., et al. (2013). Resistance to diet-induced
- 2 obesity and associated metabolic perturbations in haploinsufficient monocarboxylate
- 3 transporter 1 mice. *PLoS One* 8.
- 4 Li, H., Cheng, Y., Wu, W., Liu, Y., Wei, N., Feng, X., Xie, Z., and Feng, Y. (2014).
- 5 SRSF10 Regulates Alternative Splicing and Is Required for Adipocyte Differentiation.
- 6 *Mol. Cell. Biol.* 34, 2198–2207.
- 7 Lin, F., and Worman, H.J. (1993). Structural organization of the human gene encoding
- 8 nuclear lamin A and nuclear lamin C. *J. Biol. Chem.* 268, 16321–16326.
- 9 Liu, B., Ghosh, S., Yang, X., Zheng, H., Liu, X., Wang, Z., Jin, G., Zheng, B., Kennedy,
- 10 B.K., Suh, Y., et al. (2012). Resveratrol rescues SIRT1-dependent adult stem cell
- 11 decline and alleviates progeroid features in laminopathy-based progeria. *Cell Metab.*
- 12 16, 738–750.
- 13 Lloyd, D.J., Trembath, R.C., and Shackleton, S. (2002). A novel interaction between
- 14 lamin A and SREBP1: implications for partial lipodystrophy and other laminopathies.
- 15 *Hum. Mol. Genet.* 11, 769–777.
- 16 Locke, A.E., Kahali, B., Berndt, S.I., Justice, A.E., Pers, T.H., Day, F.R., Powell, C.,
- 17 Vedantam, S., Buchkovich, M.L., Yang, J., et al. (2015). Genetic studies of body mass
- 18 index yield new insights for obesity biology. *Nature* 518, 197–206.
- 19 Lopez-Mejia, I.C., Vautrot, V., De Toledo, M., Behm-Ansmant, I., Bourgeois, C.F.,
- 20 Navarro, C.L., Osorio, F.G., Freije, J.M.P., Stévenin, J., De Sandre-Giovannoli, A., et
- 21 al. (2011). A conserved splicing mechanism of the LMNA gene controls premature
- 22 aging. *Hum. Mol. Genet.* 20, 4540–4555.
- 23 Lopez-Mejia, I.C., de Toledo, M., Chavey, C., Lapasset, L., Cavelier, P., Lopez-
- 24 Herrera, C., Chebli, K., Fort, P., Beranger, G., Fajas, L., et al. (2014). Antagonistic
- 25 functions of LMNA isoforms in energy expenditure and lifespan. *EMBO Rep.* 15, 529–
- 26 539.
- 27 López-Otín, C., Blasco, M. a, Partridge, L., Serrano, M., and Kroemer, G. (2013). The
- 28 hallmarks of aging. *Cell* 153, 1194–1217.
- 29 Melamed, Z., Levy, A., Ashwal-Fluss, R., Lev-Maor, G., Mekahel, K., Atias, N., Gilad,
- 30 S., Sharan, R., Levy, C., Kadener, S., et al. (2013). Alternative Splicing Regulates
- 31 Biogenesis of miRNAs Located across Exon-Intron Junctions. *Mol. Cell* 50, 869–881.
- 32 Mori, M., Nakagami, H., Rodriguez-Araujo, G., Nimura, K., and Kaneda, Y. (2012).
- 33 Essential role for miR-196a in brown adipogenesis of white fat progenitor cells. *PLoS*
- 34 *Biol.* 10.
- 35 Mori, M. a., Thomou, T., Boucher, J., Lee, K.Y., Lallukka, S., Kim, J.K., Torriani, M.,
- 36 Yki-Järvinen, H., Grinspoon, S.K., Cypess, A.M., et al. (2014). Altered miRNA
- 37 processing disrupts brown/white adipocyte determination and associates with



1 lipodystrophy. *J. Clin. Invest.* **124**, 3339–3351.

2 Navarro, C.L., Cau, P., and Lévy, N. (2006). Molecular bases of progeroid syndromes.  
3 *Hum. Mol. Genet.* **15**, 151–161.

4 Ng, M., Fleming, T., Robinson, M., Thomson, B., Graetz, N., Margono, C., Mullany,  
5 E.C., Biryukov, S., Abbafati, C., Abera, S.F., et al. (2014). Global, regional, and national  
6 prevalence of overweight and obesity in children and adults during 1980-2013: a  
7 systematic analysis for the Global Burden of Disease Study 2013. *Lancet* **6736**, 1–16.

8 Nilsson, C., Raun, K., Yan, F., Larsen, M.O., and Tang-Christensen, M. (2012).  
9 Laboratory animals as surrogate models of human obesity. *Acta Pharmacol. Sin.* **33**,  
10 173–181.

11 Ortega, F.J., Moreno-Navarrete, J.M., Pardo, G., Sabater, M., Hummel, M., Ferrer, A.,  
12 Rodriguez-Hermosa, J.I., Ruiz, B., Ricart, W., Peral, B., et al. (2010). MiRNA  
13 expression profile of human subcutaneous adipose and during adipocyte  
14 differentiation. *PLoS One* **5**.

15 Ortega-Molina, A., Efeyan, A., Lopez-Guadamillas, E., Muñoz-Martin, M., Gómez-  
16 López, G., Cañamero, M., Mulero, F., Pastor, J., Martinez, S., Romanos, E., et al.  
17 (2012). Pten positively regulates brown adipose function, energy expenditure, and  
18 longevity. *Cell Metab.* **15**, 382–394.

19 Passetti, F., Ferreira, C.G., and Costa, F.F. (2009). The impact of microRNAs and  
20 alternative splicing in pharmacogenomics. *Pharmacogenomics J.* **9**, 1–13.

21 Powell, a G., Apovian, C.M., and Aronne, L.J. (2011). New drug targets for the  
22 treatment of obesity. *Clin. Pharmacol. Ther.* **90**, 40–51.

23 Rochford, J.J. (2014). Mouse models of lipodystrophy and their significance in  
24 understanding fat regulation (Elsevier Inc.).

25 Rosen, E.D., and MacDougald, O. a (2006). Adipocyte differentiation from the inside  
26 out. *Nat. Rev. Mol. Cell Biol.* **7**, 885–896.

27 Ruas, J.L., White, J.P., Rao, R.R., Kleiner, S., Brannan, K.T., Harrison, B.C., Greene,  
28 N.P., Wu, J., Estall, J.L., Irving, B. a, et al. (2012). A PGC-1 $\alpha$  isoform induced by  
29 resistance training regulates skeletal muscle hypertrophy. *Cell* **151**, 1319–1331.

30 De Sandre-Giovannoli, A., Bernard, R., Cau, P., Navarro, C., Amiel, J., Boccaccio, I.,  
31 Lyonnet, S., Stewart, C.L., Munnich, A., Le Merrer, M., et al. (2003). Lamin a truncation  
32 in Hutchinson-Gilford progeria. *Science* **300**, 2055.

33 Schulz, T.J., Huang, P., Huang, T.L., Xue, R., McDougall, L.E., Townsend, K.L.,  
34 Cypess, A.M., Mishina, Y., Gussoni, E., and Tseng, Y.-H. (2013). Brown-fat paucity  
35 due to impaired BMP signalling induces compensatory browning of white fat. *Nature*  
36 **495**, 379–383.

- 1 Seale, P. (2010). Transcriptional control of brown adipocyte development and  
2 thermogenesis. 17–23.
- 3 Seale, P., Bjork, B., Yang, W., Kajimura, S., Chin, S., Kuang, S., Scimè, A.,  
4 Devarakonda, S., Conroe, H.M., Erdjument-Bromage, H., et al. (2008). PRDM16  
5 controls a brown fat/skeletal muscle switch. *Nature* 454, 961–967.
- 6 Soret, J., Bakkour, N., Maire, S., Durand, S., Zekri, L., Gabut, M., Fic, W., Divita, G.,  
7 Rivalle, C., Dauzonne, D., et al. (2005). Selective modification of alternative splicing  
8 by indole derivatives that target serine-arginine-rich protein splicing factors. *Proc. Natl.*  
9 *Acad. Sci. U. S. A.* 102, 8764–8769.
- 10 Spann, T.P., Goldman, A.E., Wang, C., Huang, S., and Goldman, R.D. (2002).  
11 Alteration of nuclear lamin organization inhibits RNA polymerase II-dependent  
12 transcription. *J. Cell Biol.* 156, 603–608.
- 13 Spiegelman, B.M., and Heinrich, R. (2004). Biological control through regulated  
14 transcriptional coactivators. *Cell* 119, 157–167.
- 15 Suh, J.M., Gao, X., McKay, J., McKay, R., Salo, Z., and Graff, J.M. (2006). Hedgehog  
16 signaling plays a conserved role in inhibiting fat formation. *Cell Metab.* 3, 25–34.
- 17 Sun, L., Xie, H., Mori, M. a, Alexander, R., Yuan, B., Hattangadi, S.M., Liu, Q., Kahn,  
18 C.R., and Lodish, H.F. (2011). Mir193b-365 is essential for brown fat differentiation.  
19 *Nat. Cell Biol.* 13, 958–965.
- 20 Tang, J.J., Li, J.G., Qi, W., Qiu, W.W., Li, P.S., Li, B.L., and Song, B.L. (2011).  
21 Inhibition of SREBP by a small molecule, betulin, improves hyperlipidemia and insulin  
22 resistance and reduces atherosclerotic plaques. *Cell Metab.* 13, 44–56.
- 23 Tomás, P., Jiménez-Jiménez, J., Zaragoza, P., Vuligonda, V., Chandraratna, R. a S.,  
24 and Rial, E. (2004). Activation by retinoids of the uncoupling protein UCP1. *Biochim.*  
25 *Biophys. Acta - Bioenerg.* 1658, 157–164.
- 26 Trajkovski, M., Hausser, J., Soutschek, J., Bhat, B., Akin, A., Zavolan, M., Heim, M.H.,  
27 and Stoffel, M. (2011). MicroRNAs 103 and 107 regulate insulin sensitivity. *Nature* 474,  
28 649–653.
- 29 Trajkovski, M., Ahmed, K., Esau, C.C., and Stoffel, M. (2012). MyomiR-133 regulates  
30 brown fat differentiation through Prdm16. *Nat. Cell Biol.* 14, 1330–1335.
- 31 Tseng, Y.-H., Cypess, A.M., and Kahn, C.R. (2010). Cellular bioenergetics as a target  
32 for obesity therapy. *Nat. Rev. Drug Discov.* 9, 465–482.
- 33 Vaughan, R. a., Mermier, C.M., Bisoffi, M., Trujillo, K. a., and Conn, C. a. (2014).  
34 Dietary stimulators of the PGC-1 superfamily and mitochondrial biosynthesis in skeletal  
35 muscle. A mini-review. *J. Physiol. Biochem.* 70, 271–284.
- 36 Wilson, K.L., Zastrow, M.S., and Lee, K.K. (2001). Lamins and disease: insights into

- 1 nuclear infrastructure. *Cell* *104*, 647–650.
- 2 Worman, H.J., and Bonne, G. (2007). “Laminopathies”: A wide spectrum of human  
3 diseases. *Exp. Cell Res.* *313*, 2121–2133.
- 4 Xie, H., Lim, B., and Lodish, H.F. (2009). MicroRNAs induced during adipogenesis that  
5 accelerate fat cell development are downregulated in obesity. *Diabetes* *58*, 1050–  
6 1057.
- 7 Yin, H., Pasut, A., Soleimani, V.D., Bentzinger, C.F., Antoun, G., Thorn, S., Seale, P.,  
8 Fernando, P., Van Ijcken, W., Grosveld, F., et al. (2013). MicroRNA-133 controls brown  
9 adipose determination in skeletal muscle satellite cells by targeting Prdm16. *Cell*  
10 *Metab.* *17*, 210–224.

11

For Peer Review

## Figure legends

### Figure 1: Identification of ABX300 a SRSF1 partner that modulates *Imna* splicing.

(A) Confocal fluorescence microscopy of SRSF1-GFP HeLa cells ABX300 treated , ABX914 treated and control

(B) Schematic representation of the *in vitro* screening based on the LMNA-Luc splicing reporter.

(C) Classification of positive compounds from the screen.

(D) Fluorimetric titration of SRSF1 with ABX300.

(E) Fluorimetric titration of SRSF1 $\Delta$ RS with ABX300.

### Figure 2: *In vivo* Fat-dependent Efficacy of ABX300

(A) Monitoring of weight changes (left panel) along with average daily and cumulative food intake (right panel) of Untreated and Treated DIO animals (50 mg/kg) in a Curative context.

(B) Monitoring of weight changes (left panel) along with average daily and cumulative food intake (right panel) of Untreated and Treated animals (50 mg/kg) in a Preventive context.

(C) Monitoring of weight changes (left panel) along with average daily and cumulative food intake (right panel) of Untreated and Treated animals (50 mg/kg) under normal chow diet conditions.

(D) Effect of Caloric Restriction/Pair-Feeding on body weight (left panel) along with average daily and cumulative food intake (right panel), in DIO animals. ABX300 was

orally administered once daily (50 mg/kg) exclusively in the Treated group. In the CR/PF group, mice were provided everyday with the same amount of diet/biscuits/dry food that had been consumed in the Treated cages over the preceding 24 h.

**Figure 3: ABX300 decrease adiposity in DIO mice**

(A)Weights of individual organs as fold of Untreated group after 35 days of treatment (n=10).

(B)PET-CT imaging for HFD Untreated, HFD Treated and CD Untreated mice.

(C)Quantification of fat tissue volume (expressed in mm<sup>3</sup>).

(D)Representative images of HE-stained sections of WAT from HFD Untreated and HFD treated mice.

(E)Quantification of adipocyte by size from WAT of HFD Untreated and HFD Treated mice (expressed in % of lipids droplets per size range)

**Figure 4: Identification of ABX300 associated Alternative Splicing signature**

**Figure 5: Transcriptomic analysis of key genes involved in adipose tissue homeostasis.**

(A) Scatter Plot between HFD treated mice versus HFD untreated mice showing upregulated and down-regulated genes.

(B) Scatter Plot between Chow diet mice versus HFD untreated mice.

(C) Scatter Plot between HFD treated mice and Chow diet mice

We used the Mouse Adipogenesis RT<sup>2</sup> Profiler™ PCR Array profiles for analyzing the expression of 84 key genes involved in the differentiation and maintenance of mature

adipocytes. Upregulated genes are represented in red boxes and down-regulated genes in green boxes.

**Figure 6: ABX300 modulates a population of miRNAs likely mitochondrial-enriched**

(A) Heat map showing the shifts for the 52 micro-RNAs (y axis) varying between DIO Untreated and Treated animals (x axis). After one month of daily drug administration (50mg/Kg), 26 micro-RNAs appear up regulated (red) and 26 RNAs appear down regulated (green).

(B) Heat map showing the shifts for the 113 micro-RNAs (y axis) varying between DIO and lean Untreated animals (x axis). After three months of different nourishment conditions, 54 micro-RNAs appear up regulated (red) and 59 RNAs appear down regulated (green).

(C) The Venn diagram shows the number of shared and unique miRNAs expressed upon different diet and treatment conditions. Circumference's overlapping area refers to the 42 miRNAs that reverted to the lean level, healthy white adipose tissue, after ABX300 treatment and that are up-regulated (red) or down-regulated (green) in HFD Untreated versus CD Untreated (green circle), or HFD Treated (blue circle). ABX300's 10-miRNA signature proved to be mitochondrial enriched. The mitochondria overlapping area shows the miRNAs involved in this organelle's field/function/related processes. The effectuated comparisons revealed that ABX300 treatment for obesity *enhanced* a non-coding population set of 8 miR regulators of *mitochondrial* genes. The identified miRNAs are divided according to their predicted targets (miRBASE,  $\geq 80\%$  confidence) through Mitocarta analysis. All of the miRNAs shown here display more than 1.5 Fold-Change differences between the groups ( $p < 0.05$ ). Values represent  $\geq$

4 animals per group; 5–6 months old. Expression of miRNAs was determined by Genosplice, Affimetrix 3.0. The Heat maps were generated by a custom R script using gplots and RcolorBrewer libraries (see material and methods). The Fold-changes and *p*-values of individual miRNAs have been summarized in S5.

**Figure 7: ABX300 modifies DIO mice metabolism.**

(A) Monitoring of  $\text{VO}_2$  consumption (left panel) and  $\text{CO}_2$  production (right panel) over 24h (12h-light / 12h-dark) on HFD Untreated and HFD Treated mice. Values are normalized to body weight (n=11)

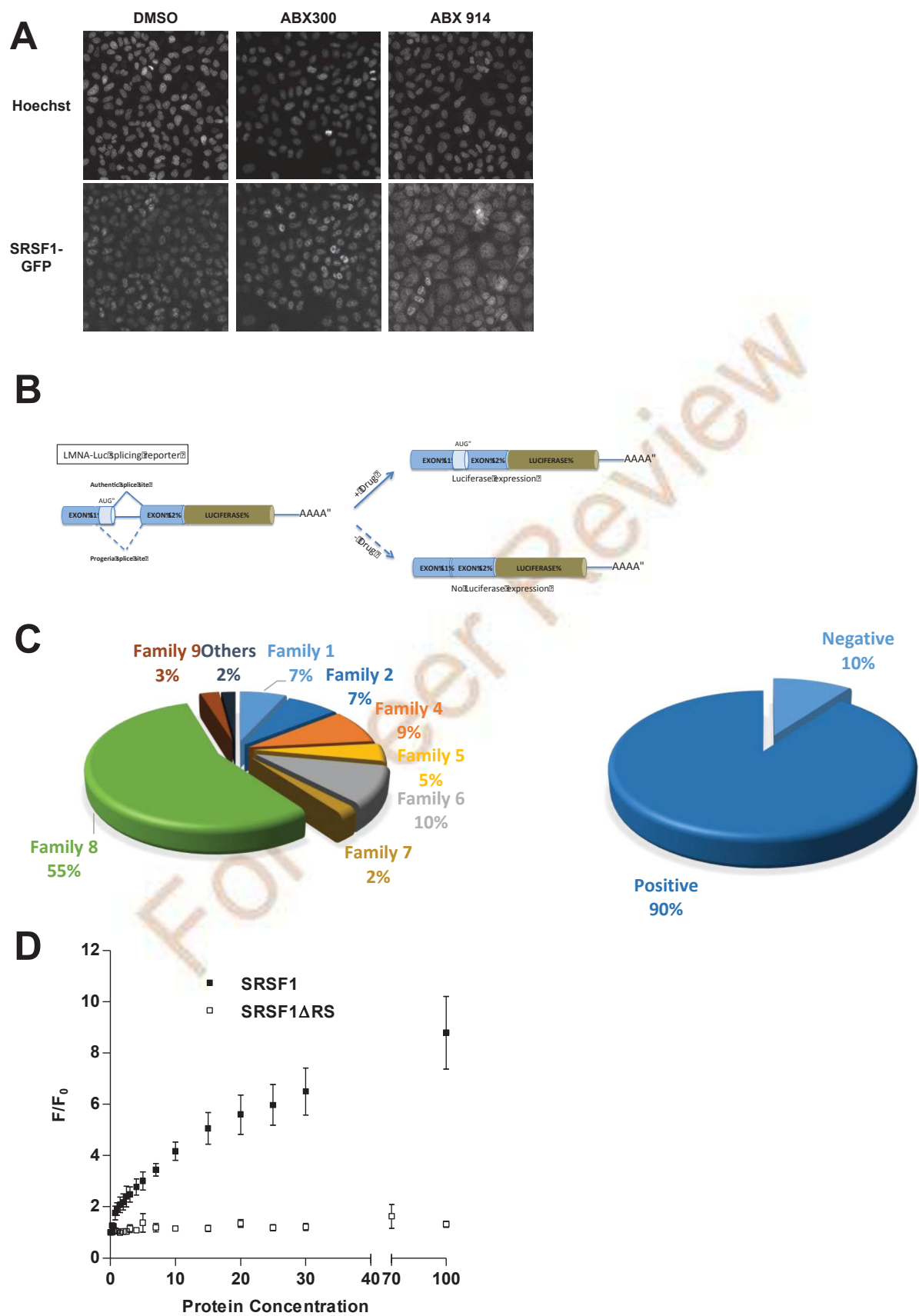
(B) Mean of  $\text{VO}_2$  consumption 8h after treatment (left panel) and 24h after treatment (right panel).

(C) Mean of  $\text{CO}_2$  production 8h after treatment (left panel) and 24h after treatment (right panel).

(D) Respiratory Exchange Ratio (RER) 8h after treatment (left panel) and 24h after treatment (right panel).

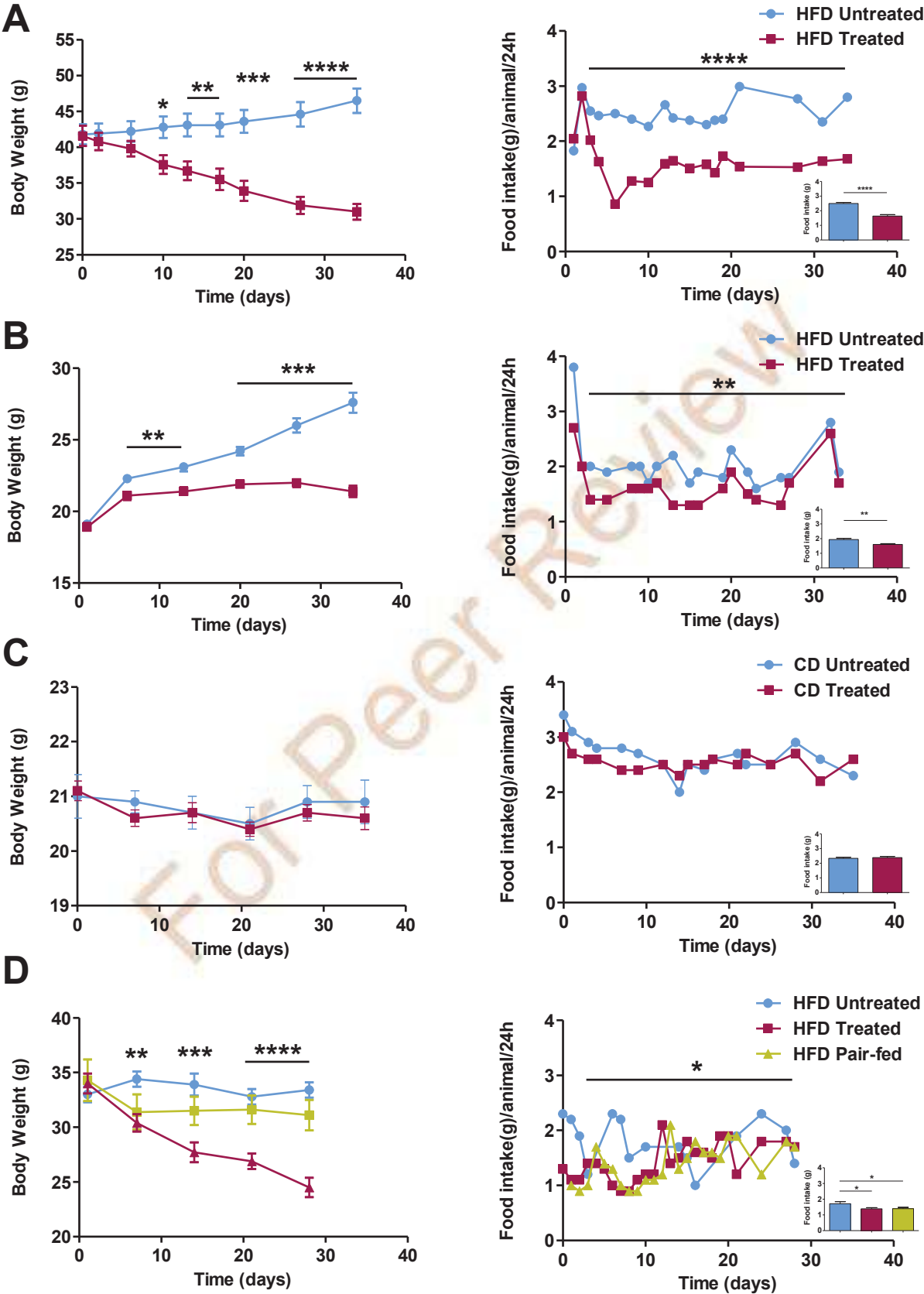


Figure 1



1

Figure 2



2

Figure 3

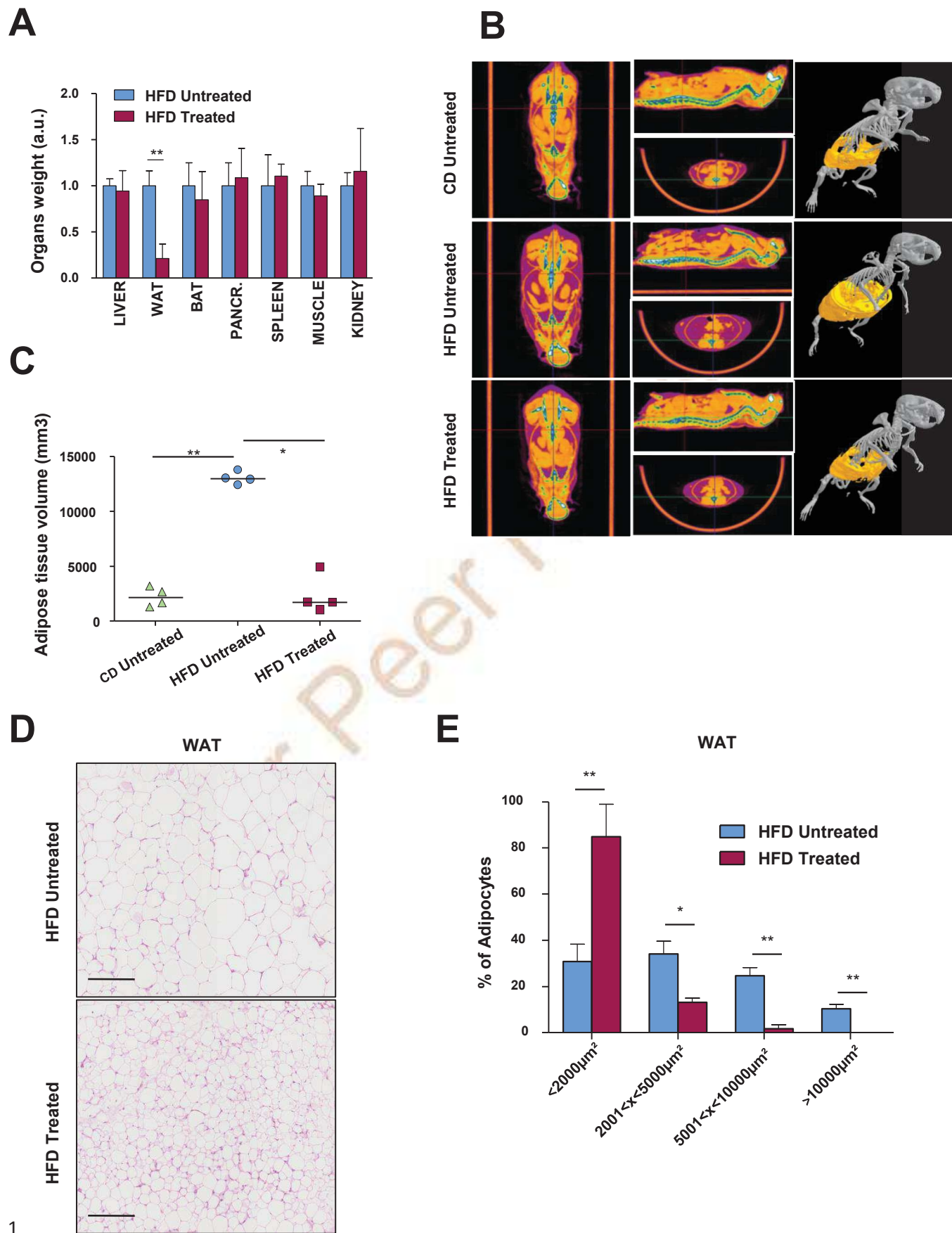


Figure 4

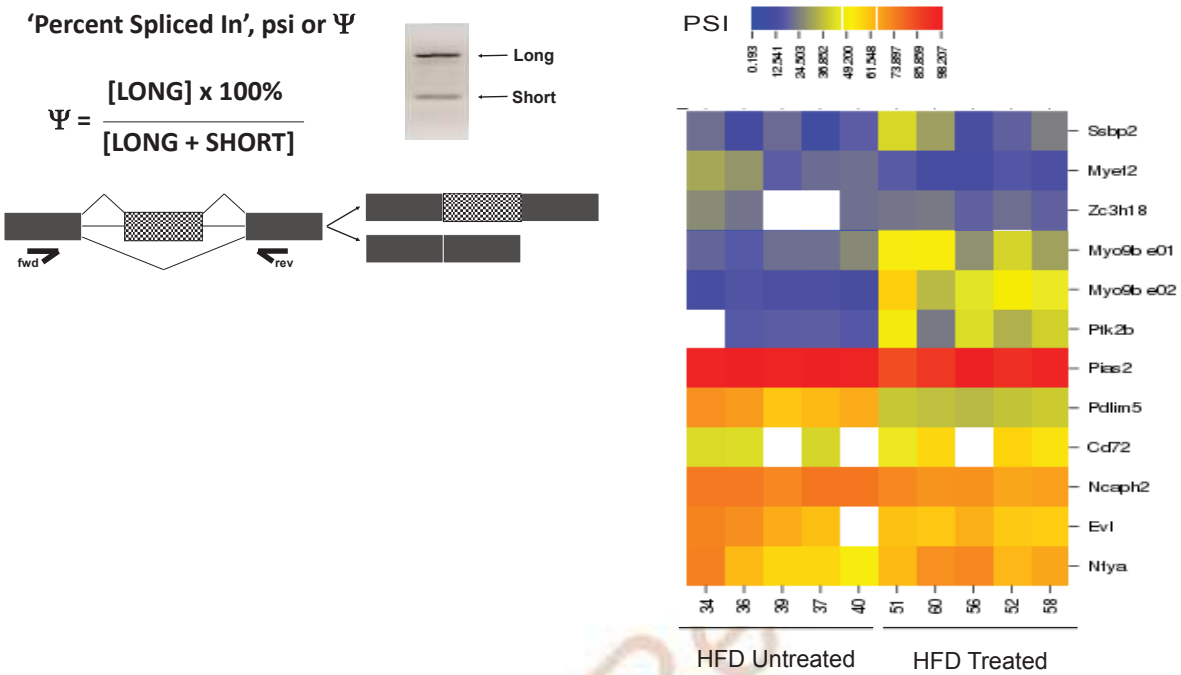


Figure 5

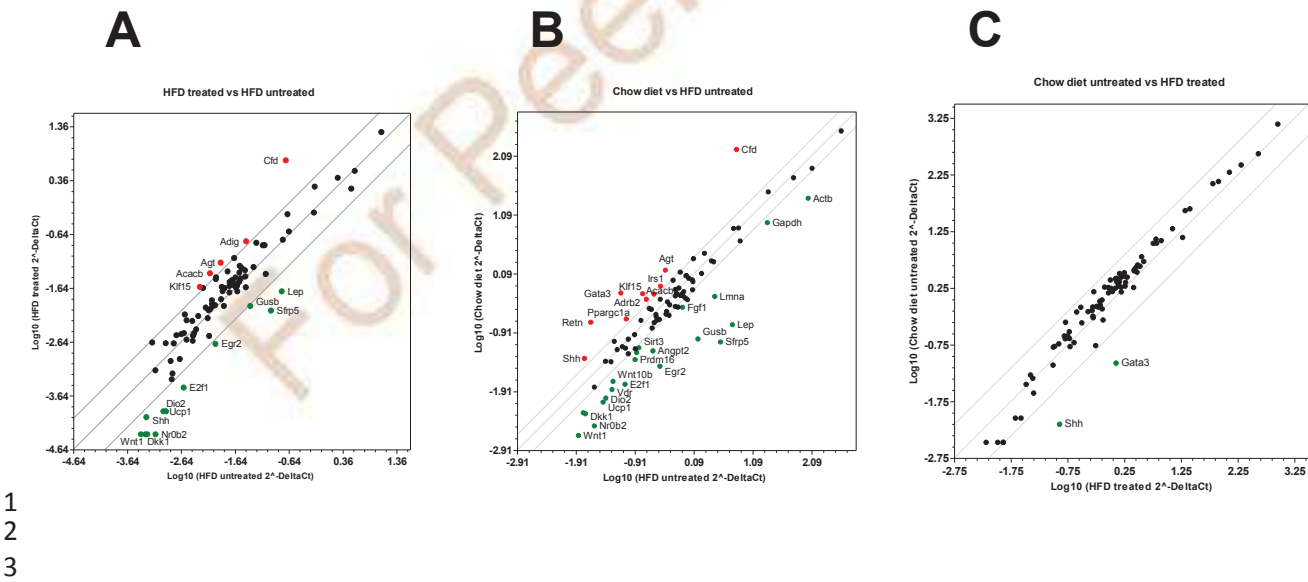


Figure 6

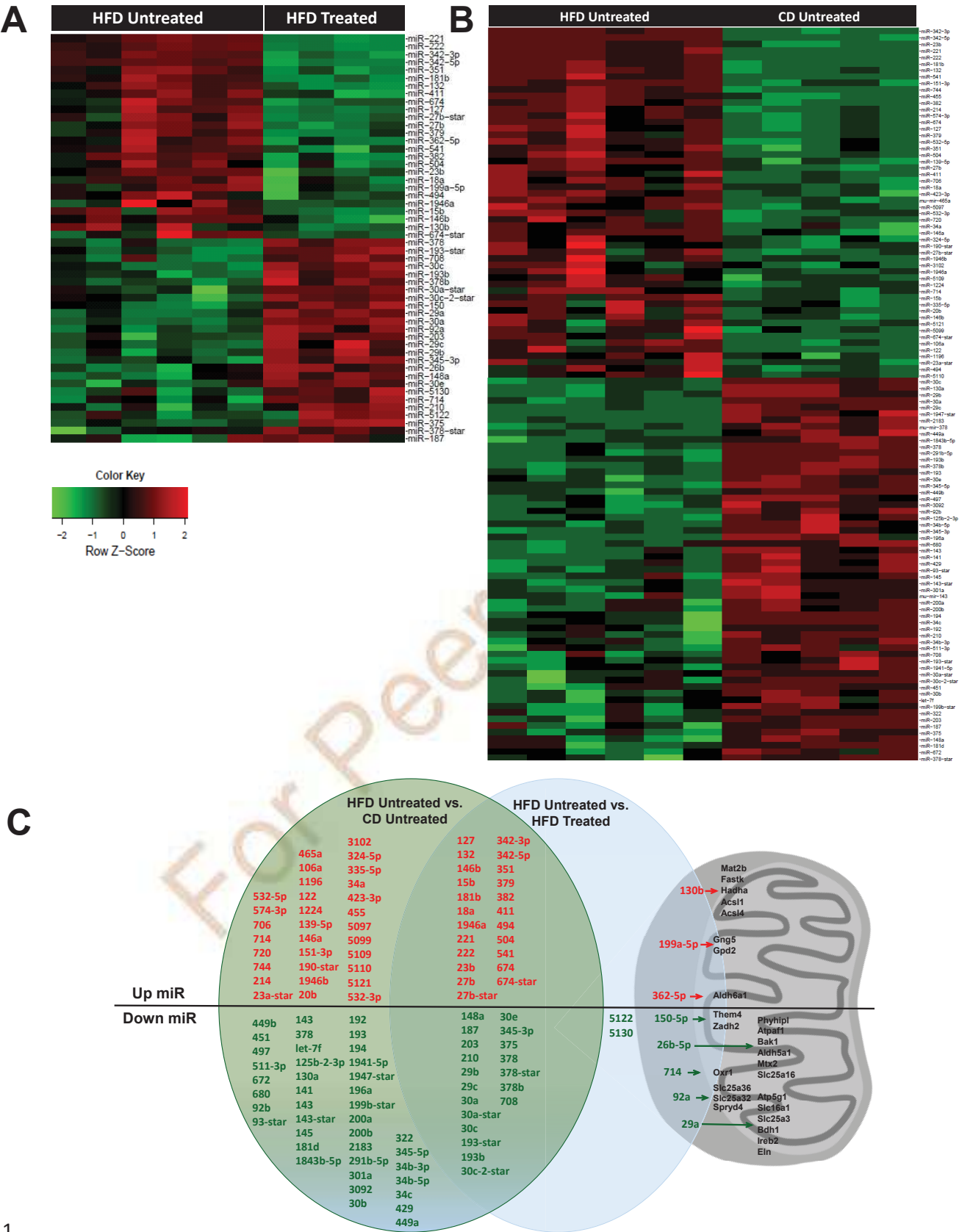
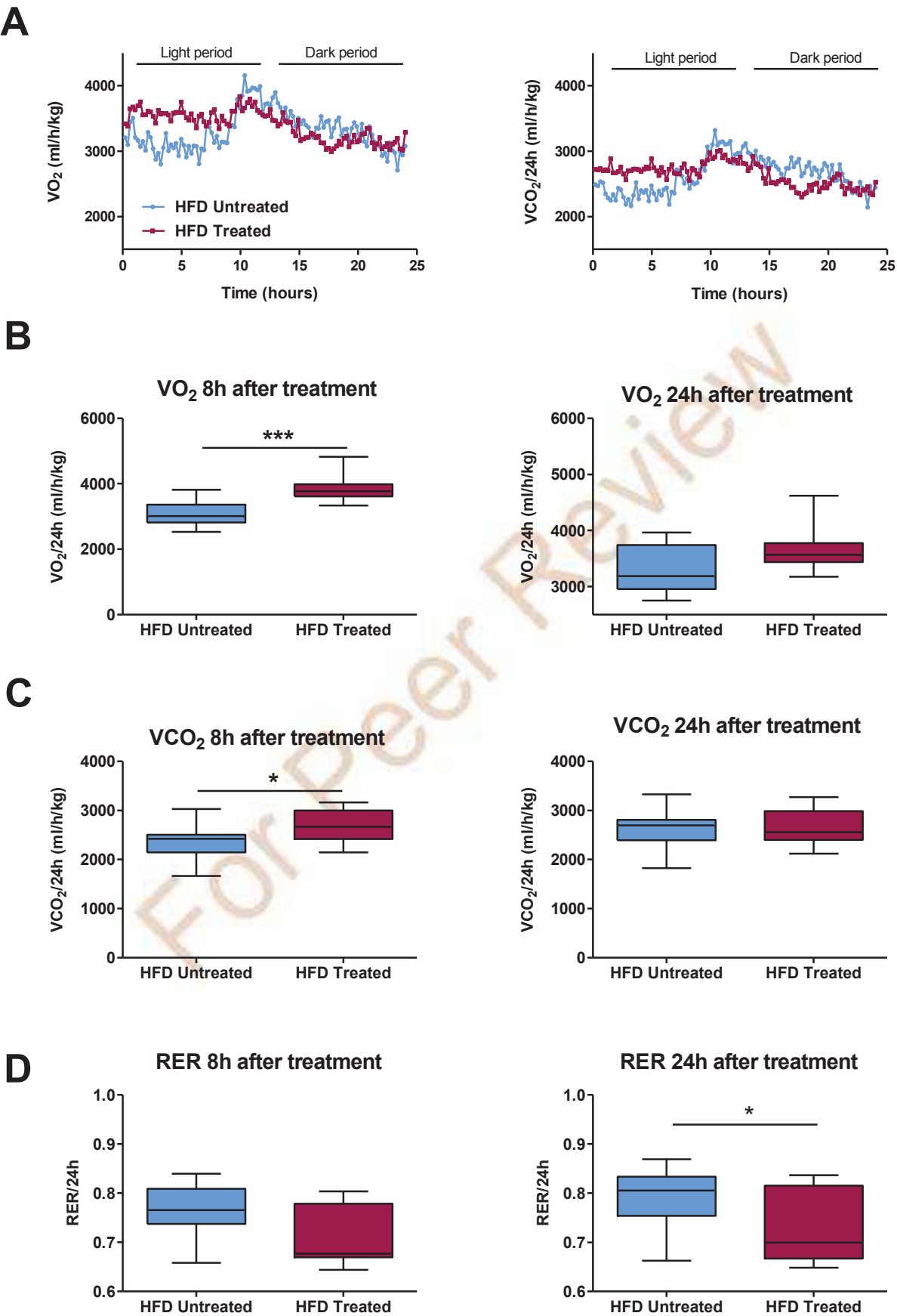
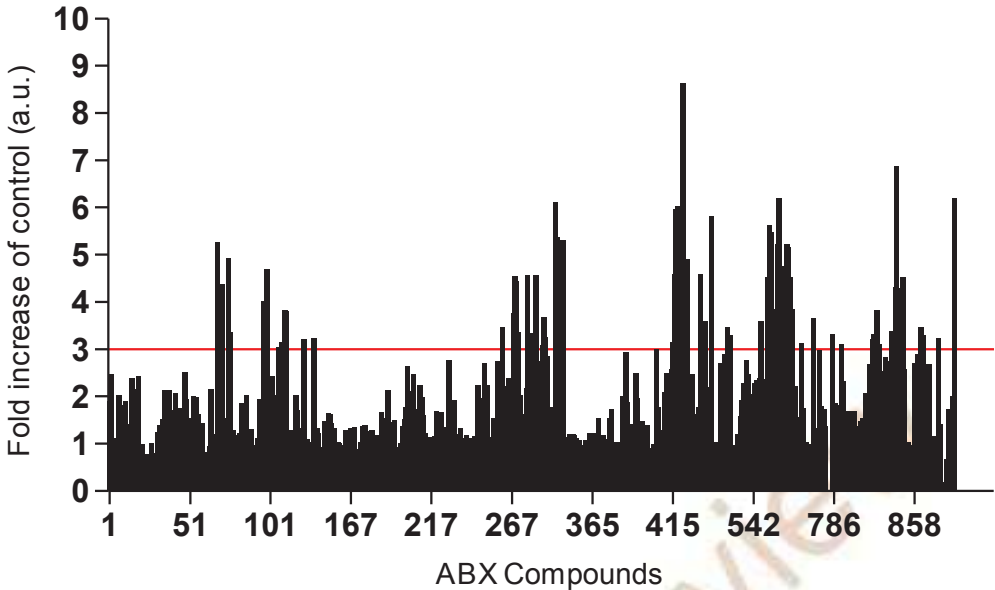


Figure 7



# Supplemental Figure 1

A



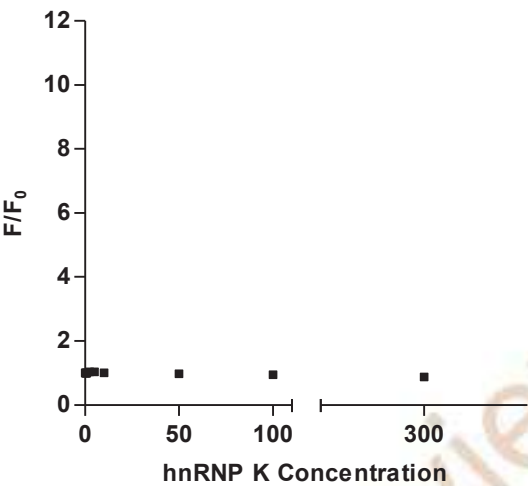
B

Abivax Compound	LMNA-luc activity	LMNA-luc toxicity (MTS)	Abivax Compound	LMNA-luc activity	LMNA-luc toxicity (MTS)
ABX68	5,25	<10 %	ABX548	3,59	10 % < x < 30%
ABX71	4,37	<10 %	ABX718	4,53	<10 %
ABX75	4,92	<10 %	ABX719	5,63	<10 %
ABX76	3,35	<10 %	ABX720	5,47	<10 %
ABX97	4,00	<10 %	ABX722	3,23	<10 %
ABX99	4,69	<10 %	ABX723	3,84	<10 %
ABX106	3,05	<10 %	ABX724	5,21	<10 %
ABX110	3,83	<10 %	ABX725	6,20	<10 %
ABX111	3,80	<10 %	ABX727	4,75	<10 %
ABX261	3,46	<10 %	ABX730	5,21	<10 %
ABX268	3,77	<10 %	ABX731	5,15	<10 %
ABX269	4,54	<10 %	ABX732	4,53	10 % < x < 30%
ABX270	4,43	<10 %	ABX733	3,84	10 % < x < 30%
ABX271	3,35	<10 %	ABX743	3,13	<10 %
ABX297	4,56	<10 %	ABX750	3,65	<10 %
ABX300	3,33	<10 %	ABX777	2,98	<10 %
ABX330	4,57	<10 %	ABX785	3,32	<10 %
ABX334	3,08	<10 %	ABX791	3,11	10 % < x < 30%
ABX335	3,66	<10 %	ABX832	3,21	<10 %
ABX336	3,25	<10 %	ABX833	3,32	<10 %
ABX405	3,00	<10 %	ABX835	3,83	<10 %
ABX415	3,15	<10 %	ABX836	3,11	10 % < x < 30%
ABX416	4,58	<10 %	ABX844	3,37	<10 %
ABX417	5,96	<10 %	ABX846	4,30	<10 %
ABX418	6,03	<10 %	ABX847	6,87	10 % < x < 30%
ABX420	4,97	<10 %	ABX848	4,29	<10 %
ABX421	8,63	10 % < x < 30%	ABX850	3,42	<10 %
ABX424	4,90	<10 %	ABX851	4,51	<10 %
ABX432	4,59	<10 %	ABX858	2,70	<10 %
ABX433	3,27	10 % < x < 30%	ABX860	2,89	<10 %
ABX435	3,59	<10 %	ABX861	2,80	<10 %
ABX448	3,87	10 % < x < 30%	ABX863	3,46	<10 %
ABX505	3,46	10 % < x < 30%	ABX865	3,29	10 % < x < 30%
ABX510	3,29	<10 %	ABX877	3,22	<10 %
ABX545	2,33	<10 %	ABX887	6,19	<10 %
ABX550	2,36	<10 %	ABX898		



**Supplemental Figure 1**  
**(continued)**

**C**



1  
2

1  
2  
3  
4  
5  
6  
7  
8  
9  
10  
11  
12  
13  
14

**Figure S1: Relative to Figure 1**

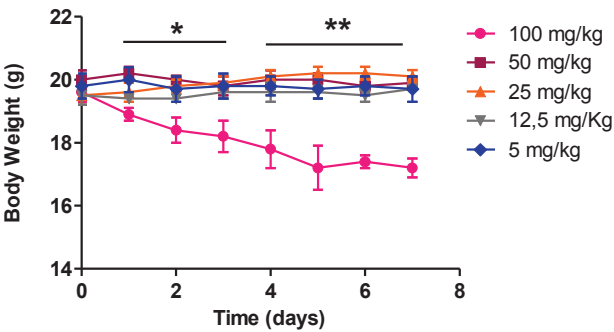
(A) Histogram recapitulating all the drugs from the ABIVAX Chemical library tested with the LMNA-luc mini gene reporter. Vertical bars represent the mean of the luciferase activity from three independent experiments. Pink bars signify the molecules tested *in vivo*. Threshold is depicted with a black line.

(B) Catalogue of all the drugs from the ABIVAX Chemical library referred to in this text. Columns show for each compound: the ABIVAX codification, their LMNA-luc activity and their LMNA-luc toxicity (MTS) (mean from three independent experiments). Pink depicts the molecules tested *in vivo*. Blue delineates activities below the established threshold

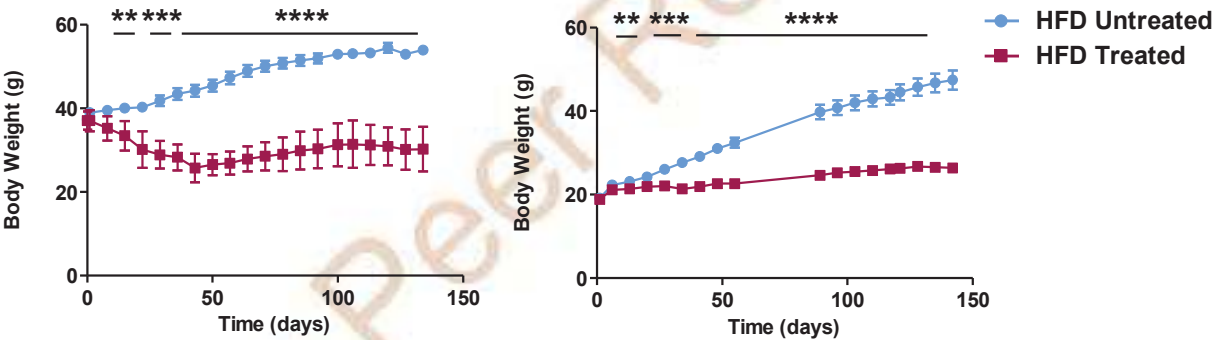
(C) Negative control for 1D). Under the same titration conditions, this figure exhibits an absence of interaction in between hnRNPK and ABX300.

Supplemental Figure 2

A



B



1

2

1 **Figure S2: Recapitulation of the Effects of ABX300 on Body Weight**

2 (A) Evaluation of ABX300 Maximal Tolerated Dose. Monitoring of weight changes  
3 of Treated DIO animals (5, 12.5, 25, 50, 100 mg/kg) under normal diet conditions.

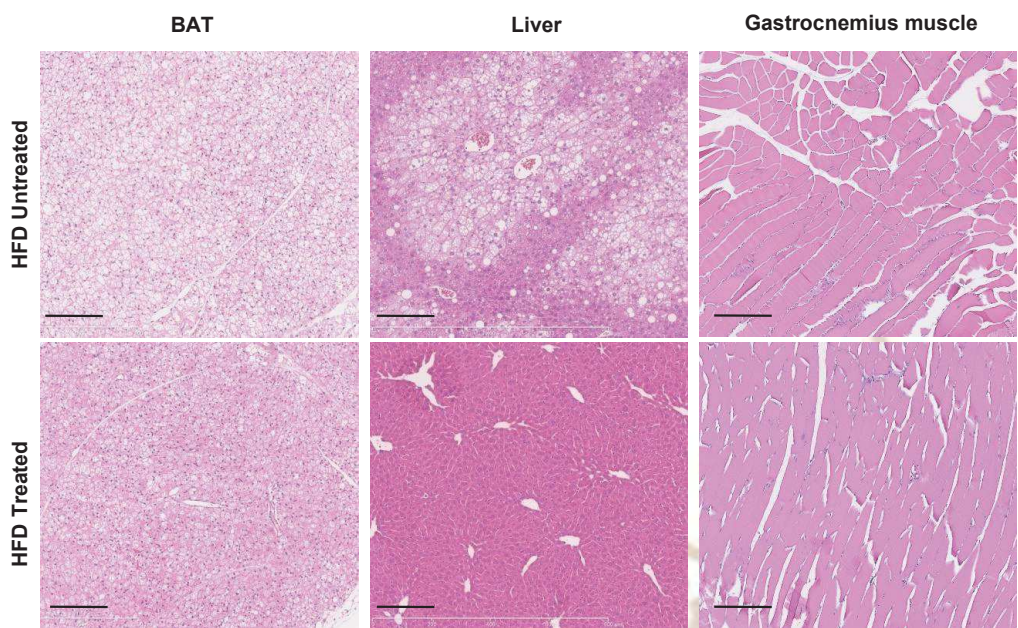
4 (B) ABX300 Time Persistence. Monitoring of weight changes of Untreated and  
5 Treated DIO animals (50 mg/kg) in a Curative and a Preventive context, under HFD  
6 conditions. Steady effects on body mass are patent after one month treatment

7

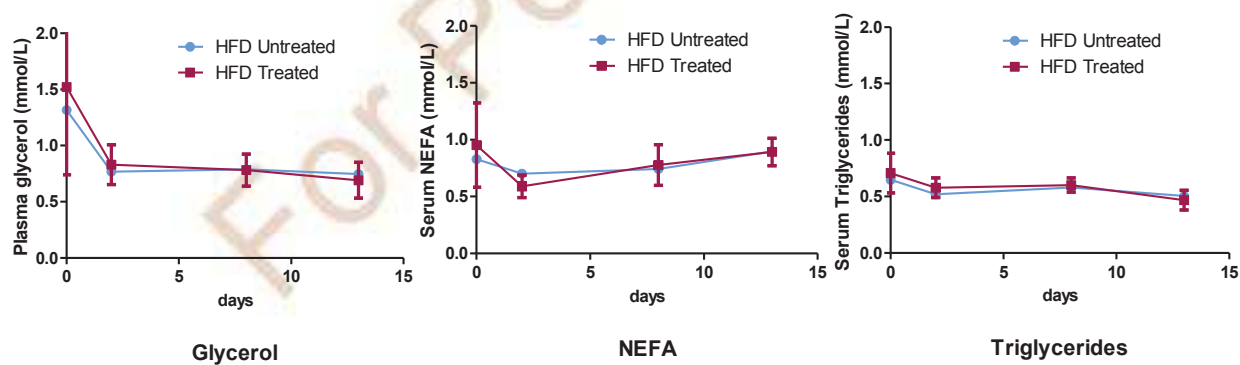
For Peer Review

Supplemental Figure 3

A



B



1

2

1 **Figure S3: Relative to Figure 3**

2 (A) Representative images of HE-stained sections of BAT, liver and gastrocnemius  
3 muscle from HFD Untreated and HFD treated mice.

4 (B) Assesment of glycerol, non-esterified fatty acids (NEFA) and triglycerides, in  
5 plasma and serum of ABX300 DIO Treated and Untreated animals

6

For Peer Review

## Supplemental Figure 4

Gene	Untreated PSI 1 (%)	ABX300 PSI 2 (%)	$\Delta$ PS1-2	Gene	Untreated PSI 1 (%)	ABX300 PSI 2 (%)	$\Delta$ PS1-2
Amigo1	9,3	81,4	-72,1	Fam76a	80,1	58,6	21,5
Pias2	38,4	100,0	-61,6	Hipk2	56,1	34,3	21,8
Odf2	28,5	72,0	-43,5	Pdlim5	41,1	18,3	22,8
Hexdc	9,7	51,1	-41,4	Tia1	88,6	65,2	23,4
Ncaph2	33,9	74,1	-40,2	Nlgn1	31,8	8,3	23,5
Cd200r3	21,3	61,3	-40,0	Gtpbp5	38,6	14,6	24,0
Myo9b	9,5	44,8	-35,3	Crybb3	100,0	74,2	25,8
Kctd18	55,1	87,5	-32,4	Lhx6	56,4	30,2	26,2
Cd226	64,3	93,9	-29,6	Vldlr	67,9	39,8	28,1
Ptk2b	14,4	43,9	-29,5	Pnpla6	72,9	44,6	28,3
Optc	71,9	100,0	-28,1	Pln	29,0	0,0	29,0
Il18r1	16,0	42,4	-26,4	Tcf20	29,3	0,0	29,3
Nfya	35,1	59,1	-24,0	Thap3	100,0	70,0	30,0
Zfp207	0,0	23,6	-23,6	Crem	45,1	14,8	30,3
Cd72	33,7	57,3	-23,6	Evl	72,6	41,6	31,0
Tcf7l2	23,6	46,9	-23,3	Ppm1b	43,0	11,6	31,4
Ntf3	0,0	22,2	-22,2	Cd6	100,0	68,6	31,4
Tssc4	28,9	50,0	-21,1	Dnmt3b	43,7	12,1	31,5
Espn	31,1	52,0	-20,9	Abi3bp	33,8	0,0	33,8
Mark3	63,3	84,1	-20,8	Zc3h18	44,5	10,4	34,2
Dctn3	79,3	100,0	-20,7	Mboat2	83,8	47,9	35,9
Entpd5	65,2	44,8	20,4	Ap3m2	36,2	0,0	36,2
Celsr2	34,2	13,8	20,4	Myef2	57,4	19,0	38,4
Fance	84,0	63,1	20,9	Trpt1	83,2	38,2	45,0
Kif21a	100,0	78,8	21,2	Myo9b	68,2	5,1	63,1
Zdhhc6	21,4	0,0	21,4	Ssbp2	80,2	12,9	67,3

1

2



1 **Figure S4: Relative to Figure 4**

2 Table recapitulating the largest PSI's variations in between HFD Untreated and  
3 ABX300 Treated groups.

4

5

6

For Peer Review

1

# Supplemental Figure 5

A

HFD Untreated vs. HFD Treated					
Up-regulated			Down-regulated		
Probe Set Name	Fold Change	P-Value	Probe Set Name	Fold Change	P-Value
mmu-miR-342-5p	10.14	3.12E-06	mmu-miR-30c-2-star	3.75	1.38E-04
mmu-miR-342-3p	5.62	1.02E-04	mmu-miR-30a	3.49	6.84E-06
mmu-miR-222	5.15	3.43E-07	mmu-miR-203	3.31	1.70E-03
mmu-miR-221	4.83	3.44E-06	mmu-miR-193b	3.20	1.22E-03
mmu-miR-541	3.09	2.66E-03	mmu-miR-210	3.13	2.42E-03
mmu-miR-146b	2.92	4.74E-03	mmu-miR-148a	2.95	4.94E-04
mmu-miR-382	2.74	5.82E-03	mmu-miR-714	2.62	1.87E-03
mmu-miR-351	2.56	4.64E-04	mmu-miR-30a	2.40	7.51E-07
mmu-miR-27b-star	2.45	1.61E-03	mmu-miR-30a-star	2.29	1.63E-04
mmu-miR-411	2.37	4.58E-03	mmu-miR-375	2.20	4.40E-02
mmu-miR-127	2.35	1.40E-03	mmu-miR-193-star	2.02	3.33E-04
mmu-miR-1946a	2.33	2.76E-02	mmu-miR-378-star	1.97	7.27E-03
mmu-miR-379	2.29	2.02E-03	mmu-miR-5122	1.86	4.41E-02
mmu-miR-18a	2.23	7.37E-03	mmu-miR-30c	1.86	1.97E-04
mmu-miR-132	1.97	2.77E-04	mmu-miR-378b	1.81	6.37E-03
mmu-miR-494	1.95	5.79E-03	mmu-miR-378	1.80	2.52E-04
mmu-miR-27b	1.85	2.41E-03	mmu-miR-29c	1.76	3.00E-02
mmu-miR-674-star	1.84	3.56E-02	mmu-miR-5130	1.65	8.90E-03
mmu-miR-674	1.83	4.94E-03	mmu-miR-26b	1.59	3.23E-03
mmu-miR-130b	1.76	6.49E-03	mmu-miR-29a	1.59	9.89E-06
mmu-miR-15b	1.76	9.48E-05	mmu-miR-187	1.57	2.20E-02
mmu-miR-181b	1.66	1.49E-04	mmu-miR-345-3p	1.56	2.37E-04
mmu-miR-504	1.62	2.68E-02	mmu-miR-708	1.55	5.56E-03
mmu-miR-362-5p	1.58	1.62E-03	mmu-miR-150	1.54	1.65E-03
mmu-miR-23b	1.53	8.42E-04	mmu-miR-29b	1.52	3.40E-03
mmu-miR-199a-5p	1.50	3.34E-02	mmu-miR-92a	1.52	2.47E-03

B

HFD Untreated vs. CD Untreated					
Up-regulated			Down-regulated		
Probe Set Name	Fold Change	P-Value	Probe Set Name	Fold Change	P-Value
mmu-miR-342-5p	13.04	2.77E-09	mmu-miR-34c	8.15	3.25E-03
mmu-miR-122	8.54	3.34E-03	mmu-miR-193	7.40	5.67E-05
mmu-miR-342-3p	8.40	6.38E-08	mmu-miR-141	5.36	2.06E-03
mmu-miR-222	6.22	3.83E-06	mmu-miR-429	4.98	1.34E-03
mmu-miR-221	4.72	2.63E-05	mmu-miR-200a	4.69	1.72E-02
mmu-miR-706	3.76	5.52E-04	mmu-miR-345-5p	4.43	9.68E-06
mmu-miR-382	3.60	1.46E-04	mmu-miR-193b	3.88	1.53E-05
mmu-miR-132	3.52	3.84E-07	mmu-miR-29b	3.77	3.23E-04
mmu-miR-541	3.21	1.37E-04	mmu-miR-200b	3.59	9.14E-03
mmu-miR-1946a	3.12	2.53E-02	mmu-miR-1947-star	3.55	2.23E-03
mmu-miR-5097	2.97	7.29E-04	mmu-miR-143-star	3.24	1.23E-03
mmu-miR-335-5p	2.95	1.75E-02	mmu-miR-34b-3p	3.18	1.19E-02
mmu-miR-27b-star	2.89	7.02E-03	mmu-miR-30e	3.15	3.25E-04
mmu-miR-423-3p	2.83	6.94E-04	mmu-miR-30c-2-star	3.04	9.18E-03
mmu-miR-351	2.49	1.76E-03	mmu-miR-451	2.94	2.53E-02
mmu-miR-1946b	2.41	1.43E-02	mmu-miR-378b	2.92	3.77E-08
mmu-miR-720	2.37	2.85E-03	mmu-miR-130a	2.90	2.20E-06
mmu-miR-532-3p	2.36	9.10E-04	mmu-miR-29c	2.76	3.69E-06
mmu-miR-674-star	2.27	1.49E-02	mmu-miR-199b-star	2.75	5.93E-03
mmu-miR-714	2.24	1.42E-02	mmu-miR-449a	2.50	2.52E-03
mmu-miR-1224	2.22	3.94E-03	mmu-miR-291b-5p	2.50	2.71E-04
mmu-miR-5099	2.22	2.92E-02	mmu-miR-30a	2.45	7.47E-06
mmu-miR-674	2.19	2.40E-04	mmu-miR-378	2.40	6.62E-06
mmu-miR-27b	2.15	8.06E-04	mmu-miR-34b-5p	2.37	1.71E-03
mmu-miR-5110	2.14	1.75E-02	mmu-miR-210	2.34	2.94E-03
mmu-miR-127	2.12	8.05E-04	mmu-miR-187	2.33	1.38E-02
mmu-miR-214	2.10	2.83E-05	mmu-miR-203	2.29	3.60E-03
mmu-miR-18a	2.08	1.58E-03	mmu-miR-192	2.25	2.70E-02
mmu-miR-411	2.03	6.11E-03	mmu-miR-143	2.23	2.40E-03
mmu-miR-455	2.03	1.03E-04	mmu-miR-125b-2-3p	2.22	3.67E-03
mmu-miR-504	1.99	1.07E-03	mmu-miR-378-star	2.22	1.34E-02
mmu-miR-532-5p	1.99	4.14E-04	mmu-miR-181d	2.14	1.05E-02
mmu-miR-5109	1.94	2.94E-03	mmu-miR-30c	2.10	5.87E-06
mmu-miR-3102	1.92	2.92E-02	mmu-miR-148a	2.09	9.68E-03
mmu-miR-574-3p	1.91	3.46E-04	mmu-miR-301a	2.09	5.00E-03
mmu-miR-379	1.89	3.02E-03	mmu-miR-194	2.07	2.60E-03
mmu-miR-181b	1.86	2.66E-06	mmu-miR-680	1.97	1.09E-03
mmu-miR-23b	1.81	1.52E-06	mmu-miR-322	1.96	1.86E-02
mmu-miR-5121	1.80	1.89E-02	mmu-miR-1843b-5p	1.94	2.53E-04
mmu-miR-146a	1.80	5.52E-03	mmu-miR-2183	1.89	7.40E-04
mmu-miR-494	1.78	7.08E-03	mmu-miR-92b	1.87	6.90E-04
mmu-miR-324-5p	1.78	5.93E-03	mmu-miR-1941-5p	1.78	3.51E-03
mmu-miR-15b	1.77	3.66E-04	mmu-miR-93-star	1.77	5.99E-04
mmu-miR-744	1.77	3.65E-05	mmu-miR-449b	1.75	5.57E-05
mmu-miR-151-3p	1.74	1.20E-04	mmu-miR-3092	1.72	9.89E-04
mmu-miR-146b	1.73	1.04E-02	mmu-miR-30a-star	1.71	2.60E-02
hp_mmu-mir-465a	1.68	7.10E-05	mmu-miR-345-3p	1.70	3.72E-03
mmu-miR-23a-star	1.68	1.70E-02	hp_mmu-mir-378	1.69	4.76E-05
mmu-miR-1196	1.63	1.99E-02	mmu-miR-497	1.69	1.59E-03
mmu-miR-190-star	1.62	3.70E-02	mmu-miR-30b	1.67	8.97E-04
mmu-miR-106a	1.59	2.63E-03	mmu-miR-196a	1.65	7.03E-03
mmu-miR-34a	1.58	8.68E-03	mmu-miR-375	1.61	2.97E-03
mmu-miR-20b	1.58	1.85E-02	mmu-miR-145	1.59	3.08E-02
mmu-miR-139-5p	1.51	2.46E-04	mmu-miR-193-star	1.56	1.12E-02
			mmu-let-7f	1.55	2.73E-02
			mmu-miR-672	1.54	1.21E-02
			mmu-miR-708	1.53	7.76E-03
			hp_mmu-mir-143	1.53	1.43E-02
			mmu-miR-511-3p	1.50	1.43E-02

2

**C**

## Supplemental Figure 5 (continued)

miRNA Name	Fold Change	P-Value	TARGET PREDICTION		
			Target Score	Gene Symbol	Gene Description
<b>mmu-miR-29a</b>	1,59	9,89E-06	81	<b>Atp5g1</b>	ATP synthase, H <sup>+</sup> transporting, mitochondrial F0 complex, subunit C1 (subunit 9)
			83	<b>Slc16a1</b>	solute carrier family 16 (monocarboxylic acid transporters), member 1
			87	<b>Slc25a3</b>	solute carrier family 25 (mitochondrial carrier, phosphate carrier), member 3
			94	<b>Bdh1</b>	3-hydroxybutyrate dehydrogenase, type 1
			97	<b>Ireb2</b>	iron responsive element binding protein 2
			100	<b>Eln</b>	elastin
<b>mmu-miR-714</b>	2,62	1,87E-03	64	<b>Oxr1</b>	oxidation resistance 1
<b>mmu-miR-92a</b>	1,52	2,47E-03	82	<b>Slc25a36</b>	solute carrier family 25, member 36
			94	<b>Slc25a32</b>	solute carrier family 25, member 32
			96	<b>Spryd4</b>	SPRY domain containing 4
<b>mmu-miR-26b</b>	1,59	3,23E-03	82	<b>Phyhipl</b>	phytanoyl-CoA hydroxylase interacting protein-like
			84	<b>Atpaf1</b>	ATP synthase mitochondrial F1 complex assembly factor 1
			86	<b>Bak1</b>	BCL2-antagonist/killer 1
			93	<b>Aldh5a1</b>	aldehyde dehydrogenase family 5, subfamily A1
			96	<b>Mtx2</b>	metaxin 2
			99	<b>Slc25a16</b>	solute carrier family 25 (mitochondrial carrier, Graves disease autoantigen), member 16
<b>mmu-miR-150</b>	1,54	1,65E-03	83	<b>Them4</b>	thioesterase superfamily member 4
			85	<b>Zadh2</b>	zinc binding alcohol dehydrogenase, domain containing 2
<b>mmu-miR-199a</b>	1,50	3,34E-02	95	<b>Gng5</b>	guanine nucleotide binding protein (G protein), gamma 5
			99	<b>Gpd2</b>	glycerol phosphate dehydrogenase 2, mitochondrial
<b>mmu-miR-362</b>	1,58	1,62E-03	94	<b>Aldh6a1</b>	aldehyde dehydrogenase family 6, subfamily A1
<b>mmu-miR-130b</b>	1,76	6,49E-03	82	<b>Mat2b</b>	methionine adenosyltransferase II, beta
			84	<b>Fastk</b>	Fas-activated serine/threonine kinase
			85	<b>Hadha</b>	hydroxyacyl-Coenzyme A dehydrogenase/3-ketoacyl-Coenzyme A thiolase/enoyl-Coenzyme A hydratase (trifunctional protein), alpha subunit
			91	<b>AcsI1</b>	acyl-CoA synthetase long-chain family member 1
			99	<b>AcsI4</b>	acyl-CoA synthetase long-chain family member 4

1

D

# Supplemental Figure 5 (continued)

miRNA Name	HFD Untreated vs. HFD Treated		HFD Untreated vs. CD Untreated		Target Prediction	
	Fold Change	P-Value	Fold Change	P-Value	Target Score	Gene Symbol
mmu-miR-132	1.97	2.77E-04	3.52	3.84E-07	81	Slc30a6
					98	Timm9
mmu-miR-146b	2.92	4.74E-03	1.73	1.04E-02	89	Tdrkh
					93	Afg3l2
mmu-miR-181b	1.66	1.49E-04	1.86	2.66E-06	89	Acsf1
					96	Acsf4
mmu-miR-15b	1.76	9.48E-05	1.77	3.66E-04	89	Gatm
					91	Lymr1
mmu-miR-18a	2.23	7.37E-03	2.08	1.58E-03	89	Oxsm
					87	Slc25a36
mmu-miR-1946a	2.33	2.76E-02	3.12	2.53E-02	92	Kif1b
					84	Ehhadp
mmu-miR-221	4.83	3.44E-06	4.72	2.63E-05	84	Gfm2
					87	Glud1
mmu-miR-222	5.15	3.43E-07	6.22	3.83E-06	83	Idh3a
					98	Mfn2
mmu-miR-23b	1.53	8.42E-04	1.81	1.52E-06	91	Mthfd1l
					82	Tatdn3
mmu-miR-27b	1.85	2.41E-03	2.15	8.06E-04	82	Tk2
					83	Rab1b
mmu-miR-342-5p	10.14	3.12E-06	13.04	2.77E-09	81	Kif1b
					88	Rexo2
mmu-miR-351	2.56	4.64E-04	2.49	1.76E-03	96	Mp140
					85	Slc25a44
mmu-miR-379	2.29	2.02E-03	1.89	3.02E-03	84	Slc30a6
					84	Slc30a6
mmu-miR-382	2.74	5.82E-03	3.60	1.46E-04	84	Slc30a6
					84	Slc30a6
mmu-miR-494	1.95	5.79E-03	1.78	7.08E-03	82	30018D20f
					90	Acsf1
mmu-miR-541	3.09	2.66E-03	3.21	1.37E-04	89	Aldh1l2
					94	Ankrd26
mmu-miR-674	1.83	4.94E-03	2.19	2.40E-04	98	Auh
					91	Gls
mmu-miR-148a	2.95	4.94E-04	2.09	9.68E-03	85	Pdk4
					93	Ppilf
mmu-miR-193b	3.20	1.22E-03	3.88	1.53E-05	83	Slc25a31
					96	Uqcrrf1
mmu-miR-203	3.31	1.70E-03	2.29	3.60E-03	99	Aldh5a1
					89	Ak2
mmu-miR-210	3.13	2.42E-03	2.34	2.94E-03	93	Mfn
					92	Pdhx
mmu-miR-29b	1.52	3.40E-03	3.77	3.23E-04	91	Pnk4
					90	Triap1
mmu-miR-29c	1.76	3.00E-02	2.76	3.69E-06	80	Gpd1
					94	Atp5c1
mmu-miR-30a-star	2.29	1.63E-04	1.71	2.60E-02	84	Ptpc7
					82	Sfxn1
mmu-miR-30a	2.40	7.51E-07	2.45	7.47E-06	84	Tfam
					88	Slc25a16
mmu-miR-30c-2-star	3.75	1.38E-04	3.04	9.18E-03	83	Sptlc2
					87	Mp149
mmu-miR-30c	1.86	1.97E-04	2.10	5.87E-06	89	Dnajc19
					97	Atad1
mmu-miR-30e	3.49	6.84E-06	3.15	3.25E-04	98	Ucp3
					83	Akap1
mmu-miR-378	1.80	2.52E-04	2.92	3.77E-08	93	Slc25a44
					83	Glsr1
mmu-miR-708	1.55	5.56E-03	1.53	7.76E-03	90	Armc1
					80	Timm8a1
mmu-miR-181b	1.66	1.49E-04	1.86	2.66E-06	92	Cyb5b
					97	Atp5g3
mmu-miR-15b	1.76	9.48E-05	1.77	3.66E-04	83	Iscu
					83	Slc16a1
mmu-miR-18a	2.23	7.37E-03	2.08	1.58E-03	81	Atp5g1
					94	Bdh1
mmu-miR-1946a	2.33	2.76E-02	3.12	2.53E-02	100	Ein
					97	Irb2
mmu-miR-221	4.83	3.44E-06	4.72	2.63E-05	87	Slc25a3
					83	Slc16a1
mmu-miR-222	5.15	3.43E-07	6.22	3.83E-06	81	Atp5g1
					94	Bdh1
mmu-miR-23b	1.53	8.42E-04	1.81	1.52E-06	100	Ein
					97	Irb2
mmu-miR-27b	1.85	2.41E-03	2.15	8.06E-04	87	Slc25a3
					83	Slc16a1
mmu-miR-342-5p	10.14	3.12E-06	13.04	2.77E-09	81	Atp5g1
					94	Bdh1
mmu-miR-351	2.56	4.64E-04	2.49	1.76E-03	100	Ein
					97	Irb2
mmu-miR-379	2.29	2.02E-03	1.89	3.02E-03	87	Slc25a3
					83	Slc16a1
mmu-miR-382	2.74	5.82E-03	3.60	1.46E-04	81	Atp5g1
					94	Bdh1
mmu-miR-494	1.95	5.79E-03	1.78	7.08E-03	100	Ein
					97	Irb2
mmu-miR-541	3.09	2.66E-03	3.21	1.37E-04	87	Slc25a3
					83	Slc16a1
mmu-miR-674	1.83	4.94E-03	2.19	2.40E-04	81	Atp5g1
					94	Bdh1
mmu-miR-148a	2.95	4.94E-04	2.09	9.68E-03	100	Ein
					97	Irb2
mmu-miR-193b	3.20	1.22E-03	3.88	1.53E-05	87	Slc25a3
					83	Slc16a1
mmu-miR-203	3.31	1.70E-03	2.29	3.60E-03	81	Atp5g1
					94	Bdh1
mmu-miR-210	3.13	2.42E-03	2.34	2.94E-03	100	Ein
					97	Irb2
mmu-miR-29b	1.52	3.40E-03	3.77	3.23E-04	87	Slc25a3
					83	Slc16a1
mmu-miR-29c	1.76	3.00E-02	2.76	3.69E-06	81	Atp5g1
					94	Bdh1
mmu-miR-30a-star	2.29	1.63E-04	1.71	2.60E-02	100	Ein
					97	Irb2
mmu-miR-30a	2.40	7.51E-07	2.45	7.47E-06	87	Slc25a3
					83	Slc16a1
mmu-miR-30c-2-star	3.75	1.38E-04	3.04	9.18E-03	81	Atp5g1
					94	Bdh1
mmu-miR-30c	1.86	1.97E-04	2.10	5.87E-06	100	Ein
					97	Irb2
mmu-miR-30e	3.49	6.84E-06	3.15	3.25E-04	87	Slc25a3
					83	Slc16a1
mmu-miR-378	1.80	2.52E-04	2.92	3.77E-08	81	Atp5g1
					94	Bdh1
mmu-miR-708	1.55	5.56E-03	1.53	7.76E-03	100	Ein
					97	Irb2

**Figure S5: Identification of ABX300 associated miRNA signature**

(A) Table showing the shifts for the 52 micro-RNAs varying between DIO Untreated and Treated animals. Up-regulated miR (26) are represented in red boxes and down-regulated miR (26) in green boxes.

(B) Table showing the shifts for the 113 micro-RNAs varying between DIO and lean untreated animals. Up-regulated miR (54) are represented in red boxes and down-regulated miR (59) in green boxes.

(C) Table showing the fold changes with their respective P-values, for the 8 miRNAs predicted to target mitochondrial genes ( $\geq 80\%$  confidence) selected from HFD Untreated vs. HFD Treated comparison. A description of these genes is also presented in the table.

(D) Table showing the fold changes with their respective P-values, for the 37 miRNAs overlapping in between the comparisons HFD Untreated vs. CD Untreated and HFD Untreated vs. HFD Treated, that have been predicted to have a mitochondrial target ( $\geq 80\%$  confidence). A description of these genes is also presented in the table.



### 3. Additional explored avenues

#### i) *Effect of ABX300 on adipocytes differentiation*

We have shown that ABX300 induces a magnificent weight lost which is translated in terms of WAT mass reduction. A decrease in AT mass can result from a reduction in adipocyte size, a reduction in adipocyte number, an impaired differentiation, or a mix of the above. Inhibiting the differentiation of adipocytes from precursor cells seems attractive as a therapeutic strategy, although it is potentially laden with pitfalls. Peripheral anti-obesity approaches that target adipogenesis alone may prove problematic given the fact that co-morbidities, notably diabetes, can result from either a paucity or plethora of fat tissue (Cummings and Schwartz, 2003). Many molecules have been shown to inhibit adipogenesis *in vitro* through the use of the 3T3-L1 adipocyte cell culture system (Grujic et al., 1997; Lin et al., 2000; Lin et al., 2001; Mallet et al., 2002; Rajala and Scherer, 2003; Trujillo and Pajvani, 2005). Moreover, 'anti-differentiation', or a loss of distinctive adipocyte morphology and function has been studied in this same cell model (Tamori et al., 2002). The 3T3-L1 cell line was derived from fibroblasts isolated from disaggregated Swiss mouse embryos, immortalized by continuous passage and sub-cloned according to their differentiation capacity. This cell line can be differentiated over a period of one week and can be induced to undergo adipogenesis. Detailed procedures for highly effective and reproducible 3T3-L1 cell differentiation are nowadays extensively available (Zebisch et al., 2012). Due to their potential to differentiate from fibroblasts to adipocytes, currently, 3T3-L1 cells are widely used for studying adipogenesis and the biochemistry of adipocytes. Although when fully differentiated they do not display unilocular intracellular fat stores but multilocular fat droplets typical of brown cells, they are considered as a relevant cellular model of WAT that can be used to test drugs that may affect adipogenesis.

Our first attempt to inspect the potential effect of ABX300 on this cell model was to treat the cells at different moments during the differentiation process, at the concentration of 5  $\mu$ M. Rosiglitazone, a PPAR $\gamma$  agonist, was used as an additional prodifferentiative agent to obtain full differentiation. Within 7 to 10 days, apparently complete differentiation was achieved. In order to characterize the differentiation rate, we performed ORO (oil red O) staining. The extraction of this colorant and the subsequent measurement of the absorbance at 520nm provide valuable information



about the content in lipid droplets, thus the degree of differentiation. ORO analysis allowed us to conclude an absence of effect for ABX300 under these specific conditions (**Figure 35A**). To try to empower the potential effect of the ABX300 molecule onto differentiation, we decided to remove rosiglitazone from experiments. As a consequence, we encountered lower differentiation rates, but still no effect of ABX300 at 1  $\mu$ M and 5  $\mu$ M (**Figure 35B**).

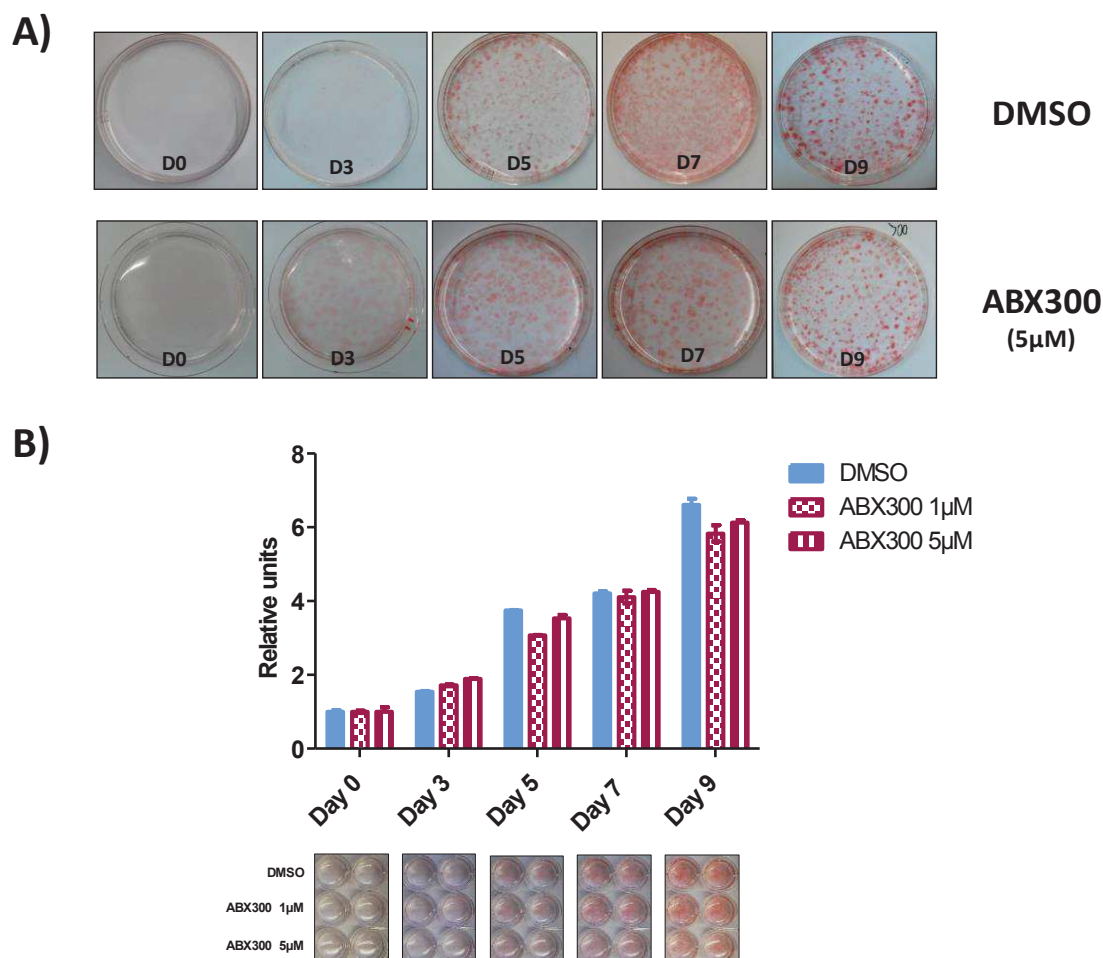


**Figure 35: Absence of ABX300 effect on 3T3-L1 differentiation.**

- A)** Representative Images of ORO-stained Petri-dishes of differentiating 3T3-L1, at days 0, 3, 5, 7 and 9, in the presence of rosiglitazone +/- ABX300. DMSO being the drug vehicle, it serves as control.
- B)** Representative Images of ORO-stained 6 wells-plates of differentiating 3T3-L1, at days 0, 3, 5, 7 and 9, in the absence of rosiglitazone. Histogram bars correspond to the absorbance of the extracted colorant from the plates (Abs=520nm).

In view of these results, rosiglitazone was further kept for every other experiment presented in this manuscript. Since it has been reported that the variability in 3T3-L1 adipocyte differentiation depends strongly on the cell culture dishes (Mehra et al., 2007), with both culture dish provider (i.e., the material and/or processing of the plastic surface) and dish type being crucial factors for 3T3-L1 differentiation, I have tested this hypothesis into different cell-culture plates. The data shown in this manuscript are representative results of the many experiments I have carried out. Taken together, all my research data do not strongly imply a role for ABX300 in 3T3-L1 adipocyte differentiation.

Consistent with these results, qPCR experiments revealed no effect of ABX300 on differentiating 3T3-L1 cells. Three biological replicates were made per time point (**Figure 36**). As I already detailed in the introduction of this manuscript, the members of the C/EBP family have shown to be very important in adipogenesis. When treating with ABX300, mRNA expression levels of two early markers of differentiation, C/EBP $\delta$  and C/EBP $\beta$ , were similar between untreated and treated cells (**Figure 36A left column**). These markers additionally contribute to the transcriptional activation of PPAR $\gamma$  in early adipogenesis, and C/EBP $\beta$  redundantly activates adipogenic genes targeted by C/EBP $\alpha$  (Ryan Alexander, Harvey Lodish, 2011). Continued expression of PPAR $\gamma$ , a master transcriptional regulator of adipogenesis, is necessary for maintaining the differentiated state. PPAR $\gamma$  also activates genes involved in terminal differentiation and mature functions of adipocytes. Following commitment to the adipocyte lineage, preadipocytes undergo terminal adipocyte differentiation, acquiring a mature adipocyte morphology, and expressing mature adipocyte markers such as FABP4 and GLUT4. Relative mRNA levels of intermediate markers: C/EBP $\alpha$  and PPAR $\gamma$ , as well as late ones: AdipoQ, FABP4 and GLUT4, did not differ between ABX300 treated and untreated conditions, suggesting an equivalent degree of differentiation (**Figure 36A middle and right columns**). Furthermore, mRNA expression levels of PGC1 $\alpha$  and UCP1 were also similar (**Figure 36B**). This evidence further indicated that ABX300 treatment did not significantly affect the adipocyte differentiation process.

As a completing strategy in the study of the mechanisms of adipogenesis and remodulation of AT, we measured TGs content in the cell culture media of ABX300 treated and untreated 3T3-L1, but repeatedly found no differences due to ABX300 administration (**Figure 36C**).

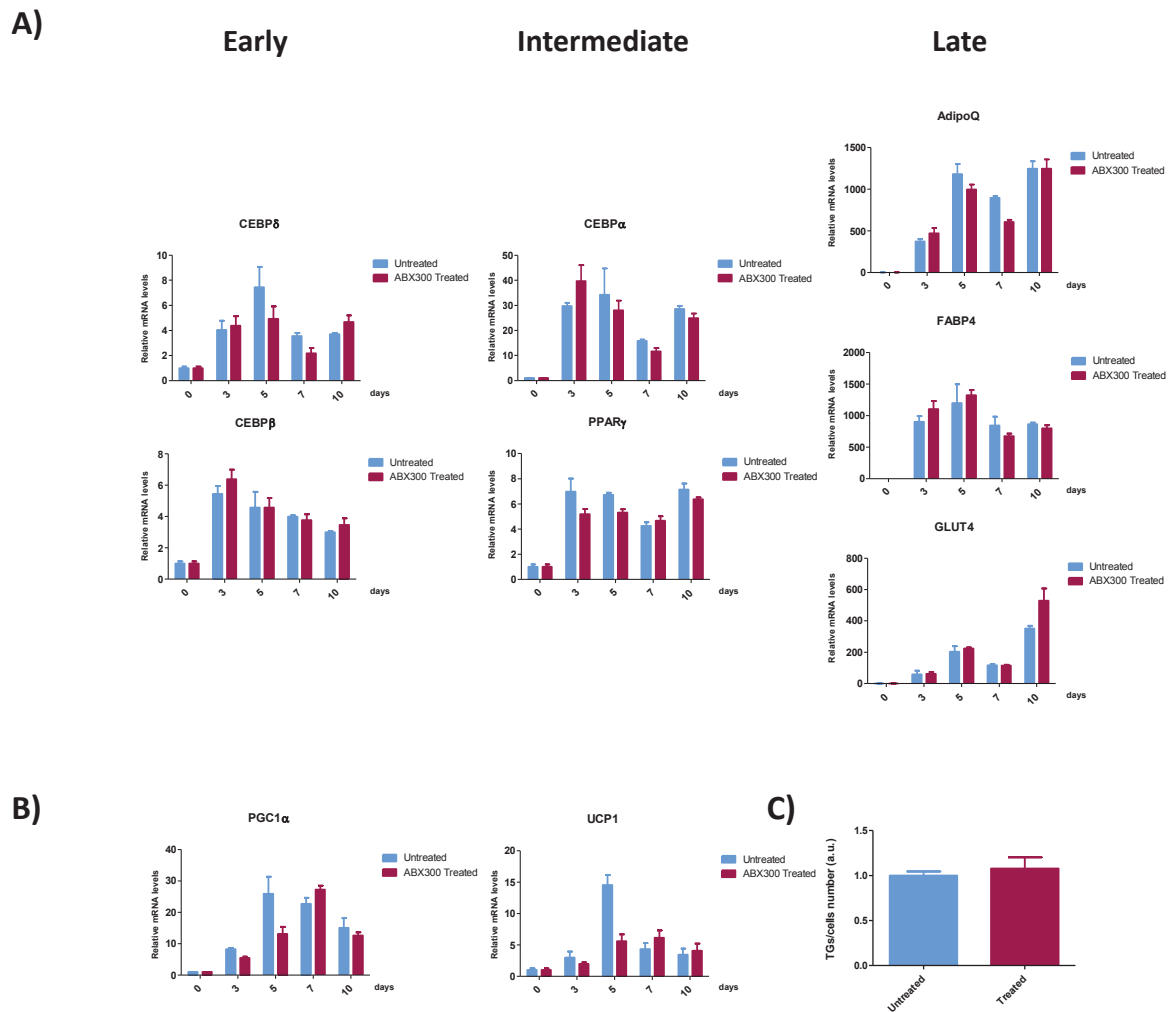


**Figure 36: Absence of ABX300 effect on relative expression of key genes during 3T3-L1 differentiation.**

- A)** Relative mRNA levels of early, intermediate and late markers of differentiating 3T3-L1, at days 0, 3, 5, 7 and 10.  
**B)** Relative mRNA levels of metabolic key genes in the same cells as in A).  
**C)** TGs supernatant content at day 10 of 3T3-L1 cells in A) and B).

All qPCR results are normalized to the housekeeping genes (NoNo and b2m).

The absence of ABX300 effect regarding 3T3-L1 differentiation was also confirmed by protein levels of key metabolic genes. **Figure 37A** shows western blotting of differentiating 3T3-L1, on PGC1α, PPARγ, UCP1 and FABP4 genes. Perilipin-A and ATGL were used as internal controls for checking on the differentiation process itself. TBP and Tubulin were used to normalize the results.

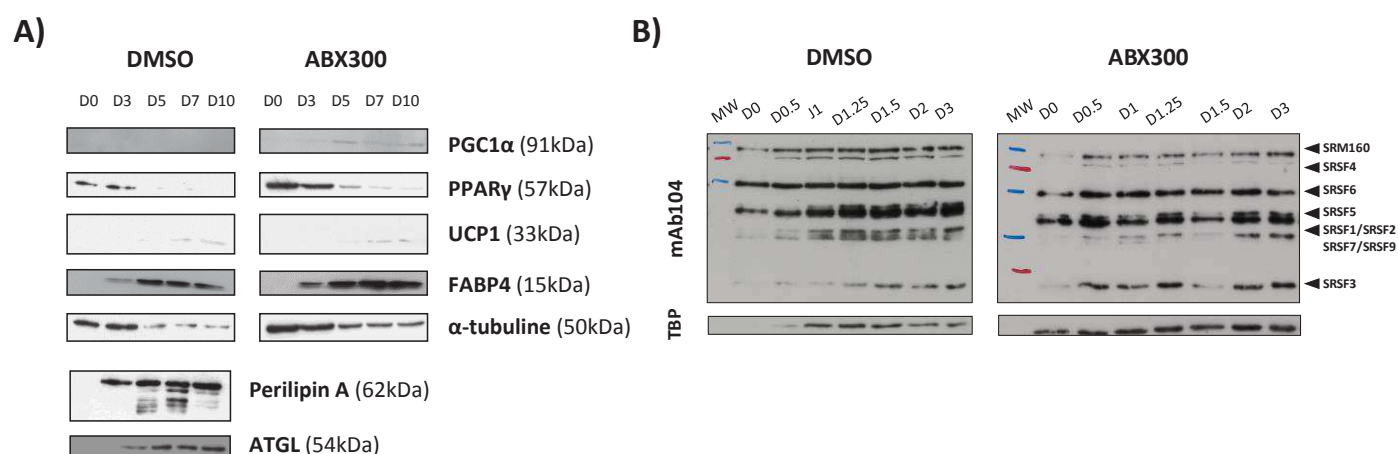


**Figure 37: Absence of ABX300 effect on protein expression of key genes involved in adipogenesis and phosphorylation of SR proteins during 3T3-L1 differentiation.**

- A)** Protein expression levels of metabolic key genes in differentiating 3T3-L1, at days 0, 3, 5, 7 and 10.  
**B)** SR proteins phosphorylation levels during 3T3-L1 differentiation, at days 0, 0.5, 1, 1.25, 1.5, 2 and 3.

Since we reported ABX300 to interact with SRSF1, and very likely also to interfere with its activity, I checked for its phosphorylation by western blotting. As already described in the introduction, the activity of this family of splicing regulators is principally dependent on their phosphorylation level. So I carried out western blotting on differentiation kinetics of 3T3-L1 cells with Mab104, a self-customized hybridoma antibody which binds to phosphorylated RS domains. Seven different time points were evaluated. Results indicate that the drug does not have a remarkable effect on the phosphorylation levels at any of the tested time points, thus in theory nor on the activity of these proteins in these experimental conditions (**Figure 37B**).

Most studies of adipocytes have been limited either to a small number of established cell lines, such as the previously described 3T3-L1, or to primary cell culture. Recently, immortalized brown adipocyte cell lines have been generated from single newborn mice of different KO mouse models (Klein et al., 2002; Whittle et al., 2012). These cell lines, presented during the introduction of this manuscript, appear as physiologically relevant for testing drugs that may prevent, delay or stop adipogenesis, and as such are likely to cause weight loss and other features.

Because we hadn't been able to verify any *in vitro* effect on adipocyte differentiation using a WAT cellular model, we evaluated ABX300 taking advantage of this newly available cell type of BAT preadipocytes.

After undergoing differentiation to brown adipocytes for eight days, in a medium containing a high concentration of insulin, triiodothyronine (T3), dexamethasone (DEX), 3-isobutyl-1-methylxanthine (IBMX) and indomethacin, I treated the cells during 48 hours, at different ABX300 concentrations (1, 2.5 and 5  $\mu$ M). No differences were observed between untreated and treated cells with regards to brown adipocyte morphology or ORO staining (**Figures 38A and B**). These experiments did not allow to confirm any effect of ABX300 in BAT preadipocytes differentiation.

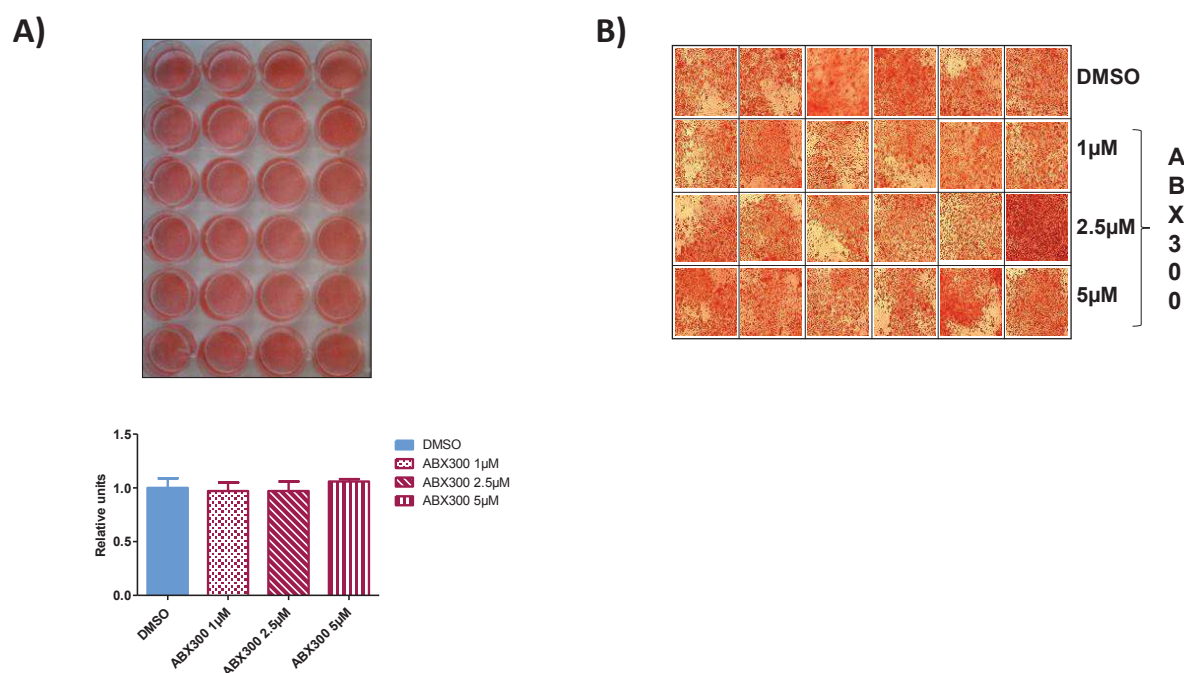


**Figure 38: Absence of ABX300 effect on differentiated BAT preadipocytes.**

- A)** Representative Picture of ORO-stained 24 wells-plates of differentiated BAT preadipocytes at day 10. ABX300 treatment took place during the preceding 48 hours. Histogram bars correspond to the mean of three independent experiments for the absorbance of the extracted colorant from the plates (Abs=520nm).
- B)** Representative Invert Microscopy Images of cells in A).

Altogether the results presented in this section point to an absence of effect of ABX300 on white and/or brown adipocytes differentiation. It is presumable that ABX300 action may occur via its metabolites. This would explain why we do not see any robust effect of the drug on the tested cell lines. Besides, it is important to note that *in vitro* differentiation of 3T3-L1 adipocytes is easily disrupted by a variety of pharmacologic interventions, suggesting a rather delicate balance between terminal differentiation and continued proliferation that may not accurately reflect *in vivo* adipogenesis (Trujillo and Pajvani, 2005). Many other features could explain the fact that we do not see an effect of ABX300 *in vitro* (see **discussion** section for further details).

## **ii) Effect of ABX300 on adipocytes lipolysis/lipogenesis**

The initial phenotypic characterization of ABX300 treated mice revealed a decline in fat tissue. Subsequent experimental work showed a clear absence of effect on differentiation of white and brown AT rodent cell models in response to the treatment. Both, the weight loss and the reduced weight gain, in ABX300 treated mice could also likely be due to increased lipolysis and/or impaired lipogenesis in response to the drug and the hyper-caloric feeding.

In the first place, to verify if ABX300 treatment was getting underway lipolytic mechanisms, we carried out a kinetics experiment in differentiated 3T3-L1 cells. Three different drug concentrations were tested, along with isoproterenol at 1 $\mu$ M, which was used as a positive control. Glycerol levels were assessed at five distinct time points (1h, 2h, 4h, 6h and 8h) (**Figure 39A**). In addition, NEFA, glycerol and TGs levels were dosed in the cell culture supernatant of differentiated cells, 24 hours after drug application (**Figure 39B**). None of these experiments allowed the confirmation of any differences in between treated and untreated wells.

Secondly, longer experiments were designed in order to check if it was a matter of time that impeded us to manage to prove an effect of ABX300. We therefore focused on periods of one to two weeks or even one month duration. During this time, 3T3-L1 cells were treated every 48h with ABX300 at 5  $\mu$ M. Results showed no differences between treated and untreated cells regarding ORO staining (**Figure 39C**), and TGs supernatant content (**Figure 39D**).

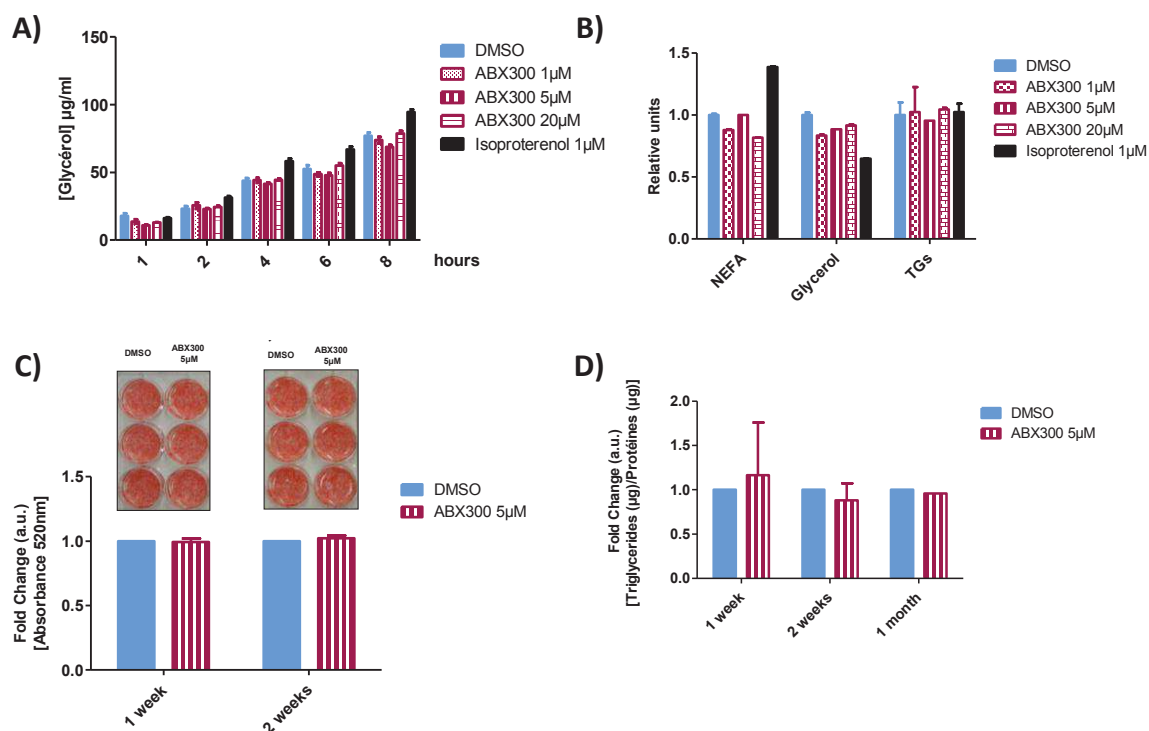


**Figure 39: Absence of ABX300 effect on lipolytic/lipogenic mechanisms in 3T3-L1 cells.**

- A)** Kinetics of glycerol relative levels in differentiated 3T3-L1, at time points 1, 2, 4, 6 and 8 (hours) under various treatment conditions.
- B)** NEFA, glycerol and TGs relative levels in differentiated 3T3-L1, after 24 hours diverse treatment conditions.
- C)** Representative picture of ORO-stained 6 wells-plates of differentiated 3T3-L1 treated every 48 hours for 7 or 14 days at 5 µM. Histogram bars correspond to the absorbance of the extracted colorant from the plates (Abs=520nm).
- D)** Relative TGs levels of cells treated similarly than in C). One surplus 30 days condition.

Because cell models are far from reproducing every single characteristic of a real tissue, the reason for not observing any effect of the molecule could still reside in this fact. Therefore additional experiments were carried out using animal explants. Wild Type (WT) and genetically obese mouse models ( $OB \leftrightarrow ob/ob$ ) were used (**Figure 40**).

The  $ob/ob$  mouse model was used according to the rapidity of the obtaining of the samples compared to the DIO model. Isoproterenol was again used as a positive control of lipolysis (1 µM). ABX300 concentration was fixed to 5 µM. Treatment times are shown in the legends of the figure. Of note is that the response to isoproterenol in the  $ob/ob$  subject's is less good than in WT's. This could be explained by their intrinsic defective metabolism due to the obese state.



These data suggest that neither increased lipolysis, nor reduced lipogenesis are the mechanisms responsible for the protection from high-fat diet-induced obesity during ABX300 treatment. Nevertheless, it is hard to conclude. Among the tested subjects there was only one adequately responding to isoproterenol.

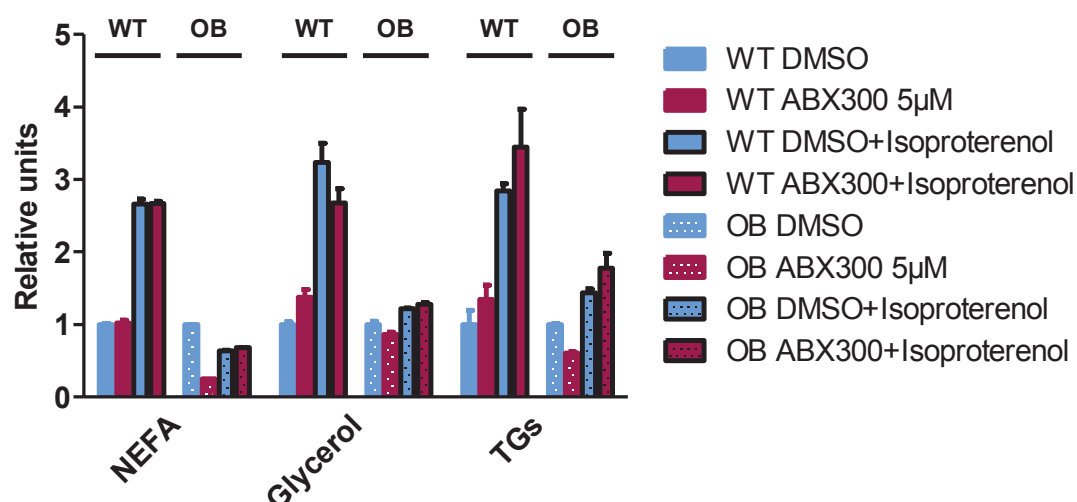


**Figure 40: Absence of ABX300 effect inducing lipolysis on ex-vivo WAT explants.**

NEFA, glycerol and TGs relative levels in supernatants from cultured WAT explants derived from WT and OB animals. ABX300 and isoproterenol *in-vitro* treatment correspond to 7 hours at 5μM and 3 hours at 1μM respectively. Data are normalized to the corresponding non-treated DMSO.

### **iii) Effect of ABX300 on Browning**

An alternative contributor to reduced fat storage in ABX300 treated mice could be increased thermogenesis. It has now been established for over a decade that WAT browning enhances this process (Cousin et al., 1992). It is important to note that even though the BAT depots are present in small amounts, the activated tissue has the potential to substantially contribute to energy expenditure (Nedergaard et al., 2007). Besides, beige cells retain a remarkable ability to powerfully turn on a robust program of respiration and EE that is equivalent to that of classical brown fat cells (see introduction). To investigate the conceivable WAT browning and to determine whether it contributed to the observed phenotype, I firstly performed qPCR experiments.

Since the different fat cells; brown, white and beige/brite, have been reported to present a unique gene expression signature (**Table 2** of the introduction section) which provides a powerful tool for investigating fat identity (Wu et al., 2012), I performed the experiments on a set of these genes. I verified the expression of a subset of the brown-selective (**Figure 41A**) and beige-selective (**Figure 41B**) genes in the basal (not cold exposed or cAMP-stimulated) state via qPCR analysis. Data demonstrated that two beige specific genes, *Tmem26* and *Tbx1*, appeared increased in subcutaneous WAT from DIO treated animals. At first sight, this could be indicative of a browning processes being settled. However, this hypothesis could not be totally confirmed due to the lack of significant variation for extra brown (*Prdm16* and *Cidea*), and yonder beige specific genes (*HoxC9*). Besides, the experimental design was not optimal for permitting the investigator to observe the desired results (see the **discussion** section for further explanations).

To complete the characterization of WAT, I checked for the expression of a few other relevant genes, revealing an increase in *Adrb3* and *PPAR $\alpha$* , accompanied by a decrease in *Leptin*, which is logically correlated to the amount of fat in the depots of the individuals (**Figure 41C**).

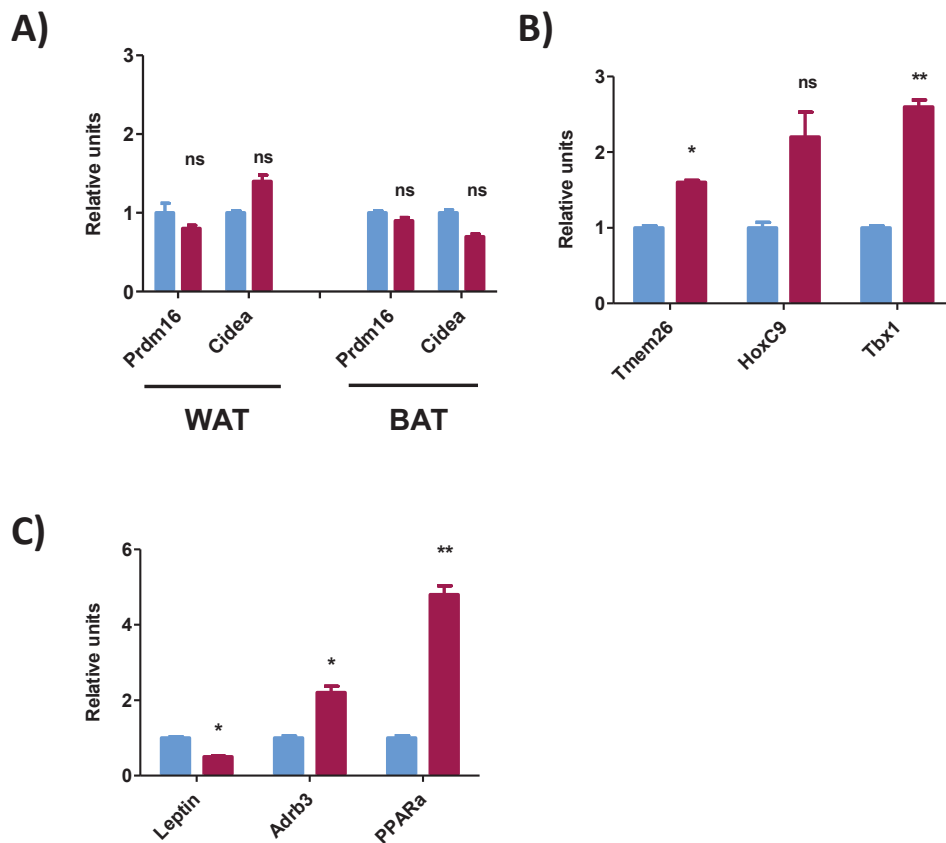


**Figure 41: Absence of a clear effect of ABX300 on browning.**

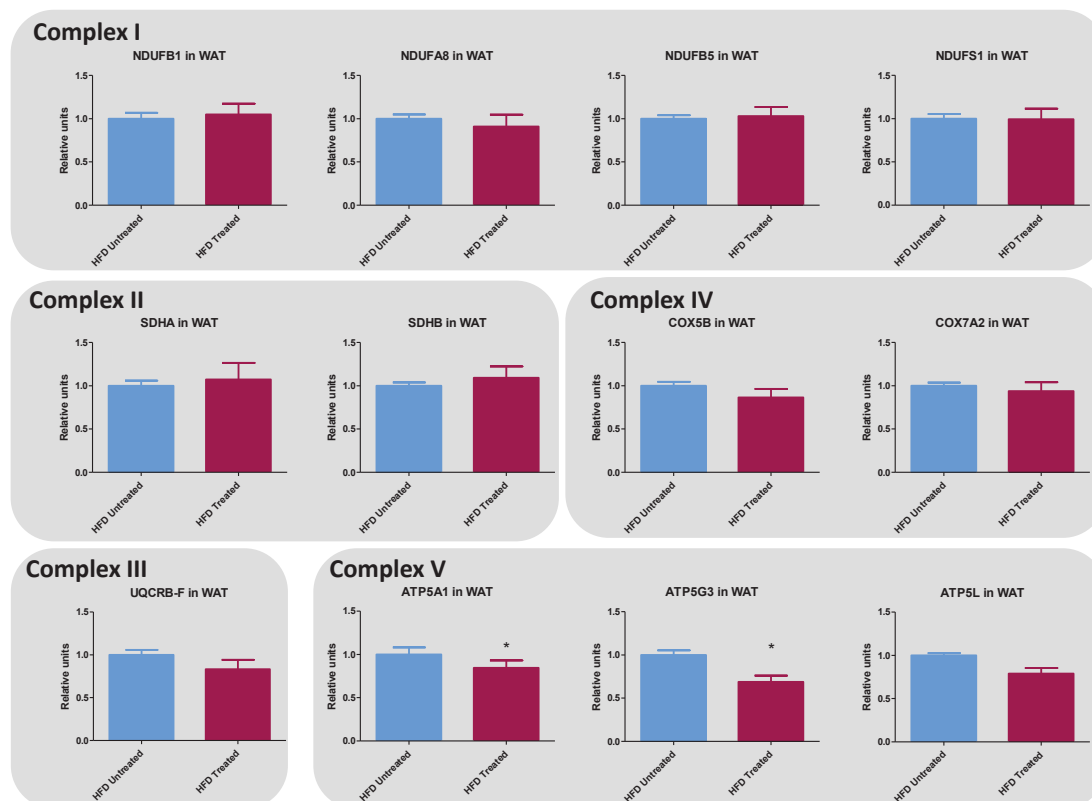
- A)** Relative mRNA expression for genes with a brown selective expression pattern was measured by qPCR in white and brown fat tissue isolated from inguinal WAT and interscapular BAT of DIO mice, in an unstimulated state.
- B)** Relative mRNA expression for genes with a beige selective expression pattern in inguinal WAT from mice in A).
- C)** qRT-PCR data showing the fold induction of the expression of the indicated genes in visceral WAT of Untreated and ABX300 DIO Treated mice.

All qPCR results are normalized to the housekeeping genes (NoNo and b2m). Values are mean  $\pm$  SEM (n = 7). \*p < 0.05; \*\*p < 0.01; \*\*\*p < 0.001.

#### iv) *Effect of ABX300 on mitochondria and oxygen consumption*

Mitochondrial number and mitochondrial-based respiration is highly adaptive in most eukaryotes, responding to environmental conditions such as diet, physical activity, and temperature (Uldry et al., 2006). For example, transgenic mice with an increased mitochondrial number have been reported as being resistant to obesity (Kopecky et al., 1995). Because, as I just showed, subcutaneous inguinal WAT from ABX300 treated mice partially acquired the appearance of BAT, expressing significantly higher levels of Tmem26 and Tbx1, I investigated the possibility that mitochondrial biogenesis in these animals occurred. Analysis using a mouse mitochondrial biogenesis qPCR Kit (72626 | NovaQUANT™), consisting on a qPCR plate with specific pre-aliquoted PCR primers showed no important variations regarding the relative mRNA levels of Oxidative Phosphorylation (OXPHOS) complex subunits I, II, III, IV and V. This last complex was represented in the plate by three different genes. Among them, significant differences were apparent in response to ABX300 treatment for ATP5G3 in both, white and brown fat tissues, and for ATP5A1 exclusively in WAT (**Figures 42A and B**).

A)



B)

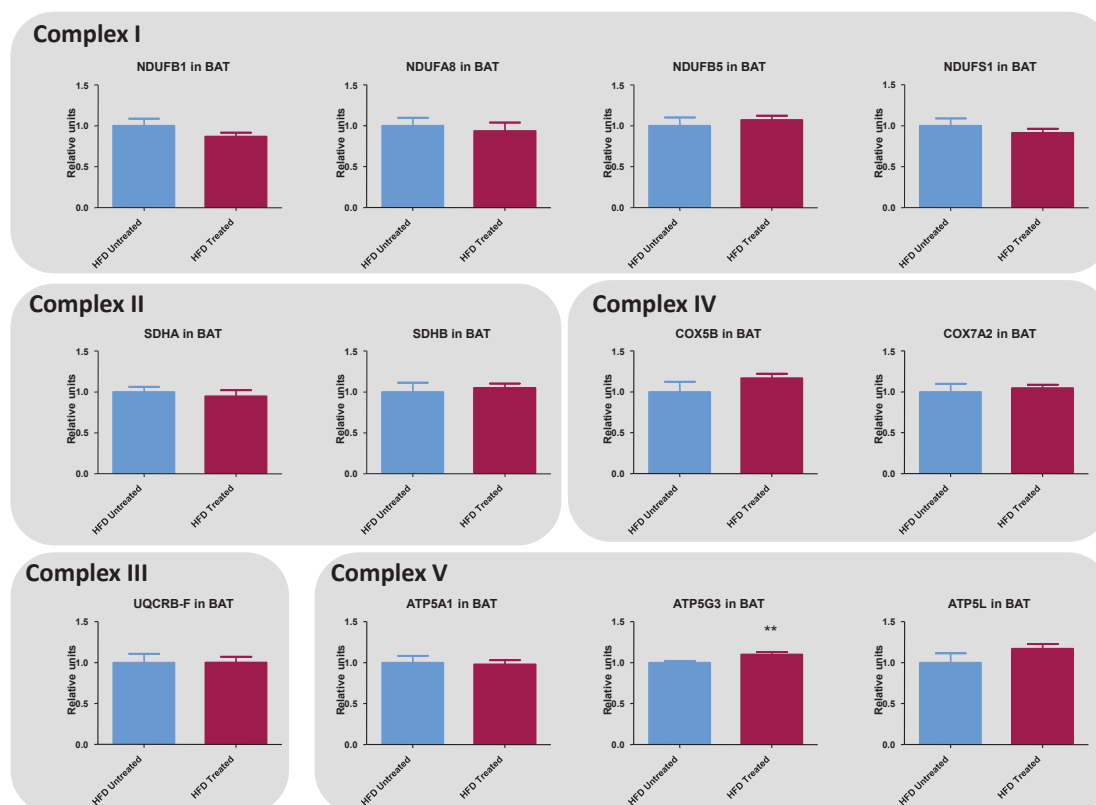


**Figure 42: ABX300 does not modulate the relative mRNA expression of key genes involved in mitochondrial biogenesis in WAT and BAT.**

- A)** Relative mRNA expression of OXPHOS complex subunits I, II, III, IV and V in WAT.  
**B)** Relative mRNA expression of OXPHOS complex subunits I, II, III, IV and V in BAT.

The mRNA for the house keeping genes used in were mRP11, mRPL27 and mOAZ1. Individuals correspond to one month of treatment with ABX300 in a curative context. Values are mean  $\pm$  SEM (n = 5). \*p < 0.05; \*\*p < 0.01; \*\*\*p < 0.001.

Mitochondrial number was further evaluated in WAT and BAT by quantification of mitochondrial DNA. This was done by calculating the ratio between mitochondrial and genomic DNA, using commercial pre-coated plates too (72621 | NovaQUANT™). This kit contains a set of four optimized PCR primer pairs targeting two nuclear (*BECN1* and *NEB*) and two mitochondrial (*trLEV* and *12s*) genes Compared to the untreated condition, the amount of mtDNA was significantly higher in BAT from HFD ABX300 treated mice. In contrast, no differences were observed in WAT (**Figure 43A**).

**Figure 43B** depicts qPCR analysis of mRNA relative expression of supplementary OXPHOS genes in WAT and BAT, and some of the obtained results encounter those previously exhibited in figure 41. The discrepancy in between these analysis might be due to the distinct origin of the samples or to the disparate design of the primers. This last factor could influence in amplicon size, as well as RT-PCR efficiency, which brings on a bias that could account for the intriguingly uneven results. Surprisingly, no differences between groups were previously apparent for complexes II, III and IV whereas variations are evident along the qPCR represented in the left column of **Figure 43B**, which refers to WAT. Regarding BAT, no modulations were apparent any of the studied genes, except for Cox1 (complex IV) (**Figure 43B right column**). Cox1 is a component in the respiratory chain which catalyzes the reduction of O<sub>2</sub> to H<sub>2</sub>O, CO-I being the catalytic subunit of the enzyme. The possibility of novel anti-obesity therapies to increase oxygen consumption is a tantalizing speculation. In fact, this elevated O<sub>2</sub> consumption is what we have somehow shown within the Figure 7 of López Herrera *et al.* An action of ABX300 thereupon may account for the protection from high-fat diet-induced obesity during the treatment.

Withal, an alternative explanation for the observed phenotype would be if mitochondrial FAO was sufficiently elevated to prevent the accumulation of the excess dietary fat. We assessed genes described in the literature as being essential during  $\beta$ -oxidation in WAT and BAT (**Figure 43C**). Out of the seven genes studied in inguinal WAT, results showed an absence of ABX300 regulation for Cpt1, Sirt1 and GPx1 while up-regulations were exhibited for Pgc1a, Cpt2 and Sod1. Nevertheless, the results concerning Pgc1a and Cpt1 must be interpreted cautiously because these genes were amplified after 30 cycles of qPCR. For Pgc1a, this situation of late peaks on the amplification plots was reproduced in BAT. This trouble was unexpected, since BAT is a tissue where the expression of this gene is known to be much more abundant. No changes were observed for Cpt1, nor Cpt2 in BAT. Lastly, mCAD appeared down-regulated in both, WAT and BAT from ABX300 treated animals.

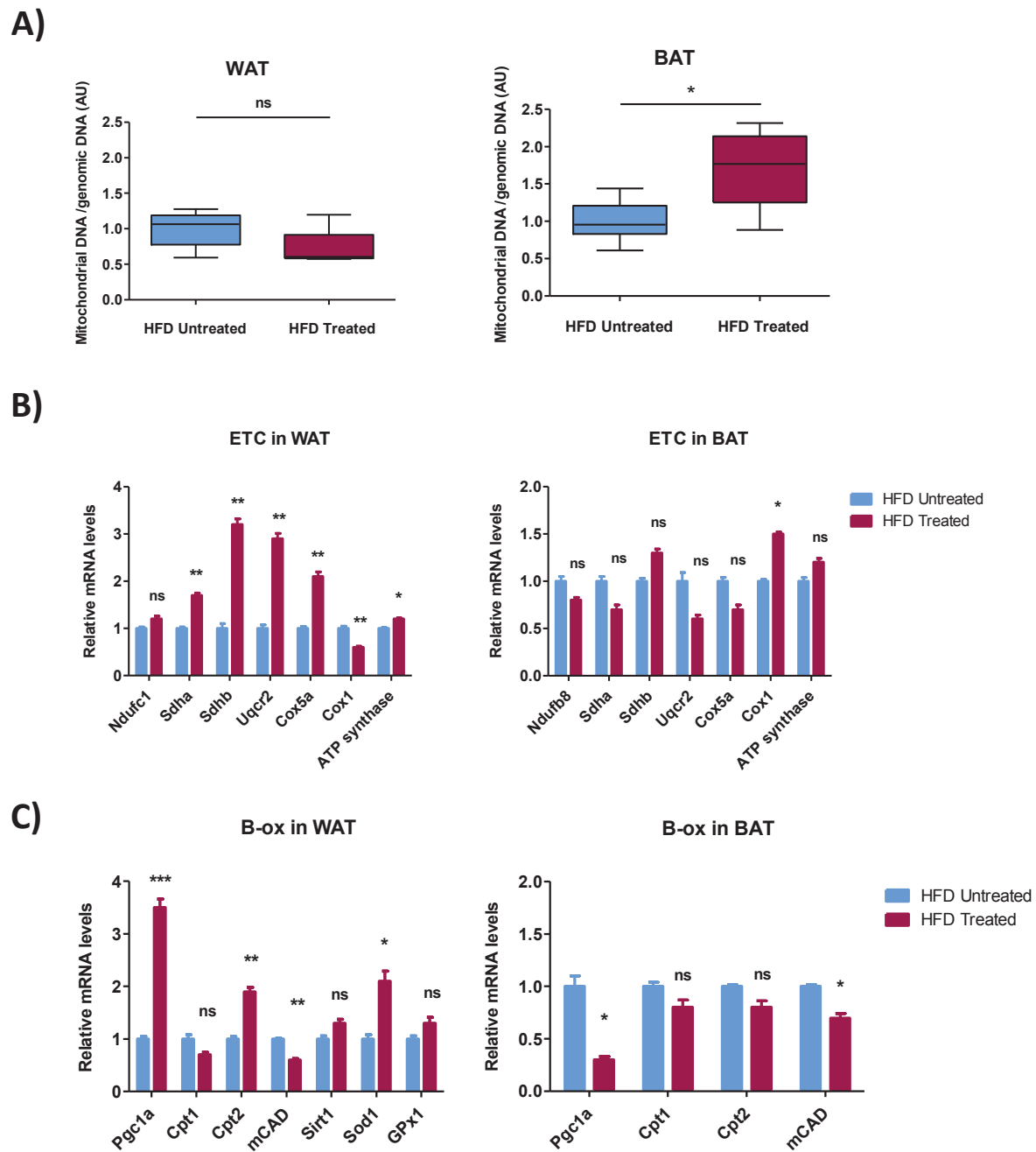


**Figure 43: ABX300 influence on the mitochondrial amount and on the relative expression levels of genes implicated in mitochondrial ETC and Beta Oxidation.**

- A)** Ratio between mitochondrial and genomic DNA to evaluate mitochondrial number.  
**B)** Relative mRNA levels of genes from the mitochondrial ETC.  
**C)** Relative mRNA levels of genes involved in mitochondrial  $\beta$ -Oxidation.

All qPCR results are normalized to the housekeeping genes (NoNo and b2m).  
 Values are mean  $\pm$  SEM (n = 5-8). \*p < 0.05; \*\*p < 0.01; \*\*\*p < 0.001.



To try to solve out the conspicuous contradictions in between figures 42 and 43, and check if the changes observed at the mRNA level were or not evident at the protein level, I carried out Western Blot analysis of the different subunits of each of the five complexes assembling the ETC. Protein detection with the 'Total OXPHOS Rodent WB Antibody Cocktail (ab110413)' did not allow to note any changes in WAT (**Figure 44A**). However, an increase of the protein expression levels of Cytochrome c oxidase subunit 1 (Cox1) was shown in BAT (**Figure 44B**). This result is in accordance with the observations at the transcriptional level showed in the right panel of **Figure 43B**.

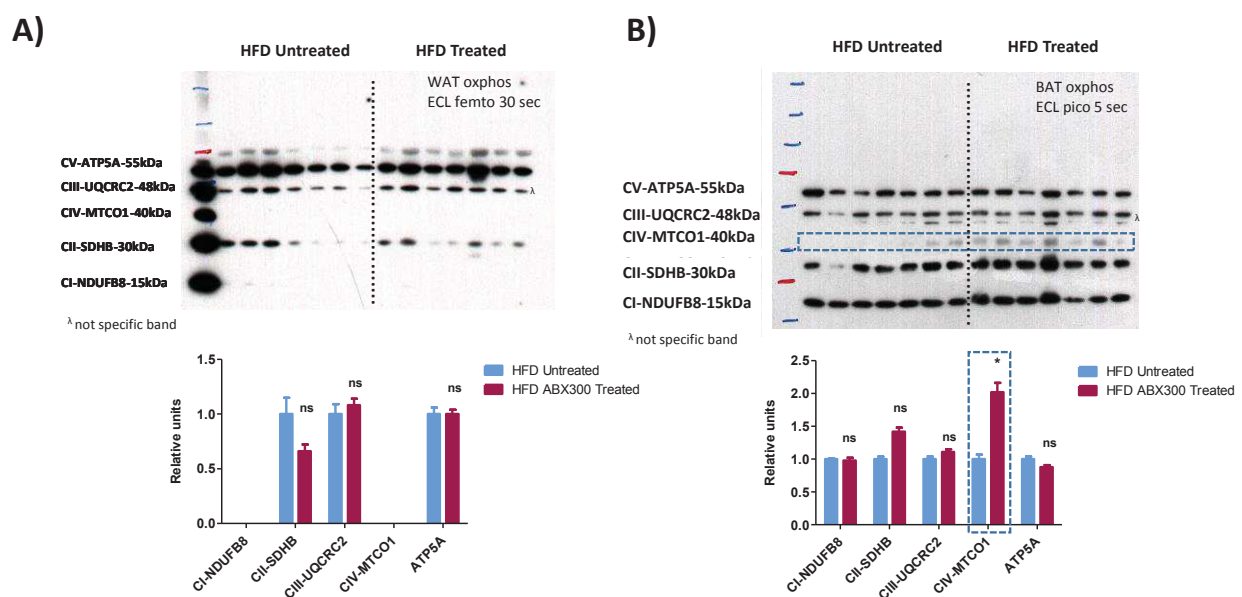


**Figure 44: Protein levels of mitochondrial total oxidative phosphorylation (OXPHOS) in WAT and BAT of ABX300 treated and untreated mice.**

- A)** Representative blots of OXPHOS complexes I–V and bands intensity quantification (Image J) in WAT.  
**B)** Similar than A) but in BAT.  
 Values are mean  $\pm$  SEM (n = 7). \*p < 0.05; \*\*p < 0.01; \*\*\*p < 0.001.

This variation could be indicative of a different activity of the ETC complexes. In order to evaluate if this was indeed the case, as an adjacent step we measured oxygen consumption ratio (OCR) in different cell models, using the Seahorse XF24 Extracellular Flux Analyzer (Seahorse Bioscience, North Billerica, MA).

These two cell lines were measured with quintuplicate wells per experimental condition. Cells were seeded and differentiated directly into special XF24 cell culture plates and

incubated at 37°C, CO<sub>2</sub> free, for one hour in unbuffered, serum-free DMEM media prior to analysis. The length of differentiation was fixed to seven days for both cellular models. The molecule was mixed within the cell culture media and dispatched into the wells when changing medium, which corresponds to four times for 3T3-L1 cells (days 1, 3, 5 and 7 of the differentiation protocol), and five times for BAT preadipocytes (days 1, 2, 3, 5 and 7 of the differentiation protocol). In both cases the cells were as well treated during four hours, the morning of the Seahorse run, which took place systematically during the afternoon. ABX300 treatment after differentiation partook during four consecutive days in a daily fashion (≈96 hours).

ABX300 Treated cells exhibited no important differences when compared to control (**Figure 45**) in 3T3-L1 (**A** and **B**) and BAT preadipocytes (**C** and **D**). I carried drug treatment at various concentrations both, during differentiation (**A** and **C**), and once the cells were differentiated (**B** and **D**) in twain cell models, without exhibiting any robust and reproducible effect.

Bioenergetic profiling (**Figure 45**) was performed by monitoring basal oxygen consumption for 30 minutes followed by the sequential injection of three inhibitors. The final concentrations for 3T3-L1 or BAT preadipocytes, were: (**a**) oligomycin (1 or 3 μM), (**b**) cyanide p-trifluoromethoxy-phenylhydrazine (FCCP) (600 or 300 nM), and (**c**) rotenone (1 μM for both). Basal oxygen consumption, was calculated from the primary data and is represented in the histograms appearing on the left side of the figure. Seahorse profiles on the right part give us information about the proper conduct of the experiment. Analysis of the profiles more in depth would allow us to obtain hints about ATP production, maximal respiration, spare capacity and non-mitochondrial respiration.

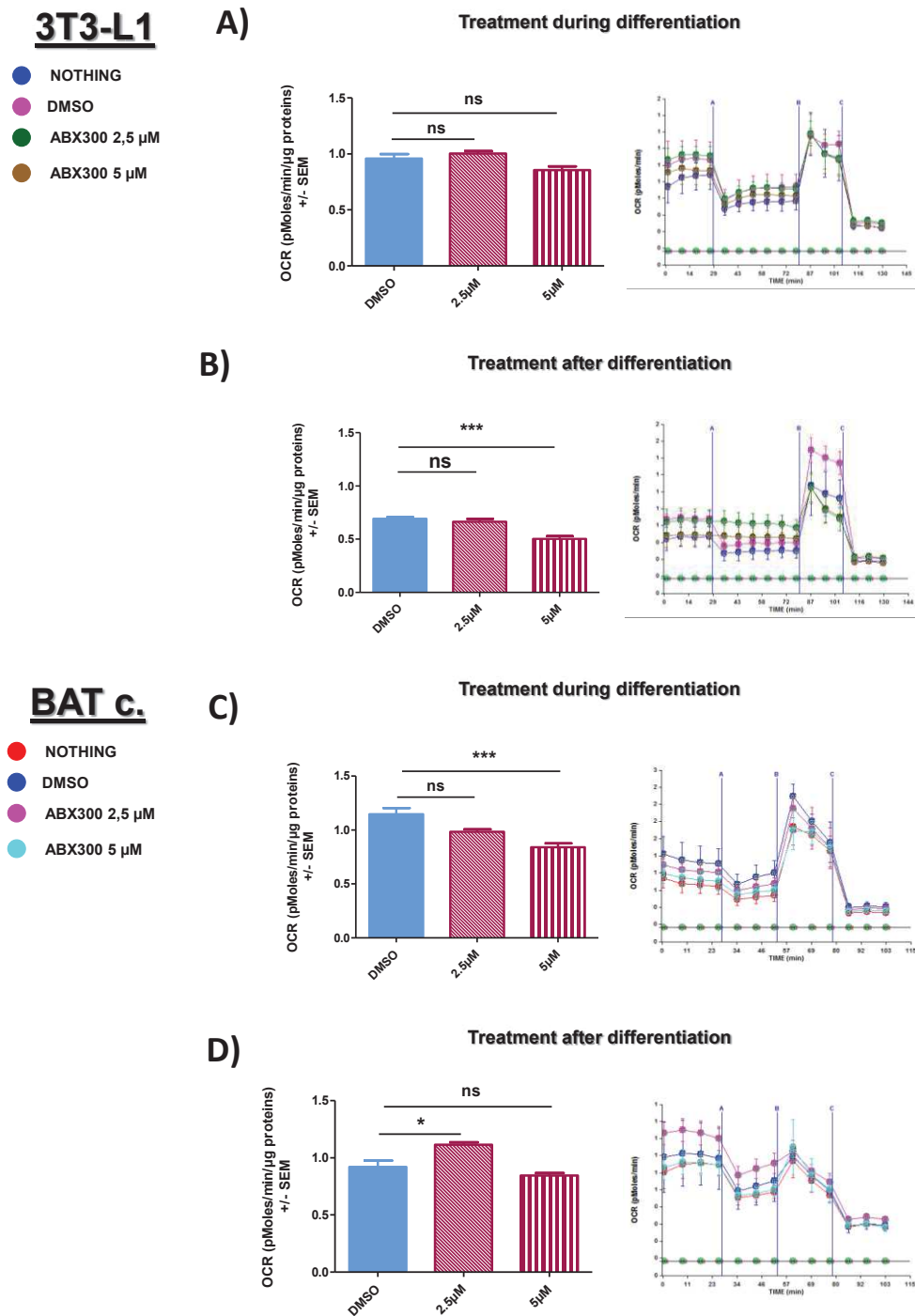


**Figure 45: ABX300 does not change profiling of Seahorse XF Stress Test**

- A) 3T3-L1 cells treated with ABX300 during white adipocyte differentiation.  
 B) 3T3-L1 cells treated with ABX300 after white adipocyte differentiation.  
 C) BAT preadipocytes treated with ABX300 during white adipocyte differentiation.  
 D) BAT preadipocytes treated with ABX300 after white adipocyte differentiation.

Because we were rather convinced that our treatment had indeed an effect on mitochondrial respiration, even if using the Seahorse technology we unable to clearly show it on these cellular models, we decided for Mouse Embryonic Fibroblasts (MEFs) to face a more physiological and complete conditions. Unfortunately, we were still unable to confirm any effect of our treatment on OCR (**data not shown**). In the same way I could not surely observe confident results when working with pieces of AT from distinct depots (**data not shown**); and ditto when trying to isolate intact mitochondria from the preceding tissues.

Although we did not succeed with the demonstration of ABX300's effect on OCR using *in vitro* cellular models, we strongly believe that ABX300 impacts mitochondrial activity. In fact, this is what the results from the metabolic cages experiments shown in López Herrera *et al.* suggest. Setting up the appropriate parameters to further apply the Seahorse technology to *ex-vivo* samples and isolated mitochondria would be necessary for the completion of the project.

#### v) **Effect of ABX300 on LMNA**

To further understand the opposing effects of the distinct isoforms encoded by the *LMNA* gene on energy metabolism, we analyzed CD/HFD ABX300 Un/Treated animals. We found by Western Blotting that, as a consequence of a dietary switch, protein expression levels of both lamin A and lamin C, were altered in WAT, whereas they remained unchanged in BAT (**Figure 46, left panel**). Nevertheless, following ABX300 treatment of DIO mice, changes were measurable for several metabolic organs; including WAT, BAT, liver and muscle, where increased expression levels of lamins A/C were exhibited. No differences were described for other tissues (**Figure 46, right panel** and **data not shown**).

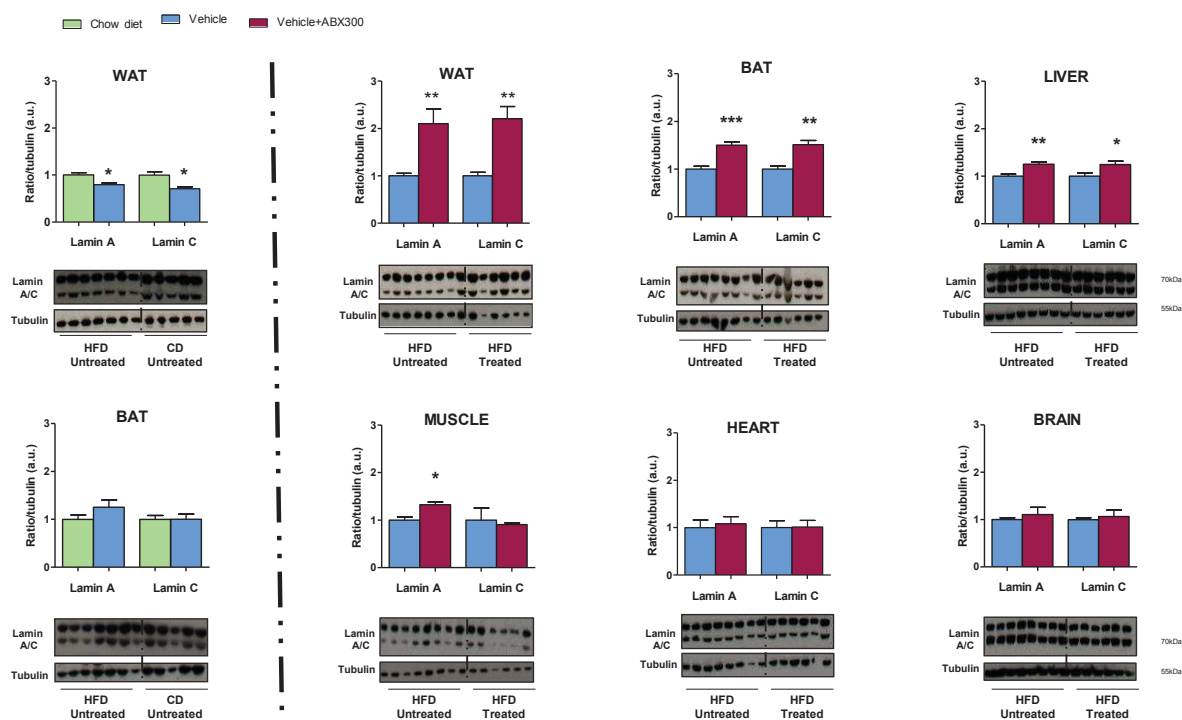


**Figure 46: Tissue specific expression of lamins depending on diet condition and ABX300 treatment.**

Protein level of Lamin A/C in WAT, BAT, Muscle, Liver, Heart and Brain were determined by western blot. Tubulin levels were used as a control. Analysis showing quantification of protein expression levels using ImageJ software. All these experiments were done with C57BL/6 mice ( $n = 6-8$  /group). Values are given as mean  $\pm$  SEM. \*\* $p < 0.001$  and \*\*\* $p < 0.0001$ . Antibodies references are Lamin A/C (H-110): sc-20681 and  $\alpha$  Tubulin (DM1A): sc-32293.

For concretizing our results, we tested ABX300 in murine models exclusively expressing the Lamin C isoform of the LMNA gene (LCS) (Osorio et al., 2011). We put the animals under HFD to force them to rapid obesity and exacerbate the conceivable effects of the molecule (**Figure 47A**). WT mice lost in average 11.82 grams (**Figure 47B**). On their side, results regarding the LCS animals were not concluding because, after 50 days, responses to ABX300 treatment differed according to the individuals' genetic background. LCS male mice breeding from heterozygous LCS progenitors (WT/LCS) lost in average 12.3 grams (**Figure 47C**). Whereas, the LCS offspring

proceeding from homozygous parents (LCS/LCS), barely lost 0.3 grams (**Figure 47D**). These experiments must be redesigned keeping into higher consideration the provenance of the animals. Moreover, the completely epitomizing of the drug would require also its administration in murine models deficient for A-type lamins (Lloyd et al., 2002; Fong et al., 2006; Davies et al., 2010; Coffinier et al., 2010).

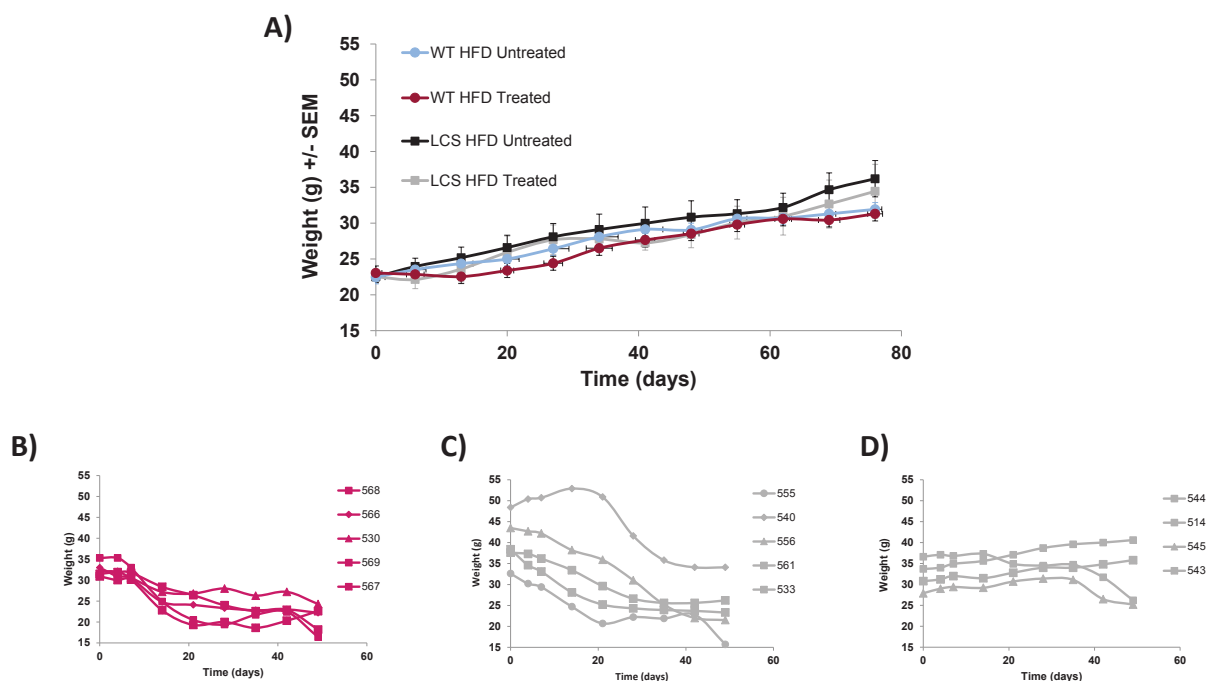


**Figure 47: LCS mice response to ABX300 diverges according to their genetic background.**

- A)** Weight monitoring of untreated and ABX300 treated WT and LCS mice under HFD conditions.
- B)** Weight monitoring of WT HFD ABX300 Treated mice.
- C)** Weight monitoring of LCS HFD ABX300 Treated WT/LCS mice.
- D)** Weight monitoring of LCS HFD ABX300 Treated LCS/LCS mice.

### vi) Further phenotypic characterization of ABX300 treated mice

To try to get rid of the kidney toxic effects *in vivo* (see “clinical development”) while maintaining efficacy, we carried out three sort of experiments. In the first kind, we diminished the frequency of the drug administration to three times per week (50mg/Kg) (**Figure 48A**). In the second kind we changed the administration dose, adapting the drug amount to the animal’s lean-mass ( $\approx 31\text{g}$ ) (**Figure 48B**). Finally, in the third case, we diminished downright to 20mg/Kg (**Figure 48C**).

In the two first cases, ABX300 had the same effect on weight evolution than when administrated daily at 50mg/Kg. But unfortunately, kidney toxicity was still present (**data not shown**). The third concentration was below the required threshold for an appreciable action, and animal groups did not present any differences regarding weight evolution.

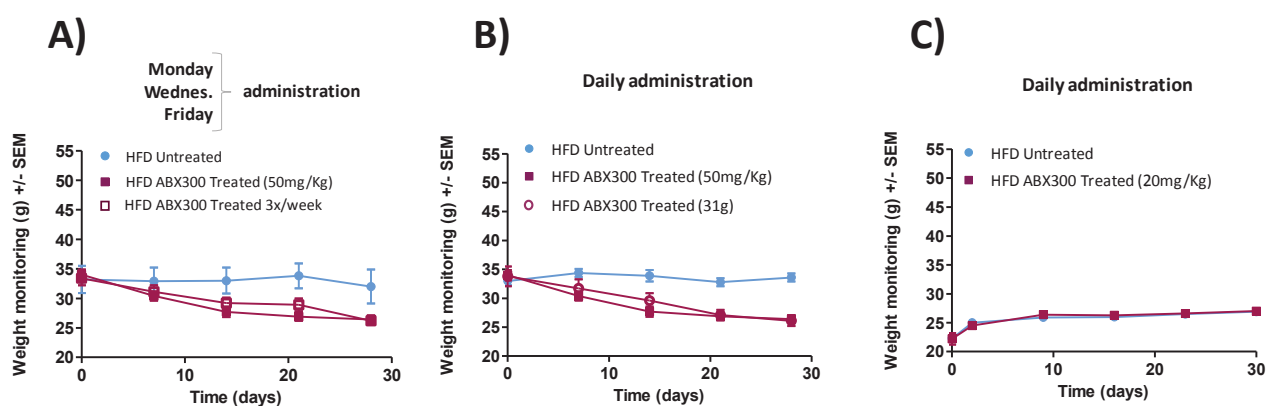


**Figure 48: Different treatment schemes of ABX300 do not affect its effect on weight loss after one month treatment.**

The general diminution of the fat size, as well as the aspect of other metabolic organs from these three and other treatment schemes previously mentioned can be observed in **Figure 49**.



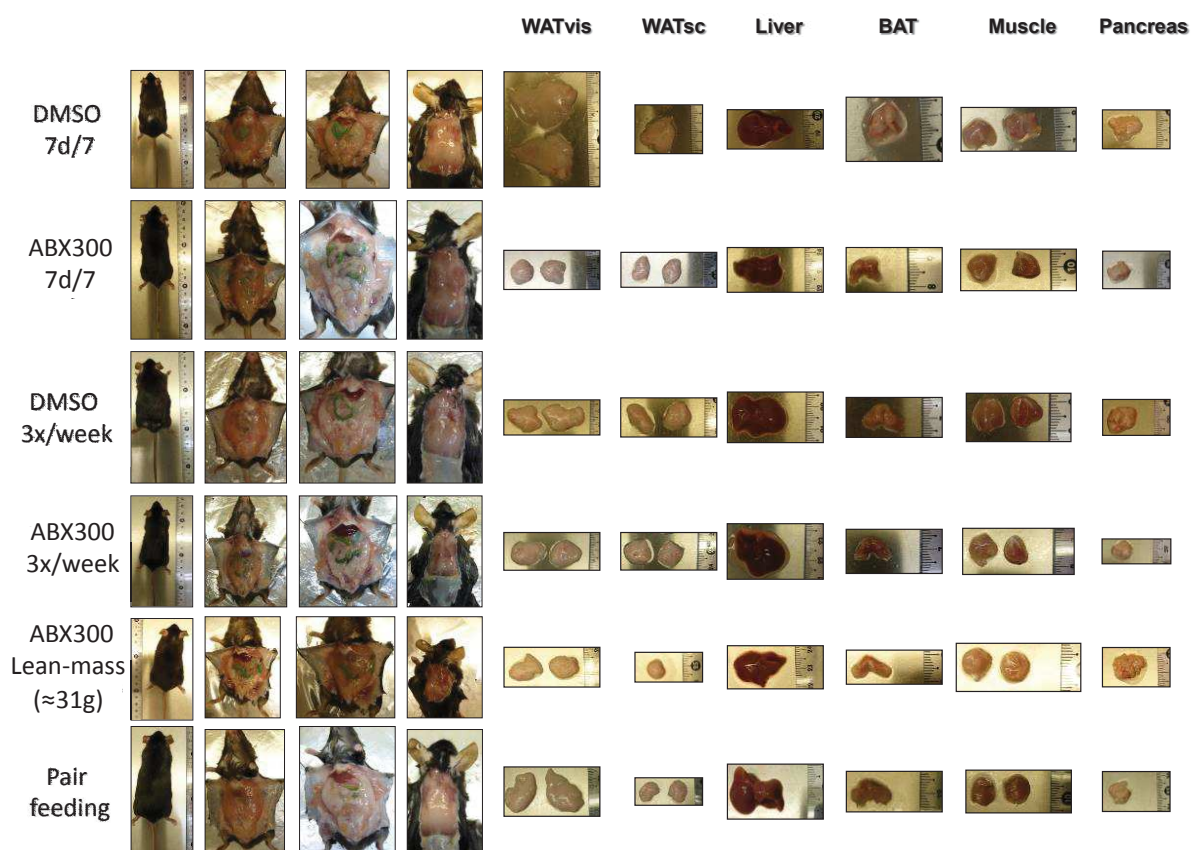


**Figure 49: Noteworthy macroscopic effects induced by ABX300 on WAT.**

Pictures of metabolic organs from exemplary individuals in very many of the so-mentioned ABX300 protocols in this manuscript (See Figure 48 on this same page and Figure 2 of López Herrera *et al.*)

The experiences depicted in **Figures 48 A)** and **B)** are quite curious because if we take into account the total amount of drug, and this in a weekly fashion:  $50\text{mg} \times 3 = 150$ , and  $20\text{mg} \times 7 = 140$ , which corresponds to almost the same quantity of ABX300 administrated per week. This observation suggests the existence of some kind of mechanism that will not be activated if the dose is not high enough, some threshold to be surpassed at once, not with the potential accumulation of the compound over time. To study the accumulation of the molecule over time, and the memory effect of ABX300 we designed an experiment into which we would arrest treatment and check for weight evolution (**Figure 50**).

We monitored the weight changes of untreated and ABX300 treated mice went from a normal chow diet (CD) (yellow cage) to a high fat diet (HFD) (grey cage). At the start of

the experiment, under normal diet conditions, the mice weight did not significantly differ between groups. At day 60 (a), all animals were put to a HFD (a) and two groups were made from the initially treated group. In the one that ABX300 treatment was arrested, mice began to gain weight (green squares) gradually approaching the vehicle group (blue circles). ABX300 long term treated animals (maroon squares), maintained their original weight, reproducing the preventing effect of the molecule that we had already proven. To check for reversibility of our effect, at day 110 these two groups were inversed (b). The graph shows how the group that re-started the treatment, immediately lost weight (green triangles) and the group that had been treated for over three months, slightly started to re-gain weight (maroon triangles). On day 150, when the experiment was terminated, the weight of the mice belonging to the inversed groups was in the range of 22–23 g, whereas untreated animals had reached 27g. These data led us to conclude that lipotrophy induced by ABX300 is reversible upon cessation of treatment, in other words, that ABX300 enhances weight loss in obese mice without inducing resistance.

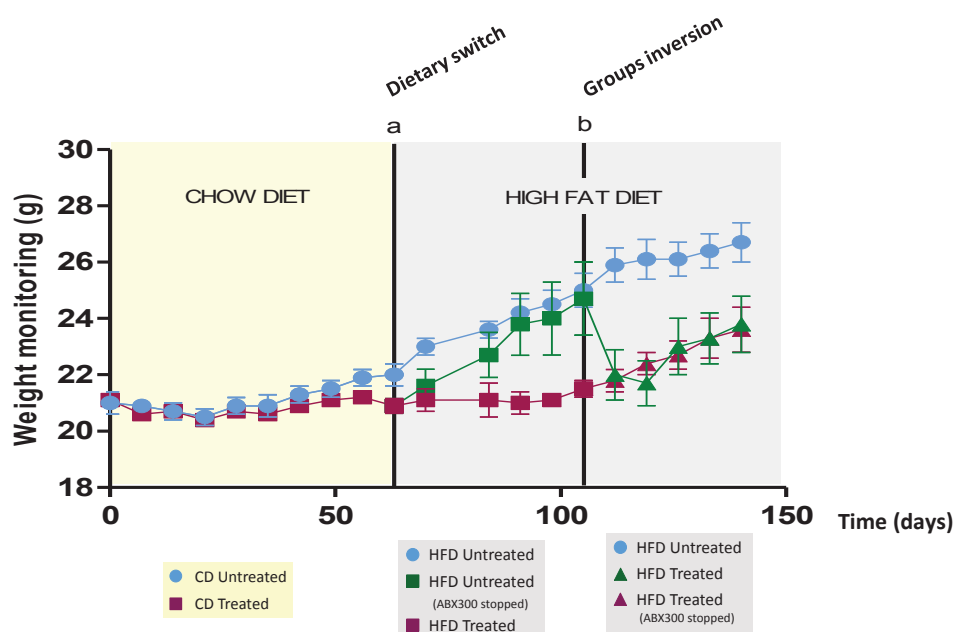


**Figure 50: Long term effect and efficacy of ABX300 to enhance weight loss in obese but not lean mice**

Because of this food dependent effect of ABX300 treatment, we decided to focus on more metabolic aspects. Regarding carbohydrates metabolism, a couple of tests were carried out in order to evaluate the physiological response to a given dose of glucose. To determine how mice's organism broke sugar down, we carried out an OGTT (Oral Glucose Tolerance Test) experiment. Four hours fasting subjects were orally given of glucose. Blood samples were collected every thirty minutes for further glycemic evaluation. If insulin secretion befallen normally, data obtained in this manner would allow the experimenter to observe a decrease of the glucose present in the blood, and indeed, this was the case. Results in **Figure 51A** show a slight improvement in regard to glucose tolerance after 1 month of ABX300 treatment. Moreover, this test is usually used to assess diabetes, insulin resistance, and sometimes rare disorders of carbohydrate metabolism.

Besides OGTT, individuals were also conducted through ITT (Insulin Tolerance Test). This analysis measures the body's ability to respond to an intra-peritoneal (IP) injection of insulin. Similarly to the previous experience, we followed the levels of blood glucose every fifteen minutes during the 45 minutes following insulin injection. However, this time not improvement of the ability of ABX300 treated mice to respond to IP injected insulin was observed (**Figure 51B**).

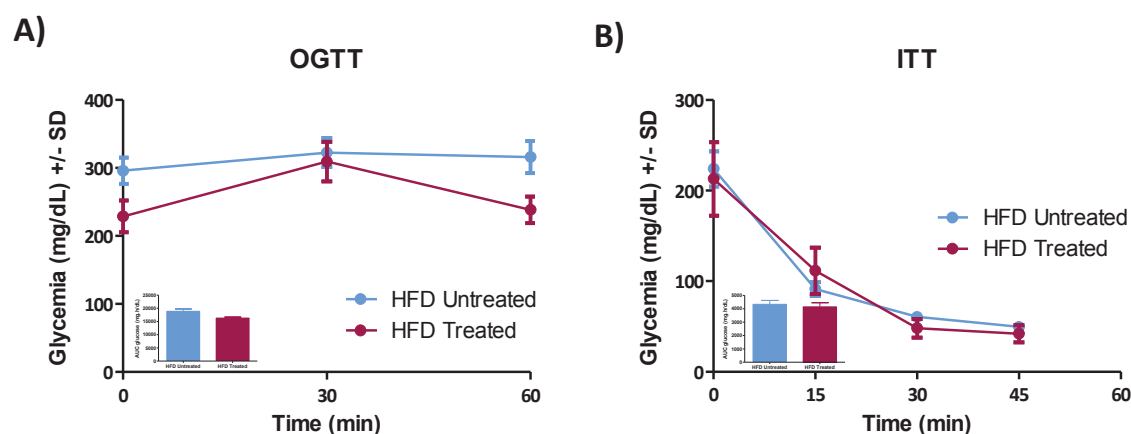


**Figure 51: ABX300 does not induce robust changes in glucose metabolism.**

- A)** ITT monitoring after insulin intra-peritoneal injection on treated and control groups.  
**B)** OGTT monitoring after glucose oral administration on treated and control groups.  
 OGTT → 1 gram of glucose per kg; ITT → 1U insulin per kg (n=7-8/metabolic test).

#### 4. Clinical development of ABX300

##### *i) Adverse effects of ABX300 on hERG*

In preclinical safety trials, studies on the mechanisms of hERG (human Ether-à-go-go-Related Gene) channel inhibition are nowadays an unavoidable step for the development process of any pharmaceutical compound. These channels are essential for the normal electrical activity of the heart. A molecule is considered acceptable when administered at 1 $\mu$ M, the enhanced hERG inhibition remains below 10%. Several blockbuster drugs have been withdrawn from the market due to undesirable side effects on these channels. Repercussions usually involve long QT syndromes, which create a concomitant risk of sudden death (Sanguinetti and Tristani-Firouzi, 2006).

In the laboratory, before my arrival, extensive studies had been conducted on ABX300 toxicity, including evaluation of the rabbit Purkinje fibers. The obtained results had determined too high risks for a potential clinical development. To try to get rid of this conceivable cardiotoxicity, together with chemists, we worked on ABX300 SAR (Structure-Activity Relationship). My second project's objective relates to this issue and seeks to solve it in order to obtain a druggable compound clinically developable.

Unluckily, the majority of the designed ABX300 homologues which were positive within our screening systems (see López Herrera *et al.*), compounds conserved an unacceptable hERG (**Table 4**), and the ones that did not, did not prompt the desired *in vivo* response (**Figure 56**).

Abivax Compound	LMNA-luc activity	LMNA-luc toxicity (MTS)	hERG	
			1 $\mu$ M	10 $\mu$ M
<b>ABX300</b>	3,33	<10 %	26	70,3
<b>ABX418</b>	6,03	<10 %	12	20
<b>ABX420</b>	4,97	<10 %	9,3	15
<b>ABX435</b>	3,59	<10 %	14,7	48,3
<b>ABX448</b>	3,87	10 % < x < 30%	11	59
<b>ABX545</b>	2,33	<10 %	5,3	5,3
<b>ABX550</b>	2,36	<10 %	8	9,3
<b>ABX719</b>	5,63	<10 %	4	38
<b>ABX720</b>	5,47	<10 %	9	34
<b>ABX722</b>	3,23	<10 %	22	60
<b>ABX725</b>	6,20	<10 %	2	10
<b>ABX730</b>	5,21	<10 %	3	11
<b>ABX777</b>	2,98	<10 %	5,7	8
<b>ABX791</b>	3,11	10 % < x < 30%	5	13,7
<b>ABX833</b>	3,32	<10 %	9	22
<b>ABX835</b>	3,83	<10 %	5	13
<b>ABX844</b>	3,37	<10 %	5	55
<b>ABX858</b>	2,70	<10 %		
<b>ABX860</b>	2,89	<10 %	10	43
<b>ABX861</b>	2,80	<10 %	7	19
<b>ABX898</b>				

**Table 4: Activity and cardiotoxicity of all the *in vivo* tested ABIVAX compounds.**

The three first columns show for each *in vivo* tested compound: the Abivax nomenclature, their LMNA-luc activity and their LMNA-luc toxicity (MTS) (mean from three independent experiments). The two last columns exhibit hERG data at 1 and 10  $\mu$ M. Blue delineates activities below the established threshold, red shows toxicity and green points to a safe cardiac response to the products. Grey illustrates the period of my PhD.



## ii) *Adverse effects of ABX300 on kidneys*

When carrying out the sacrifices of the animals, we frequently noticed an abnormal kidney aspect on the treated mice that, we were afraid, was pointing to a nephrotoxicity potentially induced by the treatment. Notably, we could check that ABX300 induced alterations in the size, morphology and structure of these organs. Histopathological analyzes of kinetics (**Figure 52**) revealed: Clogged renal tubules (**A**), fibrosis (**B**), and numerous inflammatory cells infiltrations (**A**, **B**, **C**). These features were apparent after only six days of ABX300 drug administration, and this independently of the regime conditions.

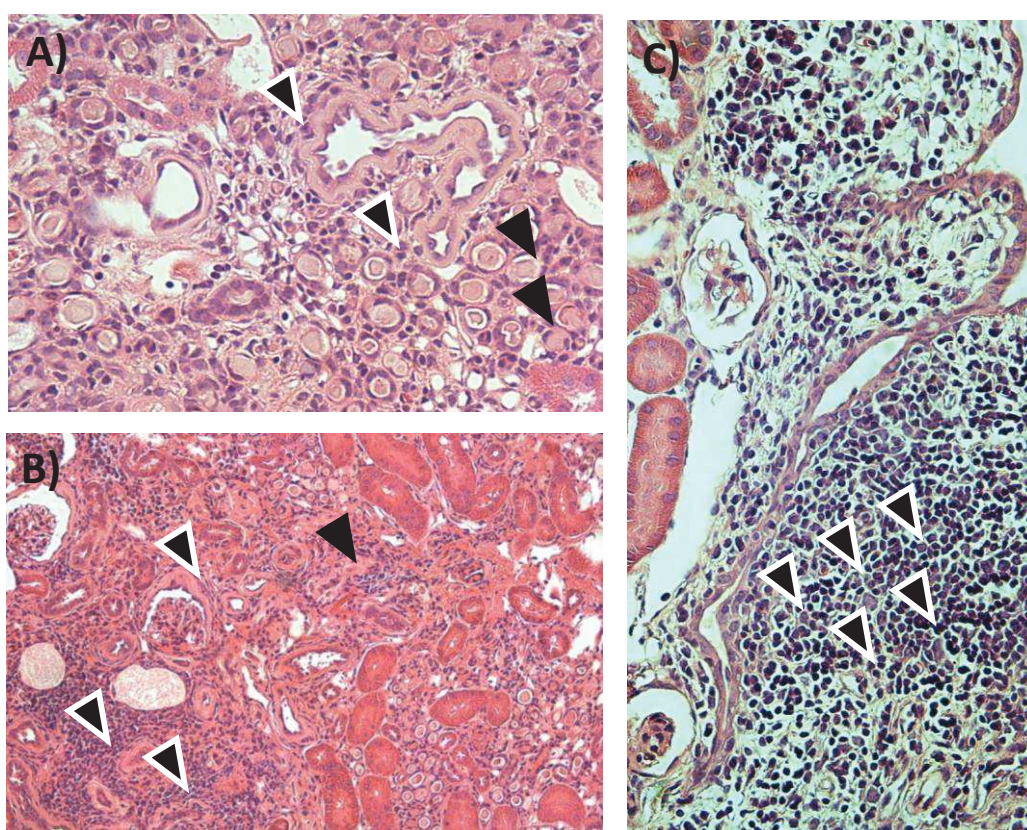


**Figure 52: Kidney sections of kidneys from ABX300 DIO treated mice.**

Haematoxylin-Eosin staining of representative sections of kidney embedded in paraffin after 1 month of treatment. See text for further details.

### iii) ABX300 skin biopsies in vitro (absorption experiments)

Facing the impossibility of making away with hERG and kidney side effects, we explored the possibility of developing an ABX300 topic treatment. Overlooking a potential future cream, we did some experiments on dermal absorption, using *in vitro* skin biopsies. The aim of the study that took place at C.RIS Pharma, was to evaluate the dermal and epidermal absorption of ABX300 by using fresh *ex-vivo* human skin biopsies (Nativeskin). Biopsies were treated at T0min and collected at T1h and T24h for further analysis of ABX300 content in dermal and epidermal tissues by HPLC-MS/MS method.

Results uncovered the ability of ABX300 to go across these samples. Scarcely 1 hour was sufficient to be able to detect ABX300, both in the epidermis and the dermis. Logically, after 24h of ABX300 exposure time, its concentration was increased (**Figure 53**). We concluded a satisfactory permeability of the skin to our molecule. These findings imply the possibility of a potential and promising development of ABX300 with cosmetic purposes.

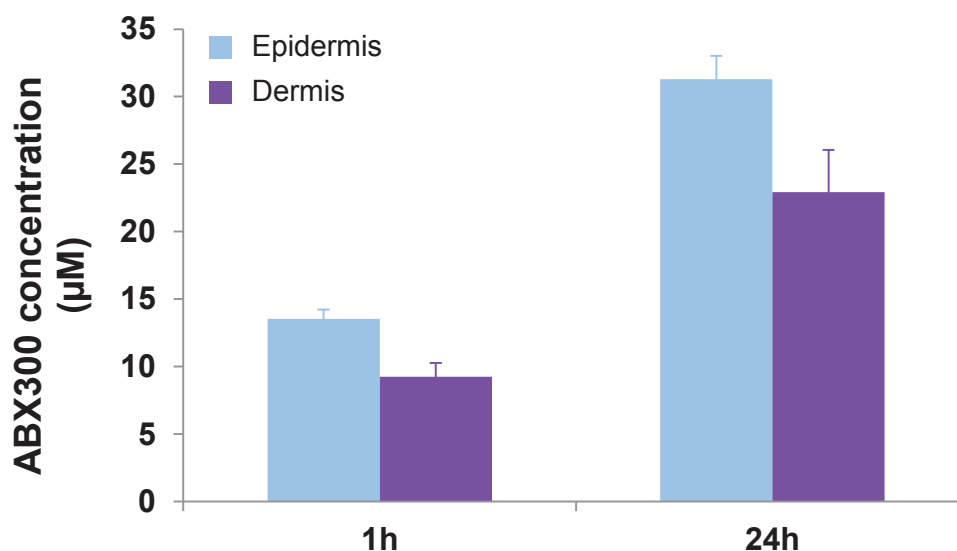


**Figure 53:** *In vitro* ABX300 dermal absorption experiment on skin biopsies.



## Project 2: Identification of molecules targeting *LMNA* splicing to avoid use of the progerin 5' SS

### 1. Aim of the project

Commonly, drugs fail along the development process for two main reasons. The first is that they do not work, and the second is that they are not safe. For ABX300, case number two is what explains the “no go” decision referring to its continuity into clinics. Because of the many existing drawbacks to pharmaceutically develop this molecule, the second objective of my PhD has been the identification of novel molecules, mainly ABX300 analogues but not exclusively, targeting *LMNA* splicing, and thus theoretically having an impact on weight evolution. Chemical modifications were implemented into the principal drug skeleton. On the frame of this second project of my PhD, we intended to find a back-up molecule. Ideally, this drug would not have adverse side effects of any kind while maintaining the activity and efficacy of ABX300 on weight modulation.

## 2. Modulation of the luciferase activity of the mini gene reporter by the ABIVAX Chemical Library

The ABIVAX Chemical Library is emplaced in the Curie Institute, in Paris. Further information about the origins of this drugs collection can be found in Soret *et al.*, 2005 and Bakkour *et al.*, 2007. Practically the entire presently existing library has been screened by means of the mini-gene luciferase reporter shown within **Figure 1B** of López Herrera *et al.* Since the beginning of this project in 2009, the number of tested drugs totals 887. This work has been mostly fulfilled by Julien Santo, an ABIVAX employee. He has also set up several parameters for the screening test, such as the optimal amount of cells to be seeded ( $10^4$ /well), the best cell clone to be used (clone 8) and the appropriate reading time (1s).

Because the background signal was very high in the HEK293 stable cell line, an elevated threshold was established in order to avoid selecting false positive compounds. Indeed, only molecules increasing 3 fold the luminescence signal compared to the control were selected for further exploration. Keeping this limit into consideration, 62 drugs out of the 887, are above the established threshold (**Figure 54**). Additionally, a toxicity test that reflects the number of viable cells based on the mitochondrial respiratory chain reactions (MTS) is systematically run to discard potentially toxic compounds. Once this second criterion is checked for, only 52 out of the 887 prevail eligible.

During the period of my PhD 110 molecules were screened from the ABIVAX chemical library. Only a few of these seemed to have an effect on *LMNA* splicing with no toxicity, and were investigated *in vivo*.

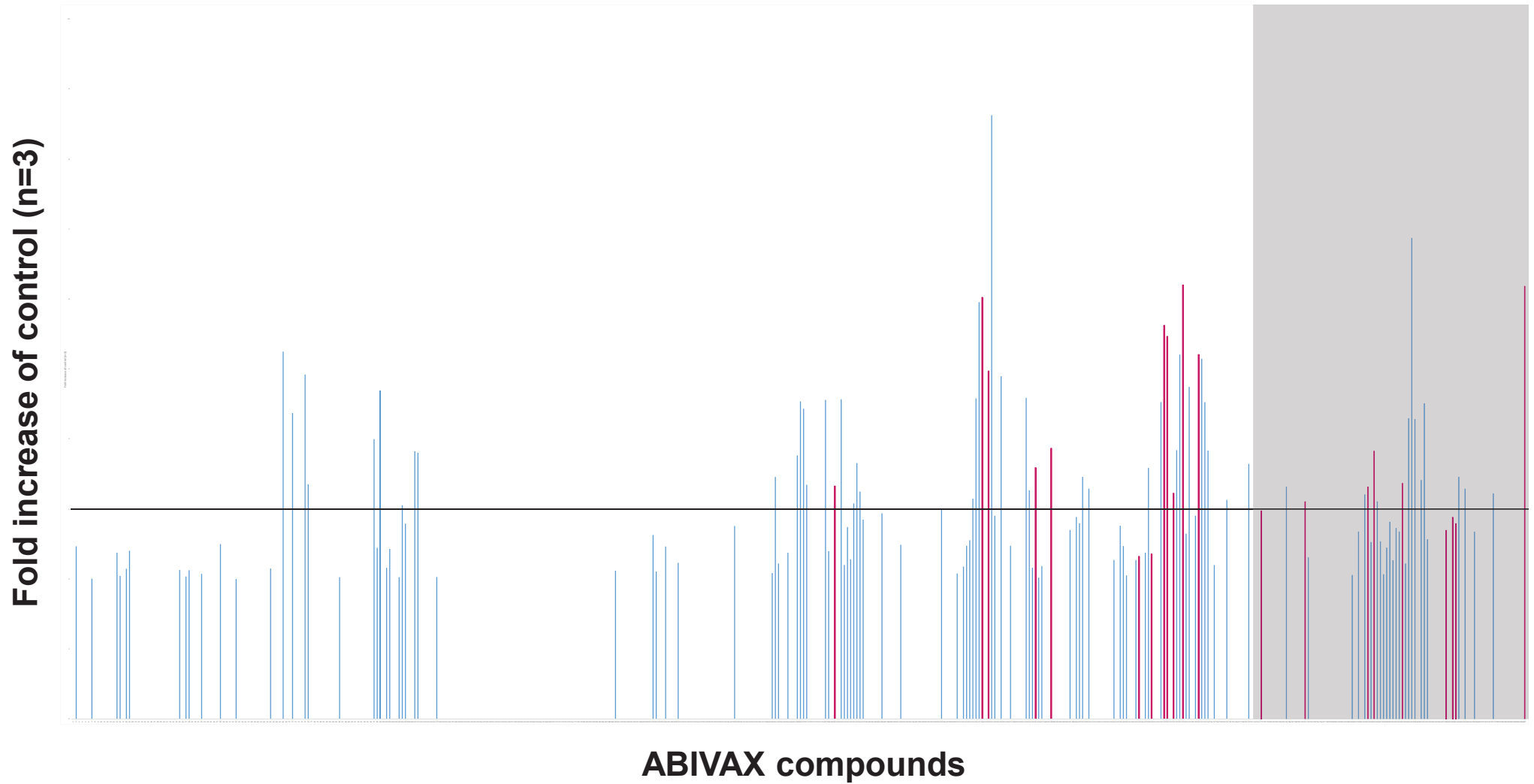


**Figure 54: Histogram recapitulating all the drugs from the ABIVAX Chemical Library tested with the LMNA-luc mini gene reporter.**

Vertical bars represent the mean of the luciferase activity from three independent experiments. Pink bars signify the molecules tested in vivo. The grey rectangle illustrates the period of my PhD. Threshold is depicted with a black line.

*i) Regulation of body weight through splicing modulation*

To bypass the so-mentioned negative effects of ABX300, the chemists that we work with, focused on ABX300's SAR studies. A summary of the modified chemical moieties is depicted in **figure 55**.

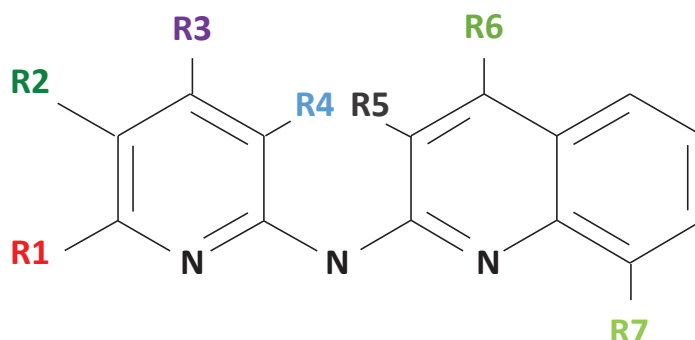


**Figure 55: Modified moieties during the SAR studies.**

Countless modifications have been done in the structure. However, only 21 ABIVAX drugs have been proved *in vivo*, in obesity models. They appear maroon colored on **Figure 54**. Before my arrival to the lab, the team had already tested six analogues (from 2009 to 2012) ABX418, ABX420, ABX545, ABX550, ABX725 and ABX730. Unsuccessfully none of them was proved effective relative to weight loss. During the period of my PhD (from 2012 to 2015), we tested another 14 whose *in vitro* activity was very close to three or beyond, and that corresponded elsewhere to the rest of the eligible criteria that had been previously determined (see text). These molecules correspond to ABX435, ABX448, ABX719, ABX720, ABX722, ABX777, ABX791, ABX833, ABX835, ABX844, ABX858, ABX860, ABX861 and ABX898. As a positive control, ABX300 (the 21<sup>st</sup> to complete the list), was simultaneously administered in every experiment.

Treatments were administrated daily by a tube feeding protocol. Animal groups were composed of 7 to 10 mice and the period of administration oscillated from 30 to 60 days. The amount of drug was set according to the weight of each mouse at a dose of 50mg/Kg, and this for all of the molecules. An exceptional situation exists for ABX898 where three different doses were tested; 5, 25 and 50mg/Kg. This is because this compound is in fact a pro-drug of ABX887, into which the addition of a phosphate group to the scaffold of the molecule was intended to solubilize it rendering it more available for the organism (Gasparik et al., 2012). All the molecules were tested in a curative context, except for two of them, ABX777 and ABX791, which were administrated in a preventive manner. ABX448 was also *in vivo* tested, but graphs are not shown in this manuscript because the treatment had to be stopped after one week due to the severe *in vivo* toxicity of the molecule.

Unfortunately, when the totality of the compounds were tested on DIO mice models, none of them showed an effect on weight evolution. The weight of untreated animals, in blue, progressed in parallel to that one belonging to treated animals, in maroon (**Figure 56**).

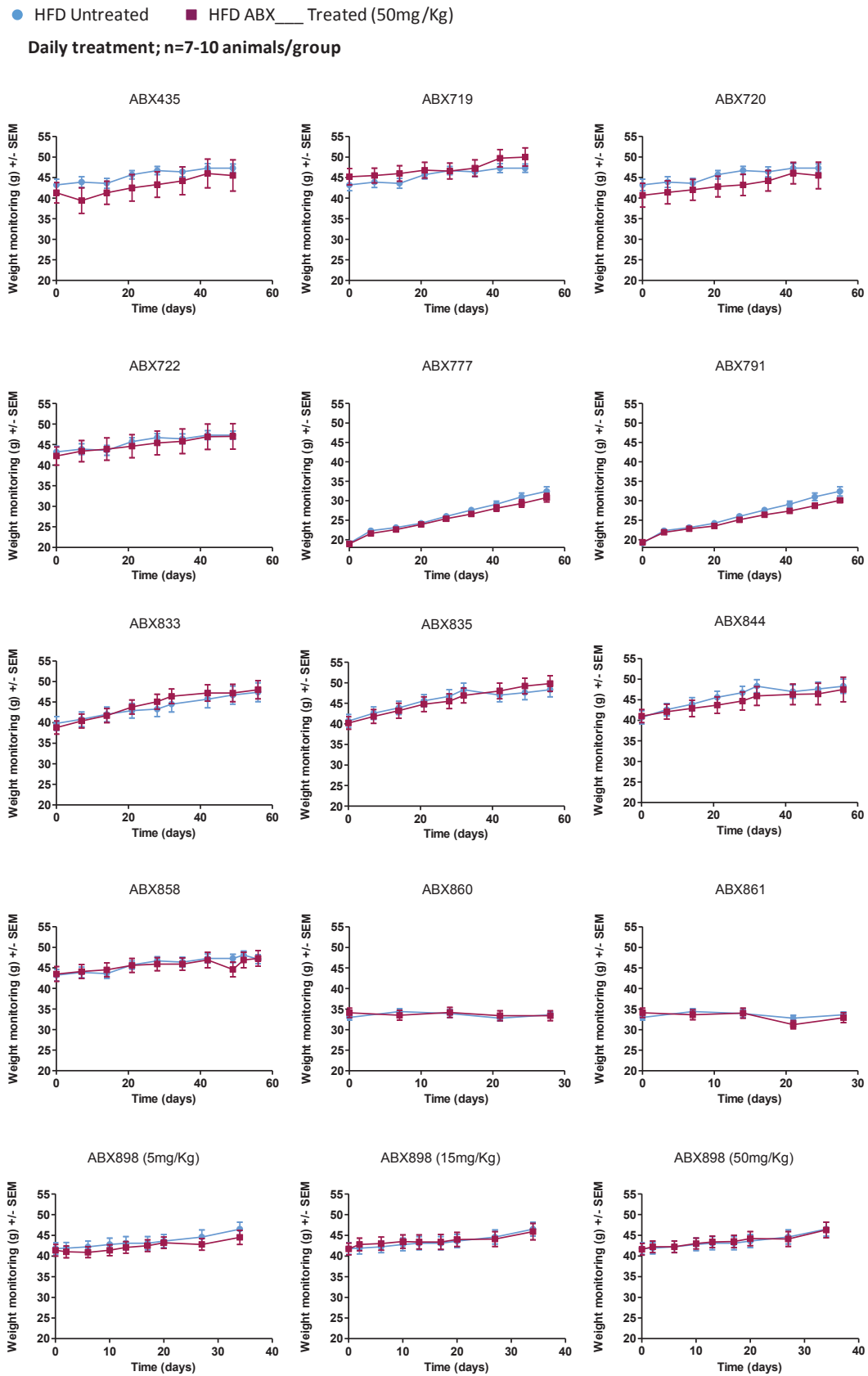


Figure 56: Absence of in vivo efficiency on weight loss of ABX

## DISCUSSION

---



## GENERAL DISCUSSION

*LMNA* is a gene coding for three major protein isoforms that have been classically implicated in nuclear architecture, gene expression, DNA replication, transcription signaling, chromatin organization and aging (Worman and Bonne, 2007; Dechat et al., 2008; Worman et al., 2009; Schreiber and Kennedy, 2013). To procure these distinct protein products, the *LMNA* gene is subjected to alternative processing. Alternative polyadenylation will give rise to lamins A and C while AS will produce lamin A and progerin. In the laboratory, we have shown that this splicing process is mainly regulated by two SR proteins, which correspond to SRSF1 and SRSF6. These two factors have been reported to play opposite roles in *LMNA* splicing (Lopez-Mejia et al., 2011). Furthermore, recent evidence indicates that *LMNA* is an active player in metabolism (Tang et al., 2011; Liu et al., 2012). Moreover, our laboratory has demonstrated that the different *LMNA* isoforms have antagonistic functions in EE and lifespan (Lopez-Mejia et al., 2014). This gene had already been proclaimed as a potential target for pharmacological modulation of WAT formation and, ultimately obesity. Various studies had identified *LMNA* as a strong candidate for targeting metabolic disorders (Rochford, 2014), but none of them had considered targeting *LMNA*'s splicing mechanism for this purpose. To better understand how *LMNA* influences AT homeostasis and the essential link of this gene with obesity, my thesis work has addressed two aims: the investigation of the MoA of ABX300, a modulator of the *LMNA* gene splicing with a striking effect on weight evolution; and the identification of other small molecules targeting the AS of *LMNA*.

Along this project, we have concretely been interested in the AS of the *LMNA* gene. We employed animal models to determine a concrete role for A-type lamins expression in the regulation of BMI and/or metabolism. In this regard, our data point to a favoring of the mechanisms leading to Lamin-A production. Our results are in line with previous evidence suggesting a metabolic role for lamins (Tang et al., 2011; Liu et al., 2012). One mechanism via which mutations in *LMNA* are proposed to influence AT is via interaction with the transcription factor SREBP1c (Lloyd et al., 2002). Beyond a role in regulating transcription factors, the lamins interact directly with many other nuclear proteins and form lamina-associated

domains (LADs) that are repressive regions rich in heterochromatin. By changing Lamin-A outcome, ABX300 could possibly affect AT-related gene expression. Lamin-A seems to be one important core module that modulates various transcriptional pathways, among which SREBP1 is comprised, in enhancing matrix elasticity-directed differentiation (Swift et al., 2013).

The interaction of SREBP1 with lamins A and C was characterized more than ten years ago, after a yeast-two hybrid interaction screen. SREBP1c plays a key role in adipocyte differentiation, inducing the expression of many genes of the mature adipocyte (Kim and Spiegelman, 1996). It acts as a transcription factor, that attached to the nuclear membrane and the endoplasmic reticulum regulates the expression and activity of PPAR $\gamma$  and PGC1 $\alpha$ . Several lines of evidence have suggested a role for SREBP-1 as a key mediator in the induction of lipogenesis during experimental caloric excess, regardless of whether the calories are derived largely from dietary carbohydrates or dietary fats. Furthermore, inhibition of SREBP by one small molecule, betulin, ameliorated obesity and increased EE in mice (Tang et al., 2011).

In my concrete project, for selecting the compounds capable of modulating *LMNA* AS, two screening systems were designed. A first one based on SRSF1 localization, and a second one based on the splicing event that occurs between exons 11 and 12 of the *LMNA* gene in the frame of HGPS (C>T  $\rightarrow$  activation of progerin 5'SS). On this second reporting system, it would be advisable to test ABX300 on the corresponding WT/non-mutated mini-gene. By doing so, we would get rid of any potential transcriptional effect of the drugs and could really recline on this construction with a closer reliability. Alternatively, we could have used other approaches for compound screening. Small-molecule screening techniques in drug discovery have been reviewed by Kedhar and colleagues. (Khedkar et al., 2009).

In the course of our experiments, we were able to establish an interaction between SRSF1 and ABX300. Having accomplished this, we would like to continue the study with other members of this same family of splicing regulators. With respect to the regulation of *LMNA*'s AS by SRSF1, a counteraction has been shown to be exerted by SRSF5 and SRSF6, (Fong et al., 2009; Lopez-Mejia et al., 2011), which enhance the use of the *LMNA* 5'SS at the expenses of progerin

5'SS. It would be intriguing to determine whether they bind to ABX300 or not. In addition, it is not superfluous to think that it is possible the existence of many other RNA Binding Proteins (RBPs) that would also interact with our candidate-drug. Another potential RBP would be Sam68, which has been recently identified to control prelamins A (Lattanzi et al., 2014), and which in addition has been proposed to be a key regulator of AS during adipogenesis, by binding the mammalian target of rapamycin (mTOR) (Huot et al., 2012). To recover other potential interactions we could use techniques of affinity chromatography or SPR (Surface Plasmon Resonance) in combination with mass spectrometry (MS). SPR quantifies interactions between proteins and ligands whereas MS deciphers the structural features of the bound proteins. In addition, since computational prediction of interactions between drugs and their target proteins is of great importance for drug discovery and design, we could also help ourselves with *in silico* prediction methods.

When we turn our attention to global expression analyses, an overall alteration in AT specific splicing may also contribute to the striking effect on weight evolution caused by ABX300 treatment in this tissue. When we evaluated the impact of ABX300 on cellular splicing, we determined that it did not seem to globally interfere with this process. The relative abundance of the alternatively spliced products did not show variations between conditions, suggesting no large impact of our treatment on AS. Moreover, it might be interesting to demonstrate that ABX300 does not stall the spliceosome assembly, like they do some known drugs, such as Spliceostatin A (Roybal and Jurica, 2010), Isoginkgetin (Bonnal et al., 2012) or Pladienolide B (Shi et al., 2015). One adequate method to verify this would be the performance of radioactive assays. To get beyond about this point, high-throughput analysis of RNA splicing (HTS) could shed extra light into how ABX300 contributes to weight loss by modulating splicing of specific pre-mRNA in a genome-wide scale. RNA-Seq seems to be more flexible and powerful than microarrays. When sequencing polyA<sup>+</sup> RNAs with stranded protocol, the quality of the data is very good. Besides, by using also small RNA sequencing (selecting RNAs of length <100nt and then sequencing this fraction), it would be possible to assess the effect of the treatment on miRNA biogenesis.

Moreover, it has been shown that primary sequence and RNA structure are key regulators in miRNA biogenesis (Ha and Kim, 2014). Complementary, it has been demonstrated that alterations in miRNA levels correlate with various metabolic diseases (Hartig et al., 2015). However, there is limited knowledge on how diet influences miRNA expression in AT. Experiments in 3T3-L1 cells and primary adipocytes suggest changes in miRNA expression may occur in response to nutrient availability (Klötting et al., 2009). Given the growing number of adipogenic and anti-adipogenic miRNAs identified, it is highly plausible that these miRNAs will also respond to dietary changes. Indeed our results show food-dependent variations for 113 miRNA. In a correlative manner, some studies have shown that nutrient supplementation can reduce the adverse consequences of a HFD and also coincidentally modulate miRNA expression in AT (Parra et al., 2010; Murase et al., 2011). Our work additionally shows a modulatory effect of ABX300 on the miR found in AT. After intersection of the several generated datasets, our miRNA analysis demonstrated that ABX300 modulates a population of miRNAs likely mitochondrial-enriched, and this independently of the nutritional regime. Since regarding SRSF1, data are available for CLIP (cross-linking immunoprecipitation) and ChIP-seq (chromatin immunoprecipitation combined with massively parallel DNA sequencing) (Ji et al., 2013; Pandit et al., 2013), it would be of great interest to determine if this splicing factor, which interacts with our candidate-drug, does also bind to any of the 26 mitochondrial genes that are predicted to be targeted by the eight miRNAs modulated by ABX300 (miRBASE,  $\geq 80\%$  confidence). Additionally, in future studies it would also be interesting to analyze how ABX300 affects interactions of SR proteins with mRNAs by co-IP or CLIP-Seq. Furthermore, it is worth noting that more direct evidence is now needed to document and validate the described ABX300-miR modulations, as well as the modulations of the miR-predicted targets.

It has been recently reported that there exists an interplay in between miRNA silencing efficiency and mitochondrial activity (Huang et al., 2011). It is tempting to think that ABX300 treatment could possibly have an impact on RISC assembly, a process for which mitochondrial activity is required. Mitochondrial main activity is respiration, and it appears to act as a canonical central mechanism integrating central and peripheral regulation of energy stores. Our

studies highlight a mitochondrial's major role in the regulation of the energy balance and suggest that the functioning of these organelles could be regulated by the ABX300 treatment. By the achieved comparisons we obtained information about the amount of these organelles in WAT and BAT. Interestingly, we showed that the content of these organelles was higher in BAT from treated animals. This finding might seem unexpected given the absence of ABX300 hearty modulations of the genes implicated in mitochondrial biogenesis, and the diminution we observe in PGC1 $\alpha$  relative expression levels in BAT from treated animals. Intriguingly, these results regarding mitochondrial genes are a little bit convoluted, but as swiftly discussed all along the results themselves, it is possible that the explanation lies in the fact that both, individuals and primers were different between the different experiences. An increase in the number of individuals used for the *in vivo* experiments would also be recommendable.

We presume that the mitochondrial amount could be related to mitochondrial activity, even if several lines of evidence suggest that this is not always necessarily the case (Galgani et al., 2008). Although we failed to *in vitro* identify this hypothetical increased mitochondrial activity using the Seahorse Technology, we believe that ABX300 treatment is inexorably linked to the functioning of this organelle. Nevertheless, much more complete analysis shall be performed to confirm this statement.

Today's research has described that disturbance of mitochondrial functioning and of fatty acid metabolism might be involved in the pathophysiology of obesity (Li et al., 2015). Furthermore, energy sensors such as AMPK, have been suggested to represent a central node linking energy metabolism to diseases correlated with aberrant AS (Finley, 2014). Measuring AMPK's activity could help us characterize ABX300's MoA. Besides, two recent reviews (Kaminska and Pihlajamäki, 2013; Lin, 2015) provided a brief overview of the basic aspects of splicing regulation in adipocytes differentiation, obesity and insulin resistance with specific examples. They suggested that understanding of the molecular mechanisms behind the spliced transcripts may provide opportunities for new diagnostic approaches. One concrete example is the association between a concrete spliced isoform and reduced adiposity. The

authors showed a selective reduction in the mass of fat depots in mice with skeletal muscle-specific transgenic expression of PGC-1 $\alpha$ 4, a form of PGC-1 $\alpha$  that resulted from alternative promoter usage and splicing of the primary transcript (Ruas et al., 2012). PGC1 is a key factor in mitochondrial biogenesis and thermogenesis. Interestingly, PGC1 $\alpha$  has two regions rich in serine-arginine pairs. These two RS domains make PGC1 $\alpha$  an SR-like protein. Like for SR proteins, the activity of PGC1 $\alpha$  is modulated by posttranslational modifications of the RS domain. PGC1 $\alpha$  has been shown to be activated, together with SIRT1, by an outstanding compound known as resveratrol. This activation improved mitochondrial function and protected against metabolic disease (Lagouge et al., 2006). Compelling data also demonstrated that specific SIRT1 activation mimicked low energy levels and protected against diet-induced metabolic disorders by enhancing fat oxidation (Feige et al., 2008). Furthermore, in genetically modified mice phenocopying the HGPS pathology (Zmpste24 $^{-/-}$ ), resveratrol was shown to activate SIRT1 in a Lamin A-dependent manner, thus associate with the nuclear matrix (Liu et al., 2012). SIRT1 is a NAD $^{+}$ -dependent protein deacetylase that regulates various metabolic pathways (Haigis and Sinclair, 2010). Loss of SIRT1 abolishes many beneficial effects of caloric restriction (CR). On the contrary, transgenic mice with additional copies of SIRT1 show phenotypes resembling CR (Guarente, 2013). Putting this in context with our data, we could assimilate ABX300 action to resveratrol's and hypothesize that our molecule might act by enhancing SIRT1 action. However, experiments assessing potential SIRT1 activation by ABX300 would be required to affirm this. Lamins distribution upon ABX300 treatment should also be checked for; along with the locomotory activity of ABX300 treated animals. In terms of the coinciding effects of ABX300 and resveratrol regarding the leanness of the CR induced phenotype, we have demonstrated that ABX300 action on feeding cannot entirely explain the observed changes in body weight. Our PF results demonstrated that ABX300's anorexigenic effect *solo* was not sufficient to explain the observed phenotype. It would also be interesting to determine which is the exact triggering effect, i.e. if diminish food intake precedes weight loss or it is the other way around. Additionally it would be interesting to evaluate the effects of ABX300 on the circulating levels of the principal neuropeptides related with appetite and satiety.



In the literature we encounter several lipolytic conditions among which beta-adrenoceptor agonist treatment is described. The finding that the relative mRNA expression of *Adrb3* appeared increased in WAT from ABX300 treated mice is suggestive of elevated sympathetic activation. Higher sympathetic tone and activation of the beige cells, which are known to be present in this tissue, might lead to an increased EE and partially account for the observed leanness and DIO protection in treated animals. We could not conveniently demonstrate increased levels of beige adipocytes selective markers in WAT from treated animals. Supplementary experiments adequately challenging beige cells emergence would be required. This may be done by cold-exposure (4°C), CL316,243 ( $\beta$ 3-AR adrenoceptor agonist) administration, or the just described creatine-substrate for mitochondrial respiration enhancement in beige fat (Kazak et al., 2015). Alternatively, to verify the fate of FFA in ABX300 treated mice, we could perform metabolomics/ lipidomics analyses and trace the clearance of lipids by using radioactive-labeled palmitate ([13C], [1-14C], [U-14C], and [16-14C]). Some other attainable experiences for this same purpose comprise among others following the lipid clearance from the circulation in response to a bolus fat load or the injection of lipid emulsions (olive oil for example). More readily, we could expose our animals to 24 hours of food deprivation and check which group lost more mass. We predict the observation of an exaggerated loss of fat mass in the ABX300 treated mice. This result would be indicative of an increase in the metabolic rate enhanced by the treatment.

Indeed, when we recapitulate the experiments that we have carried out to check for a plausible lipolysis being established in treated cells/explants, we realize that in none of the experiences we have kept into consideration the likely re-esterification of fatty acids and glycerol. This could have been overcome by the addition of Triacsin C into the culture media. Triacsin is a potent inhibitor of long fatty acyl CoA synthetase, and thus of triglyceride synthesis.

The one exact mechanism by which ABX300 in fat tissue affects systemic metabolism remains unknown at this time. Despite our efforts to observe ABX300's effect *in vitro* we did not succeed to prove any group differences. However, based on the current results we can speculate, that perhaps a metabolite, i.e. a molecule derived signaling molecule, enters the circulatory



system and subsequently affects metabolism in peripheral tissues. One experiment that would allow us to further confirm or dismiss this hypothesis would be to collect the serum from treated animals, to subsequently extract the potential metabolites and to thereafter use it *in-vitro* on different cellular models. Documenting the metabolites obtained from ABX300 could be doable with the help of techniques using microsomes. These are vesicle-like artifacts re-formed from pieces of the endoplasmic reticulum when eukaryotic cells are broken-up in the laboratory. A bank of readily available well-characterized human and animal hepatic microsomal fractions has been established and is available for this purpose (Lacarelle et al., 1991). Besides characterizing ABX300 metabolites, microsomal studies may also help to elucidate their pathways, and make suggestions for further *in vivo* testing (Jia and Liu, 2007).

Historically, deciphering the mechanism of action of small molecules identified through cell-based screening has often brought new insights into biology (Schreiber and Kennedy, 2013). Such was the case for IDC16 and ABX464, two compounds targeting specifically SR proteins and inhibiting HIV RNA biogenesis respectively *in vitro* (Bakkour et al., 2007) and *in vivo* (Campos et al., 2015).

For the advancement of basic science and drug development it is important to understand the interactions between small molecules and proteins. This can be approached from different perspectives. Particular methodologies have been developed to identify protein-small molecule and protein-metabolite interactions (McFedries et al., 2013). To carry out proteomics in the specific case of ABX300 we would need to heavily rely on chemistry to link our compound to a solid support (different attachment sites could be tried according to prior information from SAR). In the drug discovery field, the classic target validation tool is the small bioactive molecule that interacts with and functionally modulates effector proteins (Hughes et al., 2011). The effector proteins that ABIVAX focuses on are namely the Serine/Arginine-Rich Splicing Factors (SR proteins). ABIVAX *leitmotiv* is to target the AS mechanism in order to cure various diseases. In joint collaboration with the CNRS (French National Center of Scientific Research), this company is developing novel drug candidates for the treatment of metabolic and viral disorders, along with exploring novel therapeutic space. Drug discovery and

development in ABIVAX involve the utilization of *in vitro* and *in vivo* experimental models. Unluckily, the leading drug candidate of my PhD project, ABX300, was proved to be inappropriate for the clinical advancement. Its narrow therapeutic index is illustrated by the adverse effects that result from early takes. Therefore, ABX300 research was compromised and forced to put an end before reaching the late stages of clinical trials phases, corresponding to human subjects.

Maybe partially because of the difficulty of trespassing these last steps, few efficient treatments for obesity are currently available in the market, despite the fact that distinct possibilities for approaching these lifestyle related pandemics have been the subject of numerous studies over the last decade (Butsch, 2015; Jackson et al., 2015). Nonetheless, hopes for breakthrough therapies for obesity and diabetes are as high as they have ever been. The pace of discovery in the field of metabolism indicates that this is an area growing rapidly, and new insights are unfolding with each passing month (Rosen and Spiegelman, 2006). It remains to be seen how these discoveries will be translated into patients, because restrictions regarding safety concerns in obesogenic treatments are very high. At any rate, the transfer of ideas from bench to bedside is rarely a straight forward path.

## APPENDIX

---



# Antagonistic functions of *LMNA* isoforms in energy expenditure and lifespan

Isabel C Lopez-Mejia<sup>1,2,†</sup>, Marion de Toledo<sup>1,†</sup>, Carine Chavey<sup>1</sup>, Laure Lapasset<sup>1</sup>, Patricia Cavelier<sup>1</sup>, Celia Lopez-Herrera<sup>1</sup>, Karim Chebli<sup>1</sup>, Philippe Fort<sup>3</sup>, Guillaume Beranger<sup>4</sup>, Lluís Fajas<sup>2</sup>, Ez Z Amri<sup>4</sup>, François Casas<sup>5</sup> & Jamal Tazi<sup>1,\*</sup>

## Abstract

Alternative RNA processing of *LMNA* pre-mRNA produces three main protein isoforms, that is, lamin A, progerin, and lamin C. *De novo* mutations that favor the expression of progerin over lamin A lead to Hutchinson-Gilford progeria syndrome (HGPS), providing support for the involvement of *LMNA* processing in pathological aging. Lamin C expression is mutually exclusive with the splicing of lamin A and progerin isoforms and occurs by alternative polyadenylation. Here, we investigate the function of lamin C in aging and metabolism using mice that express only this isoform. Intriguingly, these mice live longer, have decreased energy metabolism, increased weight gain, and reduced respiration. In contrast, progerin-expressing mice show increased energy metabolism and are lipodystrophic. Increased mitochondrial biogenesis is found in adipose tissue from HGPS-like mice, whereas lamin C-only mice have fewer mitochondria. Consistently, transcriptome analyses of adipose tissues from HGPS and lamin C-only mice reveal inversely correlated expression of key regulators of energy expenditure, including *Pgc1a* and *Sfrp5*. Our results demonstrate that *LMNA* encodes functionally distinct isoforms that have opposing effects on energy metabolism and lifespan in mammals.

**Keywords** aging; energy expenditure; *LMNA* protein isoforms; mitochondria biogenesis; RNA processing

**Subject Categories** Metabolism; Physiology

**DOI** 10.1002/embr.201338126 | Received 18 October 2013 | Revised 7 February 2014 | Accepted 11 February 2014 | Published online 17 March 2014

**EMBO Reports (2014) 15: 529–539**

See also: **IA Chatzispyrou & RH Houtkooper** (May 2014)

## Introduction

Multiple signaling pathways affect senescent decline and aging. Studies in simple model organisms have led to remarkable

progress in understanding the molecular pathways that modulate aging and senescence [1–3]. However, the mechanisms mediating senescent decline and aging in mammals remain unclear. Thus, it is important to understand which cells or tissues coordinate the aging process at the level of the whole organism.

The Hutchinson-Gilford progeria syndrome (HGPS or progeria) is a rare syndrome that causes premature aging [4]. Progeria is typically due to a silent *de novo* mutation in exon 11 of the *LMNA* gene (1824C > T, G608G). This mutation increases the usage of a natural splice donor site in exon 11 of *LMNA* [5–7], leading to an in-frame deletion of 150 nucleotides, including the cleavage motif required for the last maturation step of lamin A by the ZMPSTE24 endoprotease [8]. Both *Zmpste24*-deficient mice (*Zmpste24*<sup>−/−</sup>) and farnesylated progerin (*Lmna*<sup>HG/+</sup>) knock-in mice present HGPS-like phenotypes [8,9], implying that defects in prelamin A processing rather than the loss of lamin A are responsible for premature aging. Interestingly, knock-in mouse models lacking either the lamin A (lamin C-only) or lamin C (lamin A-only) isoform do not exhibit disease phenotypes [9,10].

The RNA processing mechanisms leading to progerin and lamin C production are highly conserved in humans and mice [7,10,11]. Lamin C has not yet been identified outside of the mammalian lineage (Fig 1, [8,11]), and the polyadenylation site responsible for lamin C production is conserved between mammals. Since progerin expression is mutually exclusive with lamin C expression, we examined whether lamin C and progerin have opposite effects on lifespan. *Lmna* knock-in mice in which *Lmna* exons 11 and 12 are not transcribed and thus progerin-specific splicing cannot be performed were used in this study. Our results show that lamin C and progerin trigger antagonistic signals in adipose tissue that regulate mitochondrial biogenesis and energy expenditure. This study introduces a characterization of lamin C-only-expressing mouse model that exhibits obese phenotypes and increased lifespan.

<sup>1</sup> Institut de Génétique Moléculaire de Montpellier, CNRS UMR 5535, Universities of Montpellier 1 and Montpellier 2, Montpellier, France

<sup>2</sup> Département de Physiologie, Université de Lausanne, Lausanne, Switzerland

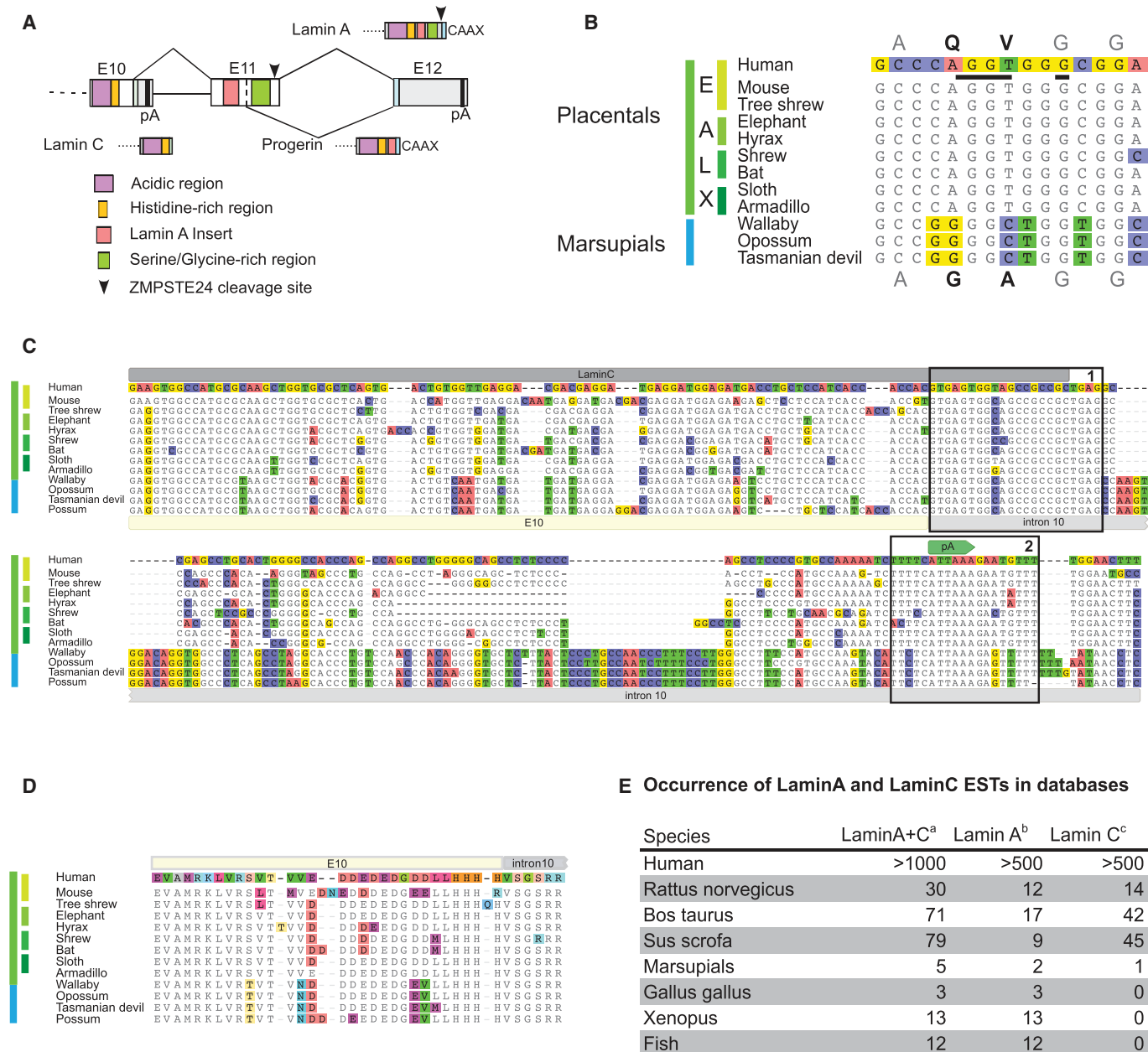
<sup>3</sup> CNRS, Centre de Recherche de Biochimie Macromoléculaire de Montpellier, Montpellier, France

<sup>4</sup> Faculté de Médecine, Inserm U844, Institut de Biologie de Valrose, UMR CNRS 7277 – UMR INSERM 1091, Université de Nice Sophia Antipolis, Nice, France

<sup>5</sup> UMR Dynamique Musculaire et Métabolisme, NRA - CAMPUS SUPAGRO 2 place Viala, Montpellier, France

\*Corresponding author. Tel: +33 4 34 359685; Fax: +33 4 34 359634; E-mail: jamal.tazi@igmm.cnrs.fr

<sup>†</sup>These authors contributed equally to this work.

**Figure 1. LMNA RNA processing isoforms during evolution.**

- A Schematic view of the three variable C-termini produced by the *LMNA* locus. Only the region spanning over exon 10 (E10), intron 10, exon 11 (E11), intron 11, and exon 12 (E12) is presented. pA are the polyadenylation sites producing lamin C and lamin A.
- B The alignment of progerin 5' splice site shows that it is conserved in the four placental super-orders (E: Euarchontoglires; A: Afrotheria; L: Laurasiatheria; X: Xenarthra).
- C Lamin C is conserved in Therians. Alignment of the genomic sequences spanning over exon 10 and the 5' end of intron 10 (IVS 10). Boxes labeled 1 and 2 show the high levels of conservation of the exon/intron borders and polyadenylation signals, respectively.
- D Alignment of the amino acids encoded by the genomic sequences (end of exon 10 and beginning of intron 10) shown in (C).
- E Occurrence of lamin A and lamin C ESTs in databases.

## Results and Discussion

### Complexity of the C-terminus of lamin A during evolution

In order to infer functional relationship between LMNA isoforms, we first examined when production of progerin and lamin C isoforms was selected during evolution. We found that the splice site responsible for progerin production is included in a region highly conserved throughout the four placental super-orders but absent in the exon 11 sequences of marsupials from three distinct orders (Fig 1B). In contrast, lamin C transcripts and a conserved polyadenylation signal site in intron 10 were identified in all placentals and marsupials examined (Fig 1C–E). Furthermore, intron 10 nucleotide sequences proximal to the splice sites (Fig 1C) and the corresponding encoded peptides (Fig 1D) showed extreme conservation. This supports a scenario in which lamin C production was selected first in mammals, followed by progerin in placentals. Lamin C lacks the residues encoded by exons 11 and 12 of the LMNA gene; therefore, the complex maturation process involving proteolytic cleavage of the C-terminal part of prelamin A does not occur. Failure of prelamin A processing leads to the progeroid phenotype [8,12]; thus, the production of lamin C by alternative RNA processing may be an evolutionary adaptation to counteract the deleterious effects that result from inefficient prelamin A maturation. This also suggests that the production of LMNA isoforms may have physiological outcomes. This hypothesis was further tested here using mouse models.

### Lifespan and growth of mice carrying different *Lmna* alleles

The first mouse model of progeria to recapitulate the premature aging phenotype and splicing alteration observed in HGPS was recently described [7,10]. The progeria allele (*Lmna*<sup>G609G</sup> allele) was created by a knock-in strategy involving another mutant allele that encodes lamin C alone (*Lmna*<sup>LCS</sup> allele). This allele carries a floxed neo cassette just downstream of the polyadenylation site of lamin C and the G609G mutation in exon 11 (Fig 2A). *Lmna*<sup>G609G/+</sup> and *Lmna*<sup>LCS/+</sup> mice were intercrossed to generate *Lmna*<sup>G609G/G609G</sup>, *Lmna*<sup>G609G/+</sup>, *Lmna*<sup>LCS/+</sup>, and *Lmna*<sup>LCS/LCS</sup> mice used in this study. *Lmna*<sup>+/+</sup> obtained from both crosses were used as controls. Specific *Lmna* isoform expression was confirmed by Western blot (Fig 2A, and [7,10]).

As expected, mice homozygous for the G609G mutation lived < 6 months. In contrast, mice carrying only one G609G allele lived for 1 year on average. Most of the control mice died after 2 years, whereas approximately 60% of the *Lmna*<sup>LCS/+</sup> and *Lmna*<sup>LCS/LCS</sup> mice remained alive (Fig 2B). The median lifespan of *Lmna*<sup>LCS/+</sup> and *Lmna*<sup>LCS/LCS</sup> mice was about 110 weeks, which was significantly longer than the lifespan of WT mice ( $P = 0.0025$  and  $P = 0.0067$ , respectively) (Fig 2B). Both male and female *Lmna*<sup>LCS/LCS</sup> mice demonstrated significantly increased longevity compared to WT mice of the same gender (Supplementary Fig S1A).

Autopsies from *Lmna*<sup>LCS/LCS</sup> old mice showed a dramatically increased tumor incidence compared to *Lmna*<sup>LCS/+</sup> and *Lmna*<sup>+/+</sup> mice (Supplementary Fig S1B). These tumors were primarily located in the abdominal cavity. Histological analysis suggested that they were of lymphoid origin (unpublished results). No visible tumors were detected in younger *Lmna*<sup>LCS/LCS</sup> mice (less than a year old),

suggesting that lymphomas developed at a late age in these mice. This finding suggests that the *Lmna*<sup>LCS/LCS</sup> mice died from the progression of tumors that blunted their lifespan extension.

Consistent with previous observations [10], all of the mice were macroscopically identical before weaning. However, *Lmna*<sup>G609G/G609G</sup> mice failed to thrive, in contrast to the other “mutant” mice (Fig 2C). *Lmna*<sup>G609G/G609G</sup> mice died at an average of 18 weeks. At 30 weeks of age, *Lmna*<sup>G609G/+</sup> mice weighed less than WT and *Lmna*<sup>LCS/+</sup> mice, whereas *Lmna*<sup>LCS/LCS</sup> mice exhibited an increased weight. The differences between *Lmna*<sup>G609G/+</sup> mice and *Lmna*<sup>LCS/LCS</sup> mice were most apparent between the ages of 35 and 45 weeks. Moreover, *Lmna*<sup>G609G/+</sup> mice in that age range were not yet cachexic. Thus, we used mice in that age group for physiological and molecular biology studies. However, food intake was not significantly different between control and transgenic mice at any age tested (Fig 2C).

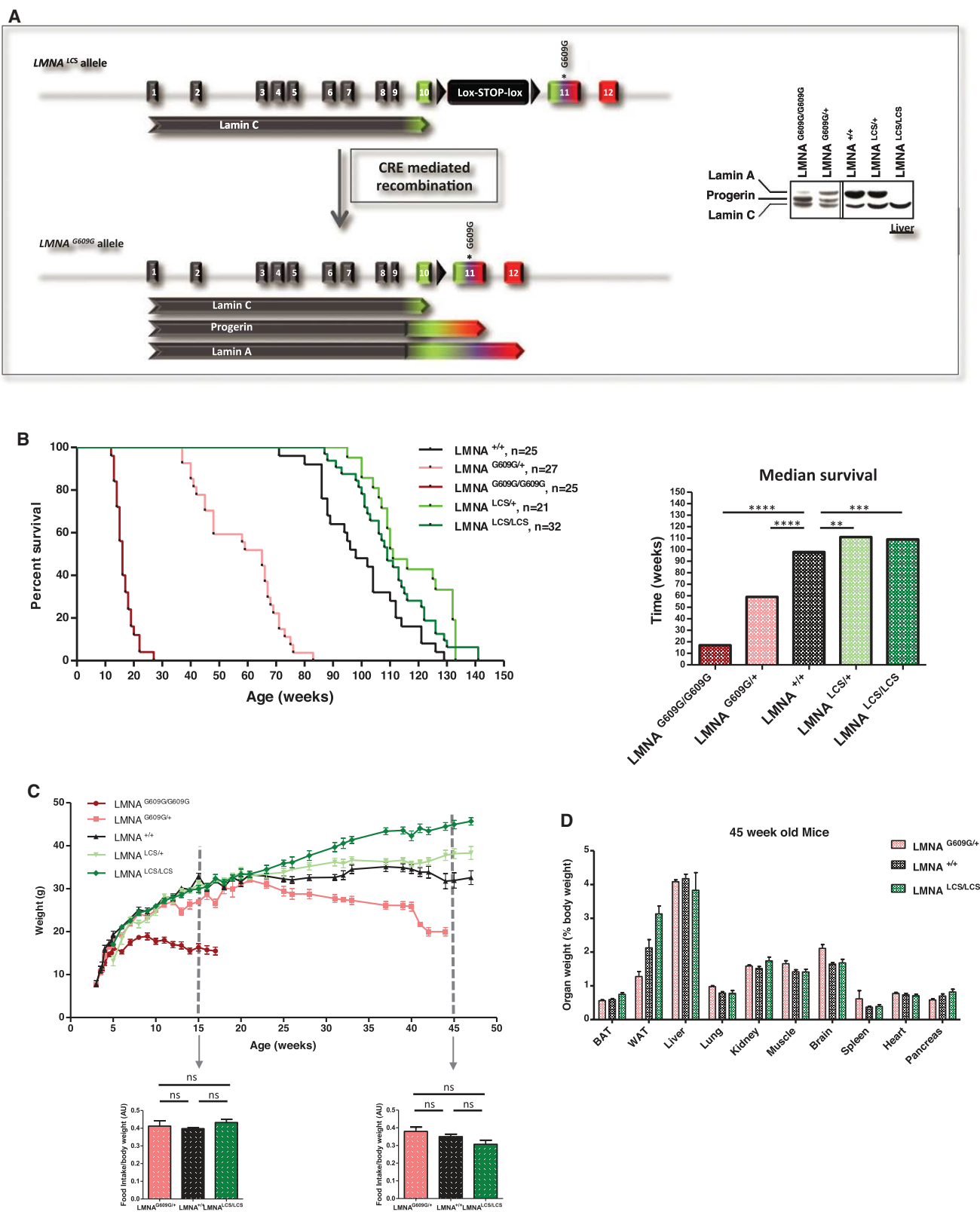
Weights of most of the tissues varied in proportion with the body weight. Exceptions were the brain, spleen, and perigonadal white adipose tissue (WAT). Brain size remained constant regardless of the size and genotype of the animals. *Lmna*<sup>LCS/LCS</sup> mice accumulated more adipose tissue, whereas *Lmna*<sup>G609G/+</sup> mice were extremely lean (Fig 2D). The adipose tissue phenotypes were interesting, as lamin C and progerin might play opposite roles in the homeostasis of this tissue, while having opposing effect on lifespan. The observation on brain weight is discussed in the legend of Supplementary Fig S1C and was not explored further.

### Adipose tissue distribution and adipocyte number in *Lmna*<sup>LCS/LCS</sup> and *Lmna*<sup>G609G/+</sup> mice

Abdominal computed tomography (CT) was performed on 40- to 45-week-old mice. Examination of the subcutaneous and intra-abdominal adipose tissue volumes indicated that all adipose tissue depots were equally affected by the expression of different *Lmna* splicing isoforms (Fig 3A). We calculated the total fat volume per animal and found that *Lmna*<sup>G609G/+</sup> mice had a twofold decrease ( $P = 0.0255$ ) in AT volume. In contrast, *Lmna*<sup>LCS/LCS</sup> mice showed a 1.5-fold increase ( $P = 0.0288$ ) in AT volume compared to the controls (Fig 3A).

Adjusting adipose tissue weight for body weight did not “correct” for the observed differences. Thus, we examined the potential reason for these discrepancies. The analysis of adipose tissue slices (Fig 3B) suggested that the differences in WAT mass were primarily due to a decrease in the average cell surface for *Lmna*<sup>G609G/+</sup> mice and an increase in the average cell surface of *Lmna*<sup>LCS/LCS</sup> mice. These results were confirmed by quantification of the surface size of adipocytes from at least five different animals per genotype (Fig 3C). Similar results were obtained with brown adipose tissue slices, where the average cell surface of brown adipocytes for *Lmna*<sup>G609G/+</sup> mice was decreased, while it was slightly increased for *Lmna*<sup>LCS/LCS</sup> mice (Fig 3B and C).

Preadipocytes from the perigonadal and subcutaneous WAT depots failed to show macroscopic differences in adipocyte differentiation. In addition, we did not observe differences in triglyceride accumulation (Supplementary Fig S2A), nor in the expression of the mature adipocyte markers aP2, Pparg, and Glut4 by RT-qPCR in differentiated preadipocytes (Supplementary Fig S2B). These results suggest that lamin C and progerin are more important for the fate of



differentiated adipocytes than for preadipocyte differentiation. Furthermore, serum lipoprotein, lipid, and cholesterol profiles did not reveal any significant difference between mice of different genotypes (Supplementary Fig S2C).

Metabolic tests indicated that fasting glycemia was low in *Lmna*<sup>G609G/+</sup>, but not significantly different in *Lmna*<sup>LCS/LCS</sup> mice compared to WT. Fasting insulin was also significantly decreased in *Lmna*<sup>G609G/+</sup> mice, while it was increased in normoglycemic



**Figure 2. *Lmna* isoforms, progerin and lamin C, affect lifespan and body weight.**

- A Left panel, structure of the targeted allele after homologous recombination. Right panel, expression levels of lamin A, progerin, and lamin C protein isoforms in the livers of *Lmna*<sup>G609G/G609G</sup>, *Lmna*<sup>G609G/+</sup>, *Lmna*<sup>+/+</sup>, *Lmna*<sup>LCS/+</sup>, and *Lmna*<sup>LCS/LCS</sup>, determined by Western blotting.
- B Left panel, survival curves of male and female *Lmna*<sup>+/+</sup> (*n* = 25), *Lmna*<sup>G609G/+</sup> (*n* = 27), *Lmna*<sup>G609G/G609G</sup> (*n* = 25), *Lmna*<sup>LCS/+</sup> (*n* = 21), and *Lmna*<sup>LCS/LCS</sup> (*n* = 32) mice. Right panel, histogram showing the median lifespan of each genotype.
- C Body weights of male *Lmna*<sup>+/+</sup> (*n* = 11), *Lmna*<sup>G609G/+</sup> (*n* = 9), *Lmna*<sup>G609G/G609G</sup> (*n* = 8), *Lmna*<sup>LCS/+</sup> (*n* = 9), and *Lmna*<sup>LCS/LCS</sup> (*n* = 12) mice. Food intake was measured for 15- and 45-week-old mice (panels below body weight curves).
- D Weights of individual organs as a percentage of total body weight for 45-week-old *Lmna*<sup>G609G/+</sup> (*n* = 15), *Lmna*<sup>LCS/LCS</sup> (*n* = 8), and *Lmna*<sup>+/+</sup> (*n* = 10) mice.
- Data information: Results were expressed as median (B) or means (C and D) ± s.e.m. The significance of differences in lifespan was determined with the log-rank (Mantel–Cox) test.

*Lmna*<sup>LCS/LCS</sup> mice (Fig 3D). *Lmna*<sup>G609G/+</sup> mice are more tolerant to glucose, as measured by an intraperitoneal glucose tolerance test (Fig 3E). Glucose tolerance of *Lmna*<sup>LCS/LCS</sup> mice is slightly decreased at this age. Moreover, *Lmna*<sup>G609G/+</sup> mice are more sensitive to insulin as measured by fasting insulin and by an insulin tolerance test (Fig 3D and F). On the other hand, *Lmna*<sup>LCS/LCS</sup> demonstrated mild insulin resistance. High levels of insulin may balance this resistance (Fig 3D). Overall, these results indicate that the *Lmna*<sup>LCS/LCS</sup> mice are moderately insulin-resistant, whereas *Lmna*<sup>G609G/+</sup> mice are more insulin-sensitive. Increased fat storage and insulin resistance are contrasting with the increased longevity of *Lmna*<sup>LCS/LCS</sup> mice, as they are expected to lead progressively to hyperglycemia. Surprisingly, 20-month-old *Lmna*<sup>LCS/LCS</sup> mice were rather hypoglycemic (Supplementary Fig S2D), showing that they are able to compensate for obesity and aging-induced insulin resistance, thus highlighting a possible function of lamin C in the maintenance of energy balance.

#### Energy expenditure and mitochondrial content in *Lmna*<sup>LCS/LCS</sup> and *Lmna*<sup>G609G/+</sup> mice

Oxygen consumption (VO<sub>2</sub>), CO<sub>2</sub> production (VCO<sub>2</sub>), respiratory exchange ratios (RER), and energy expenditure were monitored with the Oxymax System. The absolute VO<sub>2</sub> and VCO<sub>2</sub> values are comparable between different genotypes, but when normalized to body weight *Lmna*<sup>G609G/+</sup> mice showed a marked increase in VO<sub>2</sub> and VCO<sub>2</sub>, whereas *Lmna*<sup>LCS/LCS</sup> mice consumed less O<sub>2</sub> and produced less CO<sub>2</sub> (Fig 4A). *Lmna*<sup>G609G/+</sup> mice exhibited higher energy expenditure, whereas *Lmna*<sup>LCS/LCS</sup> mice exhibited lower energy expenditure. These results indicate that progerin increases the metabolic rate, whereas lamin C reduces overall energy consumption. Interestingly, similar to obese mice, *Lmna*<sup>LCS/LCS</sup> mice demonstrated lower RERs, suggesting that they mainly consume fatty acids [13]. The contribution of fat oxidation to energy expenditure calculated from Lusk equations indicated that *Lmna*<sup>LCS/LCS</sup> mice burned 80% fat, WT mice used 55% fat, whereas *Lmna*<sup>G609G/+</sup> mice consumed only 41% fat. The fact that lamin C-only mice use more fat and less carbohydrates, whereas progerin-expressing mice do the opposite, clearly indicates a prominent role for *Lmna* gene in metabolic fuel partitioning. Interestingly, the amount of mitochondrial DNA was significantly higher in *Lmna*<sup>G609G/+</sup> mice and lower in *Lmna*<sup>LCS/LCS</sup> mice compared to WT mice (Fig 4B), suggesting global mitochondrial activity. These results were confirmed by the examination of white and brown adipose tissue electron microscopic micrographs (Supplementary Fig S3).

Mouse embryonic fibroblasts (MEFs) derived from *Lmna*<sup>G609G/+</sup> and *Lmna*<sup>LCS/LCS</sup> embryos exhibited similar variations in mitochondrial DNA content as in the adipose tissues (Fig 4C). Mitochondrial function was studied with a mitochondrial stress test on an XF24 Seahorse analyzer. When compared to control MEFs, *Lmna*<sup>G609G/+</sup> MEFs showed a basal oxygen consumption rate (OCR) that was 1.5-fold higher, whereas *Lmna*<sup>LCS/LCS</sup> MEFs showed a modest but significant decrease in basal respiration (Fig 4D and E). Inhibition of ATP synthesis by oligomycin revealed a significantly higher ATP production in *Lmna*<sup>G609G/+</sup> and a decreased ATP production in *Lmna*<sup>LCS/LCS</sup> MEFs, but this difference was not significant. FCCP was used to determine the maximal OXPHOS capacity. *Lmna*<sup>G609G/+</sup> MEFs showed a 1.13-fold increase in maximal respiration and a 1.3-fold increase in mitochondrial spare capacity, whereas *Lmna*<sup>LCS/LCS</sup> showed a 1.4-fold decrease in maximal OCR and a twofold decrease in mitochondrial spare capacity. Proton leak was significantly increased in *Lmna*<sup>G609G/+</sup> MEFs and slightly decreased in *Lmna*<sup>LCS/LCS</sup> MEFs. The differences in mitochondrial basal and maximal respiration and in proton leak could mainly be due to the differences in mitochondrial number. However, the fact that *Lmna*<sup>G609G/+</sup> MEFs have increased spare capacity strongly suggests that their mitochondria were more oxidative. In contrast, the mitochondrial content of *Lmna*<sup>LCS/LCS</sup> MEFs was reduced and their mitochondria have less oxidative potential. The results obtained with MEFs are consistent with the global energy expenditure phenotypes of both *Lmna*<sup>G609G/+</sup> and *Lmna*<sup>LCS/LCS</sup> mice. The reduction in oxidative capacity of the adipose tissue is expected to lead to the obese phenotype of *Lmna*<sup>LCS/LCS</sup> mice that have less capacity to burn lipids and therefore gain more weight.

#### Gene expression analysis of adipose tissue samples from *Lmna*<sup>LCS/LCS</sup> and *Lmna*<sup>G609G/+</sup> mice

PGC1α (Ppargc1α) is a master regulator of mitochondrial biogenesis [14–16]. UCP1 (uncoupling protein 1) is a PGC1α target gene and a key thermogenic protein. Induced expression of UCP1 in WAT reduces obesity and improves insulin sensitivity [14,17]. The expression in adipose tissue of PGC1α and UCP1, both at RNA (Fig 5A) and protein (Fig 5B) levels, varied in opposite ways in mice expressing progerin versus mice expressing lamin C alone. Changes in mitochondrial gene expression might thus be responsible for the observed differences in energy consumption and expenditure. RT-qPCR analysis of PGC1α target genes (*Tfam*, *NRF1*, *SOD2*, and *NRF2*), electron transport chain (ETC) genes (*ATP synthase*, *SDHA*, *cytochrome C oxidase*, and *NADPH dehydrogenase*), and fatty oxidation genes (*mCAD* and *CPT2*) showed that expression of each gene

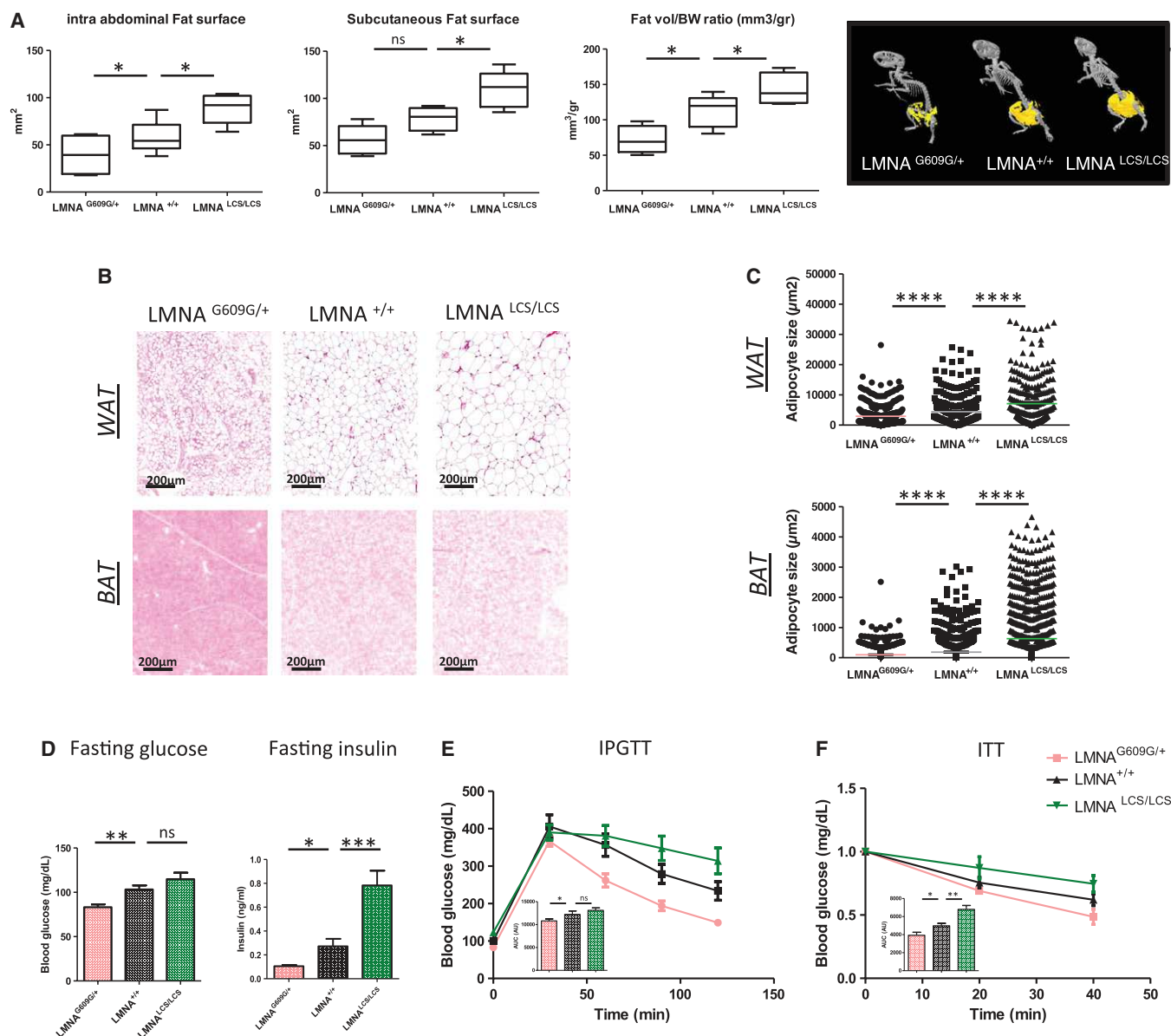


**Figure 3. Antagonistic adipose tissue alterations in *Lmna*<sup>G609G/+</sup> and *Lmna*<sup>LCS/LCS</sup> mice.**

**A** PET-CT imaging analysis showing quantification of subcutaneous fat surface, intra-abdominal fat surface, and total fat volume normalized to body weight in *Lmna*<sup>G609G/+</sup>, *Lmna*<sup>+/+</sup>, *Lmna*<sup>LCS/LCS</sup> mice ( $n = 5$  per genotype). A representative PET-CT image for each genotype is shown in the right panel.  
**B** Representative images of HE-stained sections of WAT (upper panels) and BAT (lower panels) from *Lmna*<sup>+/+</sup>, *Lmna*<sup>G609G/+</sup>, and *Lmna*<sup>LCS/LCS</sup> mice.  
**C** Quantification of adipocyte size from WAT (upper panel) and BAT (lower panel) with ImageJ software ( $n = 5$  per genotype).  
**D** Metabolic measurements (fasting glucose and insulin, intraperitoneal glucose tolerance test and insulin tolerance test) of *Lmna*<sup>+/+</sup> ( $n = 6$ ), *Lmna*<sup>G609G/+</sup> ( $n = 10$ ), and *Lmna*<sup>LCS/LCS</sup> ( $n = 7$ ) mice. Area under the curve for IPGTT and ITT was analyzed (AUC).

Data information: All experiments were conducted using 45-week-old male mice. Results were expressed as means  $\pm$  s.e.m. The significance of differences was determined with the Student's *t*-test.

[17], except for *NRF2*, varied inversely between *Lmna*<sup>LCS/LCS</sup> and *Lmna*<sup>G609G/+</sup> samples (Fig 5C), suggesting that LMNA isoforms affect mitochondrial gene expression.

In order to determine the molecular pathways altered by lamin C and progerin expression and their roles in energy metabolism and aging, we analyzed the WAT transcriptome in control mice and in *Lmna*<sup>G609G/G609G</sup> and *Lmna*<sup>LCS/LCS</sup> mice, as examples of the most

extreme aging phenotypes. We used samples from fasting 4-month-old male mice to probe Affymetrix exon arrays (results are accessible at <https://www.easana.com/>). Consistent with the essential role of lamins in nuclear architecture, WAT samples from *Lmna*<sup>G609G/G609G</sup> mice demonstrated extreme variations, with 6,509 up-regulated and 3,024 down-regulated mRNAs. Large variations were also observed at the level of alternative splicing, confirming recent observations

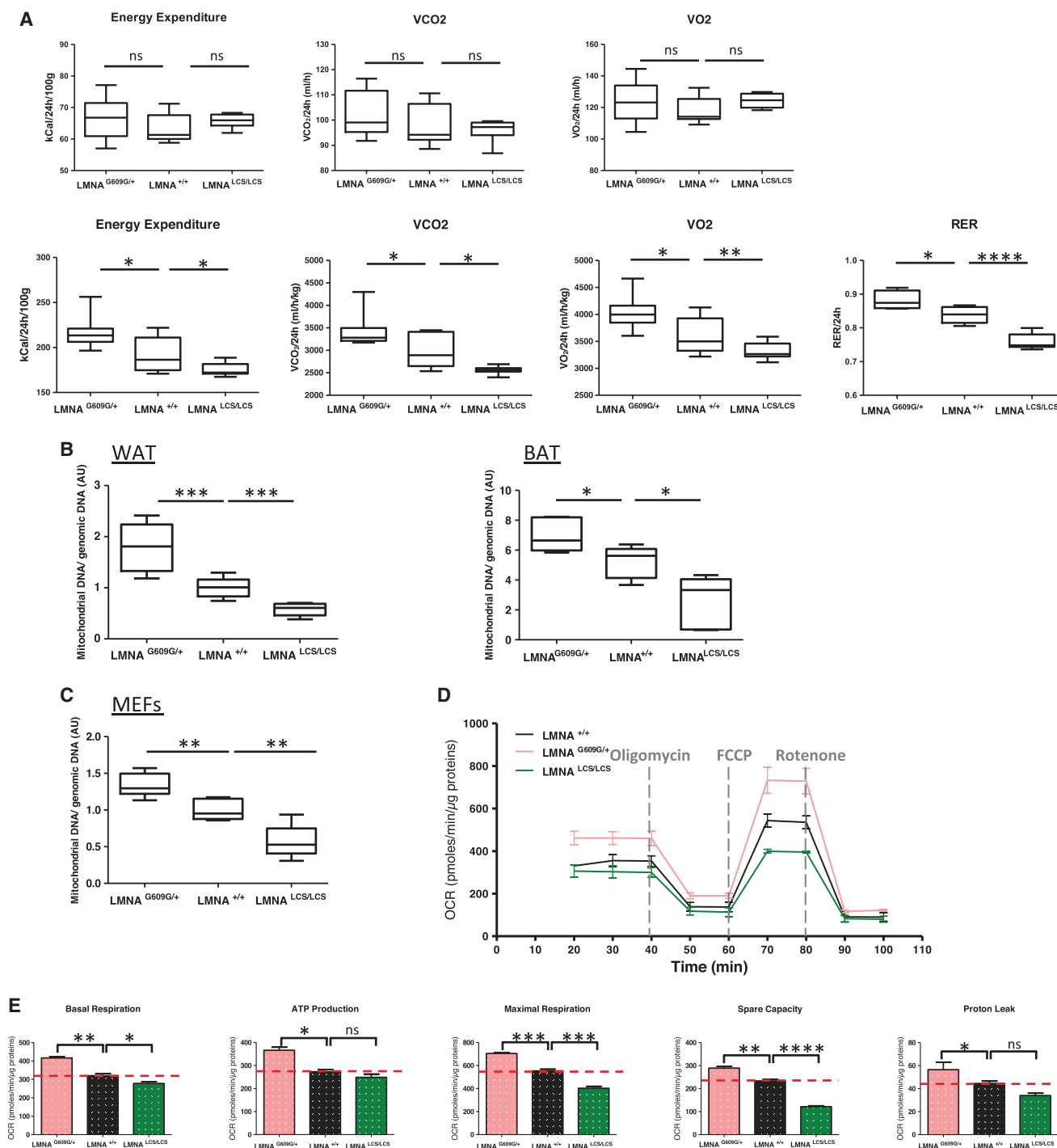


**Figure 4. LMNA isoforms modify energy expenditure and mitochondrial content in mice and in MEFs.**

**A** Upper panels correspond to absolute values of VCO<sub>2</sub>, VO<sub>2</sub>, RER, and energy expenditure. Lower panels represent the same values normalized to body weight ( $n = 5$  per genotype).

**B** Mitochondrial DNA levels in WAT and BAT were assessed by qPCR and normalized to genomic DNA ( $n = 7$  per genotype).

**C** Mitochondrial DNA levels in MEFs were assessed by qPCR and normalized to genomic DNA ( $n = 4$  clones per genotype).

**D, E** MEFs oxygen consumption rates (OCR) were determined with a Seahorse XF24 Flux analyzer in basal and stimulated conditions ( $n = 3$  clones per genotype). The areas under the curve from different sections of the experiment are shown as individual histograms (E) for basal respiration, ATP production, maximal respiration, mitochondrial spare capacity, and proton leak.

Data information: Results were expressed as means  $\pm$  s.e.m. The significance of differences was determined with the Student's *t*-test. See Supplementary Table S1 for a list of primers used for RT-qPCR.

that progerin expression triggers a senescent phenotype characterized by large changes in alternative splicing [18,19]. WAT samples from *Lmna*<sup>LCS/LCS</sup> mice showed also large variations, with 736 up-regulated and 1,563 down-regulated genes, and different alternative splicing of 2,691 exons (<https://www.easana.com/>). These observations are consistent with a recent finding showing that lamin A/C interacts with distinct spatially restricted subpromoter regions associated with distinct transcriptional outcomes in human adipose tissue stem cells [18,20].

Variations in gene expression may directly or indirectly contribute to the different phenotypes elicited by lamin C and progerin. We focused on 278 annotated genes (<https://www.easana.com/>), for which inverse expression patterns existed between the two phenotypes. Interestingly, KEGG pathway analysis of those genes showed that two of the three most regulated pathways are involved in energy metabolism (arachidonic acid metabolism and glycerolipid metabolism, Fig 5D). These data also confirmed that PGC1 $\alpha$  was one of the inversely regulated genes, further validating our approach (Fig 5E). In addition to PGC1 $\alpha$ , 29 genes involved in lipid metabolism were identified with expression controlled in an inverse way by lamin C and progerin. These 30 genes could be involved in the process of aging (Fig 5E).

We used dedicated qPCR arrays (Adipogenesis and Fatty acid metabolism RT<sup>2</sup> Profiler<sup>TM</sup> PCR Arrays) designed to study 84 genes per pathway to further confirm these results (Supplementary Fig S4A and B). Only six genes showed inverse expression on both arrays (*Ppargc1a*, *Lep*, *Sfrp5*, *Acot3*, *Acsn3*, and *Bdh2*). Four (*Ppargc1a*, *Lep*, *Sfrp5*, and *Acsn3*) were already on the list of 30 genes obtained from the Affymetrix analysis. Thus, these four genes were considered candidate genes accounting for the phenotypes associated with the lamin isoforms. Interestingly, 29 of 84 genes involved in the regulation of fatty acid metabolism were up-regulated in the adipose tissue from progeria mice. In contrast, all of the genes that we examined in this pathway (8 out of 84) were down-regulated in the adipose tissue from lamin C-only mice, further confirming that these two lamin isoforms have antagonistic functions in the regulation of fatty acid metabolism (Supplementary Fig S4B).

One of the four candidate genes, *Sfrp5* suppresses oxidative metabolism, is strongly induced during adipocyte differentiation, and is up-regulated in adipocytes during obesity and likely counteracts WNT signaling [21]. Moreover, *SFRP5*-deficient mice are phenotypically similar to *Lmna*<sup>G609G/+</sup> mice (same numbers of adipocytes but fewer large adipocytes and increased mitochondrial activity, partially mediated by PGC1 $\alpha$ ). However, changes in leptin expression cannot explain the metabolic phenotypes, since increased

expression of leptin in *Lmna*<sup>LCS/LCS</sup> mice would result in reduced food intake and increased energy expenditure. While increased adipose tissue mass is always correlated with leptin expression, *Lmna*<sup>LCS/LCS</sup> mice display only slight decrease in food intake that is not statistically significant, suggesting that the increase in the expression of *leptin* mRNA is not sufficient to increase circulating leptin levels. Alternatively, *Lmna*<sup>LCS/LCS</sup> mice are leptin resistant.

## Concluding remarks

Our results support the notion that RNA processing of the *Lmna* gene is an active conserved mechanism that contributes to metabolic adaptations of adipose tissue in mammals. While some of the phenotypes of *Lmna*<sup>LCS/LCS</sup> mice are contrasting with their increased longevity, both in MEFs and mice, lamin C-only expression results in low mitochondrial activity, whereas progerin expression strongly increases organelle activity. Strikingly, these distinct effects on mitochondrial activity correlate with opposing effects of these lamins on lifespan. Although these could be independent phenotypes, recent studies have linked mitochondrial function to lifespan [22]. The finding that old *Lmna*<sup>LCS/LCS</sup> mice are able to compensate for deleterious effects triggered by obesity suggests that lamin C protects against increased oxidative stress associated with fat accumulation [23]. In contrast, progerin increases energy expenditure and mitochondrial activity, which probably induces potent oxidative stress, characteristic of senescence [24–26] and one of the central hallmarks of the normal aging process [26]. The lamin isoforms by changing the nuclear envelope architecture may also contribute to changes in the expression of genes involved in mitonuclear imbalance controlling longevity.

## Materials and Methods

### Database searches and sequence analysis

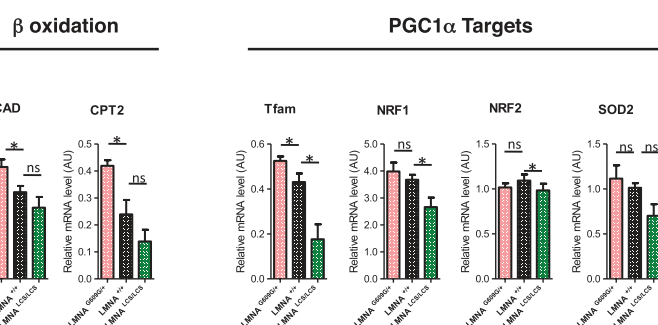
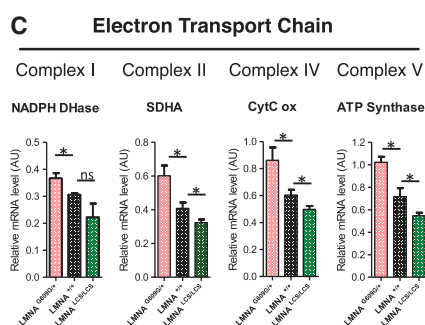
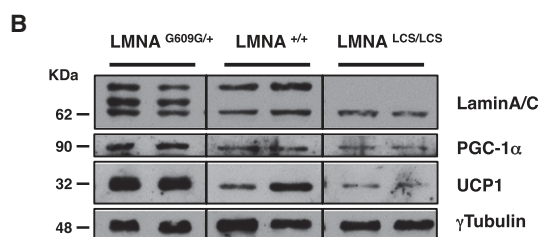
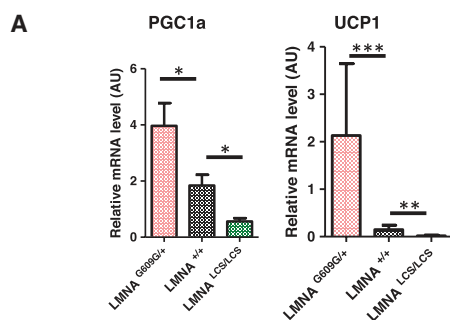
Lamin A/C gene sequences were retrieved from Ensembl (<http://www.ensembl.org/>) and aligned with MAFFT in the Geneious package (v 6.1.5 created by Biomatters, available from <http://www.geneious.com/>).

The occurrence of lamin A/C ESTs in databases was determined with BLAST (<http://blast.ncbi.nlm.nih.gov>) using protein and nucleic acid queries specific for either of the lamin isoforms (exon 11 for lamin A, intron 10 for lamin C) or for a sequence common to both isoforms (other exons). A more detailed description of sequence analysis can be found in Supplementary Methods.

### Figure 5. Gene expression profiling of WAT adipose tissue from *Lmna* mutant mice.

- A Relative mRNA levels of *PGC1 $\alpha$*  and *UCP1* in WAT were determined by RT-qPCR.
- B Protein levels of *PGC1 $\alpha$*  and *UCP1* in WAT were determined by Western blotting. Lamin A/C levels and  $\gamma$ -tubulin levels were used as controls.
- C Relative mRNA levels of mitochondrial markers in WAT were assessed by RT-qPCR.
- D Table representing KEGG pathways significantly and antagonistically regulated by progerin and lamin C derived from exon array analysis of WAT from 18-week-old *Lmna*<sup>G609G/G609G</sup> and *Lmna*<sup>LCS/LCS</sup> mice ( $n = 5$  per genotype).
- E Metabolic genes that are oppositely regulated in WAT from 18-week-old *Lmna*<sup>G609G/G609G</sup> and *Lmna*<sup>LCS/LCS</sup> mice versus *Lmna*<sup>+/+</sup> mice ( $n = 5$  per genotype). Up-regulated genes are in red boxes, and down-regulated genes are in green boxes.

Data information: RT-qPCR and WB were performed with 45-week-old *Lmna*<sup>+/+</sup>, *Lmna*<sup>G609G/+</sup>, and *Lmna*<sup>LCS/LCS</sup> mice samples ( $n = 5$  per genotype). Results were expressed as means  $\pm$  s.e.m. The significance of differences was determined with the Student's *t*-test. See Supplementary Table S1 for a list of primers used for RT-qPCR.

**D**

Significant Pathways (10)					
KEGG Pathway ID	Pathway Description (KEGG)	Nb Genes in Pathway	Nb Genes regulated in Pathway	P-Value	% of regulated genes
mmu04610	Complement and coagulation cascades	75	7	6.08.10 <sup>-4</sup>	9.33
mmu00590	Arachidonic acid metabolism	83	6	6.08.10 <sup>-3</sup>	7.23
mmu04270	Vascular smooth muscle contraction	120	7	6.66.10 <sup>-3</sup>	5.83
mmu05414	Dilated cardiomyopathy	92	6	9.34.10 <sup>-3</sup>	6.52
mmu00561	Glycerolipid metabolism	47	4	2.81.10 <sup>-2</sup>	8.51
mmu04512	ECM-receptor interaction	83	5	2.92.10 <sup>-2</sup>	6.02
mmu05410	Hypertrophic cardiomyopathy (HCM)	84	5	3.03.10 <sup>-2</sup>	5.95
mmu05416	Viral myocarditis	94	5	4.31.10 <sup>-2</sup>	5.32
mmu00564	Glycerophospholipid metabolism	67	4	6.82.10 <sup>-2</sup>	5.97
mmu05412	Arrhythmogenic right ventricular cardiomyopathy (ARVC)	75	4	8.88.10 <sup>-2</sup>	5.33

**E**

Protein	G609G/G609G vs +/-		LCS/LCS vs +/-		Function
	Fold change	P-value	Fold change	P-value	
Lep	33.09	9.90E-08	2.11	3.87E-05	Leptin plays a key role in regulating energy intake and energy expenditure, including appetite/hunger and metabolism
Cyp4f18	1.68	1.58E-03	2.22	9.36E-04	Belongs to Cyp4 family of enzymes that catalyze the oxidation of fatty acid
Sod3	3.61	1.19E-04	1.84	8.54E-03	This gene encodes a member of the superoxide dismutase (SOD) protein family that play a key antioxidant role
Gcmt4	5.58	1.58E-05	1.74	6.63E-04	Belongs to the family of acyltransferases that participates to aminosugar metabolism
Mrps6	2	1.39E-02	1.75	6.20E-03	Mammalian mitochondrial ribosomal proteins are encoded by nuclear genes and help in protein synthesis within the mitochondrion
Sfrp5	14.79	3.25E-04	2.83	6.97E-04	Sfrp5 is an anti-inflammatory adipokine that modulates metabolic dysfunction in obesity
Dgat2	6.5	1.90E-05	1.63	2.38E-04	This gene encodes one of two enzymes that catalyzes the final reaction of triglycerides synthesis
Slc1a1	5.52	1.09E-06	1.8	1.00E-04	Plays an essential role in transporting glutamate (a key compound in cellular metabolism) across plasma membranes
Lpgat1	5.28	1.74E-05	1.65	7.42E-03	catalyzes the recylation of LPG to phosphatidylglycerol, a phospholipid that is an important precursor for the synthesis of cardiolipin
Pnpla3	3.38	1.96E-05	1.95	2.25E-05	Also known as Adiponutrin, a lipase that mediates triacylglycerol hydrolysis in adipocytes and may be involved in the balance of energy usage/storage in adipocytes
Paqr9	3.24	1.58E-03	1.6	2.73E-02	Receptor of adiponectin, which is an adipokine that modulates glucose metabolism and fatty acid oxidation
Hgfac	3.05	4.59E-04	1.87	9.99E-05	Acts as a serine protease that converts hepatocyte growth factor from his precursor to his active form
Pla2g5	2.93	1.40E-03	2.61	6.16E-05	Catalyzes the hydrolysis of membrane phospholipids to generate lysophospholipids and free fatty acids including arachidonic acid
Dhcr24	2.87	1.64E-05	1.71	1.18E-04	Encodes a (FAD)-dependent oxidoreductase which catalyzes the reduction of the delta-24 double bond of sterol intermediates during cholesterol biosynthesis
Lipf	2.84	8.43E-04	2	2.20E-03	Gastric lipase involved in the digestion of triglycerides in the gastrointestinal tract, responsible for 30% of fat digestion processes occurring in human
Sfrp4	2.67	8.84E-04	1.73	6.11E-05	Secreted Frizzled-Related Protein 4 reduces insulin secretion and is overexpressed in Type 2 Diabetes
Slc7a5	2.58	4.09E-07	1.62	1.01E-04	Involved in cellular amino-acid uptake
Igfals	2.43	3.57E-02	1.68	4.46E-03	Crucial role in determining the endocrine effect of IGF on target tissues
Dhrs3	2.2	1.39E-04	1.65	1.04E-04	p53-Inducible DHR3 is an endoplasmic reticulum protein associated with lipid droplet accumulation
Alox15	1.67	2.04E-04	1.95	1.62E-03	Lipoxygenases (LOXs) are a family of non-heme iron dioxygenases that participates in arachidonic acid metabolism and linoleic acid metabolism
Gpd1	1.95	4.36E-05	1.66	3.78E-05	The encoded protein plays a critical role in carbohydrate and lipid metabolism
Akr1b7	2.08	6.27E-05	10.79	2.20E-03	Induced in response to oxidative stress
Pgam2	3.98	1.95E-04	3.94	6.40E-04	Phosphoglycerate mutase (PGAM) catalyzes the reversible reaction of 3-phosphoglycerate (3-PGA) to 2-phosphoglycerate
Scd3	5.25	1.79E-05	2.72	8.63E-04	Stearoyl-coenzyme A (CoA) desaturase (SCD) is a key enzyme involved in the conversion of saturated fatty acids into monounsaturated fatty acids
Ptgs2	3.86	6.30E-07	2.77	1.20E-02	Prostaglandin endoperoxide H synthase, COX 2, converts arachidonic acid (AA) to prostaglandin endoperoxide H2
Cyp4a12b	1.67	1.01E-02	4.93	4.99E-04	Belongs to Cyp4 family of enzymes that catalyze the oxidation of fatty acid
AcsM3	1.94	7.63E-05	1.61	4.84E-04	Has medium-chain fatty acid-CoA ligase activity. The protein is activated by the deacetylation of lysine residues of the active site by Sirt3.
Slc38a4	1.74	1.86E-03	2.4	1.04E-04	Sodium-dependent amino acid transporter. Mediates electrogenic symport of neutral amino acids and sodium ions
Fabp3	1.52	1.21E-02	2.31	1.04E-02	H-FABP (FABP3) is involved in active fatty acid metabolism where it transports fatty acids from the cell membrane to mitochondria for oxidation
Ppargc1a	2.07	6.30E-05	1.58	8.78E-03	Transcription coactivator that plays a central role in the regulation of cellular energy metabolism



## Animal experiments & ethics statement

Transgenic mice (LMNA<sup>G609G/+</sup> and LMNA<sup>LCS/LCS</sup>) were generated as previously described [10]. A more detailed description of the breeding strategy, tumor evaluation, micro-computed tomography, metabolic evaluation, and Oxymax analysis can be found in Supplementary Methods.

All animal procedures were conducted in strict adherence with the European Community Council Directive of November 24, 1986 (86-609/EEC). Mice were maintained in pathogen-free conditions in our animal facility (E34-172-16). All experiments were conducted by authorized personnel (agreements JT 34-236; MDT 34-433; IL-M 34-467; KC 34-028; CC has legal training) and approved by the Institutional Review Board at the Animal Facility of the Institut de Génétique Moléculaire de Montpellier (agreement no CEEA-LR-12112).

Food intake was measured three times over a period of 72 h with seven animals per genotype in individual cages.

## Microarray data analysis

All the data are deposited in GEO (NCBI) under accession number GSE51204. Affymetrix Mouse Exon 1.0 ST arrays were hybridized by GenoSplice technology (www.genosplice.com) according to their standard protocol. A detailed description of the procedure can be found in Supplementary Methods.

## Statistical analysis

The survival curves were completed using the Kaplan–Meier curve. The median survival is representative of the survival curves. We use the log-rank (Mantel–Cox) test to perform the statistical analyses of the survival curves.

All the other results were expressed as means  $\pm$  standard error of the means (s.e.m.). The significance of differences was determined with the Student's *t*-test, with significance defined as  $P < 0.05$  (\* $P < 0.05$ , \*\* $P < 0.005$ , \*\*\* $P < 0.0005$ , \*\*\*\* $P < 0.00005$ ).

**Supplementary information** for this article is available online: <http://embor.embopress.org>

## Acknowledgements

This work was supported by grants from Fondation pour la Recherche Médicale and Splicos Therapeutics. JT is senior member of the Institut Universitaire de France. We are grateful to N. Levy and C. Lopez-Otin for providing *Lmna*<sup>LCS/+</sup> mice and the Montpellier-RIO imaging platform (Montpellier, France), to the Histology Experimental Network of Montpellier, to the "Centre de Ressources en Imagerie Cellulaire de Montpellier" (France), and to the IGMM animal facilities. The authors are grateful to C. Cazevielle and C. Sanchez for their technical assistance and P. de la Grange from Genosplice. I.L.-M. was supported by a graduate fellowship from the Ministère Délégué à la Recherche et aux Technologies and CNRS. C. L.-H is supported by ITN RNPnet Grant.

## Author contributions

ICLM and MDT performed most of the experiments and contributed to writing the manuscript. CC performed the metabolic data and contributed to writing the paper. LL performed the qPCR experiments. EZA, GB, and FC

contributed to CT scan and metabolic cages experiments. PC contributed to histological data. PF and KC have made the sequence alignment. LF provided critical metabolic discussions. JT designed the study and wrote the manuscript.

## Conflict of interests

The authors declare that they have no conflict of interest.

## References

1. Bishop NA, Guarente L (2007) Genetic links between diet and lifespan: shared mechanisms from yeast to humans *Nat Rev Genet* 8: 835–844
2. Kenyon C (2005) The plasticity of aging: insights from long-lived mutants *Cell* 120: 449–460
3. Houtkooper RH, Williams RW, Auwerx J (2010) Metabolic networks of longevity *Cell* 142: 9–14
4. Hennekam RCM (2006) Hutchinson–Gilford progeria syndrome: review of the phenotype *Am J Med Genet A* 140: 2603–2624
5. De Sandre-Giovannoli A, Bernard R, Cau P, Navarro C, Amiel J, Boccaccio I, Lyonnet S, Stewart CL, Munnich A, Le Merrer M et al (2003) Lamin A truncation in Hutchinson–Gilford progeria *Science* 300: 2055
6. Eriksson M, Brown WT, Gordon LB, Glynn MW, Singer J, Scott L, Erdos MR, Robbins CM, Moses TY, Berglund P et al (2003) Recurrent *de novo* point mutations in lamin A cause Hutchinson–Gilford progeria syndrome *Nature* 423: 293–298
7. Lopez-Mejia IC, Vautrot V, De Toledo M, Behm-Ansmant I, Bourgeois CF, Navarro CL, Osorio FG, Freije JMP, Stévenin J, De Sandre-Giovannoli A et al (2011) A conserved splicing mechanism of the LMNA gene controls premature aging *Hum Mol Genet* 20: 4540–4555
8. Berge MO, Gavino B, Ross J, Schmidt WK, Hong C, Kendall LV, Mohr A, Meta M, Genant H, Jiang Y et al (2002) Zmpste24 deficiency in mice causes spontaneous bone fractures, muscle weakness, and a prelamin A processing defect *Proc Natl Acad Sci USA* 99: 13049–13054
9. Fong LG, Ng JK, Lammerding J, Vickers TA, Meta M, Coté N, Gavino B, Qiao X, Chang SY, Young SR et al (2006) Prelamin A and lamin A appear to be dispensable in the nuclear lamina *J Clin Invest* 116: 743–752
10. Osorio FG, Navarro CL, Cadiñanos J, Lopez-Mejia IC, Quirós PM, Bartoli C, Rivera J, Tazi J, Guzmán G, Varela I et al (2011) Splicing-directed therapy in a new mouse model of human accelerated aging *Sci Transl Med* 3: 106ra107
11. Peter A, Reimer S (2012) Evolution of the lamin protein family: what introns can tell *Nucleus* 3: 44–59
12. Pendás AM, Zhou Z, Cadiñanos J, Freije JMP, Wang J, Hultenby K, Astudillo A, Wernerson A, Rodríguez F, Tryggvason K et al (2002) Defective prelamin A processing and muscular and adipocyte alterations in Zmpste24 metalloproteinase-deficient mice *Nat Genet* 31: 94–99
13. Martin TL, Alquier T, Asakura K, Furukawa N, Preitner F, Kahn BB (2006) Diet-induced obesity alters AMP kinase activity in hypothalamus and skeletal muscle *J Biol Chem* 281: 18933–18941
14. Fislis JS, Warden CH (2006) Uncoupling proteins, dietary fat and the metabolic syndrome *Nutr Metab (Lond)* 3: 38
15. Handschin C, Spiegelman BM (2006) Peroxisome proliferator-activated receptor gamma coactivator 1 coactivators, energy homeostasis, and metabolism *Endocr Rev* 27: 728–735
16. Finck BN, Kelly DP (2006) PGC-1 coactivators: inducible regulators of energy metabolism in health and disease *J Clin Invest* 116: 615–622

17. Austin S, St-Pierre J (2012) PGC1 $\alpha$  and mitochondrial metabolism—emerging concepts and relevance in ageing and neurodegenerative disorders *J Cell Sci* 125: 4963–4971
18. Lund E, Oldenburg A, Delbarre E, Freberg C, Duband-Goulet I, Eskeland R, Buendia B, Collas P (2013) Lamin A/C-promoter interactions specify chromatin state-dependent transcription outcomes *Genome Res* 23: 1580–1589
19. Cao K, Blair CD, Faddah DA, Kieckhafer JE, Olive M, Erdos MR, Nabel EG, Collins FS (2011) Progerin and telomere dysfunction collaborate to trigger cellular senescence in normal human fibroblasts *J Clin Invest* 121: 2833–2844
20. Miranda M, Chacón MR, Gutiérrez C, Vilarrasa N, Gómez JM, Caubet E, Megía A, Vendrell J (2008) LMNA mRNA expression is altered in human obesity and type 2 diabetes *Obesity* 16: 1742–1748
21. Mori H, Prestwich TC, Reid MA, Longo KA, Gerin I, Cawthorn WP, Susulic VS, Krishnan V, Greenfield A, Macdougald OA (2012) Secreted frizzled-related protein 5 suppresses adipocyte mitochondrial metabolism through WNT inhibition *J Clin Invest* 122: 2405–2416
22. Houtkooper RH, Mouchiroud L, Ryu D, Moullan N, Katsyuba E, Knott G, Williams RW, Auwerx J (2013) Mitonuclear protein imbalance as a conserved longevity mechanism *Nature* 497: 451–457
23. Bondia-Pons I, Ryan L, Martinez JA (2012) Oxidative stress and inflammation interactions in human obesity *J Physiol Biochem* 68: 701–711
24. Fischer F, Hamann A, Osiewacz HD (2012) Mitochondrial quality control: an integrated network of pathways *Trends Biochem Sci* 37: 284–292
25. Bratic A, Larsson N-G (2013) The role of mitochondria in aging *J Clin Invest* 123: 951–957
26. Lopez-Otin C, Blasco MA, Partridge L, Serrano M, Kroemer G (2013) The hallmarks of aging *Cell* 153: 1194–1217



## REFERENCES

---

- Abizaid, A., Gao, Q., Horvath, T.L., 2006. Thoughts for Food: Brain Mechanisms and Peripheral Energy Balance. *Neuron* 51, 691–702. doi:10.1016/j.neuron.2006.08.025
- Aguirre, E., Cadenas, S., 2010. GDP and carboxyatractylate inhibit 4-hydroxynonenal-activated proton conductance to differing degrees in mitochondria from skeletal muscle and heart. *Biochim. Biophys. Acta - Bioenerg.* 1797, 1716–1726. doi:10.1016/j.bbabo.2010.06.009
- Ahima, R.S., Antwi, D. a., 2008. Brain Regulation of Appetite and Satiety. *Endocrinol. Metab. Clin. North Am.* 37, 811–823. doi:10.1016/j.ecl.2008.08.005
- Almind, K., Manieri, M., Sivitz, W.I., Cinti, S., Kahn, C.R., 2007. Ectopic brown adipose tissue in muscle provides a mechanism for differences in risk of metabolic syndrome in mice. *Proc Natl Acad Sci U S A* 104, 2366–2371. doi:0610416104 [pii]10.1073/pnas.0610416104
- Ameisen, J.C., 2002. On the origin, evolution, and nature of programmed cell death: a timeline of four billion years. *Cell Death Differ.* 9, 367–393. doi:10.1038/sj.cdd.4400950
- Ameur, A., Stewart, J.B., Freyer, C., Hagström, E., Ingman, M., Larsson, N.-G., Gyllenstein, U., 2011. Ultra-Deep Sequencing of Mouse Mitochondrial DNA: Mutational Patterns and Their Origins. *PLoS Genet.* 7, e1002028. doi:10.1371/journal.pgen.1002028
- Anczuków, O., Rosenberg, A.Z., Akerman, M., Das, S., Zhan, L., Karni, R., Muthuswamy, S.K., Krainer, A.R., 2012. The splicing factor SRSF1 regulates apoptosis and proliferation to promote mammary epithelial cell transformation. *Nat. Struct. Mol. Biol.* 19, 220–228. doi:10.1038/nsmb.2207
- Andrade, J.M.O., Frade, A.C.M., Guimarães, J.B., Freitas, K.M., Lopes, M.T.P., Guimarães, A.L.S., de Paula, A.M.B., Coimbra, C.C., Santos, S.H.S., 2014. Resveratrol increases brown adipose tissue thermogenesis markers by increasing SIRT1 and energy expenditure and decreasing fat accumulation in adipose tissue of mice fed a standard diet. *Eur. J. Nutr.* 1–8. doi:10.1007/s00394-014-0655-6
- Arai, Y., Takayama, M., Abe, Y., Hirose, N., 2011. Adipokines and aging. *J. Atheroscler. Thromb.* 18, 545–550. doi:10.5551/jat.7039
- Ardilouze, J.L., Fielding, B. a., Currie, J.M., Frayn, K.N., Karpe, F., 2004. Nitric Oxide and ??-Adrenergic Stimulation Are Major Regulators of Preprandial and Postprandial Subcutaneous Adipose Tissue Blood Flow in Humans. *Circulation* 109, 47–52. doi:10.1161/01.CIR.0000105681.70455.73
- Arner, P., Kulyté, A., 2015. MicroRNA regulatory networks in human adipose tissue and obesity. *Nat. Rev. Endocrinol.* 11, 276–288. doi:10.1038/nrendo.2015.25
- Austin, S., St-Pierre, J., 2012. PGC1 and mitochondrial metabolism - emerging concepts and relevance in ageing and neurodegenerative disorders. *J. Cell Sci.* 125, 4963–4971. doi:10.1242/jcs.113662

- Azevedo, R. De, Luvizotto, M., Conde, S.J., Oliveira, M. De, Sibio, M.T. De, Jr, K.N., Nogueira, C.R., 2012. Obesity and Weight Loss : The Influence of Thyroid Hormone on Adipokines.
- Azzu, V., Affourtit, C., Breen, E.P., Parker, N., Brand, M.D., 2008. Dynamic regulation of uncoupling protein 2 content in INS-1E insulinoma cells. *Biochim. Biophys. Acta - Bioenerg.* 1777, 1378–1383. doi:10.1016/j.bbabbio.2008.07.001
- Baboota, R.K., Sarma, S.M., Boparai, R.K., Kondepudi, K.K., Mantri, S., Bishnoi, M., 2015. Microarray Based Gene Expression Analysis of Murine Brown and Subcutaneous Adipose Tissue: Significance with Human. *PLoS One* 10, e0127701. doi:10.1371/journal.pone.0127701
- Badoud, F., Lam, K.P., Perreault, M., Zulyniak, M. a., Britz-McKibbin, P., Mutch, D.M., 2015. Metabolomics Reveals Metabolically Healthy and Unhealthy Obese Individuals Differ in their Response to a Caloric Challenge. *PLoS One* 10, e0134613. doi:10.1371/journal.pone.0134613
- Bakkour, N., Lin, Y.L., Maire, S., Ayadi, L., Mahuteau-Betzer, F., Chi, H.N., Mettling, C., Portales, P., Grierson, D., Chabot, B., Jeanteur, P., Branlant, C., Corbeau, P., Tazi, J., 2007. Small-molecule inhibition of HIV pre-mRNA splicing as a novel antiretroviral therapy to overcome drug resistance. *PLoS Pathog.* 3, 1530–1539. doi:10.1371/journal.ppat.0030159
- Baluka, F., 2009. Cell-cell channels, viruses, and evolution: Via infection, parasitism, and symbiosis toward higher levels of biological complexity. *Ann. N. Y. Acad. Sci.* 1178, 106–119. doi:10.1111/j.1749-6632.2009.04995.x
- Bartelt, A., Heeren, J., 2014. Adipose tissue browning and metabolic health. *Nat. Rev. Endocrinol.* 10, 24–36. doi:10.1038/nrendo.2013.204
- Baur, J. a, Pearson, K.J., Price, N.L., Jamieson, H. a, Lerin, C., Kalra, A., Prabhu, V. V, Allard, J.S., Lopez-Lluch, G., Lewis, K., Pistell, P.J., Poosala, S., Becker, K.G., Boss, O., Gwinn, D., Wang, M., Ramaswamy, S., Fishbein, K.W., Spencer, R.G., Lakatta, E.G., Le Couteur, D., Shaw, R.J., Navas, P., Puigserver, P., Ingram, D.K., de Cabo, R., Sinclair, D. a, 2006. Resveratrol improves health and survival of mice on a high-calorie diet. *Nature* 444, 337–342. doi:10.1038/nature05354
- Begrache, K., Massart, J., Robin, M., Borgne-sanchez, A., Fromenty, B., 2011. Review Drug-induced toxicity on mitochondria and lipid metabolism : Mechanistic diversity and deleterious consequences for the liver. *J. Hepatol.* 54, 773–794. doi:10.1016/j.jhep.2010.11.006
- Bertrand, C., Valet, P., Castan-Laurell, I., 2015. Apelin and energy metabolism. *Front. Physiol.* 6, 115. doi:10.3389/fphys.2015.00115
- Bibb, M.J., Van Etten, R.A., Wright, C.T., Walberg, M.W., Clayton, D.A., 1981. Sequence and gene organization of mouse mitochondrial DNA. *Cell* 26, 167–180. doi:10.1016/0092-8674(81)90300-7
- Blackstone, N.W., 2013. Evolution and cell physiology. 2. The evolution of cell signaling: from mitochondria to Metazoa. *Am. J. Physiol. Cell Physiol.* 305, C909–

15. doi:10.1152/ajpcell.00216.2013
- Blanc, J., Alves-Guerra, M.C., Esposito, B., Rousset, S., Gourdy, P., Ricquier, D., Tedgui, a., Miroux, B., Mallat, Z., 2003. Protective role of uncoupling protein 2 in atherosclerosis. *Circulation* 107, 388–390. doi:10.1161/01.CIR.0000051722.66074.60
- Bland, M.L., Birnbaum, M.J., 2011. Cell biology. ADaPting to energetic stress. *Science* 332, 1387–1388. doi:10.1126/science.1208444
- Blencowe, B.J., 2006. Alternative Splicing: New Insights from Global Analyses. *Cell* 126, 37–47. doi:10.1016/j.cell.2006.06.023
- Bogenhagen, D., Lowell, C., Clayton, D. a, 1981. Mechanism of mitochondrial DNA replication in mouse L-cells. Replication of unicircular dimer molecules. *J. Mol. Biol.* 148, 77–93.
- Bonnal, S., Vigevani, L., Valcárcel, J., 2012. The spliceosome as a target of novel antitumour drugs. *Nat. Rev. Drug Discov.* 11, 847–59. doi:10.1038/nrd3823
- Borisov, V.B., 2002. Defects in mitochondrial respiratory complexes III and IV, and human pathologies. *Mol. Aspects Med.* 23, 385–412. doi:10.1016/S0098-2997(02)00013-4
- Boss, O., Samec, S., Paoloni-Giacobino, A., Rossier, C., Dulloo, A., Seydoux, J., Muzzin, P., Giacobino, J.P., 1997. Uncoupling protein-3: A new member of the mitochondrial carrier family with tissue-specific expression. *FEBS Lett.* 408, 39–42. doi:10.1016/S0014-5793(97)00384-0
- Bouchard, C. et al., 1990. The response to long-term overfeeding in identical twins.
- Bournat, J.C., Brown, C.W., 2010. Mitochondrial dysfunction in obesity. *Curr. Opin. Endocrinol. Diabetes. Obes.* 17, 446–52. doi:10.1097/MED.0b013e32833c3026
- Bourne, H., 1993. © 19 9 3 Nature Publishing Group. *Nature* 363.
- Brand, M.D., 2000. Uncoupling to survive? The role of mitochondrial inefficiency in ageing. *Exp. Gerontol.* 35, 811–820. doi:10.1016/S0531-5565(00)00135-2
- Butsch, W.S., 2015. Obesity medications. *Curr. Opin. Endocrinol. Diabetes Obes.* 22, 360–366. doi:10.1097/MED.0000000000000192
- Cadenas, S., Buckingham, J. a., Samec, S., Seydoux, J., Din, N., Dulloo, A.G., Brand, M.D., 1999. UCP2 and UCP3 rise in starved rat skeletal muscle but mitochondrial proton conductance is unchanged. *FEBS Lett.* 462, 257–260. doi:10.1016/S0014-5793(99)01540-9
- Cadenas, S., Echtay, K.S., Harper, J. a., Jekabsons, M.B., Buckingham, J. a., Grau, E., Abuin, A., Chapman, H., Clapham, J.C., Brand, M.D., 2002. The basal proton conductance of skeletal muscle mitochondria from transgenic mice overexpressing or lacking uncoupling protein-3. *J. Biol. Chem.* 277, 2773–2778. doi:10.1074/jbc.M109736200
- Cambier, L., Rassam, P., Chabi, B., Mezghenna, K., Gross, R., Eveno, E., Auffray, C.,

- Wrutniak-Cabello, C., Lajoix, A.-D., Pomiès, P., 2012. M19 modulates skeletal muscle differentiation and insulin secretion in pancreatic  $\beta$ -cells through modulation of respiratory chain activity. *PLoS One* 7, e31815. doi:10.1371/journal.pone.0031815
- Campos, N., Renier, M., Aude, G., Audrey, V., Laure, L., Erika, N., Florence, M.-B., Romain, N., Pauline, F., Katjana, T., Eugénia, B., Martial, S., Julian, V.P., Bernard, P., Edouard, B., Wainberg, A.M., Roberto, S.F., Didier, S., Jamal, T., 2015. Retrovirology Long lasting control of viral rebound with a new drug ABX464 targeting Rev – mediated viral RNA biogenesis. doi:10.1186/s12977-015-0159-3
- Canals, I., Carmona, M.C., Amigó, M., Barbera, A., Bortolozzi, A., Artigas, F., Gomis, R., 2009. A functional leptin system is essential for sodium tungstate antiobesity action. *Endocrinology* 150, 642–50. doi:10.1210/en.2008-0881
- Cannon, B., 2004. Brown Adipose Tissue: Function and Physiological Significance. *Physiol. Rev.* 84, 277–359. doi:10.1152/physrev.00015.2003
- Carracedo, A., Cantley, L.C., Pandolfi, P.P., 2013. Cancer metabolism: fatty acid oxidation in the limelight. *Nat. Rev. Cancer* 13, 227–32. doi:10.1038/nrc3483
- Carroll, J., Fearnley, I.M., Skehel, J.M., Shannon, R.J., Hirst, J., Walker, J.E., 2006. Bovine complex I is a complex of 45 different subunits. *J. Biol. Chem.* 281, 32724–32727. doi:10.1074/jbc.M607135200
- Casas, F., Pessemesse, L., Grandemange, S., Seyer, P., Gueguen, N., Baris, O., Lepourry, L., Cabello, G., Wrutniak-Cabello, C., 2008. Overexpression of the mitochondrial T3 receptor p43 induces a shift in skeletal muscle fiber types. *PLoS One* 3, e2501. doi:10.1371/journal.pone.0002501
- Casas, F., Rochard, P., Rodier, A., Cassar-Malek, I., Marchal-Victorion, S., Wiesner, R.J., Cabello, G., Wrutniak, C., 1999. A variant form of the nuclear triiodothyronine receptor c-ErbA $\alpha$ 1 plays a direct role in regulation of mitochondrial RNA synthesis. *Mol. Cell. Biol.* 19, 7913–24.
- Chan, C.B., Harper, M.-E., 2006. Uncoupling proteins: role in insulin resistance and insulin insufficiency. *Curr. Diabetes Rev.* 2, 271–283. doi:10.2174/157339906777950660
- Chentouf, M., Dubois, G., Jahannaut, C., Castex, F., Lajoix, A.D., Gross, R., Peraldi-Roux, S., 2011. Excessive food intake, obesity and inflammation process in Zucker fa/fa rat pancreatic islets. *PLoS One* 6, e22954. doi:10.1371/journal.pone.0022954
- Chinnery, P.F., 2003. Searching for nuclear-mitochondrial genes. *Trends Genet.* 19, 60–62. doi:10.1016/S0168-9525(02)00030-6
- Cho, S., Hoang, A., Sinha, R., Zhong, X.-Y., Fu, X.-D., Krainer, A.R., Ghosh, G., 2011. Interaction between the RNA binding domains of Ser-Arg splicing factor 1 and U1-70K snRNP protein determines early spliceosome assembly. *Proc. Natl. Acad. Sci. U. S. A.* 108, 8233–8238. doi:10.1073/pnas.1017700108

- Cinti, S., 2005. The adipose organ. Prostaglandins Leukot. Essent. Fat. Acids 73, 9–15. doi:10.1016/j.plefa.2005.04.010
- Clapham, J.C., Arch, J.R., Chapman, H., Haynes, a, Lister, C., Moore, G.B., Piercy, V., Carter, S. a, Lehner, I., Smith, S. a, Beeley, L.J., Godden, R.J., Herrity, N., Skehel, M., Changani, K.K., Hockings, P.D., Reid, D.G., Squires, S.M., Hatcher, J., Trail, B., Latcham, J., Rastan, S., Harper, a J., Cadenas, S., Buckingham, J. a, Brand, M.D., Abuin, a, 2000. Mice overexpressing human uncoupling protein-3 in skeletal muscle are hyperphagic and lean. *Nature* 406, 415–418. doi:10.1038/35019082
- Cline, G.W., Vidal-Puig, A.J., Dufour, S., Cadman, K.S., Lowell, B.B., Shulman, G.I., 2001. In Vivo Effects of Uncoupling Protein-3 Gene Disruption on Mitochondrial Energy Metabolism. *J. Biol. Chem.* 276, 20240–20244. doi:10.1074/jbc.M102540200
- Clostre, F., 2001. [Mitochondria: recent pathophysiological discoveries and new therapeutic perspectives]. *Ann. Pharm. françaises* 59, 3–21.
- Coffinier, C., Jung, H.J., Li, Z., Nobumori, C., Yun, U.J., Farber, E. a., Davies, B.S., Weinstein, M.M., Yang, S.H., Lammerding, J., Farahani, J.N., Bentolila, L. a., Fong, L.G., Young, S.G., 2010. Direct synthesis of lamin A, bypassing prelamina processing, causes misshapen nuclei in fibroblasts but no detectable pathology in mice. *J. Biol. Chem.* 285, 20818–20826. doi:10.1074/jbc.M110.128835
- Cotter, D., Guda, P., Fahy, E., Subramaniam, S., 2004. MitoProteome: mitochondrial protein sequence database and annotation system. *Nucleic Acids Res.* 32, D463–D467. doi:10.1093/nar/gkh048
- Cousin, B., Cinti, S., Morroni, M., Raimbault, S., Ricquier, D., Pénicaud, L., Casteilla, L., 1992. Occurrence of brown adipocytes in rat white adipose tissue: molecular and morphological characterization. *J. Cell Sci.* 103 ( Pt 4, 931–942.
- Cummings, D.E., Schwartz, M.W., 2003. Genetics and pathophysiology of human obesity. *Annu. Rev. Med.* 54, 453–471. doi:10.1146/annurev.med.54.101601.152403
- Davies, B.S.J., Barnes, R.H., Tu, Y., Ren, S., Andres, D. a., Peter Spielmann, H., Lammerding, J., Wang, Y., Young, S.G., Fong, L.G., 2010. An accumulation of non-farnesylated prelamina A causes cardiomyopathy but not progeria. *Hum. Mol. Genet.* 19, 2682–2694. doi:10.1093/hmg/ddq158
- De Conti, L., Baralle, M., Buratti, E., 2013. Exon and intron definition in pre-mRNA splicing. *Wiley Interdiscip. Rev. RNA* 4, 49–60. doi:10.1002/wrna.1140
- Dechat, T., Pflieger, K., Sengupta, K., Shimi, T., Shumaker, D.K., Solimando, L., Goldman, R.D., 2008. Nuclear lamins: Major factors in the structural organization and function of the nucleus and chromatin. *Genes Dev.* 22, 832–853. doi:10.1101/gad.1652708
- Deiuliis, J. a, 2015. MicroRNAs as regulators of metabolic disease: Pathophysiologic significance and emerging role as biomarkers and therapeutics. *Int. J. Obes.* 1–



50. doi:10.1038/ijo.2015.170
- Dempersmier, J., Sul, H.S., 2015. Shades of Brown: A Model for Thermogenic Fat. *Front. Endocrinol. (Lausanne)*. 6, 1–6. doi:10.3389/fendo.2015.00071
- Dimauro, S., Schon, E.A., 2003. Mitochondrial Respiratory-Chain Diseases 2656–2668.
- Dimroth, P., Kaim, G., Matthey, U., 2000. Crucial role of the membrane potential for ATP synthesis by F(1)F(o) ATP synthases. *J. Exp. Biol.* 203, 51–59.
- Divakaruni, A.S., Brand, M.D., 2011. The regulation and physiology of mitochondrial proton leak. *Physiology (Bethesda)*. 26, 192–205. doi:10.1152/physiol.00046.2010
- Dulloo, a G., Jacquet, J., Solinas, G., Montani, J.-P., Schutz, Y., 2010. Body composition phenotypes in pathways to obesity and the metabolic syndrome. *Int. J. Obes. (Lond)*. 34 Suppl 2, S4–S17. doi:10.1038/ijo.2010.234
- Elabd, C., Chiellini, C., Carmona, M., Galitzky, J., Cochet, O., Petersen, R., Pénicaud, L., Kristiansen, K., Bouloumié, A., Casteilla, L., Dani, C., Ailhaud, G., Amri, E.-Z., 2009. Human multipotent adipose-derived stem cells differentiate into functional brown adipocytes. *Stem Cells* 27, 2753–60. doi:10.1002/stem.200
- Elstner, M., Andreoli, C., Klopstock, T., Meitinger, T., Prokisch, H., 2009. The mitochondrial proteome database: MitoP2. *Methods Enzymol.* 457, 3–20. doi:10.1016/S0076-6879(09)05001-0
- Enríquez, J.A., Fernández-Sílv, P., Montoya, J.,. Autonomous regulation in mammalian mitochondrial DNA transcription. *Biol. Chem.* 380, 737–47. doi:10.1515/BC.1999.094
- Eriksson, M., Brown, W.T., Gordon, L.B., Glynn, M.W., Singer, J., Scott, L., Erdos, M.R., Robbins, C.M., Moses, T.Y., Berglund, P., Dutra, A., Pak, E., Durkin, S., Csoka, A.B., Boehnke, M., Glover, T.W., Collins, F.S., 2003. Recurrent de novo point mutations in lamin A cause Hutchinson-Gilford progeria syndrome. *Nature* 423, 293–298. doi:10.1038/nature01629
- Fain, J.N., 2010. Release of inflammatory mediators by human adipose tissue is enhanced in obesity and primarily by the nonfat cells: A review. *Mediators Inflamm.* 2010. doi:10.1155/2010/513948
- Fajas, L., 2003. Adipogenesis: a cross-talk between cell proliferation and cell differentiation. *Ann. Med.* 35, 79–85.
- Fajas, L., Auboeuf, D., Raspé, E., Schoonjans, K., Lefebvre, a M., Saladin, R., Najib, J., Laville, M., Fruchart, J.C., Deeb, S., Vidal-Puig, a, Flier, J., Briggs, M.R., Staels, B., Vidal, H., Auwerx, J., 1997. The organization, promoter analysis, and expression of the human PPARgamma gene. *J. Biol. Chem.* 272, 18779–18789. doi:10.1074/jbc.272.30.18779
- Farmer, S.R., 2006. Transcriptional control of adipocyte formation. *Cell Metab.* 4, 263–273. doi:10.1016/j.cmet.2006.07.001



- Fasshauer, M., Bluher, M., 2015. Adipokines in health and disease. *Cell Press* 36, 69–88. doi:10.1007/978-1-4419-1607-5\_4
- Fasshauer, M., Blüher, M., Stumvoll, M., 2014. Adipokines in gestational diabetes. *lancet. Diabetes Endocrinol.* 2, 488–99. doi:10.1016/S2213-8587(13)70176-1
- Feige, J.N., Lagouge, M., Canto, C., Strehle, A., Houten, S.M., Milne, J.C., Lambert, P.D., Matak, C., Elliott, P.J., Auwerx, J., 2008. Specific SIRT1 Activation Mimics Low Energy Levels and Protects against Diet-Induced Metabolic Disorders by Enhancing Fat Oxidation. *Cell Metab.* 8, 347–358. doi:10.1016/j.cmet.2008.08.017
- Fernández-Sánchez, A., Madrigal-Santillán, E., Bautista, M., Esquivel-Soto, J., Morales-González, A., Esquivel-Chirino, C., Durante-Montiel, I., Sánchez-Rivera, G., Valadez-Vega, C., Morales-González, J. a, 2011. Inflammation, oxidative stress, and obesity. *Int. J. Mol. Sci.* 12, 3117–32. doi:10.3390/ijms12053117
- Finan, B., Ma, T., Ottaway, N., Müller, T.D., Habegger, K.M., Heppner, K.M., Kirchner, H., Holland, J., Hembree, J., Raver, C., Lockie, S.H., Smiley, D.L., Gelfanov, V., Yang, B., Hofmann, S., Bruemmer, D., Drucker, D.J., Pfluger, P.T., Perez-Tilve, D., Gidda, J., Vignati, L., Zhang, L., Hauptman, J.B., Lau, M., Brecheisen, M., Uhles, S., Riboulet, W., Hainaut, E., Sebkova, E., Conde-Knape, K., Konkar, A., DiMarchi, R.D., Tschöp, M.H., 2013. Unimolecular dual incretins maximize metabolic benefits in rodents, monkeys, and humans. *Sci. Transl. Med.* 5, 209ra151. doi:10.1126/scitranslmed.3007218
- Finley, J., 2014. Alteration of splice site selection in the LMNA gene and inhibition of progerin production via AMPK activation. *Med. Hypotheses* 83, 580–587. doi:10.1016/j.mehy.2014.08.016
- Fisher, M., Kleiner, S., Douris, N., Fox, E.C., Mepani, R.J., Verdeguer, F., Wu, J., Kharitonov, A., Flier, J.S., Maratos-flier, E., Spiegelman, B.M., 2012. adaptive thermogenesis FGF21 regulates PGC-1 $\alpha$  and browning of white adipose tissues in adaptive thermogenesis 271–281. doi:10.1101/gad.177857.111
- Fleury, C., Neverova, M., Collins, S., Raimbault, S., Champigny, O., Levi-Meyrueis, C., Bouillaud, F., Seldin, M.F., Surwit, R.S., Ricquier, D., Warden, C.H., 1997. Uncoupling protein-2: a novel gene linked to obesity and hyperinsulinemia. *Nat. Genet.* 15, 269–72. doi:10.1038/ng0397-269
- Fong, L.G., Ng, J.K., Lammerding, J., Vickers, T.A., Meta, M., Coté, N., Gavino, B., Qiao, X., Chang, S.Y., Young, S.R., Yang, S.H., Stewart, C.L., Lee, R.T., Bennett, C.F., Bergo, M.O., Young, S.G., 2006. Prelamin A and lamin A appear to be dispensable in the nuclear lamina 116, 743–752. doi:10.1172/JCI27125.with
- Fong, L.G., Vickers, T. a., Farber, E. a., Choi, C., Yun, U.J., Hu, Y., Yang, S.H., Coffinier, C., Lee, R., Yin, L., Davies, B.S.J., Andres, D. a., Spielmann, H.P., Bennett, C.F., Young, S.G., 2009. Activating the synthesis of progerin, the mutant prelamin A in Hutchinson-Gilford progeria syndrome, with antisense oligonucleotides. *Hum. Mol. Genet.* 18, 2462–2471. doi:10.1093/hmg/ddp184
- Friedman, R.C., Farh, K.K.H., Burge, C.B., Bartel, D.P., 2009. Most mammalian

- mRNAs are conserved targets of microRNAs. *Genome Res.* 19, 92–105. doi:10.1101/gr.082701.108
- Gabaldón, T., Huynen, M. a., 2004. Shaping the mitochondrial proteome. *Biochim. Biophys. Acta - Bioenerg.* 1659, 212–220. doi:10.1016/j.bbabbio.2004.07.011
- Gaich, G., Chien, J.Y., Fu, H., Glass, L.C., Deeg, M.A., Holland, W.L., Kharitonov, A., Bumol, T., Schilske, H.K., Moller, D.E., 2013. The Effects of LY2405319, an FGF21 Analog, in Obese Human Subjects with Type 2 Diabetes. *Cell Metab.* 18, 333–340. doi:10.1016/j.cmet.2013.08.005
- Galgani, J.E., Moro, C., Ravussin, E., 2008. Metabolic flexibility and insulin resistance. *Am. J. Physiol. Endocrinol. Metab.* 295, E1009–17. doi:10.1152/ajpendo.90558.2008
- Garcia-Blanco, M. a, Baraniak, A.P., Lasda, E.L., 2004. Alternative splicing in disease and therapy. *Nat. Biotechnol.* 22, 535–546. doi:10.1038/nbt964
- Gasparik, V., Daubeuf, F., Hachet-Haas, M., Rohmer, F., Gizzi, P., Haiech, J., Galzi, J.L., Hibert, M., Bonnet, D., Frossard, N., 2012. Prodrugs of a CXC chemokine-12 (CXCL12) neutraligand prevent inflammatory reactions in an asthma model in vivo. *ACS Med. Chem. Lett.* 3, 10–14. doi:10.1021/ml200017d
- Gesta, S., Blüher, M., Yamamoto, Y., Norris, A.W., Berndt, J., Kralisch, S., Boucher, J., Lewis, C., Kahn, C.R., 2006. Evidence for a role of developmental genes in the origin of obesity and body fat distribution. *Proc. Natl. Acad. Sci. U. S. A.* 103, 6676–6681. doi:10.1073/pnas.0601752103
- Gesta, S., Tseng, Y.H., Kahn, C.R., 2007. Developmental Origin of Fat: Tracking Obesity to Its Source. *Cell* 131, 242–256. doi:10.1016/j.cell.2007.10.004
- Ghorbani, M., Claus, T.H., Himms-Hagen, J., 1997. Hypertrophy of brown adipocytes in brown and white adipose tissues and reversal of diet-induced obesity in rats treated with a  $\beta_3$ -adrenoceptor agonist. *Biochem. Pharmacol.* 54, 121–131. doi:10.1016/S0006-2952(97)00162-7
- Gillum, A.M., Clayton, D. a, 1978. Mechanism of mitochondrial DNA replication in mouse L-cells: kinetics of synthesis and turnover of the initiation sequence. *J. Mol. Biol.* 119, 49–68. doi:10.1016/0022-2836(78)90269-3
- Giralt, M., Villarroya, F., 2013. White, brown, beige/brite: Different adipose cells for different functions? *Endocrinology* 154, 2992–3000. doi:10.1210/en.2013-1403
- González, M., del Mar Bibiloni, M., Pons, A., Llompарт, I., Tur, J.A., 2012. Inflammatory markers and metabolic syndrome among adolescents. *Eur. J. Clin. Nutr.* 66, 1141–5. doi:10.1038/ejcn.2012.112
- Goodyear, L.J., 2008. The Exercise Pill — Too Good to Be True? *N. Engl. J. Med.* 359, 1842–1844. doi:10.1056/NEJMcibr0806723
- Gospodarska, E., Nowialis, P., Kozak, L.P., 2015. Mitochondrial Turnover: A Phenotype Distinguishing Brown Adipocytes from Interscapular Brown Adipose Tissue and White Adipose Tissue. doi:10.1074/jbc.M115.637785

- Granata, S., Zaza, G., Simone, S., Villani, G., Latorre, D., Pontrelli, P., Carella, M., Schena, F.P., Grandaliano, G., Pertosa, G., 2009. Mitochondrial dysregulation and oxidative stress in patients with chronic kidney disease. *BMC Genomics* 10, 388. doi:10.1186/1471-2164-10-388
- Gray, M.W., 2012. Mitochondrial evolution. *Cold Spring Harb. Perspect. Biol.* 4. doi:10.1101/cshperspect.a011403
- Green, H., Kehinde, O., 1975. An established preadipose cell line and its differentiation in culture. II. Factors affecting the adipose conversion. *Cell* 5, 19–27. doi:10.1016/0092-8674(75)90087-2
- Gregory, R.I., Yan, K.-P., Amuthan, G., Chendrimada, T., Doratotaj, B., Cooch, N., Shiekhattar, R., 2004. The Microprocessor complex mediates the genesis of microRNAs. *Nature* 432, 235–240. doi:10.1038/nature03120
- Grujic, D., Susulic, V.S., Harper, M.E., Himms-Hagen, J., Cunningham, B. a, Corkey, B.E., Lowell, B.B., 1997. Beta3-adrenergic receptors on white and brown adipocytes mediate beta3-selective agonist-induced effects on energy expenditure, insulin secretion, and food intake. A study using transgenic and gene knockout mice. *J. Biol. Chem.* 272, 17686–17693. doi:10.1074/jbc.272.28.17686
- Guarente, L., 2013. Calorie restriction and sirtuins revisited. *Genes Dev.* 27, 2072–85. doi:10.1101/gad.227439.113
- Guénant, a. C., Briand, N., Bidault, G., Afonso, P., Béréziat, V., Vazier, C., Lascols, O., Caron-Debarle, M., Capeau, J., Vigouroux, C., 2014. Nuclear envelope-related lipodystrophies. *Semin. Cell Dev. Biol.* 29, 148–157. doi:10.1016/j.semcdb.2013.12.015
- Guerra, C., Koza, R. a., Yamashita, H., Walsh, K., Kozak, L.P., 1998. Emergence of brown adipocytes in white fat in mice is under genetic control effects on body weight and adiposity. *J. Clin. Invest.* 102, 412–420. doi:10.1172/JCI3155
- Ha, M., Kim, V.N., 2014. Regulation of microRNA biogenesis. *Nat. Rev. Mol. Cell Biol.* 15, 509–524. doi:10.1038/nrm3838
- Haigis, M.C., Sinclair, D.A., 2010. Mammalian Sirtuins: Biological Insights and Disease Relevance. *Annu. Rev. Pathol. Mech. Dis.* 5, 253–295. doi:10.1146/annurev.pathol.4.110807.092250
- Harms, M., Seale, P., 2013. Brown and beige fat: development, function and therapeutic potential. *Nat. Med.* 19, 1252–63. doi:10.1038/nm.3361
- Harper, M.-E., Green, K., Brand, M.D., 2008. The efficiency of cellular energy transduction and its implications for obesity. *Annu. Rev. Nutr.* 28, 13–33. doi:10.1146/annurev.nutr.28.061807.155357
- Hartig, S.M., Hamilton, M.P., Bader, D.A., McGuire, S.E., 2015. The miRNA Interactome in Metabolic Homeostasis. *Trends Endocrinol. Metab.* doi:10.1016/j.tem.2015.09.006
- Hegele, R. a., Huff, M.W., Young, T.K., 2001. Common genomic variation in LMNA

- modulates indexes of obesity in Inuit. *J. Clin. Endocrinol. Metab.* 86, 2747–2751. doi:10.1210/jc.86.6.2747
- Hegele, R.A., Cao, H., Harris, S.B., Zinman, B., Hanley, A.J., Anderson, C.M., 2000. Genetic variation in LMNA modulates plasma leptin and indices of obesity in aboriginal Canadians. *Physiol. Genomics* 3, 39–44.
- Hill, B.G., 2015. Insights into an adipocyte whitening program. *Adipocyte* 4, 75–80. doi:10.4161/21623945.2014.960351
- Himms-Hagen, J.E. in a P.F. of E.E.T., 2004. Exercise in a Pill: Feasibility of Energy Expenditure Targets.
- Hoskins, A. a., Moore, M.J., 2012. The spliceosome: A flexible, reversible macromolecular machine. *Trends Biochem. Sci.* 37, 179–188. doi:10.1016/j.tibs.2012.02.009
- Huang, L., Mollet, S., Souquere, S., Le Roy, F., Ernoult-Lange, M., Pierron, G., Dautry, F., Weil, D., 2011. Mitochondria Associate with P-bodies and Modulate MicroRNA-mediated RNA Interference. *J. Biol. Chem.* 286, 24219–24230. doi:10.1074/jbc.M111.240259
- Hughes, J.P., Rees, S.S., Kalindjian, S.B., Philpott, K.L., 2011. Principles of early drug discovery. *Br. J. Pharmacol.* 162, 1239–1249. doi:10.1111/j.1476-5381.2010.01127.x
- Hui, X., Gu, P., Zhang, J., Nie, T., Pan, Y., Wu, D., Feng, T., Zhong, C., Wang, Y., Lam, K.S.L., Xu, A., 2015. Adiponectin Enhances Cold-Induced Browning of Subcutaneous Adipose Tissue via Promoting M2 Macrophage Proliferation. *Cell Metab.* 22, 279–290. doi:10.1016/j.cmet.2015.06.004
- Hunte, C., Koepke, J., Lange, C., Roßmanith, T., Michel, H., 2000. Structure at 2.3 Å resolution of the cytochrome bc<sub>1</sub> complex from the yeast *Saccharomyces cerevisiae* co-crystallized with an antibody Fv fragment. *Structure* 8, 669–684. doi:10.1016/S0969-2126(00)00152-0
- Huot, M.-É., Vogel, G., Zabarauskas, A., Ngo, C.T.-A., Coulombe-Huntington, J., Majewski, J., Richard, S., 2012. The Sam68 STAR RNA-binding protein regulates mTOR alternative splicing during adipogenesis. *Mol. Cell* 46, 187–99. doi:10.1016/j.molcel.2012.02.007
- Hüttemann, M., Lee, I., Samavati, L., Yu, H., Doan, J.W., 2007. Regulation of mitochondrial oxidative phosphorylation through cell signaling. *Biochim. Biophys. Acta* 1773, 1701–20.
- Ibrahim, M.M., 2010. Subcutaneous and visceral adipose tissue: Structural and functional differences. *Obes. Rev.* 11, 11–18. doi:10.1111/j.1467-789X.2009.00623.x
- Itoh, N., 2014. FGF21 as a hepatokine, adipokine, and myokine in metabolism and diseases. *Front. Endocrinol. (Lausanne)*. 5, 4–7. doi:10.3389/fendo.2014.00107
- Jackson, V.M., Breen, D.M., Fortin, J.-P., Liou, A., Kuzmiski, J.B., Loomis, A.K., Rives,

- M.-L., Shah, B., Carpino, P.A., 2015. Latest approaches for the treatment of obesity. *Expert Opin. Drug Discov.* 1–15. doi:10.1517/17460441.2015.1044966
- Jakobs, S., 2006. High resolution imaging of live mitochondria. *Biochim. Biophys. Acta* 1763, 561–575. doi:10.1016/j.bbamcr.2006.04.004
- Jastroch, M., Divakaruni, A.S., Mookerjee, S., Treberg, J.R., Martin, D., 2011. NIH Public Access 53–67. doi:10.1042/bse0470053.Mitochondrial
- Ji, X., Zhou, Y., Pandit, S., Huang, J., Li, H., Lin, C.Y., Xiao, R., Burge, C.B., Fu, X.-D., 2013. SR proteins collaborate with 7SK and promoter-associated nascent RNA to release paused polymerase. *Cell* 153, 855–68. doi:10.1016/j.cell.2013.04.028
- Jia, L., Liu, X., 2007. The Conduct of Drug Metabolism Studies Considered Good Practice (II): In Vitro Experiments | BenthamScience. *Curr Drug Metab.*
- Johnson, D.T., Harris, R. a, French, S., Blair, P. V, You, J., Bemis, K.G., Wang, M., Balaban, R.S., 2007. Tissue heterogeneity of the mammalian mitochondrial proteome. *Am. J. Physiol. Cell Physiol.* 292, C689–C697. doi:10.1152/ajpcell.00108.2006
- Jung, H.-J., Coffinier, C., Choe, Y., Beigneux, A.P., Davies, B.S.J., Yang, S.H., Barnes, R.H., Hong, J., Sun, T., Pleasure, S.J., Young, S.G., Fong, L.G., 2012. Regulation of prelamin A but not lamin C by miR-9, a brain-specific microRNA. *Proc. Natl. Acad. Sci. U. S. A.* 109, E423–31. doi:10.1073/pnas.1111780109
- Kaminska, D., Pihlajamäki, J., 2013. Regulation of alternative splicing in obesity and weight loss 143–147.
- Karpe, F., Pinnick, K.E., 2015. Biology of upper-body and lower-body adipose tissue--link to whole-body phenotypes. *Nat. Rev. Endocrinol.* 11, 90–100. doi:10.1038/nrendo.2014.185
- Kazak, L., Chouchani, E.T., Jedrychowski, M.P., Gygi, S.P., Bruce, M., Kazak, L., Chouchani, E.T., Jedrychowski, M.P., Erickson, B.K., Shinoda, K., Cohen, P., Vetrivelan, R., Lu, G.Z., Laznik-bogoslavski, D., Hasenfuss, S.C., Kajimura, S., Gygi, S.P., Spiegelman, B.M., 2015. Article A Creatine-Driven Substrate Cycle Enhances Energy Expenditure and Thermogenesis in Beige Fat Article A Creatine-Driven Substrate Cycle Enhances Energy Expenditure and Thermogenesis in Beige Fat. *Cell* 163, 643–655. doi:10.1016/j.cell.2015.09.035
- Kelemen, O., Convertini, P., Zhang, Z., Wen, Y., Shen, M., Falaleeva, M., Stamm, S., 2013. Function of alternative splicing. *Gene* 514, 1–30. doi:10.1016/j.gene.2012.07.083
- Kelly, D.P., Scarpulla, R.C., 2004. Transcriptional regulatory circuits controlling mitochondrial biogenesis and function. *Genes Dev.* 18, 357–368. doi:10.1101/gad.1177604
- Kharitonov, A., Shiyanova, T.L., Koester, A., Ford, A.M., Micanovic, R., Galbreath, E.J., Sandusky, G.E., Hammond, L.J., Moyers, J.S., Owens, R. a, Gromada, J., Brozinick, J.T., Hawkins, E.D., Wroblewski, V.J., Li, D.S., Mehrbod, F., Jaskunas,



- S.R., Shanafelt, A.B., 2005. FGF-21 as a novel metabolic regulator. *J. Clin. Invest.* 115, 1627–1635. doi:10.1172/JCI23606
- Khedkar, V., Verma, J., Coutinho, E., 2009. Small-molecule screening techniques in drug discovery 3–7.
- Kim, J.B., Spiegelman, B.M., 1996. ADD 1/SREBP1 promotes adipocyte differentiation and gene expression linked to fatty acid metabolism. *Genes Dev.* 10, 1096–1107.
- Kishore, S., Stamm, S., 2006. The snoRNA HBII-52 Regulates 311, 230–232.
- Klötting, N., Berthold, S., Kovacs, P., Schön, M.R., Fasshauer, M., Ruschke, K., Stumvoll, M., Blüher, M., 2009. MicroRNA expression in human omental and subcutaneous adipose tissue. *PLoS One* 4, 2–7. doi:10.1371/journal.pone.0004699
- Knauf, C., Drougard, A., Fournel, A., Duparc, T., Valet, P., 2013. Hypothalamic actions of apelin on energy metabolism: new insight on glucose homeostasis and metabolic disorders. *Horm. Metab. Res.* 45, 928–34. doi:10.1055/s-0033-1351321
- Konarska, M.M., Vilardell, J., Query, C.C., 2006. Repositioning of the reaction intermediate within the catalytic center of the spliceosome. *Mol. Cell* 21, 543–53. doi:10.1016/j.molcel.2006.01.017
- Kopecky, J., Clarke, G., Enerbäck, S., Spiegelman, B., Kozak, L.P., 1995. Expression of the mitochondrial uncoupling protein gene from the aP2 gene promoter prevents genetic obesity. *J. Clin. Invest.* 96, 2914–2923. doi:10.1172/JCI118363
- Kornberg, H., 2000. Krebs and his trinity of cycles. *Nat. Rev. Mol. Cell Biol.* 1, 225–228. doi:10.1038/35043073
- Kornblihtt, A.R., Schor, I.E., Alló, M., Dujardin, G., Petrillo, E., Muñoz, M.J., 2013. Alternative splicing: a pivotal step between eukaryotic transcription and translation. *Nat. Rev. Mol. Cell Biol.* 14, 153–65. doi:10.1038/nrm3525
- Krauss, S., Cy, Z., Scorrano, L., Lt, D., St-Pierre, J., St, G., Bb, L., 2003. Superoxide-mediated activation of uncoupling protein 2 causes pancreatic beta cell dysfunction.[see comment]. 112, 1831–1842. doi:10.1172/JCI19774
- Krebs, H. a, Johnson, W. a, 1937. Acetopyruvic acid (alphagamma-diketovaleric acid) as an intermediate metabolite in animal tissues. *Biochem. J.* 31, 772–779.
- Lacarelle, B., Marre, F., Blanc-Gauthier, T., Zhou, X.J., Placidi, M., Catalin, J., Rahmani, R., 1991. Use of human and animal liver microsomes in drug metabolic studies. *Eur. J. Drug Metab. Pharmacokinet. Spec No* 3, 458–65.
- Lagouge, M., Argmann, C., Gerhart-Hines, Z., Meziane, H., Lerin, C., Daussin, F., Messadeq, N., Milne, J., Lambert, P., Elliott, P., Geny, B., Laakso, M., Puigserver, P., Auwerx, J., 2006. Resveratrol improves mitochondrial function and protects against metabolic disease by activating SIRT1 and PGC-1alpha. *Cell* 127, 1109–22. doi:10.1016/j.cell.2006.11.013
- Lancaster, C.R.D., 2002. Succinate : quinone oxidoreductases : an overview 1553, 1–6.

- Langin D, Frühbeck G, Frayn KN, L.M., 2009. Adipose tissue: development, anatomy and functions. John Wiley & Sons, Ltd, Chichester, UK.  
doi:10.1002/9780470712221
- Langin, D., 2006. Adipose tissue lipolysis as a metabolic pathway to define pharmacological strategies against obesity and the metabolic syndrome. *Pharmacol. Res.* 53, 482–491. doi:10.1016/j.phrs.2006.03.009
- Larder, R., O’Rahilly, S., 2012. Shedding pounds after going under the knife: Guts over glory—why diets fail. *Nat. Med.* 18, 666–667. doi:10.1038/nm.2747
- Lattanzi, G., Ortolani, M., Columbaro, M., Prencipe, S., Mattioli, E., Lanzarini, C., Maraldi, N.M., Cenni, V., Garagnani, P., Salvioli, S., Storci, G., Bonafè, M., Capanni, C., Franceschi, C., 2014. Lamins are rapamycin targets that impact human longevity: a study in centenarians. *J. Cell Sci.* 127, 147–57. doi:10.1242/jcs.133983
- Lee, Y., Rio, D.C., 2015. Mechanisms and Regulation of Alternative Pre-mRNA Splicing. *Annu. Rev. Biochem.* 84, 291–323. doi:10.1146/annurev-biochem-060614-034316
- Lenhard, J.M., 2011. Lipogenic enzymes as therapeutic targets for obesity and diabetes. *Curr. Pharm. Des.* 17, 325–31.
- Lewis, B.P., Burge, C.B., Bartel, D.P., 2005. Conserved seed pairing, often flanked by adenosines, indicates that thousands of human genes are microRNA targets. *Cell* 120, 15–20. doi:10.1016/j.cell.2004.12.035
- Li, J., Zhao, W.-G., Shen, Z.-F., Yuan, T., Liu, S.-N., Liu, Q., Fu, Y., Sun, W., 2015. Comparative Proteome Analysis of Brown Adipose Tissue in Obese C57BL/6J Mice Using iTRAQ-Coupled 2D LC-MS/MS. *PLoS One* 10, e0119350. doi:10.1371/journal.pone.0119350
- Liebling, D.S., Eisner, J.D., Gibbs, J., Smith, G.P., 1975. Intestinal satiety in rats. *J. Comp. Physiol. Psychol.* 89, 955–65.
- Liesa, M., Shirihai, O.S., 2013. Mitochondrial dynamics in the regulation of nutrient utilization and energy expenditure. *Cell Metab.* 17, 491–506. doi:10.1016/j.cmet.2013.03.002
- Lim, L.P., Burge, C.B., 2001. A computational analysis of sequence features involved in recognition of short introns. *Proc. Natl. Acad. Sci. U. S. A.* 98, 11193–8. doi:10.1073/pnas.201407298
- Lin, C.S., Klingenberg, M., 1980. Isolation of the Uncoupling Protein From Brown Adipose Tissue 113.
- Lin, J. et al., 2002. Transcriptional co-activator PGC-1 $\alpha$  drives the formation of slow-twitch muscle fibres. *Nature* 418, 797–801. doi:10.1038/nature00936.1.
- Lin, J.-C., 2015. Impacts of Alternative Splicing Events on the Differentiation of Adipocytes. *Int. J. Mol. Sci.* 16, 22169–22189. doi:10.3390/ijms160922169



- Lin, Y., Lee, H., Berg, a. H., Lisanti, M.P., Shapiro, L., Scherer, P.E., 2000. The lipopolysaccharide-activated Toll-like receptor (TLR)-4 induces synthesis of the closely related receptor TLR-2 in adipocytes. *J. Biol. Chem.* 275, 24255–24263. doi:10.1074/jbc.M002137200
- Lin, Y., Rajala, M.W., Berger, J.P., Moller, D.E., Barzilai, N., Scherer, P.E., 2001. Hyperglycemia-induced Production of Acute Phase Reactants in Adipose Tissue. *J. Biol. Chem.* 276, 42077–42083. doi:10.1074/jbc.M107101200
- Lin, Z., Tian, H., Lam, K.S.L., Lin, S., Hoo, R.C.L., Konishi, M., Itoh, N., Wang, Y., Bornstein, S.R., Xu, A., Li, X., 2013. Adiponectin mediates the metabolic effects of FGF21 on glucose homeostasis and insulin sensitivity in mice. *Cell Metab.* 17, 779–789. doi:10.1016/j.cmet.2013.04.005
- Link, T.A., 1995. between the precursor , the intermediate , and the mature form of the FeS protein from *Neurospora* . 34 Interestingly the FeS protein from potato undergoes only one-step processing and the cytochrome-c reductase / processing peptidase complex is the on 126.
- Liu, B., Ghosh, S., Yang, X., Zheng, H., Liu, X., Wang, Z., Jin, G., Zheng, B., Kennedy, B.K., Suh, Y., Kaerberlein, M., Tryggvason, K., Zhou, Z., 2012. Resveratrol rescues SIRT1-dependent adult stem cell decline and alleviates progeroid features in laminopathy-based progeria. *Cell Metab.* 16, 738–50. doi:10.1016/j.cmet.2012.11.007
- Lloyd, D.J., Trembath, R.C., Shackleton, S., 2002. A novel interaction between lamin A and SREBP1: implications for partial lipodystrophy and other laminopathies. *Hum. Mol. Genet.* 11, 769–777. doi:10.1093/hmg/11.7.769
- Lopez-Mejia, I.C., de Toledo, M., Chavey, C., Lapasset, L., Cavelier, P., Lopez-Herrera, C., Chebli, K., Fort, P., Beranger, G., Fajas, L., Amri, E.Z., Casas, F., Tazi, J., 2014. Antagonistic functions of LMNA isoforms in energy expenditure and lifespan. *EMBO Rep.* 15, 529–39. doi:10.1002/embr.201338126
- Lopez-Mejia, I.C., Vautrot, V., De Toledo, M., Behm-Ansmant, I., Bourgeois, C.F., Navarro, C.L., Osorio, F.G., Freije, J.M.P., Stévenin, J., De Sandre-Giovannoli, A., Lopez-Otin, C., Lévy, N., Branlant, C., Tazi, J., 2011. A conserved splicing mechanism of the LMNA gene controls premature aging. *Hum. Mol. Genet.* 20, 4540–55. doi:10.1093/hmg/ddr385
- López-Otín, C., Blasco, M. a, Partridge, L., Serrano, M., Kroemer, G., 2013. The hallmarks of aging. *Cell* 153, 1194–217. doi:10.1016/j.cell.2013.05.039
- Lowell, B.B., Shulman, G.I., 2005. Mitochondrial dysfunction and type 2 diabetes. *Science* 307, 384–387. doi:10.1126/science.1104343
- Lowell, B.B., S-Susulic, V., Hamann, A., Lawitts, J. a, Himms-Hagen, J., Boyer, B.B., Kozak, L.P., Flier, J.S., 1993. Development of obesity in transgenic mice after genetic ablation of brown adipose tissue. *Nature* 366, 740–742. doi:10.1038/366740a0
- Luco, R.F., Allo, M., Schor, I.E., Kornblihtt, A.R., Misteli, T., 2011. Epigenetics in

- alternative pre-mRNA splicing. *Cell* 144, 16–26. doi:10.1016/j.cell.2010.11.056
- Lukeš, J., Archibald, J.M., Keeling, P.J., Doolittle, W.F., Gray, M.W., 2011. How a neutral evolutionary ratchet can build cellular complexity. *IUBMB Life* 63, 528–537. doi:10.1002/iub.489
- Lund, L.R., Georg, B., Nielsen, L.S., Mayer, M., Danø, K., Andreasen, P. a, 1988. Plasminogen activator inhibitor type 1: cell-specific and differentiation-induced expression and regulation in human cell lines, as determined by enzyme-linked immunosorbent assay. *Mol. Cell. Endocrinol.* 60, 43–53.
- Lutz, T.A., Woods, S.C., 2013. Overview of Animal Models of Obesity 1–22. doi:10.1002/0471141755.ph0561s58.Overview
- Maes, H.H., Neale, M.C., Eaves, L.J., 1997. Genetic and environmental factors in relative body weight and human adiposity. *Behav. Genet.* 27, 325–51.
- Makeyev, E. V, Maniatis, T., 2008. Multilevel regulation of gene expression by microRNAs. *Science* 319, 1789–1790. doi:10.1126/science.1152326
- Mallet, V.O., Mitchell, C., Guidotti, J.-E., Jaffray, P., Fabre, M., Spencer, D., Arnoult, D., Kahn, A., Gilgenkrantz, H., 2002. Conditional cell ablation by tight control of caspase-3 dimerization in transgenic mice. *Nat. Biotechnol.* 20, 1234–1239. doi:10.1038/nbt762
- Mao, W., Yu, X.X., Zhong, A., Li, W., Brush, J., Sherwood, S.W., Adams, S.H., Pan, G., 1999. UCP4, a novel brain-specific mitochondrial protein that reduces membrane potential in mammalian cells. *FEBS Lett.* 443, 326–330. doi:10.1016/S0014-5793(98)01713-X
- Mardinoglu, A., Agren, R., Kampf, C., Asplund, A., Nookaew, I., Jacobson, P., Walley, A.J., Froguel, P., Carlsson, L.M., Uhlen, M., Nielsen, J., 2013. Integration of clinical data with a genome-scale metabolic model of the human adipocyte. *Mol. Syst. Biol.* 9, 649. doi:10.1038/msb.2013.5
- Martin, G., Schoonjans, K., Staels, B., Auwerx, J., 1998. PPAR $\gamma$  activators improve glucose-homeostasis by stimulating fatty- acid uptake in the adipocytes. *Atherosclerosis* 137, S75–S80.
- Martin, W., 2010. Evolutionary origins of metabolic compartmentalization in eukaryotes. *Philos. Trans. R. Soc. Lond. B. Biol. Sci.* 365, 847–855. doi:10.1098/rstb.2009.0252
- Martínez, J.A., 2006. Mitochondrial oxidative stress and inflammation: an slalom to obesity and insulin resistance. *J. Physiol. Biochem.* 62, 303–6.
- Matera, A.G., Wang, Z., 2014. A day in the life of the spliceosome. *Nat. Rev.* 34, 455–464. doi:10.1038/nrm3742
- Matlin, A.J., Clark, F., Smith, C.W.J., 2005. Understanding alternative splicing: towards a cellular code. *Nat. Rev. Mol. Cell Biol.* 6, 386–98. doi:10.1038/nrm1645
- Mattick, J.S., 2003. Challenging the dogma: The hidden layer of non-protein-coding

- RNAs in complex organisms. *BioEssays* 25, 930–939. doi:10.1002/bies.10332
- McFedries, A., Schwaid, A., Saghatelian, A., 2013. Methods for the elucidation of protein-small molecule interactions. *Chem. Biol.* 20, 667–673. doi:10.1016/j.chembiol.2013.04.008
- Mehra, A., Macdonald, I., Pillay, T.S., 2007. Variability in 3T3-L1 adipocyte differentiation depending on cell culture dish. *Anal. Biochem.* 362, 281–283. doi:10.1016/j.ab.2006.12.016
- Meirhaeghe, A., Crowley, V., Lenaghan, C., Lelliott, C., Green, K., Stewart, A., Hart, K., Schinner, S., Sethi, J.K., Yeo, G., Brand, M.D., Cortright, R.N., O'Rahilly, S., Montague, C., Vidal-Puig, A.J., 2003. Characterization of the human, mouse and rat PGC1 beta (peroxisome-proliferator-activated receptor-gamma co-activator 1 beta) gene in vitro and in vivo. *Biochem. J.* 373, 155–165. doi:10.1042/BJ20030200
- Meisinger, C., Sickmann, A., Pfanner, N., 2008. The Mitochondrial Proteome: From Inventory to Function. *Cell* 134, 22–24. doi:10.1016/j.cell.2008.06.043
- Melamed, Z., Levy, A., Ashwal-Fluss, R., Lev-Maor, G., Mekahel, K., Atias, N., Gilad, S., Sharan, R., Levy, C., Kadener, S., Ast, G., 2013. Alternative Splicing Regulates Biogenesis of miRNAs Located across Exon-Intron Junctions. *Mol. Cell* 50, 869–881. doi:10.1016/j.molcel.2013.05.007
- Mifflin, M.D., St Jeor, S.T., Hill, L. a, Scott, B.J., Daugherty, S. a, Koh, Y.O., 1990. A new predictive equation in healthy individuals<sup>3</sup> for resting energy. *Am. J. Clin. Nutr.* 51, 241–247.
- Miranda, M., Chacón, M.R., Gutiérrez, C., Vilarrasa, N., Gómez, J.M., Caubet, E., Megía, A., Vendrell, J., 2008. LMNA mRNA expression is altered in human obesity and type 2 diabetes. *Obesity (Silver Spring)*. 16, 1742–1748. doi:10.1038/oby.2008.276
- MITCHELL, P., 1961. Coupling of phosphorylation to electron and hydrogen transfer by a chemi-osmotic type of mechanism. *Nature* 191, 144–8.
- Moitra, J., Mason, M.M., Olive, M., Krylov, D., Gavrilova, O., Marcus-Samuels, B., Feigenbaum, L., Lee, E., Aoyama, T., Eckhaus, M., Reitman, M.L., Vinson, C., 1998. Life without white fat: A transgenic mouse. *Genes Dev.* 12, 3168–3181. doi:10.1101/gad.12.20.3168
- Monteiro, R., Azevedo, I., 2010. Chronic inflammation in obesity and the metabolic syndrome. *Mediators Inflamm.* 2010. doi:10.1155/2010/289645
- Mori, M. a., Thomou, T., Boucher, J., Lee, K.Y., Lallukka, S., Kim, J.K., Torriani, M., Yki-Järvinen, H., Grinspoon, S.K., Cypess, A.M., Kahn, C.R., 2014. Altered miRNA processing disrupts brown/white adipocyte determination and associates with lipodystrophy. *J. Clin. Invest.* 124, 3339–3351. doi:10.1172/JCI73468
- Murase, T., Misawa, K., Minegishi, Y., Aoki, M., Ominami, H., Suzuki, Y., Shibuya, Y., Hase, T., 2011. Coffee polyphenols suppress diet-induced body fat accumulation

- by downregulating SREBP-1c and related molecules in C57BL/6J mice. *Am. J. Physiol. Endocrinol. Metab.* 300, E122–E133. doi:10.1152/ajpendo.00441.2010
- Myers, M.G., Cowley, M. a, Münzberg, H., 2008. Mechanisms of leptin action and leptin resistance. *Annu. Rev. Physiol.* 70, 537–556. doi:10.1146/annurev.physiol.70.113006.100707
- Nam, M., Cooper, M.P., 2015. Role of Energy Metabolism in the Brown Fat Gene Program. *Front. Endocrinol. (Lausanne)*. 6. doi:10.3389/fendo.2015.00104
- Nasrallah, C.M., Horvath, T.L., 2014. Mitochondrial dynamics in the central regulation of metabolism. *Nat. Rev. Endocrinol.* 10, 650–8. doi:10.1038/nrendo.2014.160
- Navarro, C.L., Cau, P., Lévy, N., 2006. Molecular bases of progeroid syndromes. *Hum. Mol. Genet.* 15, 151–161. doi:10.1093/hmg/ddl214
- Naznin, F., Toshinai, K., Waise, T.M.Z., Namkoong, C., Moin, A.S.M., Sakoda, H., Nakazato, M., 2015. Diet-induced obesity causes peripheral and central ghrelin resistance by promoting inflammation. *J. Endocrinol.* doi:10.1530/JOE-15-0139
- Nedergaard, J., Bengtsson, T., Cannon, B., 2007. Unexpected evidence for active brown adipose tissue in adult humans. *Am. J. Physiol. Endocrinol. Metab.* 293, 444–452. doi:10.1152/ajpendo.00691.2006.
- Nedergaard, J., Cannon, B., 2013. How brown is brown fat? It depends where you look. *Nat. Med.* 19, 540–541. doi:10.1038/nm.3187
- Nedergaard, J., Cannon, B., 2003. The “novel” “uncoupling” proteins UCP2 and UCP3: what do they really do? Pros and cons for suggested functions. *Exp. Physiol.* 88, 65–84.
- Nicholls, D.G., Bernson, V.S., Heaton, G.M., 1978. The identification of the component in the inner membrane of brown adipose tissue mitochondria responsible for regulating energy dissipation. *Experientia. Suppl.* 32, 89–93.
- Nissan, X., Blondel, S., Navarro, C., Maury, Y., Denis, C., Girard, M., Martinat, C., De Sandre-Giovannoli, A., Levy, N., Peschanski, M., 2012. Unique preservation of neural cells in hutchinson- gilford progeria syndrome is due to the expression of the neural-specific miR-9 microRNA. *Cell Rep.* 2, 1–9. doi:10.1016/j.celrep.2012.05.015
- Ntambi, J.M., Kim, Y., 2000. Symposium : Adipocyte Function , Differentiation and Metabolism 3122–3126.
- Orang, A.V., Safaralizadeh, R., Kazemzadeh-bavili, M., 2014. Mechanisms of miRNA-Mediated Gene Regulation from Common Downregulation to mRNA-Specific Upregulation. *Int. J. Genomics* 2014.
- Orengo, J.P., Cooper, T.A., 2007. Alternative splicing in disease. *Adv. Exp. Med. Biol.* 623, 212–23.
- Ortega, F.J., Mayas, D., Moreno-Navarrete, J.M., Catalán, V., Gómez-Ambrosi, J., Esteve, E., Rodriguez-Hermosa, J.I., Ruiz, B., Ricart, W., Peral, B., Frühbeck, G.,

- Tinahones, F.J., Fernández-Real, J.M., 2010. The gene expression of the main lipogenic enzymes is downregulated in visceral adipose tissue of obese subjects. *Obesity* (Silver Spring). 18, 13–20. doi:10.1038/oby.2009.202
- Ortega-Molina, A., Efeyan, A., Lopez-Guadamillas, E., Muñoz-Martin, M., Gómez-López, G., Cañamero, M., Mulero, F., Pastor, J., Martinez, S., Romanos, E., Mar Gonzalez-Barroso, M., Rial, E., Valverde, A.M., Bischoff, J.R., Serrano, M., 2012. Pten positively regulates brown adipose function, energy expenditure, and longevity. *Cell Metab.* 15, 382–394. doi:10.1016/j.cmet.2012.02.001
- Osellame, L.D., Blacker, T.S., Duchon, M.R., 2012. Cellular and molecular mechanisms of mitochondrial function. *Best Pract. Res. Clin. Endocrinol. Metab.* 26, 711–723. doi:10.1016/j.beem.2012.05.003
- Osorio, F.G., Navarro, C.L., Cadiñanos, J., López-Mejía, I.C., Quirós, P.M., Bartoli, C., Rivera, J., Tazi, J., Guzmán, G., Varela, I., Depetris, D., de Carlos, F., Cobo, J., Andrés, V., De Sandre-Giovannoli, A., Freije, J.M.P., Lévy, N., López-Otín, C., 2011. Splicing-directed therapy in a new mouse model of human accelerated aging. *Sci. Transl. Med.* 3, 106ra107. doi:10.1126/scitranslmed.3002847
- Ouchi, N., Parker, J.L., Lugus, J.J., Walsh, K., 2011. Adipokines in inflammation and metabolic disease. *Nat. Rev. Immunol.* 11, 85–97. doi:10.1038/nri2921
- Pabis, M., Neufeld, N., Steiner, M.C., Bojic, T., Shav-Tal, Y., Neugebauer, K.M., 2013. The nuclear cap-binding complex interacts with the U4/U6·U5 tri-snRNP and promotes spliceosome assembly in mammalian cells. *RNA* 19, 1054–63. doi:10.1261/rna.037069.112
- Pagliarini, D.J., Calvo, S.E., Chang, B., Sheth, S. a., Vafai, S.B., Ong, S.E., Walford, G. a., Sugiana, C., Boneh, A., Chen, W.K., Hill, D.E., Vidal, M., Evans, J.G., Thorburn, D.R., Carr, S. a., Mootha, V.K., 2008. A Mitochondrial Protein Compendium Elucidates Complex I Disease Biology. *Cell* 134, 112–123. doi:10.1016/j.cell.2008.06.016
- Pan, Q., Shai, O., Lee, L.J., Frey, B.J., Blencowe, B.J., 2008. Deep surveying of alternative splicing complexity in the human transcriptome by high-throughput sequencing. *Nat. Genet.* 40, 1413–5. doi:10.1038/ng.259
- Pandit, S., Zhou, Y., Shiue, L., Coutinho-Mansfield, G., Li, H., Qiu, J., Huang, J., Yeo, G.W., Ares, M., Fu, X.-D., 2013. Genome-wide analysis reveals SR protein cooperation and competition in regulated splicing. *Mol. Cell* 50, 223–35. doi:10.1016/j.molcel.2013.03.001
- Pandya-Jones, A., Black, D.L., 2009. Co-transcriptional splicing of constitutive and alternative exons. *RNA* 15, 1896–1908. doi:10.1261/rna.1714509
- Parra, P., Serra, F., Palou, A., 2010. Expression of adipose MicroRNAs Is sensitive to dietary conjugated linoleic acid treatment in mice. *PLoS One* 5. doi:10.1371/journal.pone.0013005
- Pecqueur, C., Alves-Guerra, M.C., Gelly, C., Lévi-Meyrueis, C., Couplan, E., Collins, S., Ricquier, D., Bouillaud, F., Miroux, B., 2001. Uncoupling Protein 2, in Vivo



- Distribution, Induction upon Oxidative Stress, and Evidence for Translational Regulation. *J. Biol. Chem.* 276, 8705–8712. doi:10.1074/jbc.M006938200
- Peng, M., Ostrovsky, J., Kwon, Y.J., Polyak, E., Licata, J., Tsukikawa, M., Marty, E., Thomas, J., Felix, C. a., Xiao, R., Zhang, Z., Gasser, D.L., Argon, Y., Falk, M.J., 2015. Inhibiting cytosolic translation and autophagy improves health in mitochondrial disease. *Hum. Mol. Genet.* 24, 4829–4847. doi:10.1093/hmg/ddv207
- Phillips, T., 2008. Regulation of Transcription and gene expression in eukaryotes. *Nature Education* 1(1):199 [WWW Document]. *Nat. Educ.* URL <http://www.nature.com/scitable/topicpage/small-non-coding-rna-and-gene-expression-1078> (accessed 9.27.15).
- Pisani, D.F., Djedaini, M., Beranger, G.E., Elabd, C., Scheideler, M., Ailhaud, G., Amri, E.-Z., 2011. Differentiation of Human Adipose-Derived Stem Cells into “Brite” (Brown-in-White) Adipocytes. *Front. Endocrinol. (Lausanne)*. 2, 87. doi:10.3389/fendo.2011.00087
- Prokunina-Olsson, L., Welch, C., Hansson, O., Adhikari, N., Scott, L.J., Usher, N., Tong, M., Sprau, A., Swift, A., Bonnycastle, L.L., Erdos, M.R., He, Z., Saxena, R., Harmon, B., Kotova, O., Hoffman, E.P., Altshuler, D., Groop, L., Boehnke, M., Collins, F.S., Hall, J.L., 2009. Tissue-specific alternative splicing of TCF7L2. *Hum. Mol. Genet.* 18, 3795–3804. doi:10.1093/hmg/ddp321
- Puigserver, P., Wu, Z., Park, C.W., Graves, R., Wright, M., Spiegelman, B.M., 1998. A Cold-Inducible Coactivator of Nuclear Receptors Linked to Adaptive Thermogenesis. *Cell* 92, 829–839. doi:10.1016/S0092-8674(00)81410-5
- Qian, S., Tang, Y., Li, X., Liu, Y., Zhang, Y., Huang, H., Xue, R., Yu, H., 2013. BMP4-mediated brown fat-like changes in white adipose tissue alter glucose and energy homeostasis 110. doi:10.1073/pnas.1215236110/-/DCSupplemental.[www.pnas.org/cgi/doi/10.1073/pnas.1215236110](http://www.pnas.org/cgi/doi/10.1073/pnas.1215236110)
- Quinlan, C.L., Orr, a. L., Perevoshchikova, I. V., Treberg, J.R., Ackrell, B. a., Brand, M.D., 2012. Mitochondrial Complex II Can Generate Reactive Oxygen Species at High Rates in Both the Forward and Reverse Reactions. *J. Biol. Chem.* 287, 27255–27264. doi:10.1074/jbc.M112.374629
- Rajala, M.W., Scherer, P.E., 2003. Minireview: The adipocyte - At the crossroads of energy homeostasis, inflammation, and atherosclerosis. *Endocrinology* 144, 3765–3773. doi:10.1210/en.2003-0580
- Reitman, M.L., Arioglu, E., Gavrilova, O., Taylor, S.I., 2000. Lipoatrophy revisited. *Trends Endocrinol. Metab.* 11, 410–416. doi:10.1016/S1043-2760(00)00309-X
- Rice, D.R., White, A.G., Leevy, W.M., Smith, B.D., Dame, N., Sciences, G.L., Dame, N., 2015. Fluorescence Imaging of Interscapular Brown Adipose Tissue in Living Mice 3, 1979–1989. doi:10.1039/C4TB01914H.Fluorescence
- Ristow, M., Wolfrum, C., 2013. A radical opposition in body weight control. *EMBO Mol. Med.* 5, 1147–1148. doi:10.1002/emmm.201303094

- Rochford, J.J., 2014. Mouse models of lipodystrophy and their significance in understanding fat regulation, 1st ed, Current Topics in Developmental Biology. Elsevier Inc. doi:10.1016/B978-0-12-397920-9.00005-6
- Rogge, M.M., 2009. The role of impaired mitochondrial lipid oxidation in obesity. *Biol. Res. Nurs.* 10, 356–373. doi:10.1177/1099800408329408
- Rolfe, D.F., Newman, J.M., Buckingham, J. a, Clark, M.G., Brand, M.D., 1999. Contribution of mitochondrial proton leak to respiration rate in working skeletal muscle and liver and to SMR. *Am. J. Physiol.* 276, C692–C699.
- Rosen, E.D., MacDougald, O. a, 2006. Adipocyte differentiation from the inside out. *Nat. Rev. Mol. Cell Biol.* 7, 885–896. doi:10.1038/nrm2066
- Rosen, E.D., Spiegelman, B.M., 2006. Adipocytes as regulators of energy balance and glucose homeostasis. *Nature* 444, 847–53. doi:10.1038/nature05483
- Rosen, E.D., Spiegelman, B.M., 2000. of a Dipogenesis.
- Rosenwald, M., Wolfrum, C., 2014. The origin and definition of brite versus white and classical brown adipocytes. *Adipocyte* 3, 4–9. doi:10.4161/adip.26232
- Rothwell, N.J., Rothwell, N.J., Stock, M.J., Stock, M.J., 1983. Luxuskonsumption, diet-induced thermogenesis and brown fat: the case in favour. *Clin Sci* 64, 19–23. doi:10.1042/cs0640019
- Roybal, G. a., Jurica, M.S., 2010. Spliceostatin A inhibits spliceosome assembly subsequent to prespliceosome formation. *Nucleic Acids Res.* 38, 6664–6672. doi:10.1093/nar/gkq494
- Ruas, J.L., White, J.P., Rao, R.R., Kleiner, S., Brannan, K.T., Harrison, B.C., Greene, N.P., Wu, J., Estall, J.L., Irving, B. a, Lanza, I.R., Rasbach, K. a, Okutsu, M., Nair, K.S., Yan, Z., Leinwand, L. a, Spiegelman, B.M., 2012. A PGC-1 $\alpha$  isoform induced by resistance training regulates skeletal muscle hypertrophy. *Cell* 151, 1319–31. doi:10.1016/j.cell.2012.10.050
- Rüegger, S., Großhans, H., 2012. MicroRNA turnover: when, how, and why. *Trends Biochem. Sci.* 37, 436–446. doi:10.1016/j.tibs.2012.07.002
- Rusk, N., 2008. When microRNAs activate translation. *Nat. Methods* 5, 122–123. doi:10.1038/nmeth0208-122a
- Rustin, P., Rötig, A., 2002. Inborn errors of complex II--unusual human mitochondrial diseases. *Biochim. Biophys. Acta* 1553, 117–122.
- Ryan Alexander, Harvey Lodish, and L.S., 2011. MicroRNAs in adipogenesis and as therapeutic targets Obesity. *Expert Opin Ther Targets* 15, 623–636. doi:10.1517/14728222.2011.561317.MicroRNAs
- Salomonis, N., Schlieve, C.R., Pereira, L., Wahlquist, C., Colas, A., Zambon, A.C., Vranizan, K., Spindler, M.J., Pico, A.R., Cline, M.S., Clark, T. a, Williams, A., Blume, J.E., Samal, E., Mercola, M., Merrill, B.J., Conklin, B.R., 2010. Alternative splicing regulates mouse embryonic stem cell pluripotency and differentiation.



- Proc. Natl. Acad. Sci. U. S. A. 107, 10514–10519. doi:10.1073/pnas.0912260107
- Sanguinetti, M.C., Tristani-Firouzi, M., 2006. hERG potassium channels and cardiac arrhythmia. *Nature* 440, 463–469. doi:10.1038/nature04710
- Santoro, A., Mattace Raso, G., Meli, R., 2015. Drug targeting of leptin resistance. *Life Sci.* doi:10.1016/j.lfs.2015.05.012
- Savage, D.B., 2009. Mouse models of inherited lipodystrophy. *Dis. Model. Mech.* 2, 554–562. doi:10.1242/dmm.002907
- Sazanov, L. a., 2007. Respiratory complex I: Mechanistic and structural insights provided by the crystal structure of the hydrophilic domain. *Biochemistry* 46, 2275–2288. doi:10.1021/bi602508x
- Scarpulla, R.C., 2008. Nuclear Control of Respiratory Chain Expression by Nuclear Respiratory Factors and PGC-1-Related Coactivator. *Ann. N. Y. Acad. Sci.* 1147, 321–334. doi:10.1196/annals.1427.006
- Scarpulla, R.C., 2006. Nuclear control of respiratory gene expression in mammalian cells. *J. Cell. Biochem.* 97, 673–683. doi:10.1002/jcb.20743
- Scarpulla, R.C., 2002. Nuclear activators and coactivators in mammalian mitochondrial biogenesis. *Biochim. Biophys. Acta - Gene Struct. Expr.* 1576, 1–14. doi:10.1016/S0167-4781(02)00343-3
- Scarpulla, R.C., 1997. Nuclear control of respiratory chain expression in mammalian cells. *J. Bioenerg. Biomembr.* 29, 109–19.
- Schneeberger, M., Gomis, R., Claret, M., 2014. Hypothalamic and brainstem neuronal circuits controlling homeostatic energy balance. *J. Endocrinol.* 220, T25–T46. doi:10.1530/JOE-13-0398
- Schon, E. a, Santra, S., Pallotti, F., Girvin, M.E., 2001. Pathogenesis of primary defects in mitochondrial ATP synthesis. *Semin. Cell Dev. Biol.* 12, 441–448. doi:10.1006/scdb.2001.0281
- Schreiber, K.H., Kennedy, B.K., 2013. When lamins go bad: nuclear structure and disease. *Cell* 152, 1365–75. doi:10.1016/j.cell.2013.02.015
- Schwartz, M.W., Woods, S.C., Seeley, R.J., Barsh, G.S., Baskin, D.G., Leibel, R.L., 2003. Is the energy homeostasis system inherently biased toward weight gain? *Diabetes* 52, 232–238. doi:10.2337/diabetes.52.2.232
- Sethi, J.K., Vidal-Puig, A.J., 2007. Thematic review series: adipocyte biology. Adipose tissue function and plasticity orchestrate nutritional adaptation. *J. Lipid Res.* 48, 1253–1262. doi:10.1194/jlr.R700005-JLR200
- Shao, X., Wang, M., Wei, X., Deng, S., Fu, N., Peng, Q., Jiang, Y., Ye, L., Lin, Y., 2015. Peroxisome Proliferator-Activated Receptor- $\gamma$ : master regulator of adipogenesis and obesity. *Curr. Stem Cell Res. Ther.*
- Shi, Y., Burn, P., 2004. Lipid metabolic enzymes: emerging drug targets for the treatment of obesity. *Nat. Rev. Drug Discov.* 3, 695–710. doi:10.1038/nrd1469

- Shi, Y., Joyner, A.S., Shadrick, W., Palacios, G., Lagiseti, C., Potter, P.M., Sambucetti, L.C., Stamm, S., Webb, T.R., 2015. Pharmacodynamic assays to facilitate preclinical and clinical development of pre-mRNA splicing modulatory drug candidates. *Pharmacol. Res. Perspect.* 3, n/a–n/a. doi:10.1002/prp2.158
- Sikaris, K. a, 2004. The clinical biochemistry of obesity. *Clin. Biochem. Rev.* 25, 165–181.
- Snyder, C., Stefano, G.B., 2015. Mitochondria and chloroplasts shared in animal and plant tissues: significance of communication. *Med. Sci. Monit.* 21, 1507–11. doi:10.12659/MSM.894481
- Soret, J., Bakkour, N., Maire, S., Durand, S., Zekri, L., Gabut, M., Fic, W., Divita, G., Rivalle, C., Dauzonne, D., Nguyen, C.H., Jeanteur, P., Tazi, J., 2005. Selective modification of alternative splicing by indole derivatives that target serine-arginine-rich protein splicing factors. *Proc. Natl. Acad. Sci. U. S. A.* 102, 8764–9. doi:10.1073/pnas.0409829102
- Soukas, A., Socci, N.D., Saatkamp, B.D., Novelli, S., Friedman, J.M., 2001. Distinct Transcriptional Profiles of Adipogenesis in Vivo and in Vitro. *J. Biol. Chem.* 276, 34167–34174. doi:10.1074/jbc.M104421200
- Spalding, K.L., Arner, E., Westermark, P.O., Bernard, S., Buchholz, B. a, Bergmann, O., Blomqvist, L., Hoffstedt, J., Näslund, E., Britton, T., Concha, H., Hassan, M., Rydén, M., Frisén, J., Arner, P., 2008. Dynamics of fat cell turnover in humans. *Nature* 453, 783–787. doi:10.1097/01.ogx.0000325910.81966.ac
- Stanley, I. a., Ribeiro, S.M., Giménez-Cassina, A., Norberg, E., Danial, N.N., 2014. Changing appetites: The adaptive advantages of fuel choice. *Trends Cell Biol.* 24, 118–127. doi:10.1016/j.tcb.2013.07.010
- Stobbe, M.D., Houten, S.M., van Kampen, a. H.C., Wanders, R.J. a., Moerland, P.D., 2012. Improving the description of metabolic networks: the TCA cycle as example. *FASEB J.* 26, 3625–3636. doi:10.1096/fj.11-203091
- Swift, J., Ivanovska, I.L., Buxboim, A., Harada, T., Dingal, P.C.D.P., Pinter, J., Pajeroski, J.D., Spinler, K.R., Shin, J.-W., Tewari, M., Rehfeldt, F., Speicher, D.W., Discher, D.E., 2013. Nuclear lamin-A scales with tissue stiffness and enhances matrix-directed differentiation. *Science* 341, 1240104. doi:10.1126/science.1240104
- Taanman, J.W., 1999. The mitochondrial genome: structure, transcription, translation and replication. *Biochim. Biophys. Acta* 1410, 103–123. doi:10.1016/S0005-2728(98)00161-3
- Taliaferro, J.M., Alvarez, N., Green, R.E., Blanchette, M., Rio, D.C., 2011. Evolution of a tissue-specific splicing network. *Genes Dev.* 25, 608–620. doi:10.1101/gad.2009011
- Tamori, Y., Masugi, J., Nishino, N., Kasuga, M., 2002. Role of peroxisome proliferator-activated receptor-?? in maintenance of the characteristics of mature 3T3-L1 adipocytes. *Diabetes* 51, 2045–2055. doi:10.2337/diabetes.51.7.2045

- Tang, J.J., Li, J.G., Qi, W., Qiu, W.W., Li, P.S., Li, B.L., Song, B.L., 2011. Inhibition of SREBP by a small molecule, betulin, improves hyperlipidemia and insulin resistance and reduces atherosclerotic plaques. *Cell Metab.* 13, 44–56. doi:10.1016/j.cmet.2010.12.004
- Tang, J.-Y., Lee, J.-C., Hou, M.-F., Wang, C.-L., Chen, C.-C., Huang, H.-W., Chang, H.-W., 2013. Alternative splicing for diseases, cancers, drugs, and databases. *ScientificWorldJournal*. 2013, 703568. doi:10.1155/2013/703568
- Tao, M., You, C., Zhao, R., Liu, S., Zhang, Z., Zhang, C., Liu, Y., 2014. Animal Mitochondria : Evolution , Function , and Disease 1–10.
- Tazi, J., Bakkour, N., Stamm, S., 2009. Alternative splicing and disease. *Biochim. Biophys. Acta - Mol. Basis Dis.* 1792, 14–26. doi:10.1016/j.bbadis.2008.09.017
- Thompson, D., Karpe, F., Lafontan, M., Frayn, K., 2012. Physical Activity and Exercise in the Regulation of Human Adipose Tissue Physiology. *Physiol. Rev.* 92, 157–191. doi:10.1152/physrev.00012.2011
- Trujillo, M.E., Pajvani, U.B., 2005. ND ES SC ACKNOWLEDGEMENTS BACKGROUND RIB 8, 1141–1145.
- Tseng, Y.-H., Cypess, A.M., Kahn, C.R., 2010. Cellular bioenergetics as a target for obesity therapy. *Nat. Rev. Drug Discov.* 9, 465–482. doi:10.1038/nrd3138
- Turer, a. T., Scherer, P.E., 2012. Adiponectin: Mechanistic insights and clinical implications. *Diabetologia* 55, 2319–2326. doi:10.1007/s00125-012-2598-x
- Twyffels, L., Gueydan, C., Kruys, V., 2011. Shuttling SR proteins: More than splicing factors. *FEBS J.* 278, 3246–3255. doi:10.1111/j.1742-4658.2011.08274.x
- Uldry, M., Yang, W., St-Pierre, J., Lin, J., Seale, P., Spiegelman, B.M., 2006. Complementary action of the PGC-1 coactivators in mitochondrial biogenesis and brown fat differentiation. *Cell Metab.* 3, 333–341. doi:10.1016/j.cmet.2006.04.002
- van Waveren, C., Moraes, C.T., 2008. Transcriptional co-expression and co-regulation of genes coding for components of the oxidative phosphorylation system. *BMC Genomics* 9, 18. doi:10.1186/1471-2164-9-18
- Vega, R.B., Huss, J.M., Kelly, D.P., 2000. The coactivator PGC-1 cooperates with peroxisome proliferator-activated receptor alpha in transcriptional control of nuclear genes encoding mitochondrial fatty acid oxidation enzymes. *Mol. Cell Biol.* 20, 1868–76. doi:10.1128/MCB.20.5.1868-1876.2000
- Vidal, H., 2001. Gene expression in visceral and subcutaneous adipose tissues. *Ann. Med.* 33, 547–55.
- Vidal-Puig, a J., Grujic, D., Zhang, C.Y., Hagen, T., Boss, O., Ido, Y., Szczepanik, a, Wade, J., Mootha, V., Cortright, R., Muoio, D.M., Lowell, B.B., 2000. Energy metabolism in uncoupling protein 3 gene knockout mice. *J. Biol. Chem.* 275, 16258–16266. doi:10.1074/jbc.M910179199
- Vohl, M.-C., Sladek, R., Robitaille, J., Gurd, S., Marceau, P., Richard, D., Hudson, T.J.,

- Tchernof, A., 2004. A survey of genes differentially expressed in subcutaneous and visceral adipose tissue in men. *Obes. Res.* 12, 1217–22. doi:10.1038/oby.2004.153
- Wahl, M.C., Lührmann, R., 2015a. SnapShot: Spliceosome Dynamics I. *Cell* 161, 1474–1474.e1. doi:10.1016/j.cell.2015.05.050
- Wahl, M.C., Lührmann, R., 2015b. SnapShot: Spliceosome Dynamics II. *Cell* 162, 456–456.e1. doi:10.1016/j.cell.2015.06.061
- Wahl, M.C., Will, C.L., Lührmann, R., 2009. The spliceosome: design principles of a dynamic RNP machine. *Cell* 136, 701–18. doi:10.1016/j.cell.2009.02.009
- Wallace, D.C., 2005. A mitochondrial paradigm of metabolic and degenerative diseases, aging, and cancer: a dawn for evolutionary medicine. *Annu. Rev. Genet.* 39, 359–407. doi:10.1146/annurev.genet.39.110304.095751
- Wang, G.-S., Cooper, T. a, 2007. Splicing in disease: disruption of the splicing code and the decoding machinery. *Nat. Rev. Genet.* 8, 749–761. doi:10.1038/nrg2164
- Wang, H., Eckel, R.H., 2009. Lipoprotein lipase : from gene to obesity 80045. doi:10.1152/ajpendo.90920.2008.
- Wang, R., Green, D.R., 2012. Metabolic checkpoints in activated T cells. *Nat. Immunol.* 13, 907–915. doi:10.1038/ni.2386
- Wang, Z., Burge, C.B., 2008. Splicing regulation: from a parts list of regulatory elements to an integrated splicing code. *RNA* 14, 802–813. doi:10.1261/rna.876308
- Warne, J.P., 2003. Tumour necrosis factor alpha: a key regulator of adipose tissue mass. *J. Endocrinol.* 177, 351–355. doi:10.1677/joe.0.1770351
- Weights, A., Confri, S., n.d. EMOTION AND PERSPIRATIO INSENSIBILIS 541, 2–4.
- Whittle, A.J., Carobbio, S., Martins, L., Slawik, M., Hondares, E., Vázquez, M.J., Morgan, D., Csikasz, R.I., Gallego, R., Rodriguez-Cuenca, S., Dale, M., Virtue, S., Villarroya, F., Cannon, B., Rahmouni, K., López, M., Vidal-Puig, A., 2012. BMP8B increases brown adipose tissue thermogenesis through both central and peripheral actions. *Cell* 149, 871–885. doi:10.1016/j.cell.2012.02.066
- Winklhofer, K.F., Haass, C., 2010. Mitochondrial dysfunction in Parkinson's disease. *Biochim. Biophys. Acta* 1802, 29–44. doi:10.1016/j.bbadis.2009.08.013
- Worman, H.J., Bonne, G., 2007. “Laminopathies”: A wide spectrum of human diseases. *Exp. Cell Res.* 313, 2121–2133. doi:10.1016/j.yexcr.2007.03.028
- Worman, H.J., Fong, L.G., Muchir, A., Young, S.G., 2009. Laminopathies and the long strange trip from basic cell biology to therapy. *J. Clin. Invest.* 119, 1825–1836. doi:10.1172/JCI37679
- Wu, H., Sun, S., Tu, K., Gao, Y., Xie, B., Krainer, A.R., Zhu, J., 2010. A Splicing-Independent Function of SF2/ASF in MicroRNA Processing. *Mol. Cell* 38, 67–77. doi:10.1016/j.molcel.2010.02.021

- Wu, J., Boström, P., Sparks, L.M., Ye, L., Choi, J.H., Giang, A.-H., Khandekar, M., Virtanen, K. a, Nuutila, P., Schaart, G., Huang, K., Tu, H., van Marken Lichtenbelt, W.D., Hoeks, J., Enerbäck, S., Schrauwen, P., Spiegelman, B.M., 2012. Beige adipocytes are a distinct type of thermogenic fat cell in mouse and human. *Cell* 150, 366–76. doi:10.1016/j.cell.2012.05.016
- Xu, H., Barnes, G.T., Yang, Q., Tan, G., Yang, D., Chou, C.J., Sole, J., Nichols, A., Ross, J.S., Tartaglia, L. a., Others, 2003. Chronic inflammation in fat plays a crucial role in the development of obesity-related insulin resistance. *J. Clin. Invest.* 112, 1821–1830. doi:10.1172/JCI200319451.Introduction
- Xue, B., Rim, J.-S., Hogan, J.C., Coulter, A. a, Koza, R. a, Kozak, L.P., 2007. Genetic variability affects the development of brown adipocytes in white fat but not in interscapular brown fat. *J. Lipid Res.* 48, 41–51. doi:10.1194/jlr.M600287-JLR200
- Yagi, T., Matsuno-Yagi, A., 2003. The proton-translocating NADH-quinone oxidoreductase in the respiratory chain: The secret unlocked. *Biochemistry* 42, 2266–2274. doi:10.1021/bi027158b
- Ye, R., Scherer, P.E., 2013. Adiponectin, driver or passenger on the road to insulin sensitivity? *Mol. Metab.* 2, 133–141. doi:10.1016/j.molmet.2013.04.001
- Yu, X.X., Mao, W., Zhong, a, Schow, P., Brush, J., Sherwood, S.W., Adams, S.H., Pan, G., 2000. Characterization of novel UCP5/BMCP1 isoforms and differential regulation of UCP4 and UCP5 expression through dietary or temperature manipulation. *FASEB J.* 14, 1611–1618. doi:10.1096/fj.14.11.1611
- Zebisch, K., Voigt, V., Wabitsch, M., Brandsch, M., 2012. Protocol for effective differentiation of 3T3-L1 cells to adipocytes. *Anal. Biochem.* 425, 88–90. doi:10.1016/j.ab.2012.03.005
- Zechner, R., Kienesberger, P.C., Haemmerle, G., Zimmermann, R., Lass, A., 2009. Adipose triglyceride lipase and the lipolytic catabolism of cellular fat stores. *J. Lipid Res.* 50, 3–21. doi:10.1194/jlr.R800031-JLR200
- Zechner, R., Zimmermann, R., Eichmann, T.O., Kohlwein, S.D., Haemmerle, G., Lass, A., Madeo, F., 2012. FAT SIGNALS - Lipases and lipolysis in lipid metabolism and signaling. *Cell Metab.* 15, 279–291. doi:10.1016/j.cmet.2011.12.018
- Zhang, J., Lieu, Y.K., Ali, A.M., Penson, A., Reggio, K.S., Rabadan, R., Raza, A., Mukherjee, S., Manley, J.L., 2015. Disease-associated mutation in *SRSF2* misregulates splicing by altering RNA-binding affinities. *Proc. Natl. Acad. Sci.* 201514105. doi:10.1073/pnas.1514105112
- Zhang, Z., Krainer, A.R., 2004. Involvement of SR proteins in mRNA surveillance. *Mol. Cell* 16, 597–607. doi:10.1016/j.molcel.2004.10.031
- Zhou, Z., Licklider, L.J., Gygi, S.P., Reed, R., 2002. Comprehensive proteomic analysis of the human spliceosome. *Nature* 419, 182–5. doi:10.1038/nature01031
- Zwerger, M., Roschitzki-voser, H., Zbinden, R., Denais, C., Herrmann, H., 2015. Altering lamina assembly identifies lamina-dependent and -independent functions

for A-type lamins *Journal of Cell Science* Accepted manuscript 41.

